WOMEN IN LIPIDS IN CARDIOVASCULAR DISEASE

EDITED BY: Catherine Martel, Nathalie Pamir, Irena Levitan and Mary G. Sorci-Thomas

PUBLISHED IN: Frontiers in Cardiovascular Medicine

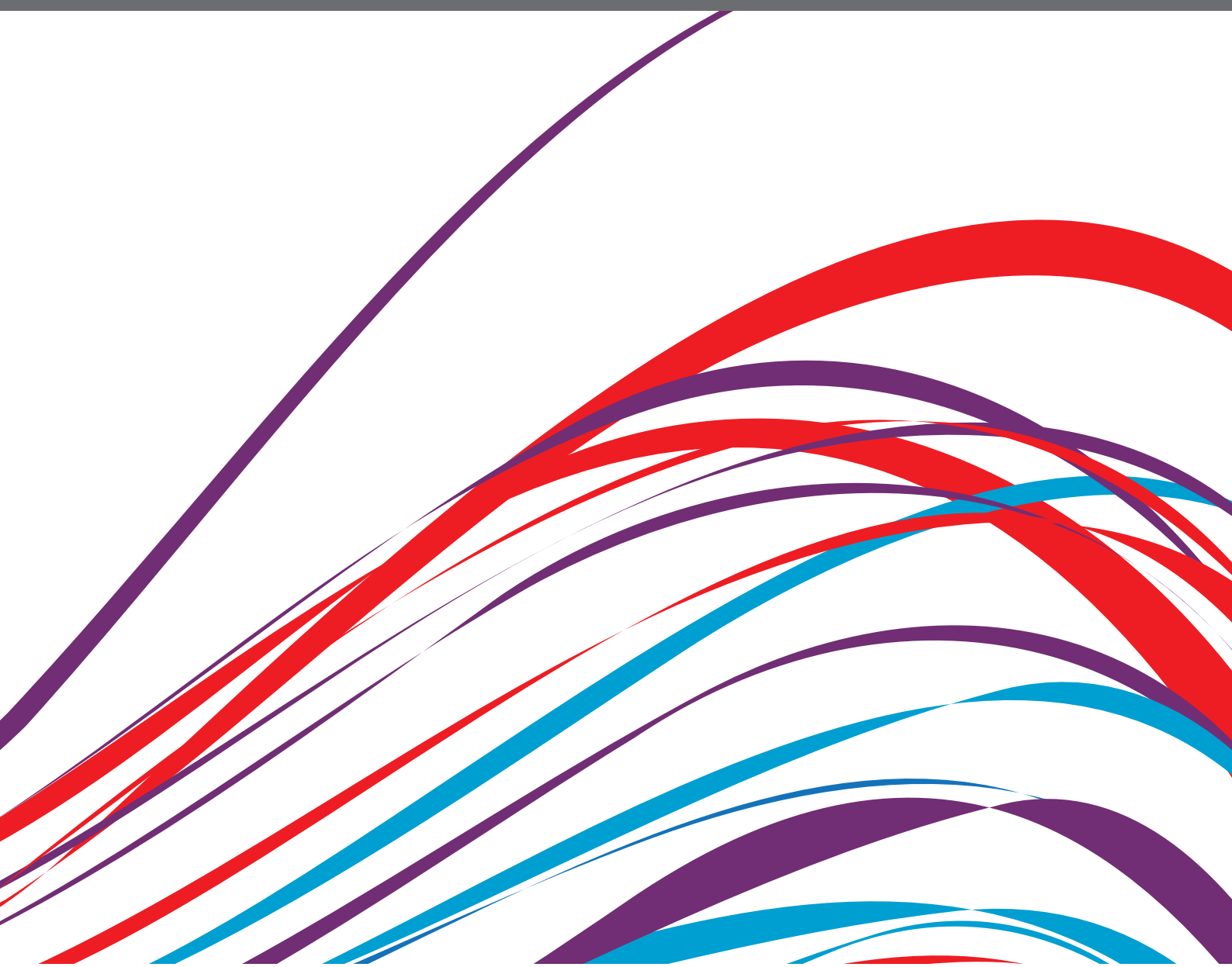

frontiers Research Topics

ISSN 1664-8714
ISBN 978-2-83250-618-9
DOI 10.3389/978-2-83250-618-9

About Frontiers

Frontiers is more than just an open-access publisher of scholarly articles: it is a pioneering approach to the world of academia, radically improving the way scholarly research is managed. The grand vision of Frontiers is a world where all people have an equal opportunity to seek, share and generate knowledge. Frontiers provides immediate and permanent online open access to all its publications, but this alone is not enough to realize our grand goals.

Frontiers Journal Series

The Frontiers Journal Series is a multi-tier and interdisciplinary set of open-access, online journals, promising a paradigm shift from the current review, selection and dissemination processes in academic publishing. All Frontiers journals are driven by researchers for researchers; therefore, they constitute a service to the scholarly community. At the same time, the Frontiers Journal Series operates on a revolutionary invention, the tiered publishing system, initially addressing specific communities of scholars, and gradually climbing up to broader public understanding, thus serving the interests of the lay society, too.

Dedication to Quality

Each Frontiers article is a landmark of the highest quality, thanks to genuinely collaborative interactions between authors and review editors, who include some of the world's best academicians. Research must be certified by peers before entering a stream of knowledge that may eventually reach the public - and shape society; therefore, Frontiers only applies the most rigorous and unbiased reviews.
Frontiers revolutionizes research publishing by freely delivering the most outstanding research, evaluated with no bias from both the academic and social point of view. By applying the most advanced information technologies, Frontiers is catapulting scholarly publishing into a new generation.

What are Frontiers Research Topics?

Frontiers Research Topics are very popular trademarks of the Frontiers Journals Series: they are collections of at least ten articles, all centered on a particular subject. With their unique mix of varied contributions from Original Research to Review Articles, Frontiers Research Topics unify the most influential researchers, the latest key findings and historical advances in a hot research area! Find out more on how to host your own Frontiers Research Topic or contribute to one as an author by contacting the Frontiers Editorial Office: frontiersin.org/about/contact

WOMEN IN LIPIDS IN CARDIOVASCULAR DISEASE

Topic Editors:
Catherine Martel, Université de Montréal, Canada
Nathalie Pamir, Oregon Health and Science University, United States
Irena Levitan, University of Illinois at Chicago, United States
Mary G. Sorci-Thomas, Medical College of Wisconsin, United States

Citation: Martel, C., Pamir, N., Levitan, I., Sorci-Thomas, M. G., eds. (2022). Women in Lipids in Cardiovascular Disease. Lausanne: Frontiers Media SA. doi: 10.3389/978-2-83250-618-9

Table of Contents

frontiers in Cardiovascular Medicine

CASE REPORT
published: 08 October 2021
doi: 10.3389/fcvm.2021.743341

Case Report: Difficulties in the Treatment of a 12-Year-Old Patient With Homozygous Familial Hypercholesterolemia, Compound Heterozygous Form – 5 Years Follow-Up

Lyudmila Vladimirova-Kitova[1,2*†], *Spas Kitov*[2†], *Mihail Ganev*[3†] *and Lubov Chochkova-Bukova*[4†]

[1] First Department of Internal Diseases, Section of Cardiology, Medical University of Plovdiv, Plovdiv, Bulgaria, [2] Clinic of Cardiology, St. George University Hospital, Plovdiv, Bulgaria, [3] Department of Medical Genetics, Medical University of Sofia, Sofia, Bulgaria, [4] Department of Paediatrics and Medical Genetics, Medical Faculty, Medical University of Plovdiv, Plovdiv, Bulgaria

OPEN ACCESS

Edited by:
Nathalie Pamir,
Oregon Health and Science University, United States

Reviewed by:
Papasani Subbaiah,
University of Illinois at Chicago, United States
Linzhang Huang,
Fudan University, China

***Correspondence:**
Lyudmila Vladimirova-Kitova
kitov@vip.bg

†These authors have contributed equally to this work and share first authorship

Specialty section:
This article was submitted to Lipids in Cardiovascular Disease, a section of the journal Frontiers in Cardiovascular Medicine

Received: 18 July 2021
Accepted: 23 August 2021
Published: 08 October 2021

Citation:
Vladimirova-Kitova L, Kitov S, Ganev M and Chochkova-Bukova L (2021) Case Report: Difficulties in the Treatment of a 12-Year-Old Patient With Homozygous Familial Hypercholesterolemia, Compound Heterozygous Form – 5 Years Follow-Up. Front. Cardiovasc. Med. 8:743341. doi: 10.3389/fcvm.2021.743341

The literature review we conducted reveals the limited use of proprotein convertase subtilisin/kexin type 9-inhibitors (PCSK9i) in children with familial hypercholesterolemia (FH). In 2015, a 10-year-old boy presented with round, xanthochromic lesions on his right knee and elbow. The values of total and LDL-cholesterol (LDL-C)—18 and 15 mmol/l, respectively—along with normal triglycerides and HDL-cholesterol (HDL-C) confirmed the lesions were xanthomas. The data suggested a homozygous form of FH. The level of lipoprotein (a) was high: 270 mg/dl. Initial treatment, based on European recommendations, included Atorvastatin 20 mg and Ezetimibe 10 mg and led to a decrease in LDL-C by 46% for 5 months; however, the patient developed severe statin intolerance. Atorvastatin was replaced with Rosuvastatin 10 mg, but the symptoms persisted. Success was achieved by switching to an intermittent regimen: Rosuvastatin 10 mg three times a week with a daily intake of Ezetimibe 10 mg. However, the results were far from the desired LDL target. LDL-apheresis was advisable, but unfortunately, it is not performed in Bulgaria. In May 2017, a genetic analysis [two pathological mutations within the *LDLR* gene: c.1519A>G; p.(Lys507Glu) and c.2403_2406del; p.(Leu802Alafs*126)] confirmed the initial diagnosis: the patient had homozygous FH with compound heterozygosity indeed. Having turned 12 in September 2017, the patient was eligible for treatment with a PCSK9i: Evolocumab 140 mg. The mean reduction of LDL-C with the triple combination reached a reduction of 52.17% for the whole 2-year period. The LDL target was reached in January 2020. The triple therapy significantly reduced Apolipoprotein B by 29.16%. No statistically significant difference was found in Lp (a) levels ($p > 0.05$) Our clinical case demonstrates that the triple lipid-lowering combination in a patient with compound heterozygous FH is a good therapeutic option for reaching the LDL-target.

Keywords: case report, homozygous familial hypercholesterolemia, child, Evolocumab, COVID-19

INTRODUCTION

The homozygous forms of familial hypercholesterolemia (HoFH) are rare (incidence is often cited to be 1:1,000,000 although estimations show that it could be as frequent as 1 in 160,000–320,000 people) and pose a significant therapeutic challenge (1, 2). In both HoFH forms (true homozygous and compound heterozygous) low-density lipoprotein (LDL) target levels are difficult to reach without treatment with LDL-apheresis, Mipomersen, or Lomitapide. The literature review reveals a limited use of proprotein convertase subtilisin/kexin type 9 inhibitors (PCSK9i) in children with FH (1–5). According to the European recommendations, diagnostic criteria of HoFH include untreated LDL-cholesterol (LDL-C) levels >13 mmol/L (500 mg/dL) and pediatric manifestations such as premature coronary heart disease, aortic valve disease, and tendon xanthomas in the hands and Achilles tendons (4, 5). The American Heart Association guidelines give a simplified clinical classification of HoFH: (1) appearance of xanthomas before the age of 10; (2) LDL-C >13 mmol/l before treatment or >7.76 mmol/l despite treatment; (3) phenotype features or documented hypercholesterolemia in both parents (6).

CASE REPORT

Case Description

In mid-2015, a 9-year-old boy first sought medical attention due to the occurrence of round, xanthochromic lesions on his right knee and right elbow as shown in the following pictures. Progression of the lesions was gradual and non-traumatic.

Physical examination showed height: 145 cm, weight: 46 kg, body mass index (BMI): 18.62 kg/m^2. The patient presented with blood pressure of 115/70 mmHg and heart rate of 95 bpm. No pathologic heart sounds were heard on auscultation; peripheral pulsations were within normal limits. Blood lipid analysis revealed extremely elevated total and LDL-C levels (18 and 15 mmol/l, respectively) with normal triglycerides (1.3 mmol/l) and HDL-C (1.4 mmol/l). Further laboratory tests revealed an Apolipoprotein-B/Apolipoprotein-A$_1$ ratio of 2.9 (Apolipoprotein-B: 3.5 g/l, Apolipoprotein-A$_1$: 1.4 g/l), which confirmed that the abovementioned lesions were xanthomas. The patient had normal thyroid function, normal vitamin D$_3$ levels, and no jaundice or anemia. We also found high levels of lipoprotein (a) (Lp(a): 270 mg/dl), which was measured by an immunoturbidimetric assay. Family history: The available data on the affected family members are presented in **Figure 1**.

According to the Simon Broome criteria, the boy was classified as having a definite FH (4, 5). Based on the early age of occurrence of xanthomas, extremely elevated LDL cholesterol levels, the presence of hypercholesterolemia in both parents, and family history of premature ischemic heart disease, we concluded that the condition was in its homozygous form (4–6).

Functional testing, electrocardiography at rest, and cardiopulmonary testing registered no abnormalities. Echocardiography revealed posterior annular calcification of the mitral valve and thickened and sclerotic aortic valve without any pathological gradient, normal ejection fraction (67%), and normal global longitudinal strain (−25%) (**Figure 2**). Additional tests for subclinical atherosclerosis were carried out in accordance with the European guidelines (7). Doppler ultrasound of the arteries of the extremities was performed by an angiologist and revealed no atherosclerotic lesions. Intima-media thickness of the carotid arteries was elevated for the patient's age and corresponded to the values of a 30-year-old male (**Figure 2**).

Treatment Approach

A multidisciplinary approach was applied with the help of a pediatrician, cardiologist, and nutritionist to reduce the total cardiovascular risk. It also included dietary recommendations and motivation for regular physical activity and psychological support to comply with the long-term treatment (4, 5).

A treatment plan for the patient was prepared in accordance with the European recommendations: administration of statins in the maximum tolerated dose and a cholesterol absorption inhibitor (3, 7) Initial treatment with Atorvastatin 20 mg in combination with Ezetimibe 10 mg was selected (8). With its help, the patient's LDL level decreased by roughly 46% for 5 months; however, he developed a severe statin intolerance: muscle weakness in his lower limbs and unwillingness to exercise. Creatin phosphokinase was elevated—approximately three times higher than the upper reference value—an insignificant finding in this case. A significant increase of the hepatic enzyme (alanine aminotransferase) levels was observed: a nearly threefold rise in comparison to baseline levels. Apart from the BMI, no other cause, potentially accountable for the statin intolerance (such as hypothyroidism, low vitamin D$_3$, or impaired kidney function) was identified. Atorvastatin was replaced with Rosuvastatin 10 mg, but the symptoms persisted. During the following year, the patient was on a treatment with Ezetimibe 10 mg only and refused to take statins, which led to an increase in the LDL-C (**Figure 3**).

In cases of HoFH, LDL apheresis is advisable. Unfortunately, the procedure is not performed in Bulgaria due to its high cost (9). Treatment with Mipomersen or Lomitapide was considered, but it was turned down due to its high financial cost (10).

We adapted an intermittent regimen for the administration of Rosuvastatin: 10 mg three times a week with a daily intake of Ezetimibe 10 mg. As a result, myalgia disappeared. The follow-up showed varying levels of LDL-C, which were far from the desired target of 5.2–11.7 mmol/l (**Figure 3**). According to ESC/EAS Guidelines for the Management of Dyslipidemias, genetic testing of children is required for accurate determination of the necessary level of aggressive lipid-lowering therapy (3, 4). In May 2017, a significant development of the case was brought in by genetic analysis: next-generation sequencing and CNV analysis of a dyslipidemia panel of 29 genes (with sensitivity of more than 99%) were performed at the Department of Clinical Genetics, Academic Medical Center at the University of Amsterdam, Netherlands. Two pathological mutations within the *LDLR* gene were identified: c.1519A>G; p.(Lys507Glu) and c.2403_2406del; p.(Leu802Alafs*126). These mutations had been previously identified only in France and the Netherlands in a small number of cases: 13 for the first mutation and three for the second one (11). No additional pathogenic mutations were identified in the remaining 28 genes of the dyslipidemia

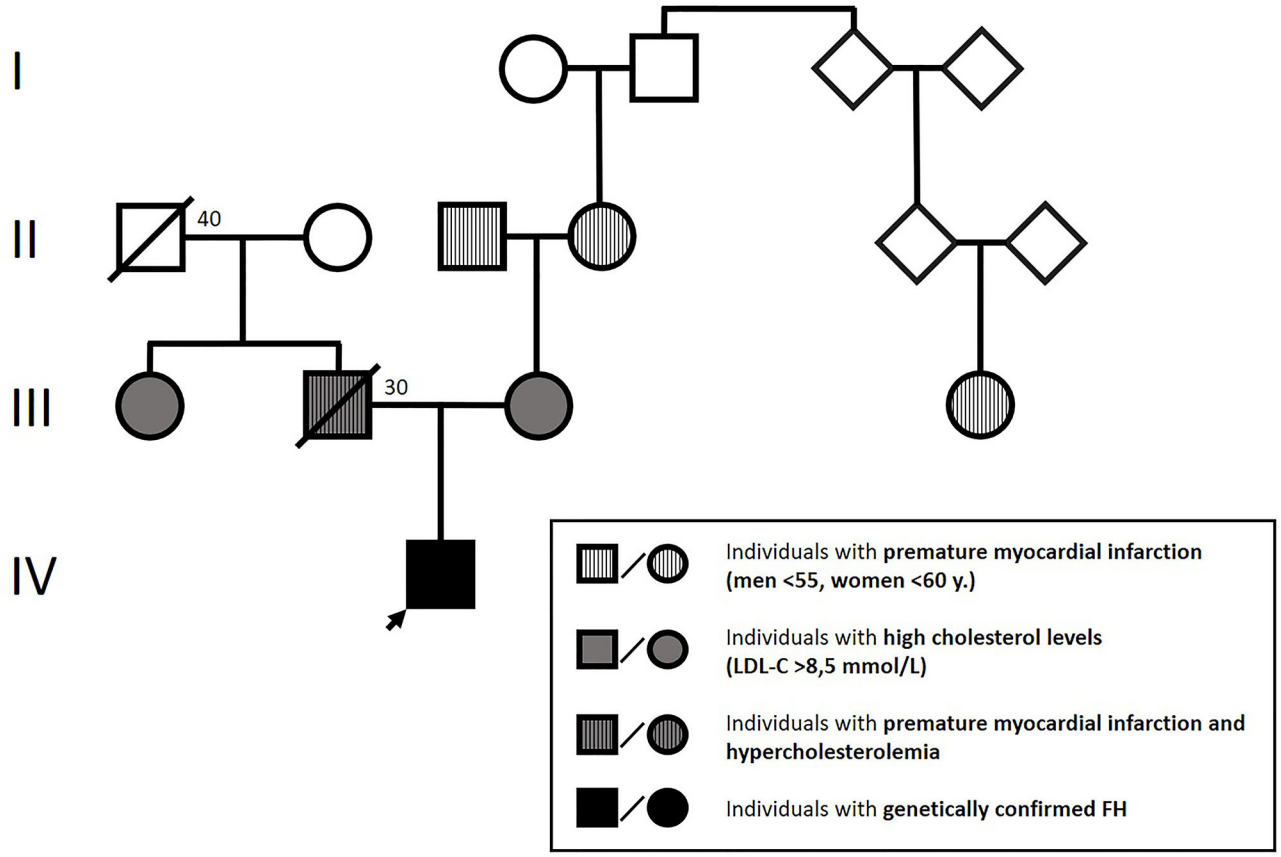

FIGURE 1 | Patient's family tree according to the boy's mother.

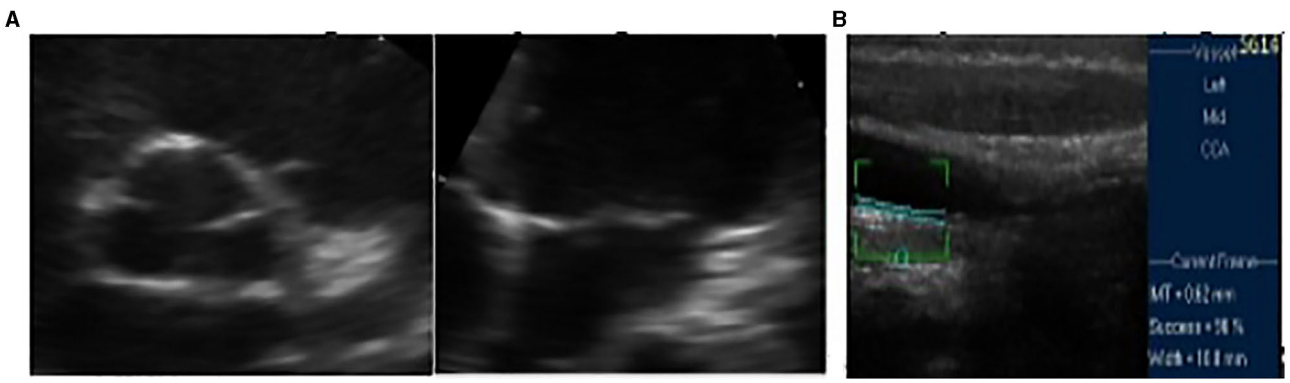

FIGURE 2 | (A) Initial fibrocalcinous changes on the aortic root and on the mitral valve annulus. **(B)** Initial intima media thickness of the last 10 mm of the right common carotid artery.

panel. The analysis confirmed the initial suspicion of HoFH. The condition was in its more common form: compound heterozygosity. The clinical severity of compound heterozygosity is considered almost equal to that of true homozygosity (11). Molecular genetics confirmation strengthened our patient's determination to be more willing to accept new treatment strategies.

In September 2017, the boy, already 12 years old, became eligible for treatment with PCSK9i (12–14). His case was reviewed by a National Committee, consisting of a cardiologist, a pediatrician, and an endocrinologist, and he was approved for adjuvant biweekly treatment with Evalocomab 140 mg with the consent of his parent. The first follow-up result was obtained at the beginning of February 2018 at week 4 after two

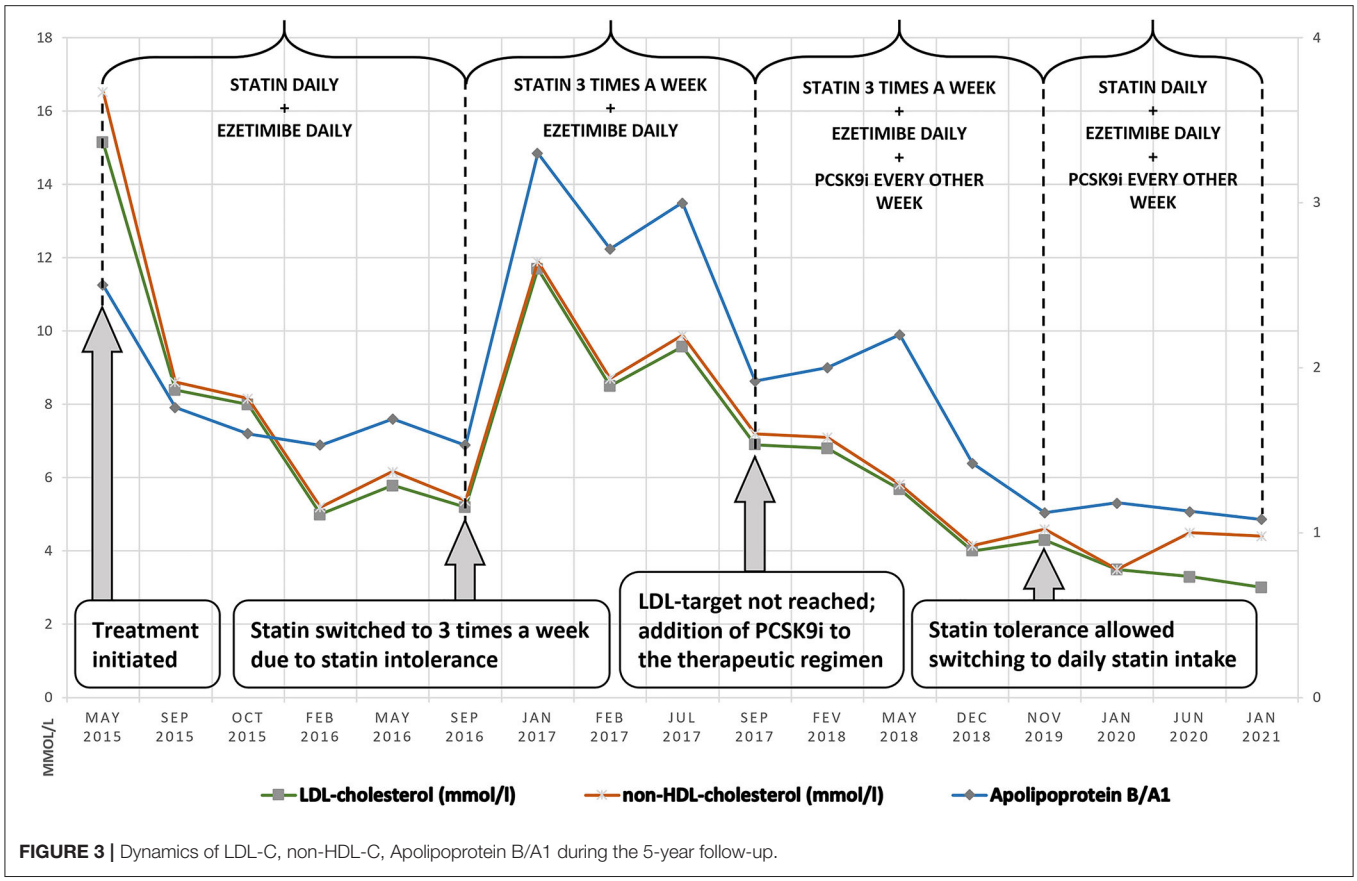

FIGURE 3 | Dynamics of LDL-C, non-HDL-C, Apolipoprotein B/A1 during the 5-year follow-up.

administrations of the drug. No reduction in the lipid levels was found: Total cholestrol was 8.8 mmol/l, and LDL-C was 6.8 mmol/l. Follow-up results at the beginning of May 2018 (nearly 6 months after the onset of the PCSK9i therapy) showed a reduction: total cholesterol was 7.46 mmol/l (15.2% reduction), and LDL-C was 5.68 mmol/l (16.4% reduction). Treatment with PCSK9i was combined with a maximum tolerated dose of Rosuvastatin 10 mg three times a week and Ezetimibe 10 mg daily. He was able to tolerate statins daily (BMI = 24.5 kg/m^2) due to the sufficient values of growth variables (height, weight, and BMI) characteristic for the patient's age (12). Subsequently, the patient started taking a combined pill of 10 mg Rosuvastatin and 10 mg Ezetimibe daily along with Evalocomab 140 mg twice a week. Follow-up evaluation was performed every 6 months. LDL-C follow-up showed a tendency for reaching the target levels. A positive result of LDL-C decrease by 50% in comparison with the initial values was achieved after the addition of Evalocomab to the dual lipid-lowering therapy. This was the reason why an increase in the statin dose was not necessary. Since January 2020, the target levels have been successfully preserved below 3.5 mmol/l. (14) (**Figure 3**).

The dynamics of the different lipid profile values during the 5-year course are displayed in **Figure 3**. The mean reduction of LDL-C by a therapeutic approach that included Rosuvastatin 20 mg daily, Ezetimibe 10 mg daily, and Evolocumab 140 mg every 2 weeks led to an initial decrease in LDL-C by 41.17% during the first year. The effect increased over time, reaching 52.17% for the whole 2-year period. The effect on LDL-C for this period increased, which indirectly indicated lack of anti-Evolocumab antibodies (the latter have not been tested). No effect on triglycerides and HDL-C was observed. As a result of the triple lipid-lowering therapy, significant reduction in the levels of Apolipoprotein-B was detected, reaching 29.16%. No statistically significant difference was found in Lp(a) levels ($p > 0.05$).

Additional laboratory assays, such as complete blood biochemistry (blood glucose and HbA_1c) and hematology analyses were carried out. The only ascertained increase was that of aminotransferase levels (three times the normal value) during the initiation of the daily statin intake. Subsequently, aminotransferase levels returned to normal.

Each year, the patient undergoes a complete cardiological examination: electrocardiography, echocardiography, duplex sonography of the carotid arteries, and stress test. No abnormalities were detected, apart from the thickness of the communal carotid artery. During the treatment, the thickness showed no alteration. Involution of xanthomas was observed in the first year of treatment with a reduction of LDL levels by almost 50%. Skin lesions' appearance during the 5-year period is shown on **Figure 4**.

Side effects, including minor flu-like symptoms, were reported by the patient's mother after the first administration of Evolocumab. An increase in the incidence of upper respiratory

FIGURE 4 | Involution of the xanthomas during the 5-year follow-up.

tract infections has been observed since the addition of the monoclonal antibody to the therapeutic scheme.

During the ongoing treatment and monitoring, it was ascertained that the child had a normal growth rate and height, which was at the 50th percentile. BMI showed the following deviations: an initial increase in BMI, which was insignificant, followed by a reduction of body mass and reaching a BMI at the third percentile at the age of 15, which requires attention and subsequent follow-up (**Supplementary Figure 1**). Because of this fact, we planned an increase in energy intake and scheduled a consultation with a pediatric dietologist. Pubertal development was at Tanner Stage 1 at the beginning of the treatment. At the age of 15, the patient was at Tanner stage 3, which was interpreted as normal development. In January 2021, while being on a triple lipid-lowering therapy, the patient suffered a mild COVID-19 infection, which had no complications.

DISCUSSION

Treatment of HoFH is often difficult despite the advances in lipid-lowering therapies (3–5). The 2016 ESC/EAS Guidelines for the Management of Dyslipidemias suggest that a healthy lifestyle and diet should be adopted by children suffering from FH, and statin treatment should be initiated as early as 8 years of age. The control of LDL-C levels is considered to be crucial. Recommended goals for children >10 years of age are LDL-C < 3.5 mmol/l (135 mg/dl) or at least a 50% reduction (3–5).

Potent statins, even at high doses, have proven to be insufficient for reaching the LDL-C targets with a reduction by 10–25% only detected in the majority of patients with HoFH. Nonetheless, they are in the basis of FH treatment (3). The addition of the cholesterol absorption inhibitor Ezetimibe lowers LDL-C further by 10–15%, adding to an overall reduction of 30–40% (3). Lipoprotein apheresis is a well-established treatment of both true homozygous (patients with two identical mutations, each in one of the copies of a certain gene) and compound heterozygous (patients with two different mutations, each in one of the copies of a certain gene) HoFH forms as well as of double heterozygous (patients with two different genes having a mutation in one of their copies) forms of FH. The high price and lifestyle requirements limit the administration of this treatment (9). Attention is currently directed at new available

lipid-lowering therapies, including Lomitapide, Mipomersen, and PCSK9i (10, 12). Both PCSK9i, Evalocomab and Alirocumab, have proven to reduce LDL-C additionally by up to 60% when added to a standard lipid-lowering therapy in heterozygous FH patients with relatively minor side effects (12–14). In HoFH (both true homozygous and compound heterozygous) and double heterozygous FH patients, the reduction at week 12 is reported to be 30.9% for Evalocomab and 41.2% for Alirocumab (15). The literature review reveals a limited use of PCSK9i in children. In the TESLA Part B trial, which included 49 individuals with HoFH over the age of 12, Evalocomab was administered in eight children, the youngest of whom was 13 years old. Two of the children were true homozygotes, and six were compound heterozygotes for *LDLR* mutations. Therapeutic reduction in cholesterol levels depended on the severity of the identified mutations and the residual activity of the *LDLR* (16). There are many other potential causes for interindividual differences in patient responses. Observations from the reported case detect a double LDL-C reduction after the addition of PCSK9i to the therapeutic scheme: during the first 6 months, reduction was by 28%; at the end of the second year, the reduction was by 52%. This demonstrates the applicability of PCSK9i in young patients with FH. The further decrease in LDL-C levels after the addition of PCSK9i to the treatment regimen suggests that there is a residual activity of the LDL receptor in our patient. Considering the results from the genetic analysis (two different *LDLR* mutations, both rare, and hence hard to reliably correlate to a specific *LDLR* activity phenotype), we assume this is indeed true; probably at least one of the mutations is "receptor-defective" and encodes a product with a partially preserved activity (as opposed to the "receptor-negative" mutations that cause complete loss of function of the product).

Our observations also confirm the TESLA Part B trial data on *LDLR* compound heterozygous HoFH of 23 patients, in which LDL-C reduction (Evolocumab compared with placebo) ranges from a mean 40.8% in 57% (28/49) of patients with either one or two mutations in *LDLR* to no response in patients with two negative or suspected negative mutations. It should be mentioned that, in the TESLA Part B trial, patients were monitored for a significantly shorter period: only 24 weeks compared with the 2-year follow-up of our case. Based on both sources, we can assume that response to Evolocumab was related to the specific underlying genetic defect causing HoFH. Furthermore, we presume that the therapeutic effect becomes more pronounced with time as observed during the 2-year PCSK9i treatment period in our patient.

In our case report, PCSK9i treatment is the main cause for reaching LDL-target levels in combination with a statin and ezetimibe. The reason behind this could be partially attributed to one or both of the following: lack of genetic defect in the *PCSK9* gene and/or residual LDLR activity. The LDL-C reduction by 52.17%, owing to the addition of PCSK9i to the therapeutic regimen, would not be sufficient by itself to reach the LDL target in HoFH when LDL-C should be even lower. The use of a triple lipid-lowering therapy employs several different mechanisms for the lowering of LDL-C, which have a more potent effect when combined and achieve significantly lower LDL-C values.

The current case study supports the results from TESLA part 2 by reporting that genetic information provides incremental insight into homozygous and compound heterozygous LDLR mutation–caused HoFH and its possible response to treatment. We also agree that the response to Evolocumab depends on the specific genotype causing HoFH with a greater reduction in LDL-C recorded in patients with *LDLR* receptor-defective mutations compared with patients with *LDLR* receptor-negative mutations (12). Therefore, it can be concluded that, in a clinical trial setting, the genetic confirmation of HoFH is a valuable source of information for assessment of the genotype–phenotype correlations. Genetic results could also prove useful in the selection of pediatric patients eligible for Evolocumab treatment in clinical practice.

This clinical case demonstrates that the triple lipid-lowering combination in a patient with compound heterozygous HoFH is a good therapeutic option for reaching the target levels as a result of reduction in LDL-C levels by more than 50% in a pediatric patient. The compound heterozygosity in our reported FH case appears not to influence the efficacy of Evolocumab with LDL-C reductions in the same range as reported for the overall pooled analysis of FH patients from an Evolocumab phase 3 trial. The LDL-C-lowering activity of Evolocumab in FH, caused by compound heterozygous LDLR genotypes, is likely to be attributable to the presence of at least one partially functional allele (receptor-defective mutation) (15).

Lp(a) is a marker that predicts and stratifies the risk of atherosclerotic cardiovascular disease in adults with FH in combination with the LDL-C level, but its role in children is debated (17, 18). Its high initial levels in our case report are consistent with previous studies suggesting that high Lp(a) levels in children may be associated with a family history of atherosclerotic cardiovascular disease (18). Lp(a) testing may also identify children with FH who could benefit from a more aggressive management to reduce atherosclerotic cardiovascular disease risk. The lack of Lp(a) reduction in our patient is discordant with the results of previous studies reporting that, in patients with either one or two defective *LDLR* alleles, Lp(a) reduction was statistically significant (16). Currently, data in regard to Lp(a) being better than LDL in stratifying the cardiovascular risk in children is lacking (18).

The lack of decrease in Lp(a) after the addition of Evolocumab is still a disappointing and disconcerting result. Data on Lp(a) in the pediatric population is limited. Previous studies show a decrease in Lp(a) but in adults and as a secondary prevention (19, 20). It should be kept in mind that the prognostic benefits that PCSK9i has in relation to Lp(a) are mainly derived from secondary analysis and not as a main goal of studies. On the other hand, we still do not have enough data on the effects of PCSK9i in primary prevention in both adult patients and children with elevated Lp(a) levels. We can suggest that the lack of effect detected in our study supports the data

in the literature that Lp(a) clearance is mediated by multiple receptors (21). Most likely due to the latter, even effective LDL-C-lowering pharmacotherapies, specifically enhancing the activity of hepatic LDL receptors, are not sufficient for an effective lowering of Lp(a) levels. This possible explanation would prove the lack of association of Lp(a) levels with the activity of any single one of the receptors expected to mediate hepatic removal of Lp(a). Targeting receptor-mediated removal of circulating Lp(a) particles for therapy may indeed require a complex approach. In accordance with the latter, recent efforts have been aimed at reducing the hepatic production rate of apolipoprotein (a). One realistic therapeutic strategy for our patient is the future use of the already approved RNAi-based PCSK9 inhibitor Inclisiran. The data from the literature proves the dose-dependent Inclisiran-mediated lowering of LDL-C and Lp(a) (22). Our team is hopeful that novel lipid-lowering therapies will help us reach the target levels of both LDL-C and Lp(a) and reduce the cardiovascular burden in the reported young individual.

Another significant problem is the thrombogenic risk associated with the persistent high levels of Lp(a) (23). It calls for a discussion on the need for antiplatelet prophylactic therapy (24). After examination of the other coagulation factors—platelets, fibrinogen, D-dimers—which were within the reference ranges and taking into account the normal vascular status, we decided to refrain from an antiplatelet treatment at this stage. We continue to monitor this issue.

Our patient had a mild COVID-19 infection a few months ago. That could be attributed to a sufficient immune response (even with Evolocumab). A few reasons can be given for the mild clinical course of the COVID-19 infection in our patient. First, statin therapy, due to its numerous pleiotropic effects on the vessel wall, may play a role because COVID-19 is an endothelial disease (25). Second, the initially elevated HDL-C levels, which remained high during the infection (HDL-C levels: 1.4 ± 0.15 mmol/l from the beginning and throughout the entire 5-year observation) probably have a connection with the administered lipid-lowering therapy: statin and PCSK9i (26, 27). Literature data suggest that PCSK9i treatment results in a more atheroprotective HDL particle profile; it decreases plasma levels of extra-large HDL particles and increases plasma levels of medium-sized HDL particles (27). The latter ones, when in high levels, are reported to be associated with a milder COVID-19 infection course (28). Similar data can be found in another observational study in which individuals with lower levels of HDL-C before the pandemic are at higher risk of suffering a severe COVID-19 infection (29, 30).

CONCLUSION

The response to Evolocumab was related to the underlying genetic defect causing HoFH with the compound heterozygous LDLR genotype. We confirm the observations of previous studies that, in compound heterozygous HoFH patients who receive stable background lipid-lowering treatment and do not undergo apheresis, biweekly treatment with Evalocomab 140 mg was well tolerated and significantly reduced LDL-C. More information is needed for the use of PCSK9i in children as far as effectiveness and possible short- and long-term side effects are concerned. The new upcoming therapies will most likely help resolve the problem of the persisting high Lp(a) levels in our patient.

LEARNING OBJECTIVES

- With the current limited literature data on the usage of PCSK9i in children with FH, the study contributes by providing additional information on the efficiency and safety within a 2-year period.
- On the other hand, the response to Evolocumab was related to the underlying genetic defect causing HoFH with compound heterozygous *LDLR* genotype. Compound heterozygous HoFH patients who receive stable background lipid-lowering treatment and do not undergo apheresis, biweekly treatment with Evalocomab 140 mg was well-tolerated and significantly reduced LDL-C for the reported period of 2 years.
- The persistent high Lp(a) level, even with the use of PSCK9 inhibitors in HoFH, is still a therapeutic challenge that we hope the new upcoming therapies will help us resolve.
- High HDL-C levels could be one of the reasons for the mild clinical COVID-19 infection course, a suggestion supported by recent literature data.

REPORTING GUIDELINES

The case report follows the consensus-based clinical case reporting guideline (CARE) checklist (30).

DATA AVAILABILITY STATEMENT

The datasets presented in this study can be found in online repositories. The names of the repository/repositories and accession number(s) can be found in the article/**Supplementary Material**.

ETHICS STATEMENT

The only living parent of the child signed an informed consent to participate in the study, genetic analysis, and data publication.

AUTHOR CONTRIBUTIONS

LV-K expert in the field of FH, aided in the diagnostic and therapeutic process, led the writing of the publication. SK constructed the family tree, provided technical support in the photo development and in writing the abstract. MG provided additional interpretation of genetic analyses data

and was responsible for the proofreading from medical genetics' standpoint. LC-B a pediatric cardiologist conducted the diagnostic tests, built the growth charts and monitored the pubescent development and treatment of the child. All authors have read and agreed to the published version of the manuscript.

ACKNOWLEDGMENTS

The case is part of a multidisciplinary project under the auspices of Medical University Plovdiv during the N14/2016 project year. With the much-appreciated help of Dr. Joep Defesche from the Department of Clinical Genetics, Academic Medical Center, Amsterdam, Netherlands, who performed the genetic analysis.

SUPPLEMENTARY MATERIAL

The Supplementary Material for this article can be found online at: https://www.frontiersin.org/articles/10.3389/fcvm.2021.743341/full#supplementary-material

Supplementary Figure 1 | BMI dynamics during the 5-year follow-up.

REFERENCES

1. Nordestgaard BG, Chapman MJ, Humphries SE, Ginsberg HN, Masana L, Descamps OS et al. Familial hypercholesterolaemia is underdiagnosed and undertreated in the general population: guidance for clinicians to prevent coronary heart disease: Consensus Statement of the European Atherosclerosis Society. *Eur Heart J.* (2013) 34:3478–90a. doi: 10.1093/eurheartj/eht273
2. Adam MP, Ardinger HH, Pagon RA, Wallace SE, Bean LJH, Mirzaa G, et al. *GeneReviews.* University of Washington, Seattle (1993). p. 202. Available online at: https://www.ncbi.nlm.nih.gov/books/NBK174884/.
3. Cuchel M, Bruckert E, Ginsberg HN, Raal FJ, Santos RD, Hegele RA, et al. Homozygous familial hypercholesterolaemia: new insights and guidance for clinicians to improve detection and clinical management. A position paper from the Consensus Panel on Familial Hypercholesterolaemia of the European Atherosclerosis Society. *Eur Heart J.* (2014) 35:2146–57. doi: 10.1093/eurheartj/ehu274
4. Wiegman A, Gidding SS, Watts GF, Chapman MJ, Ginsberg HN, Cuchel M, et al. Familial hypercholesterolaemia in children and adolescents: gaining decades of life by optimizing detection and treatment. *Eur Heart J.* (2015) 36:2425–37. doi: 10.1093/eurheartj/ehv157
5. Maliachova O, Stabouli S. Familial hypercholesterolemia in children and adolescents: diagnosis and treatment. *Curr Pharm Des.* (2018) 24:3672–7. doi: 10.2174/1381612824666181010145807
6. National Organization for Rare Disorders. *The Physician's Guide to Homozygous Familial Hypercholesterolemia* (HoFH) (2014). Available online at: https://www.rarediseases.org/for-patients-and-families/information-resources/physician-guides/homozygous-familial-hypercholesterolemia
7. Catapano AL, Graham I, De Backer G, Wiklund O, Chapman MJ, Drexel H, et al. 2016 ESC/EAS Guidelines for the management of Dyslipidaemias. New ESC Scientific Document Group. *Eur Heart J.* (2016) 37:2999–3058. doi: 10.1093/eurheartj/ehw272
8. Marais AD, Raal FJ, Stein EA, Rader DJ, Blasetto J, Palmer M, et al. A dose-titration and comparative study of rosuvastatin and atorvastatin in patients with homozygous familial hypercholesterolaemia. *Atherosclerosis.* (2008) 197:400–6. doi: 10.1016/j.atherosclerosis.2007.06.028
9. Stefanutti C, Julius U. Lipoprotein apheresis: state of the art and novelties. *Atherosclerosis Suppl.* (2013) 14:19–27. doi: 10.1016/j.atherosclerosissup.2012.10.021
10. Rader DJ, Kastelein JJ. Lomitapide and mipomersen: two first-in-class drugs for reducing low-density lipoprotein cholesterol in patients with homozygous familial hypercholesterolemia. *Circulation.* (2014) 129:1022–32. doi: 10.1161/CIRCULATIONAHA.113.001292
11. Marduel M, Carrié A, Sassolas A, Devillers M, Carreau V, Di Filippo M, et al. Molecular spectrum of autosomal dominant hypercholesterolemia in France. *Hum Mutat.* (2010) 31:E1811–24. doi: 10.1002/humu.21348
12. Stein EA, Honarpour N, Wasserman SM, Xu F, Scott R, Raal FJ. Effect of the proprotein convertase subtilisin/kexin 9 monoclonal antibody, AMG 145, in homozygous familial hypercholesterolemia. *Circulation.* (2013) 128:2113–20. doi: 10.1161/CIRCULATIONAHA.113.004678
13. Malik J, Shabeer H, Ishaq U, Chauhan HS, Akhtar HF.Modern Lipid management: a literature review. *Cureus.* (2020) 12:e9375. doi: 10.7759/cureus.9375
14. Santos RD, Ruzza A, Hovingh GK, Wiegman A, Mach F, Kurtz CE, et al. Evolocumab in pediatric heterozygous familial hypercholesterolemia. *N Engl J Med.* (2019) 383:1317–27. doi: 10.1056/NEJMoa2019910
15. Hartgers ML, Defesche JC, Langslet G, Hopkins PN, Kastelein JJP, Baccara-Dinet MT,et al. Alirocumab efficacy in patients with double heterozygous, compound heterozygous, or homozygous familial hypercholesterolemia. *J Clin Lipidol.* (2018) 12:390–6.e8. doi: 10.1016/j.jacl.2017.12.008
16. Raal FJ, Honarpour N, Blom DJ, Hovingh GK, Xu F, Scott R, et al. Inhibition of PCSK9 with evolocumab in homozygous familial hypercholesterolaemia (TESLA Part B): a randomised, double-blind, placebo-controlled trial, for the TESLA Investigators. *Lancet.* (2015) 385:341–50. doi: 10.1016/S0140-6736(14)61374-X
17. Zawacki AW, Dodge A, Woo KM, Ralphe JC, Peterson AL. In pediatric familial hypercholesterolemia, lipoprotein (a) is more predictive than LDL-C for early onset of cardiovascular disease in family members. *J Clin Lipidol.* (2018) 12:1445–51. doi: 10.1016/j.jacl.2018.07.014
18. Buonuomo PS, Mastrogiorgio G, Carletti M, Rana I, Macchiaiolo M, Gonfiantini MV, et al. New insights into the role of lipoprotein (a) as predictor of early onset of cardiovascular disease in pediatric familial hypercholesterolemia (FH). *Pediatr Cardiol.* (2020) 41:1242–3. doi: 10.1007/s00246-020-02392-1
19. Gaudet D, Kereiakes DJ, Mckenney JM, Roth EM, Hanotin C, Gipe D, et al.: Effect of alirocumab, a monoclonal proprotein convertase subtilisin/kexin 9 antibody, on lipoprotein (a) concentrations (a pooled analysis of 150 mg every two weeks dosing from phase 2 trials). *Am J Cardiol.* (2014) 114:711–5. doi: 10.1016/j.amjcard.2014.05.060
20. Raal FJ, Giugliano RP, Sabatine MS, Koren MJ, Langslet G, Bays H, et al. Reduction in lipoprotein (a) with PCSK9 monoclonal antibody evolocumab (AMG 145): a pooled analysis of more than 1,300 patients in 4 phase II trials. *J Am College Cardiol.* (2014) 63:1278–88. doi: 10.1016/j.jacc.2014.01.006
21. cCormick SPA, Schneider WJ. Lipoprotein(a) catabolism: a case of multiple receptors. *Pathology.* (2019) 51:155–64. doi: 10.1016/j.pathol.2018.11.003
22. Stoekenbroek R, Ray K, Landmesser U. Leiter LA, Wright RS, Wijngaard PL et al. Inclisiran-mediated reductions in Lp (a) in the ORION-1 trial. *Eur Heart J.* (2019) 40 (Suppl.):3021. doi: 10.1093/eurheartj/ehz746.0015
23. Vuorio A, Watts GF, Schneider WJ, Tsimikas S, Kovanen PT. Familial hypercholesterolemia and elevated lipoprotein(a): double heritable risk and new therapeutic opportunities. *J Intern Med.* (2020) 287:2–18. doi: 10.1111/joim.12981
24. Loi M, Branchford B, Kim J, Self C, Nuss R. COVID-19 anticoagulation recommendations in children. *Pediatr Blood Cancer.* (2020) 67:e28485. doi: 10.1002/pbc.28485
25. Libby P, Lüscher T. COVID-19 is, in the end, an endothelial disease. *Eur Heart J.* (2020) 41:3038–44. doi: 10.1093/eurheartj/ehaa623
26. Vuorio A, Kuoppala J, Kovanen PT, Humphries SE, Tonstad S, Wiegman A, et al. Statins for children with familial

hypercholesterolemia. *Cochrane Database Syst Rev*. (2019) 2019:CD006401. doi: 10.1002/14651858.CD006401.pub5
27. Ingueneau C, Hollstein T, Grenkowitz T, Ruidavets JB, Kassner U, Duparc T, et al. Treatment with PCSK9 inhibitors induces a more anti-atherogenic HDL lipid profile in patients at high cardiovascular risk. *Vascul Pharmacol*. (2020) 135:106804. doi: 10.1016/j.vph.2020.106804
28. Lassale C, Hamer M, Hernáez Á, Gale CR, Batty GD. Association of pre-pandemic high-density lipoprotein cholesterol with risk of COVID-19 hospitalisation and death: the UK Biobank cohort study. *medRxiv*. (2021) 26:2021.01.20.21250152. doi: 10.1101/2021.01.20.21250152
29. Wang G, Zhang Q, Zhao X, Dong H, Wu C, Wu F, et al. Low high-density lipoprotein level is correlated with the severity of COVID-19 patients: an observational study. *Lipids Health Disease*. (2020) 19:204. doi: 10.1186/s12944-020-01382-9
30. Gagnier JJ, Kienle G, Altman DG, Moher D, Sox H, Riley D. The CARE guidelines: consensus-based clinical case reporting guideline development. *BMJ Case Rep*. (2013) 110:603–8. doi: 10.3238/arztebl.2013.0603

Conflict of Interest: The authors declare that the research was conducted in the absence of any commercial or financial relationships that could be construed as a potential conflict of interest.

frontiers in Cardiovascular Medicine

ORIGINAL RESEARCH
published: 28 February 2022
doi: 10.3389/fcvm.2022.839720

Differential Biological Effects of Dietary Lipids and Irradiation on the Aorta, Aortic Valve, and the Mitral Valve

Nathalie Donis[1], Zheshen Jiang[1], Céline D'Emal[1], Alexia Hulin[1], Margaux Debuisson[1], Raluca Dulgheru[1], Mai-Linh Nguyen[1], Adriana Postolache[1], François Lallemand[2], Philippe Coucke[2], Philippe Martinive[3], Marielle Herzog[4], Dorian Pamart[4], Jason Terrell[5,6], Joel Pincemail[7], Pierre Drion[8], Philippe Delvenne[9,10], Alain Nchimi[1], Patrizio Lancellotti[1,11,12†] and Cécile Oury[1*†]*

[1] Laboratory of Cardiology, Department of Cardiology, GIGA Institute, University of Liège Hospital, CHU Sart Tilman, Liège, Belgium, [2] Department of Radiotherapy, CHU of Liège, Liège, Belgium, [3] Department Radiation Oncology, Institut Jules Bordet, Université Libre Bruxelles, Brussels, Belgium, [4] Belgian Volition Société à Responsabilité Limitée, Gembloux, Belgium, [5] Department of Oncology and Livestrong Cancer Institutes, Dell Medical School, University of Texas at Austin, Austin, TX, United States, [6] Volition America, Austin, TX, United States, [7] Clinical Chemistry, CHU of Liège, Liège, Belgium, [8] Experimental Surgery Unit, Centre de Recherche du Département de Chrirurgie, Groupe Interdisciplinaire de Géno-Protéomique Appliquée Institute, University of Liège, Liège, Belgium, [9] Department of Pathology, Centre Hospitalier Universitaire of Liège, Liège, Belgium, [10] Laboratory of Experimental Pathology, GIGA Institute, University of Liège, Liège, Belgium, [11] Gruppo Villa Maria Care and Research, Maria Cecilia Hospital, Cotignola, Italy, [12] Anthea Hospital, Bari, Italy

Aims: Dietary cholesterol and palmitic acid are risk factors for cardiovascular diseases (CVDs) affecting the arteries and the heart valves. The ionizing radiation that is frequently used as an anticancer treatment promotes CVD. The specific pathophysiology of these distinct disease manifestations is poorly understood. We, therefore, studied the biological effects of these dietary lipids and their cardiac irradiation on the arteries and the heart valves in the rabbit models of CVD.

Methods and Results: Cholesterol-enriched diet led to the thickening of the aortic wall and the aortic valve leaflets, immune cell infiltration in the aorta, mitral and aortic valves, as well as aortic valve calcification. Numerous cells expressing α-smooth muscle actin were detected in both the mitral and aortic valves. Lard-enriched diet induced massive aorta and aortic valve calcification, with no detectable immune cell infiltration. The addition of cardiac irradiation to the cholesterol diet yielded more calcification and more immune cell infiltrates in the atheroma and the aortic valve than cholesterol alone. RNA sequencing (RNAseq) analyses of aorta and heart valves revealed that a cholesterol-enriched diet mainly triggered inflammation-related biological processes in the aorta, aortic and mitral valves, which was further enhanced by cardiac irradiation. Lard-enriched diet rather affected calcification- and muscle-related processes in the aorta and aortic valve, respectively. Neutrophil count and systemic levels of platelet factor 4 and ent-8-iso-15(S)-PGF2α were identified as early biomarkers of cholesterol-induced tissue alterations, while cardiac irradiation resulted in elevated levels of circulating nucleosomes.

OPEN ACCESS

Edited by:
Xuewei Zhu,
Wake Forest Baptist Medical Center, United States

Reviewed by:
Zhenquan Jia,
University of North Carolina at Greensboro, United States
Genesio Karere,
Wake Forest School of Medicine, United States

***Correspondence:**
Patrizio Lancellotti
plancellotti@chuliege.be
Cécile Oury
cecile.oury@uliege.be

† These authors have contributed equally to this work and share last authorship

Specialty section:
This article was submitted to Lipids in Cardiovascular Disease, a section of the journal Frontiers in Cardiovascular Medicine

Received: *20 December 2021*
Accepted: *24 January 2022*
Published: *28 February 2022*

Citation:
Donis N, Jiang Z, D'Emal C, Hulin A, Debuisson M, Dulgheru R, Nguyen M-L, Postolache A, Lallemand F, Coucke P, Martinive P, Herzog M, Pamart D, Terrell J, Pincemail J, Drion P, Delvenne P, Nchimi A, Lancellotti P and Oury C (2022) Differential Biological Effects of Dietary Lipids and Irradiation on the Aorta, Aortic Valve, and the Mitral Valve. Front. Cardiovasc. Med. 9:839720. doi: 10.3389/fcvm.2022.839720

Conclusion: Dietary cholesterol, palmitic acid, and cardiac irradiation combined with a cholesterol-rich diet led to the development of distinct vascular and valvular lesions and changes in the circulating biomarkers. Hence, our study highlights unprecedented specificities related to common risk factors that underlie CVD.

Keywords: cholesterol, palmitic acid, cardiovascular diseases, arteries, heart valves, dietary lipids

INTRODUCTION

Heart diseases are a major health burden worldwide. Coronary artery disease (CAD) is the most prevalent heart disease characterized by the build-up of atherosclerotic plaques in the artery walls, which are responsible for myocardial infarction and stroke, the two leading causes of death (1). Atherosclerosis is a chronic, progressive process that remains asymptomatic for years, making it difficult to diagnose at the early stage. Consequently, atherosclerosis is most often diagnosed following an acute event. Among a population considered at low or intermediate risk of CAD, a study showed that almost 50% of patients had at least one stenotic vascular segment and more than 25% had multiple stenotic segments (2). Percutaneous coronary intervention with stent placement is recommended as the first therapy when available promptly. Afterward, chronic preventive pharmacotherapies are used to reduce the risk of future acute events. The prevalence of atherosclerotic diseases has kept increasing in the last decade, revealing the need to identify new early diagnostic tools, preventive measures, and therapeutic targets.

Valvular heart diseases (VHDs), including calcific aortic valve disease (CAVD) and degenerative mitral valve disease, are other prevalent heart diseases of the aging population (3). These cardiovascular diseases progress very slowly before the onset of the symptom. Hitherto, no pharmacotherapy exists to cure or effectively prevent VHD progression, and valve repair or replacement is the only treatment when a heart valve defect is diagnosed. Although valvular calcification and degeneration are considered active phenomena, the biological mechanisms underlying the VHD remain poorly understood.

While dyslipidemia (lifelong exposure to high cholesterol) is a well-established risk factor for atherosclerosis and CAVD (4–6), statins effectively reduce vascular atherosclerotic diseases (7, 8), but they showed no positive effect on severe CAVD (9, 10). Proprotein convertase subtilisin/kexin type 9 inhibitors are a more recent type of cholesterol-lowering drug with beneficial effects in atherosclerosis (11–13). *In vitro* data showed promising results with these inhibitors on CAVD (14). With regard to mitral valve disease, no studies have ever described a link between dyslipidemia and mitral valve degeneration.

Dietary habits and fatty acid intake are other, less-studied risk factors for heart diseases (15). Fatty acids have different impacts on cardiovascular risk, depending on their saturation degree and C-chain length. For instance, palmitic acid, a main fat component of lard, has been shown to have a deleterious effect on CAD (16). Particularly, our recent study in rabbits indicates that dietary palmitic acid can promote both arterial calcification and CAVD (17).

Beyond dietary fats, radiation therapy to the chest, as a critical component of the treatment regimen of Hodgkin lymphoma, the lung and breast cancer, can also increase the risk of death from cardiac-related causes (18–20). Radiation-induced heart disease (RIHD) is a heterogeneous disease associated with many cardiac manifestations, including CAD and left-sided heart valve diseases (21). The RIHD is a specific entity and the mechanisms underlying its pathogenesis are currently unclear.

This study aimed at evaluating and comparing the impact of the following: (1) two dietary fats, enriched with either cholesterol or lard, as a source of palmitic acid; (2) irradiation in combination with a cholesterol-rich diet, on the aorta and four heart valves. We also examined the interconnexion between circulating biomarkers related to inflammation, oxidative stress, platelet activation, and calcification.

MATERIALS AND METHODS

Ethics Statement and Animal Model

All rabbit experiments conform to the European Union guidelines for the care and use of laboratory animals and were approved by the Animal Ethical Committee of the University of Liège (file number 1951). Seventy-three eight-week-old male New Zealand White rabbits (1.83 ± 0.14 Kg) were purchased from the Charles River, France. The animals were kept in a temperature and humidity-controlled environment in an air-conditioned room with a standard rabbit chow and tap water *ad libitum*. After 2 weeks of acclimation, the rabbits were randomly assigned to seven different groups and diet habituation was conducted for 2 weeks. Protocols started when the rabbits were 12 weeks old and it lasted 16 weeks. Control group (Ctrl, $n = 13$) received a standard chow diet. Vitamin D2 group (Vit.D2, $n = 7$) received a chow diet with 15 days of Vitamin D2 supplementation (ergocalciferol, Sigma-Aldrich) in drinking water at the beginning of the protocol (25,000 U/day/2.5 Kg). The cholesterol-enriched diet group (CHT, n = 17) was treated with 0.3% of the cholesterol-enriched diet and received vitamin D2 (Vit.D2) supplementation as the Vit.D2 group. The lard-enriched

Abbreviations: Ao, aorta; AoV, aortic valve; α-SMA, α-smooth muscle actin; CAD, coronary artery disease; CAVD, calcific aortic valve disease; CVD, cardiovascular disease; DKK1, Dickkopf WNT Signaling Pathway Inhibitor 1; CHT, cholesterol; CT, computed tomography; Ctrl, control; DEG, differentially expressed genes; ECM, extracellular matrix; GAG, glycosaminoglycan; HDL, high-density lipoprotein; IR, irradiation; LDL, low-density lipoprotein; MV, mitral valve; NET, neutrophil extracellular trap; PF4, platelet factor 4; PGF2α, prostaglandin F2α; RIHD, radiation-induced heart disease; VHD, valvular heart disease; Vit.D2, Vitamin D2; Wnt, Wingless Integration site.

diet group (Lard, n =13) received 5% of the lard-enriched diet (17) with Vit.D2 supplementation. Irradiation group (IR, n = 7) received a chow diet and underwent X-ray cardiac irradiation focused on the aortic valve and the thoracic aorta during the first week of the protocol (24Gy dose divided into 3 fractions of 8Gy delivered at 48-h intervals, chosen to mimic clinically relevant doses used for anticancer radiotherapy) using image-guided radiation on an irradiator specifically made for small animals (X-Rad 225Cx, Precision X-Ray, Inc.). Irradiation combined with cholesterol-enriched diet group (IR/CHT, $n = 15$) received 0.3% of cholesterol-enriched diet plus Vit.D2 supplementation and underwent cardiac irradiation at mid protocol (e.g., after 8 weeks of cholesterol-rich diet). Cholesterol- and lard-enriched diets were produced by Safe (France). Bodyweight was measured on a weekly basis. Blood draws and cardiac CT (X-Rad 225Cx, Precision X-Ray, Inc.) were performed at baseline and at the end of every four weeks (W4, W8, W12, and W16), and aortic wall calcification was visually assessed as absent or present in each of the following segments: ascending aorta, aortic cross, and the descending aorta. An extra blood draw was performed at W2. Anesthesia was induced prior to any procedure (except for body weight measurements) by intramuscular injections of droperidol (0.625 mg/kg), xylazine (5 mg/kg), and ketamine (35 mg/kg) in the hind legs. Euthanasia was conducted in the anesthetized animals by intracardiac injection of pentobarbital (200 mg/kg).

Histological and Immunofluorescence Analyses of Rabbit Heart

Hearts were harvested, weighed, and fixed in 4% of paraformaldehyde–phosphate-buffered saline (PBS) solution for 24 h before dehydration into 70% of ethanol solution overnight at room temperature (Ctrl: $n = 6$, Vit.D2: $n = 7$, CHT: $n = 11$, Lard: $n = 6$, IR: $n = 7$, IR/CHT: $n = 7$). They were then embedded in paraffin wax and sectioned at 7 μm. Before histological and immunofluorescence analyses, the sections were incubated overnight at 58°C and rehydrated through xylene baths followed by a series of graded ethanol baths. Serial sections were used for the histological assessment of tissue structure on hematoxylin-eosin-stained sections, tissue calcification on alizarin red stained section, and extracellular matrix (ECM) composition on sirius red and Movat's pentachrome-strained sections. The aortic valve area was evaluated by isolating the aortic valve leaflets and measuring their area on multiple serial hematoxylin-eosin-stained sections (4 to 9 per rabbit) by using Adobe Photoshop software. For the immunofluorescence study, the sections were incubated overnight at 58°C prior to chemical rehydration. All sections were treated for 30 min at 96°C with Dako Target Retrieval solution, pH9 (Agilent, S2367) for antigen retrieval, then incubated for 30 min at room temperature with normal goat serum (Abcam, ab7481). Co-staining was conducted by sequential use of monoclonal mouse anti-rabbit RAM-11 primary antibody (Agilent, M0633, 1:50 dilution), TRITC-conjugated goat anti-mouse secondary antibody (Abcam, ab5885, 1:100 dilution), and AlexaFluor 488-conjugated monoclonal mouse anti-alpha smooth muscle actin (αSMA) antibody (ThermoFisher Scientific, #53-9760-82, 1:100 dilution). Nuclei were stained with 4′, 6-diamidino-2-phenylindole (DAPI) (ThermoFisher Scientific, D1306, 1:500,000 dilution). Negative controls corresponding to TRITC-conjugated goat anti-mouse secondary antibody without anti-RAM-11 primary antibody and AF488-conjugated mouse IgG2a kappa isotype control isotype were performed (**Supplementary Figure S1**). QuPath 0.2.3 software was used to analyze fluorescence staining in the delimitated aortic valve, the mitral valve, and the aorta area. Pixel classifiers were first defined to set a threshold value for each fluorochrome. A script was then applied in batch to automatically count the cell number, mean fluorescence intensities as well as the total tissue area, and the percentages of positive area for each immunostaining.

RNAseq Analysis

Aorta ring and heart valves were dissected (Ctrl: $n = 7$, CHT: $n = 6$, Lard: $n = 7$, IR/CHT: $n = 7$) at the end of the 16-week protocols, snap frozen in liquid nitrogen, and stored at −80°C until RNA extraction. Total RNA was extracted by the use of miRNeasy Mini Kit (Qiagen) according to the manufacturer's instructions. The integrity of the RNA sample was assessed on a Bioanalyser 2,100 with RNA 6,000 Nano and RNA 6,000 Pico chips (Agilent Technologies). The RNA libraries were prepared with 10 ng of RNA using the SMARTer® Stranded Total RNA-Seq Kit v2 - Pico Input Mammalian (Takara Bio USA, Inc.) according to the manufacturer's instructions. The RNA quantification and normalization were performed with the KAPA Library Quantification kit (comprising P5-P7 primers) on the ABI 7900HT system (ThermoFisher Scientific). Sequencing of the libraries was performed on a NovaSeq6000 System (Illumina) with an S4 reagent kit (300 cycles) and 1.2 nM library loading.

Paired FastQ files for all the samples were assessed for Quality Control using FastQC and then they were processed through nf-core rnaseq pipeline v1.4.2 (https://nf-co.re/rnaseq/1.4.2), with default parameters except for -clip_R2 = 3 and -nextseq-trim = 10, in order to perform mapping, quantification, and QC, and to produce the gene count matrix. The reference genome used was Oryctolagus cuniculus OryCun2.0 with annotation from Ensembl release 99 (http://jan2020.archive.ensembl.org/index.html). Gene counts were normalized by the default method (median of ratios) in the DESeq2 package (22). Gene expressions in each diet or treatment group were compared to the control group by DESeq2; a total of 29,587 tests were performed for each comparison and were followed by Benjamini and Hochberg multiple test correction. An adjusted p-value (FDR) less than 0.05 and a fold-change greater than 1.5 were used to highlight a significant difference in gene expression between the two groups. Human orthologs of differentially expressed genes (DEGs) were identified by the online tool, Better Bunny (23) with an identity of 50% as a threshold (24), and were ranked by their π-value calculated with a log-fold change (LFC) and the adjusted p-value (25). TopGO package was used to perform gene ontology (GO) analysis with a ranked gene list. The whole RNA-seq analysis was performed in R (version 4.0.4; R Foundation for Statistical Computing, Vienna, Austria).

Blood Processing

At each blood draw, differential blood cell counts (white blood cells, red blood cell indices, and platelets) were measured in 3.8% of citrated whole blood on a Cell-Dyn 3700 hematocytometer equipped with veterinary software (Abbott Laboratories). Serum aliquots were prepared after 30-min resting to allow for blood clotting followed by centrifugation at 1,700 *g* and room temperature. EDTA and 3.8% citrated plasma aliquots were prepared by two successive centrifugations at 1,700 *g* and room temperature maximum of 1 h after blood draw. Serum and plasma samples were stored at −80°C until further analysis.

Biomarker Measurements

Measurements of the levels of total cholesterol, triglycerides, LDL-c, HDL-c, calcium, phosphorous, iron, albumin, AST, ALT, creatinine, and urea were performed in serum samples on an AU480 Chemistry Analyzer (Beckman Coulter). Serum levels of IL-6 and plasma [ethylenediamine tetraacetic acid (EDTA)-anticoagulated plasma] levels of DKK1 and PF4 were measured by enzyme-linked immunosorbent assays according to the manufacturer's recommendations (Cusabio). The ent-8-iso-15(S)-PGF2α levels were measured in EDTA-plasma by the ultra-high performance liquid chromatography coupled to tandem mass spectrometry detection. Levels of circulating H3.1-nucleosomes and citrullinated histone H3R8 nucleosomes (H3R8cit-nucleosome), an epigenetic modification, were assessed by blinded Nu.Q® chemiluminescence immunoassays (Volition SRL, Belgium) in EDTA-plasma (Ctrl: $n = 7$–13, Vit.D2: $n = 7$, CHT: $n = 10$–15, Lard: $n = 7$–12, IR: $n = 7$, IR/CHT: $n = 15$).

Statistical Analysis

Between-treatment comparisons of all variables were performed by ANOVA and *post-hoc* Dunnett test on log transformed data, except for leaflet area quantification, nested GLM model, and *post-hoc* SIDAK tests were performed. Over time changes between two time points in the blood cells and circulating biomarkers were assessed by Wilcoxon signed-rank test. Data are presented as median [interquartile range (p25–p75)]. All tests were performed 2-sided and $P\text{-}value \leq 0.05$ was considered significant. All statistical analyses were performed using SAS 9.4 (SAS Institute, Cary NC).

RESULTS

Dietary Cholesterol and Palmitic Acid Induce Distinct Histological Lesions in the Aorta, Aortic Valve, and Mitral Valve

Rabbits fed for 16 weeks with lard- or cholesterol-enriched diets supplemented with Vit.D2 displayed aortic wall structural alterations that were not observed in rabbits fed with chow diet, or in those receiving the chow diet supplemented with Vit.D2 (**Figure 1A**). Alizarin red staining of heart sections from rabbits treated with a lard-enriched diet revealed massive media calcification with collagen fiber accumulation and disorganization around the calcific lesions as shown by Sirius Red and Movat's Pentachrome staining. The CT imaging revealed aortic wall calcifications in 70 to 80% of rabbits fed with lard depending on considered aorta segments (**Figure 1B**). Such macrocalcifications were not observed in Ctrl or Vit.D2 groups, except for one rabbit treated with Vit.D2 which developed calcification in the aortic cross.

In agreement with previous studies (26), rabbits fed for 16 weeks with a cholesterol-enriched diet developed atherosclerotic lesions. Hematoxylin-eosin staining of aortic sections showed intima thickening with cell and lipid infiltration, whereas Sirius Red and Movat's Pentachrome showed disorganized ECM component deposition (collagen fibers and glycosaminoglycans, GAGs). Alizarin red staining revealed calcification nodules at the intima-media junction and diffuse microcalcifications in the thickened intima. Approximately 35% of rabbits fed with a cholesterol-enriched diet displayed calcifications detected by a CT (**Figure 1B**). We also assessed the infiltration of the aortic wall by macrophages (or macrophage-like cells) by immunodetection of the rabbit RAM-11 marker (27). As described (28), a cholesterol-enriched diet-induced significant infiltration of RAM-11 positive cells in atheroma as compared to Vit.D2 alone (**Figure 4C**).

Alterations of the aortic valve structure were observed in the two diet groups (**Figure 2A**). In the cholesterol group, the aortic valve leaflets were significantly thickened with sparse calcification spots, cell infiltration and accumulation of collagen fibers, and GAGs (**Figures 2A,B**). Immunostaining of RAM-11 and of the muscle-specific αSMA marker revealed significant macrophage infiltration and few αSMA positive cells, both located in valvular ventricularis (**Figure 3**). In contrast, rabbits fed with a lard-enriched diet displayed calcific nodules in the aortic valve with only slight leaflet thickening compared to cholesterol (**Figure 2**) and no detectable RAM-11 or αSMA positive cells (**Figure 4**). No aortic valve alteration was observed in the chow diet and Vit.D2 groups.

The mitral valve was also affected in the cholesterol-enriched diet group (**Figure 3**), with cellular infiltrates and ECM remodeling in spongiosa, without leaflet thickening. The signal for RAM-11 positive cells was significantly increased as compared to the control and Vit.D2 groups (**Figure 4C**). As for the aortic valve, only few αSMA positive cells were observed in mitral valves. Rabbits from the chow diet, Vit.D2, and lard groups did not show any visible modification of the mitral valve structure.

None of the diets caused histological modifications of the tricuspid and pulmonary valves (data not shown).

Cardiac Irradiation Promotes Cell Infiltration in the Aorta, Aortic Valve, and Mitral Valve

Our histological analyses did not reveal any aortic histological alterations when cardiac irradiation was applied in rabbits fed with a chow diet kept for 8 weeks post-irradiation (**Figure 1A**). However, rabbits fed for 16 weeks with a cholesterol-enriched diet and receiving cardiac irradiation at week 9 displayed more macrocalcification in the aorta than rabbits that were not irradiated. Calcification was detected by cardiac CT in all aortic segments in 40% of rabbits (**Figure 1B**). Also, the atherosclerotic

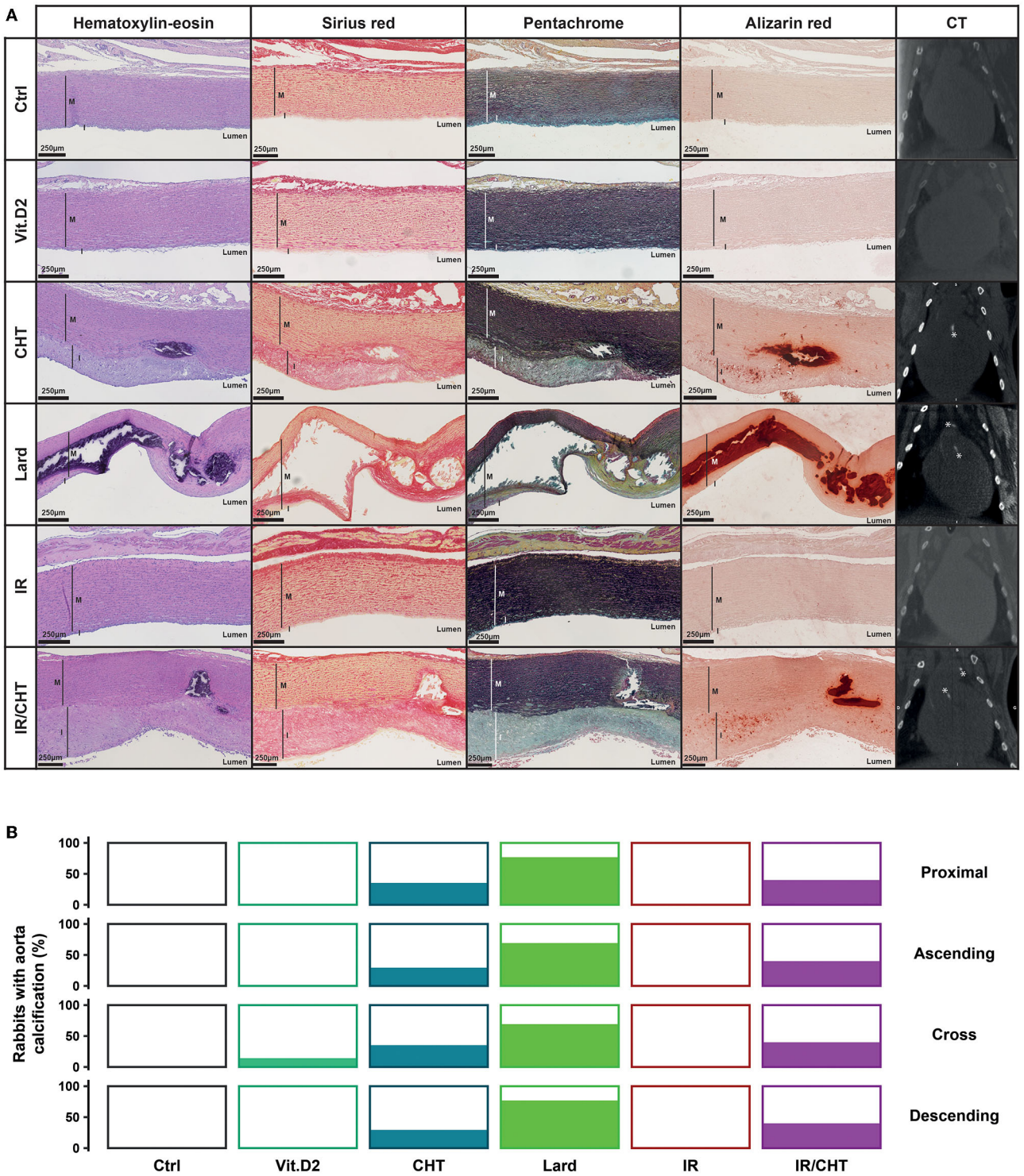

FIGURE 1 | Effect of lard- and cholesterol-enriched diets on the aorta structure. **(A)** Representative pictures of aortic wall sections stained with hematoxylin-eosin, sirius red, Movat's pentachrome, and alizarin red, and CT imaging per rabbit group as indicated. Scale bars = 250 µm. Calcifications observed by CT are indicated by asterisks. **(B)** Percentage of rabbits from each group that presented CT-detected calcification in the different portions of the aorta (Ctrl, $n = 13$; Vit.D2, $n = 7$; CHT, $n = 17$; Lard, $n = 13$; IR, $n = 7$; IR/CHT, $n = 15$). I, indicates intima; M, indicates media.

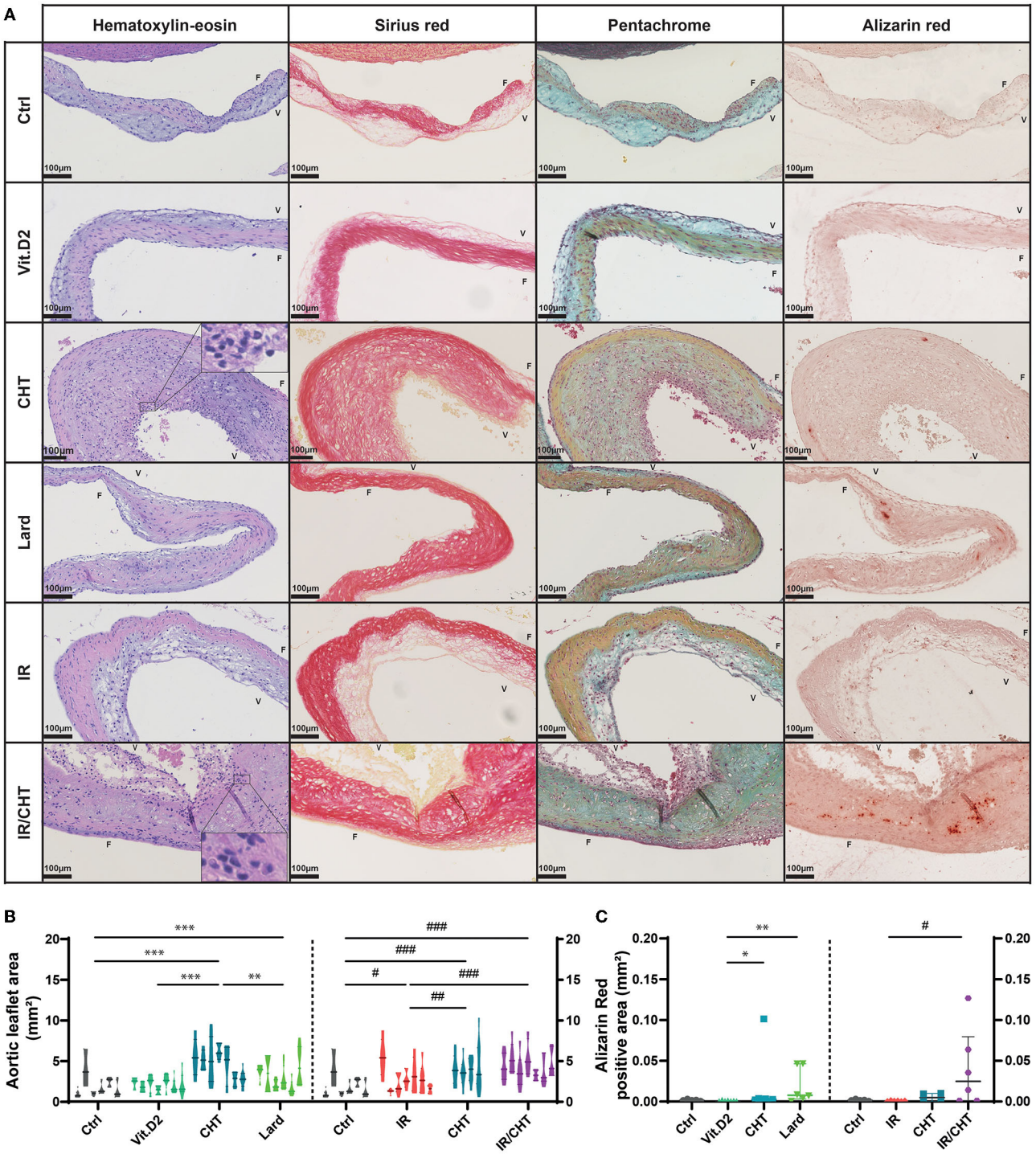

FIGURE 2 | Effect of lard- and cholesterol-enriched diets on the aortic valve leaflet histology. **(A)** Representative pictures of aortic valve leaflet sections stained with hematoxylin-eosin, sirius red, Movat's pentachrome, and alizarin red per rabbit group as indicated. Magnified areas depict neutrophil infiltrates in valvular ventricularis. Scale bars = 100 µm. **(B)** Violin plots represent aortic valve leaflet area measured on hematoxylin-eosin-stained aortic valve sections (each violin box represents one rabbit, 4–8 slides per rabbit). Four-group comparisons were performed by using a nested-GLM model and *post-hoc* SIDAK test on log-transformed data. **(C)** The graph represents the positive area for Alizarin Red staining on the aortic valve sections. Data are presented as medians with P25-P75 interquartiles. Four-group comparisons were performed by ANOVA and *post-hoc* Dunnett's test on log-transformed data (Left: Ctrl, $n = 5$; Vit.D2, $n = 7$; CHT, $n = 7$; Lard, $n = 6$; Right: Ctrl, $n = 5$; IR, $n = 6$; CHT, $n = 4$; IR/CHT, $n = 6$). $^{*}P \leq 0.05$; $^{**}P \leq 0.01$; $^{***}P \leq 0.001$; $^{\#}P \leq 0.05$; $^{\#\#}P \leq 0.01$; $^{\#\#\#}P \leq 0.001$. F, indicates fibrosa side; V, indicates ventricular side.

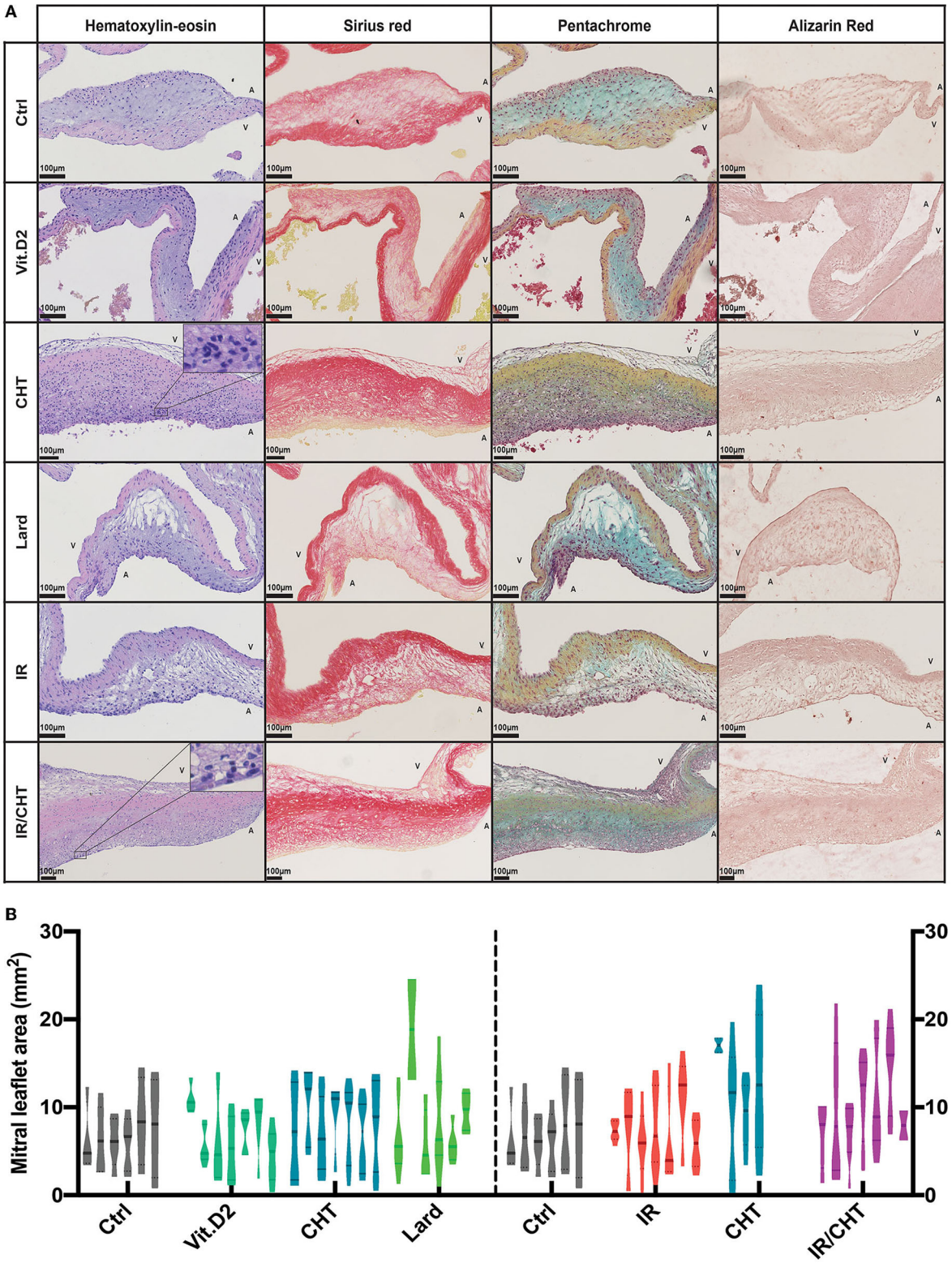

FIGURE 3 | Effect of cholesterol-enriched diets on the mitral valve leaflet histology. **(A)** Representative pictures of mitral valve leaflet sections stained with hematoxylin-eosin, sirius red, and Movat's pentachrome per rabbit group as indicated. Magnified areas depict neutrophil infiltrates in valvular atrialis. Scale bars = 100 µm. **(B)** Violin plots represent mitral valve leaflet area measured on the histological mitral valve sections (each violin box represents one rabbit, 4–8 slides per rabbit) stained with hematoxylin-eosin. Four-group comparisons were performed by using a nested-GLM model and *post-hoc* SIDAK test on log-transformed data. *P* = non-significant. A, indicates atrial side; V, indicates ventricular side.

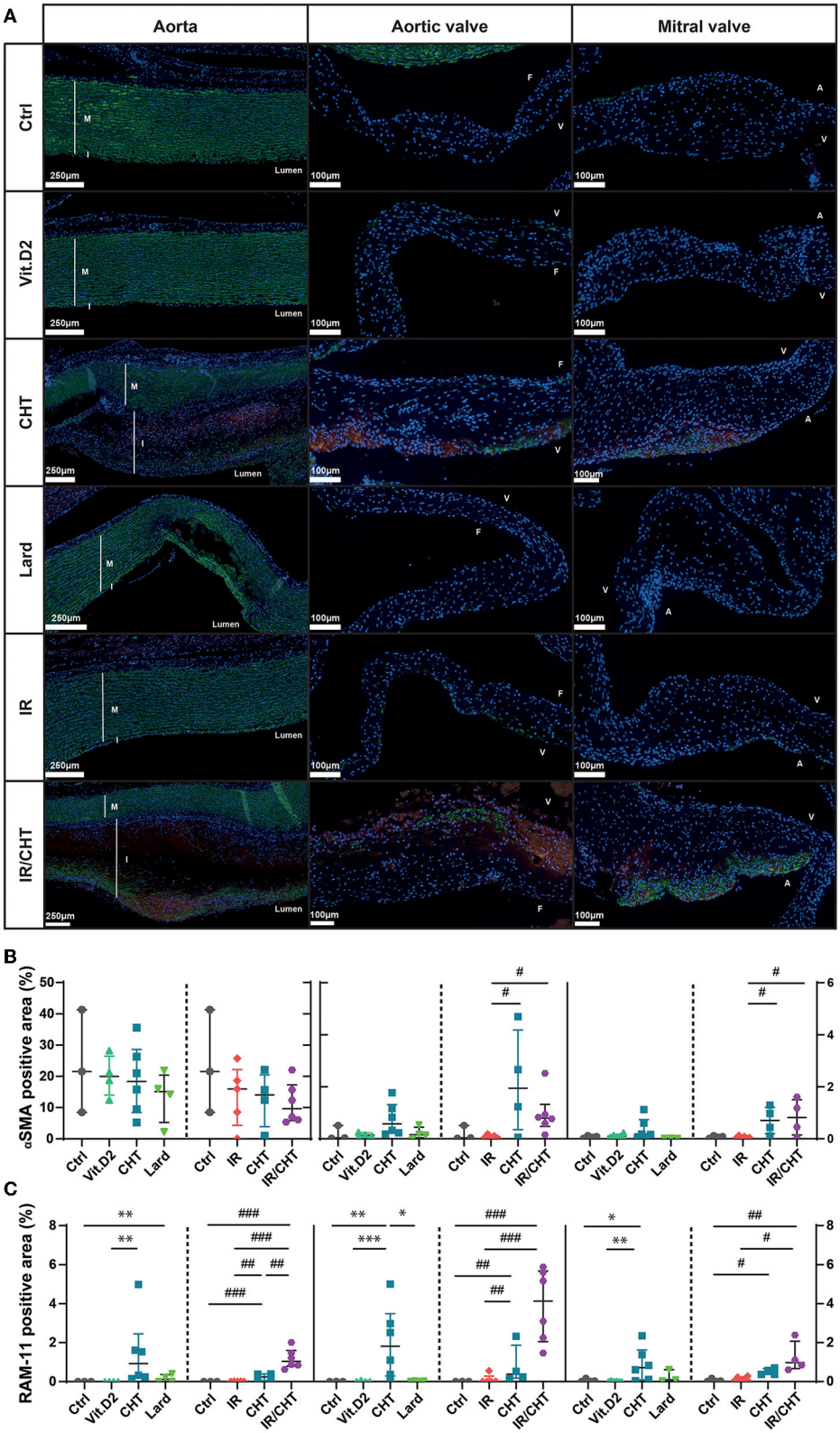

FIGURE 4 | Immuno-detection of RAM-11- and αSMA positive cells in the aorta and heart valves. **(A)** Representative pictures of RAM-11 and αSMA immunofluorescence costaining performed on the aorta, the aortic valve, and the mitral valve sections. Nuclei are stained with DAPI and appear in blue. αSMA- and

(Continued)

FIGURE 4 | RAM-11-positive cells are shown in green and red, respectively. Scale bars = 250 μm for aorta and 100 μm for the aortic and mitral valves. **(B)** Quantification of αSMA-positive cells in terms of fluorescence area percentage in the aorta (left), aortic valve (middle), and the mitral valve (right). **(C)** Quantification of RAM-11-positive cells in terms of fluorescence area percentage in the aorta (left), aortic valve (middle), and the mitral valve (right). Data are presented as median with P25–P75 interquartiles. Four-group comparisons were performed by ANOVA and *post-hoc* Dunnett's test on log-transformed data. Aorta: left: Ctrl, $n = 3$; Vit.D2, $n = 4$; CHT, $n = 6$; Lard, $n = 4$; right: Ctrl, $n = 3$; IR, $n = 5$; CHT, $n = 4$; IR/CHT, $n = 6$. Aortic valve: left: Ctrl, $n = 3$; Vit.D2, $n = 6$; CHT, $n = 6$; Lard, $n = 3$; right: Ctrl, $n = 3$; IR, $n = 5$; CHT, $n = 4$; IR/CHT, $n = 6$. Mitral valve: left: Ctrl, $n = 4$; Vit.D2, $n = 7$; CHT, $n = 7$; Lard, $n = 6$; right: Ctrl, $n = 4$; IR, $n = 6$; CHT, $n = 4$; IR/CHT, $n = 4$. $^{*}P \leq 0.05$; $^{**}P \leq 0.01$; $^{***}P \leq 0.001$; $^{\#}P \leq 0.05$; $^{\#\#}P \leq 0.01$; $^{\#\#\#}P \leq 0.001$. A, atrial side; F, fibrosa side; I, intima; M, media; V, ventricular side.

plaque core of rabbits that received cardiac irradiation combined with cholesterol diet significantly increased in the numbers of RAM-11 positive cells as compared to rabbits fed with a chow diet, a cholesterol diet without irradiation, and in rabbits that received irradiation whilst on chow diet (**Figures 4A,C**).

The addition of irradiation to the cholesterol-enriched diet induced the aortic valve structure alterations that were not observed in the irradiation-only group. Thickened aortic valve leaflets displayed more cellular infiltrates and RAM-11 positive cells than the control groups (**Figures 4A,C**). Aortic valves were more calcified than those of rabbits from the cholesterol group (**Figures 2A,B**).

As for mitral valves, the combination of irradiation with the cholesterol diet led to increased infiltration of RAM-11 positive cells as compared to the irradiation alone (**Figure 4C**).

Differential RNA Expression Profiles in the Aorta, Aortic Valve, and Mitral Valve in Response to Lard- and Cholesterol-Enriched Diets

To get insight into the biological mechanisms underlying vascular and valvular modifications, we then performed RNAseq experiments on RNA extracted from the dissected proximal aorta and all cardiac valves. The RNAseq identified 29.587 genes annotated in the rabbit genome, among which 15.135 genes could be assigned to human genes. The cholesterol-rich diet modified the expression of 1.102 (898 unique human orthologs) genes in the aorta, 612 (492) genes in the aortic valve, 281 (229) genes in the mitral valve, and only 4 (3) and 6 (6) genes in the tricuspid and pulmonary valve, respectively. The lard-rich diet yielded much less DEGs than the cholesterol-rich diet, comprising 76 (66) genes in the aorta and 40 (36) genes in the aortic valve. No DEGs were found in the three other cardiac valves in response to the lard diet.

We then assessed the impact of these changes in RNA expression on biological processes in each tissue. To detect the differential effects of each diet in every tissue, both tissue-specific and common DEGs were included in these analyses.

We first studied the effect of a cholesterol-rich diet on the aorta and aortic valve. Among the 612 DEGs identified in the aortic valve of rabbits from the cholesterol group, 443 DEGs were commonly affected in the aorta (**Figure 5A**, **Supplementary Tables S1–S3**). These common DEGs were involved in inflammatory and cellular defense responses, including the production of major inflammatory cytokines and neutrophil degranulation. Mitotic spindle organization was also affected, pointing to an effect on cell division. The 659 aorta-specific DEGs were enriched in genes contributing to additional effects on immune response and signaling pathways, positive regulation of cell migration, angiogenesis, and platelet degranulation, while the 169 aortic valve-specific DEGs were involved in cardiac muscle contraction, tissue morphogenesis, and myofibril assembly. These data indicate that inflammation likely contributes to aortic valve alterations induced by a cholesterol-rich diet similarly as in the aorta, but additional muscle-related processes could also be affected.

We next focused on the comparison between the aortic valve and mitral valve in the cholesterol-fed group. Whereas the DEGs commonly found in the mitral and aortic valves included genes involved in inflammation and cellular defense response, we surprisingly observed that the cholesterol-rich diet mainly affected lipid biosynthetic and metabolic processes as well as folic acid transport in the mitral valve (**Figure 5B**, **Supplementary Tables S4–S6**). This finding may thus reveal that not only inflammation but also key metabolic cellular processes underlie the mitral valve alterations in hypercholesterolemia.

We did not identify the genes that were commonly affected in the aorta and aortic valve by the lard-rich diet. The few DEGs that were found to be specific to the aortic valve were all involved in muscle-related processes, including contraction, filament sliding, and sarcomere organization (**Figure 5D**, **Supplementary Tables S7, S8**). Intriguingly, these processes were similarly found to be affected by the cholesterol-rich diet, suggesting that dietary cholesterol and palmitate could have a similar biological impact on the aortic valve. In contrast, in the aorta, ECM organization, osteoblast differentiation, and ossification processes were more prevalent in response to lard than cholesterol. Of interest, inflammation would not be the main process induced by the lard diet, which is in sharp contrast to the cholesterol diet.

Cardiac Irradiation Enhances Changes in the Expression of Inflammation-Related Genes

The addition of irradiation to a cholesterol-rich diet significantly increased the numbers of DEGs both in the aorta and the aortic valve. This was particularly true for the aortic valve. Indeed, 2,097 (1714) and 3,474 (2715) DEGs were identified in the aorta and aortic valve, respectively, which indicated that the aortic valve might be more impacted than the aorta following irradiation. The addition of irradiation to the cholesterol-rich diet modified the expression of 15 (12) additional genes in the aorta and 602 (512) genes in the aortic valve as compared to cholesterol without irradiation. Interestingly, we observed that the common DEGs identified both in the aorta and aortic valve

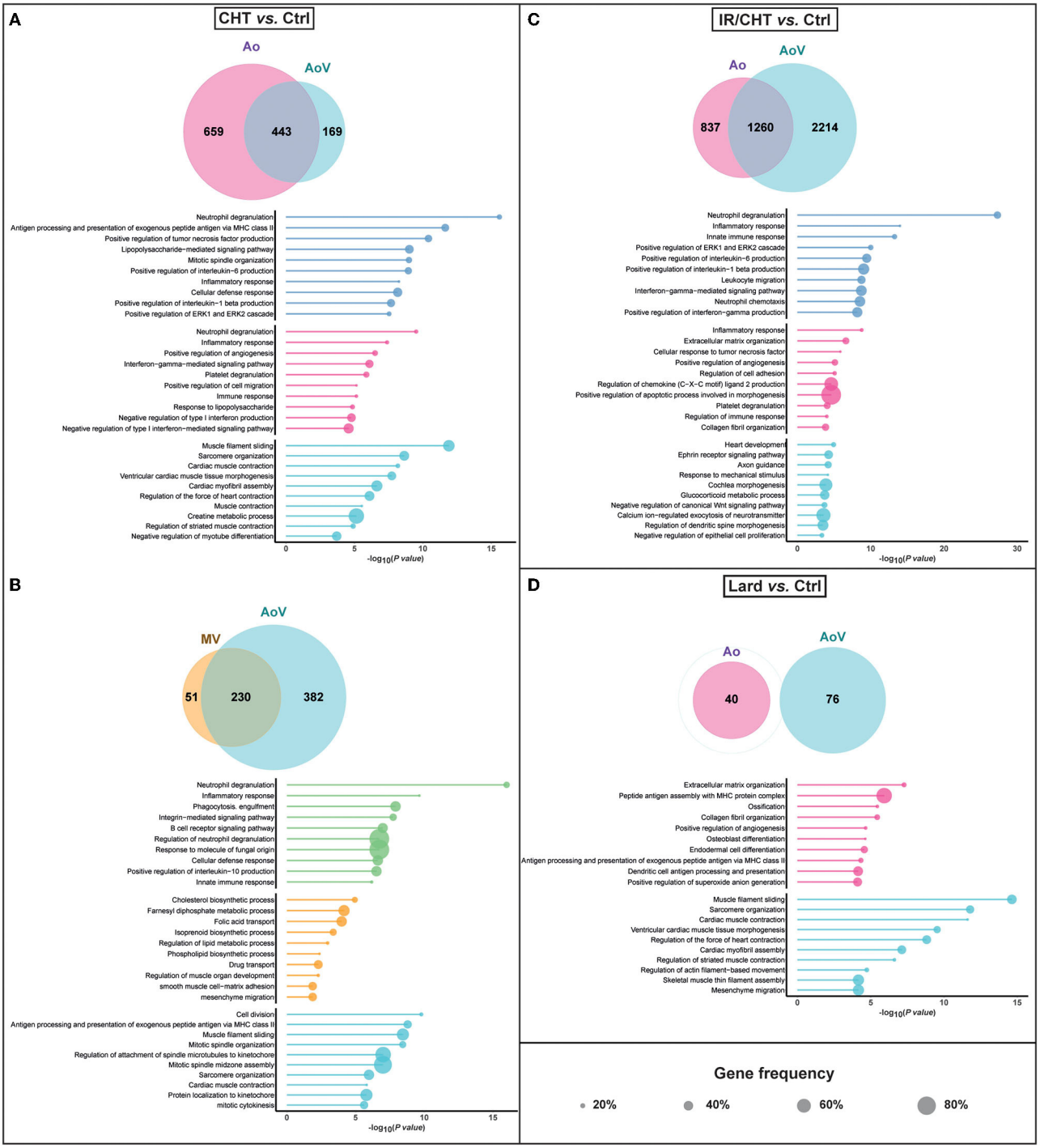

FIGURE 5 | RNA sequencing (RNAseq) analysis of differentially expressed genes (DEGs) in the aorta, the aortic valve, and the mitral valve induced by cholesterol-enriched diet (CHT), alone or combined with irradiation (IR/CHT), and lard-enriched diet as compared to chow diet (Ctrl) (Ctrl, $n = 7$; CHT, $n = 6$; Lard, $n = 7$; IR/CHT, $n = 7$). Venn diagrams represent numbers of specific and common DEGs between tissue pairs for each comparison. Lollipop plots of gene ontology (GO) terms depict the top 10 biological processes affected by specific and common DEGs, with corresponding gene frequency and -$\log_{10}$ (*P*-value) (Wald test in DESeq2 package). Detailed statistical methods are provided in the Methods section. **(A)** Comparison of DEGs and affected biological processes in the aorta and aortic valve following 16-week treatment with a cholesterol-rich diet. **(B)** Comparison of DEGs and affected biological processes in the aortic and mitral valves following 16-week treatment with a cholesterol-rich diet. **(C)** Comparison of DEGs and affected biological processes in the aorta and aortic valve following 16-week treatment with a cholesterol-rich diet combined with irradiation. **(D)** Comparison of DEGs and affected biological processes in the aorta and the aortic valve following 16-week treatment with a lard-rich diet. Ao, aorta; AoV, aortic valve; MV, mitral valve.

contributed to the same biological processes as a cholesterol-rich diet alone, namely neutrophil degranulation, inflammatory, and immune responses (**Figure 5C**, **Supplementary Tables S9–S11**). However, the gene frequency in these processes was doubled by the addition of irradiation, indicating that irradiation could promote inflammation in a neutrophil-dependent manner (**Figures 5A,C**). Processes, such as neutrophil chemotaxis and leukocyte migration indeed became predominant. In the aortic valve, specific processes were nevertheless affected, such as ephrin receptor and Wnt signaling pathways, heart development, and glucocorticoid metabolism, suggesting that irradiation could disturb aortic valve tissue homeostasis and metabolism. In the aorta, effects on collagen fibril and ECM organization predominated in addition to inflammation and platelet degranulation (**Figures 5A,C**).

Circulating Levels of Lipids and Biomarkers Related to Calcification, Inflammation, Oxidative Stress, and Platelet Activation

We wanted to determine whether diet- and irradiation-induced structural and RNA changes could be reflected systemically. For this purpose, we measured the plasma levels of biomarkers related to some of the biological processes identified in our RNAseq dataset. These measurements were performed at baseline and after 16 weeks. We first analyzed differential blood cell counts. Neutrophil count was the only parameter to be increased in the cholesterol-treated rabbits, with or without cardiac irradiation, as compared to Ctrl rabbits (**Supplementary Table S12**). We then studied the effects of lard-enriched diet and cholesterol-rich diet, combined either with irradiation or without irradiation on the circulating levels of conventional lipid biomarkers (**Table 1**). As expected, feeding rabbits for 16 weeks with a cholesterol-enriched diet increased their circulating levels of triglycerides, total cholesterol, LDL, and HDL. Surprisingly, rabbits from the irradiation-only group had increased levels of triglycerides. In agreement with our recent study (17), the lard-enriched diet did not induce changes in conventional lipid biomarkers. The hepatic marker, asparate transaminase, increased upon the intake of a cholesterol-enriched diet, whereas the albumin levels were elevated in rabbits receiving cholesterol combined either with or without irradiation (**Supplementary Table S13**).

We then analyzed the levels of biomarkers involved in calcification, inflammation, oxidative stress, and platelet activation (**Supplementary Figure S2**). Rabbits fed for 16 weeks with a lard-rich diet had reduced circulating levels of DKK1, an inhibitor of the Wnt signaling pathway which is involved in the calcification processes (**Figure 6A**). In contrast, rabbits that received cardiac irradiation combined with a cholesterol diet had elevated levels of DKK1 compared to baseline. Changes in DKK1 levels were neither observed in response to cholesterol diet alone nor in the irradiation alone.

Cholesterol-enriched diet increased the plasma levels of the specific platelet activation marker, platelet factor-4 (PF4), as

TABLE 1 | Effects of cholesterol- and lard-enriched diets as well as cardiac irradiation in addition to cholesterol-enriched diet on the circulating levels of conventional lipid biomarkers.

	CHT			Lard			IR/CHT		
	Pre	Post	*P-value*	Pre	Post	*P-value*	Pre	Post	*P-value*
Triglycerides (mg/dl)	78.98 (58.73–99.14)	134.65 (59.31–159.69)	0.010	61.36 (51.39–81.67)	69.67 (53.09–184.29)	0.301	87.15 (67.47–132.15)	172.98 (115.58–296.14)	0.005
Cholesterol (mg/dl)	33.07 (24.57–48.23)	849.50 (846.72–857.80)	<0.0001	42.00 (30.31–47.71)	22.44 (14.93–40.16)	0.052	37.85 (29.77–49.31)	841.43 (836.43–847.31)	<0.0001
LDL (mg/dl)	15.48 (12.24–26.99)	651.34 (550.05–778.28)	<0.0001	19.80 (13.52–26.90)	11.54 (7.25–20.58)	0.204	21.59 (15.47–28.59)	692.38 (600.64–804.07)	<0.0001
HDL (mg/dl)	21.61 (15.158–24.84)	110.36 (74.21–130.27)	<0.0001	25.96 (19.57–28.54)	13.34 (8.54–15.53)	0.016	20.84 (14.63–25.77)	129.28 (91.38–151.54)	<0.0001

LDL, Low-density lipoprotein; HDL, High-density lipoprotein. P-value: Wilcoxon signed-rank test.

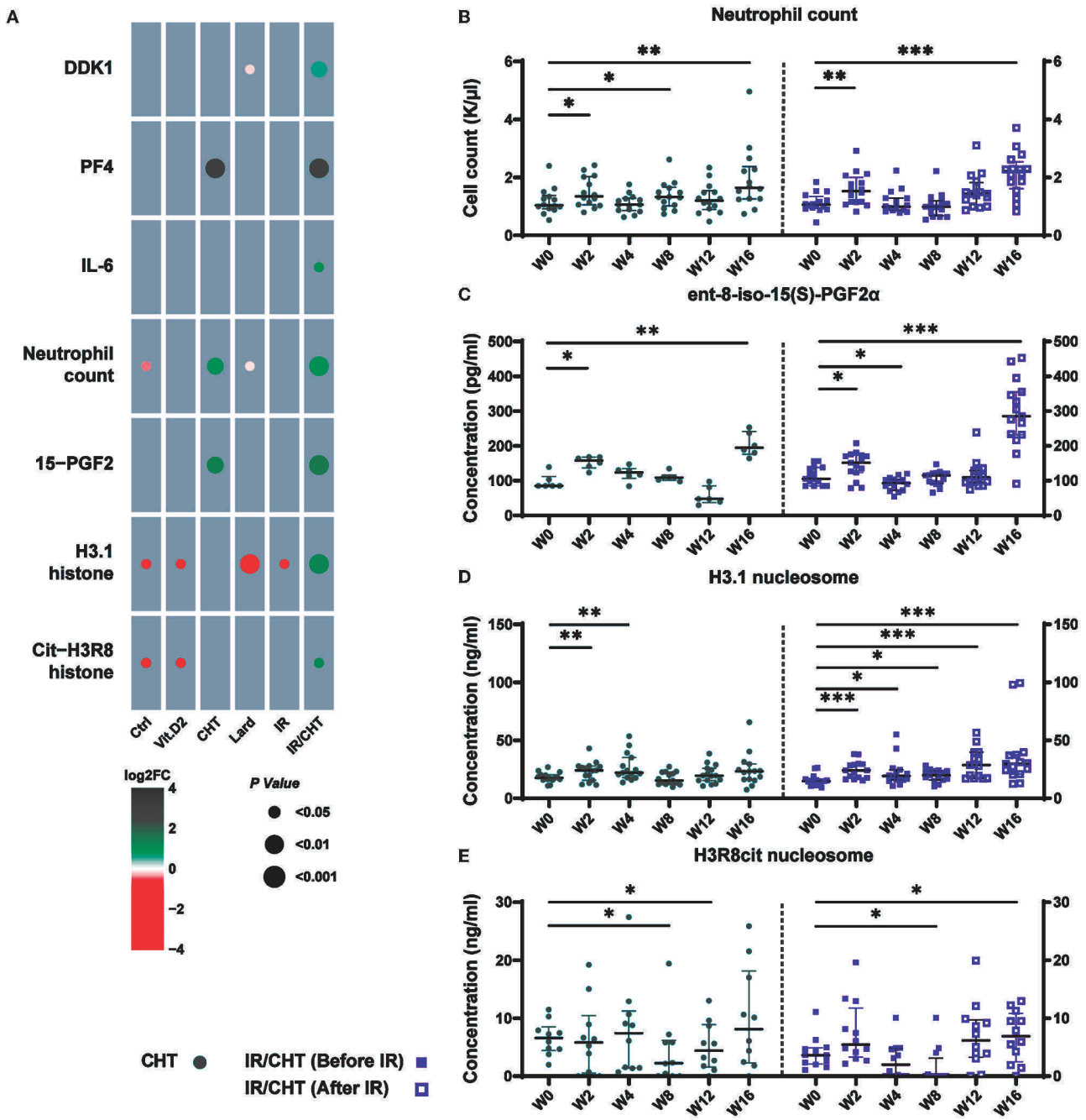

FIGURE 6 | Effect of cholesterol- and lard-enriched diets, and irradiation on the circulating biomarkers of calcification, platelet activation, inflammation, oxidative stress, and on circulating nucleosomes. **(A)** Bubble plot represents concentration fold-change of biomarkers of interest between week 16 (W16) and baseline. Over time evolution of neutrophil count. **(B)** 15-PGF2 **(C)** and circulating nucleosomes **(D,E)**. Graphs represent median with P25-P75 interquartiles. $^{*}P \leq 0.05$; $^{**}P \leq 0.01$; $^{***}P \leq 0.001$ (Wilcoxon signed-rank test; Ctrl, $n = 7$–13; Vit.D2, $n = 7$; CHT, $n = 10$–15; Lard, $n = 7$–12; IR, $n = 7$; IR/CHT, $n = 15$).

well as the neutrophil count and the oxidative stress marker, ent-8-iso-15(S)-prostaglandin F2α (ent-8-iso-15(S)-PGF2α) (**Figures 6C,E,F**). Combined irradiation and a cholesterol-rich diet induced a significant increase in the plasma levels of the major inflammatory cytokine IL-6. as well as the levels of H3.1-nucleosome and citrullinated H3R8-nucleosome (**Figure 6A**) are consistent with our data of RAM-11 staining and our RNAseq findings on a predominant role of inflammation and neutrophil degranulation in this rabbit group.

Lard-enriched diet did not increase inflammation- or oxidative stress-related biomarkers, in accordance with large, calcified area observed in the aorta and aortic valve without the

major implication of inflammatory processes as found in the RNAseq analyses.

To identify possible early biomarkers of lesion development, we performed serial measurements of the neutrophil count, ent-8-iso-15(S)-PGF2α, H3.1-nucleosome, and citrullinated H3R8-nucleosome levels in cholesterol-enriched diet and irradiation combined with cholesterol-enriched diet groups. The neutrophil count increased as early as after 15 days following the dietary cholesterol intake (**Figure 6B**). Levels of the oxidative stress marker, ent-8-iso-15(S)-PGF2α, were also elevated after 15 days of cholesterol diet (**Figure 6C**). In the cholesterol diet group, circulating H3.1-nucleosome levels quickly rose after 15 days and 4 weeks and dropped thereafter, while it went on increasing when irradiation was applied at mid-protocol (**Figure 6D**). Only rabbits that received irradiation combined with a cholesterol diet had increased the circulating levels of citrullinated H3R8-nucleosome after 16 weeks (**Figure 6E**).

DISCUSSION

Our study demonstrates differential effects on the vascular and valvular structures induced by cholesterol- and lard-enriched diet, as well as by combining the cholesterol diet with cardiac irradiation.

Cholesterol-rich diet not only induced well described atherosclerotic lesions but also aortic valve thickening. In addition, calcification occurred in the aortic valve leaflets. The two left-sided aortic and mitral valves displayed cellular infiltrates, including macrophages as observed by RAM-11 immunostaining, and excess ECM deposition. In contrast, a lard-rich diet caused massive aortic media calcification with no intima thickening, and the aortic valve calcified without changes in the leaflet thickness and obvious ECM remodeling. The RNAseq analyses of the aorta, aortic valve, and mitral valve revealed distinct predominant biological processes in lesion development depending on the diet. A cholesterol-rich diet mostly triggered inflammation-related processes in all three tissues. Aorta-specific biological processes were also identified that were involved in processes, such as platelet degranulation, angiogenesis, and cell migration, which are well known to contribute to atherogenesis (29–31). The affected aortic valve-specific biological processes were involved in muscle-related processes. Interestingly, inflammation-related biological processes were also enhanced by a cholesterol-enriched diet in the mitral valve, as well as the processes involved in lipid biosynthesis and metabolism. This is consistent with the recent observations of increased infiltration of inflammatory cells and lipids on the histological sections of the mitral valve and their association with serum cholesterol levels (32). In contrast to a cholesterol-rich diet, a lard-enriched diet did not promote inflammatory processes in the aorta, but rather the processes involved in ECM organization, osteoblast differentiation, and ossification. This indicates that a lard-enriched diet, i.e., dietary palmitate intake could impact arteries *via* different mechanisms than a cholesterol-rich diet, leading to distinct structural lesions. Likewise, while muscle-related mechanisms are likely to be involved in the development of aortic valve alterations in response to cholesterol- and lard-enriched diet, inflammatory processes would specifically contribute to the effect of cholesterol diet on the valve.

The addition of cardiac irradiation to a cholesterol-enriched diet led to similar histological lesions in the aorta, the aortic valve, and the mitral valve. However, atherosclerotic plaque and aortic valve and mitral valve leaflets had higher content in RAM-11 positive cells when irradiation was combined with cholesterol-rich diet than with a cholesterol diet alone. Also, the observed increase of αSMA positive cells in the mitral valve suggests an ongoing transdifferentiation process of valvular cells. Valvular interstitial cells could transform into myofibroblasts following cardiac irradiation, which could promote valve remodeling and ECM production (33). These findings support a possible enhancement of tissue inflammation following cardiac irradiation. This proposition was confirmed by our RNAseq data. Indeed, cardiac irradiation doubled the number of genes involved in inflammation-related processes as compared to a cholesterol-enriched diet alone. Neutrophil degranulation was a predominant activated biological process following cardiac irradiation, suggesting a major contribution of this cell type to the RIHD development mechanism. This observation can be of major clinical importance in view of key roles for neutrophils in CVD (34) and a recent report on a link between the severity of aortic stenosis and NETosis (35). Furthermore, the neutrophil-to-lymphocyte ratio has been associated with worse patient survival after chemoradiotherapy (36).

Blood neutrophil count was increased in rabbits fed with cholesterol-enriched diets, combined with cardiac irradiation or without cardiac irradiation. In addition, the circulating levels of IL-6 were higher when cardiac irradiation was added to a cholesterol-rich diet, confirming RNA-seq results of increased inflammation in response to cardiac irradiation. Neutrophil activation could promote vascular and valvular lesions through increased oxidative stress, as suggested by increased plasma levels of ent-8-iso-15(S)-PGF2α, but also through histone-mediated mechanisms as indicated by the increased levels of H3.1 and citrullinated H3R8 nucleosomes. Extracellular histones have been associated with cardiac injury in patients with septic shock (37). They can promote inflammation through activation of the Toll-like receptors, which are implicated in atherosclerosis pathogenesis (38–40). Extracellular histone can mediate lytic cell death and recent findings showed that citrullinated histones can promote foam cell formation *in vitro* (41, 42). The levels of H3.1-nucleosome were increased as early as after 2 weeks following diet administration, making it a possible good biomarker candidate for early diagnosis of atherosclerosis and aortic valve lesion development. Citrullinated H3R8-nucleosome also represent circulating biomarkers of NETosis. The elevation of these modified histones in response to cholesterol combined with cardiac irradiation may point to new NET-related mechanisms leading to RIHD. Its role as a biomarker of early RIHD also deserves further investigation.

Some biological processes were also specifically triggered by cardiac irradiation in the aorta (e.g., ECM remodeling, platelet degranulation) and aortic valve (e.g.,

ephrin signaling pathway, Wnt signaling pathway, and glucocorticoid metabolism).

Platelet degranulation was found to be increased in the aorta tissue of rabbit groups fed with a cholesterol-enriched diet, combined either with cardiac irradiation or without cardiac irradiation. This result was corroborated by increased plasma levels of PF4 in both groups. Importantly, PF4 has already been associated with atherosclerosis development and could represent another biomarker of atherosclerosis (43) and possibly of valve remodeling.

LIMITATIONS

Our study has some limitations, including that only male rabbits were included. Also, we did not detect any impact of irradiation by itself on the cardiac structures over the analyzed 8-week period. Longer time protocols should be undertaken to evaluate the sole effect of irradiation, without the influence of any diet. Also, the addition of cardiac irradiation to a lard-enriched diet would be interesting to determine whether irradiation-mediated inflammation would potentiate lard-induced lesions. Furthermore, tissue structure was only assessed by histological analyses, which did not allow for 3D visualization of the lesions, which could provide insights into their cellular and extracellular composition. Finally, RNAseq analysis was performed on complete tissues and therefore identification of specific cellular types was not possible. Single-cell RNA sequencing could bring further information regarding the impact of treatments on tissue-specific cellular type enrichment and cellular process activation or inhibition.

CONCLUSION

Our study showed that cholesterol- and lard-enriched diets, and cardiac irradiation combined with a cholesterol-enriched diet induce the development of distinct lesions in the aorta, the aortic valve, and the mitral valve. Lard- and cholesterol-induced valvular and vascular lesions were different both in terms of histological modifications and in the underlying biological process. While cholesterol led to a global increase of inflammation-related processes, lard causes arterial and aortic valve calcification *via* distinct muscle-related mechanisms. Cardiac irradiation enhanced inflammatory processes and calcification in the arteries and aortic valve. At the systemic level, markers of platelet activation, neutrophils, and specific histone modifications in nucleosomes could represent new highly valuable biomarkers for the early diagnosis of ongoing inflammation-related atherosclerosis and heart valve remodeling.

DATA AVAILABILITY STATEMENT

The datasets presented in this study can be found in online repositories. The names of the repository/repositories and accession number(s) can be found below: https://www.ncbi.nlm.nih.gov/geo/query/acc.cgi?acc=GSE193060.

ETHICS STATEMENT

The animal study was reviewed and approved by Commission Ethique Animale ULiège, Université de Liège, Liège, Belgium.

AUTHOR CONTRIBUTIONS

CO, PL, and AN contributed to the conception and design of the study. ZJ performed the statistical analysis. ND and CO wrote the manuscript. CD'E, AH, MH, RD, M-LN, AP, DP, and ND performed the experiments. MH, JT, PDe, and PL contributed to data interpretation. FL, PC, PM, JP, PDe, and PDr performed the experiments of provided tools and expertise for setting up the animal models. All authors contributed to manuscript revision, read, and approved the submitted version.

FUNDING

This project was supported by grants from the Région Wallonne (Projet Complément FEDER BIOMED HUB, convention 1510605) and the Fonds Léon Frédéricq (FLF, Prix de la Province de Liège 2019-2020). CO is Research Director at the National Funds for Scientific Research, Belgium (FRS-FNRS). This study was sponsored by Volition SRL. This study received funding from Belgian Volition SRL. The funder was involved in the study design and in the collection, analysis, and interpretation of the data of nucleosome plasma levels.

ACKNOWLEDGMENTS

We thank the GIGA-technological platforms and core facilities (Immunohistochemistry, SPF animal facility, Genomics, Cell Imaging & Flow Cytometry) for technical support.

SUPPLEMENTARY MATERIAL

The Supplementary Material for this article can be found online at: https://www.frontiersin.org/articles/10.3389/fcvm.2022.839720/full#supplementary-material

REFERENCES

1. World Health Organization. The top 10 causes of death. (2020)
2. Lambert MA, Weir-McCall JR, Salsano M, Gandy SJ, Levin D, Cavin I, et al. Prevalence and distribution of atherosclerosis in a low- to intermediate-risk population: Assessment with whole-body MR angiography. *Radiology*. (2018) 287:795–804. doi: 10.1148/radiol.2018171609
3. Coffey S, Roberts-Thomson R, Brown A, Carapetis J, Chen M, Enriquez-Sarano M, et al. Global epidemiology of valvular heart disease. *Nat Rev Cardiol*. (2021) 18:853–64. doi: 10.1038/s41569-021-00570-z

4. Stewart BF, Siscovick D, Lind BK, Gardin JM, Gottdiener JS, Smith VE, et al. Clinical factors associated with calcific aortic valve disease. *J Am Coll Cardiol.* (1997) 29:630–4. doi: 10.1016/S0735-1097(96)00563-3
5. Castelli WP, Anderson K, Wilson PWF, Levy D. Lipids and risk of coronary heart disease The Framingham Study. *Ann Epidemiol.* (1992) 2:23–8. doi: 10.1016/1047-2797(92)90033-M
6. Nazarzadeh M, Pinho-Gomes AC, Bidel Z, Dehghan A, Canoy D, Hassaine A, et al. Plasma lipids and risk of aortic valve stenosis: A Mendelian randomization study. *Eur Heart J.* (2020) 41:3913–20B. doi: 10.1093/eurheartj/ehaa070
7. Jukema WJ, Bruschke AVG, van Boven AJ, Reiben JHC, Bal ET, Zwinderman AH, et al. Effects of lipid lowering by pravastatin on progression and regression of coronary artery disease in symptomatic men with normal to moderately elevated serum cholesterol levels - the regression growth evaluation statin study (REGRESS). *Circulation.* (1995) 91:2528–40. doi: 10.1161/01.CIR.91.10.2528
8. Rouleau J. Improved outcome after acute coronary syndromes with an intensive versus standard lipid-lowering regimen: Results from the Pravastatin or Atorvastatin Evaluation and Infection Therapy-Thrombolysis in Myocardial Infarction 22 (PROVE IT-TIMI 22) trial. *Am J Med.* (2005) 118:28S—35S. doi: 10.1016/j.amjmed.2005.09.014
9. Lee SE, Chang HJ, Sung JM, Park HB, Heo R, Rizvi A, et al. Effects of statins on coronary atherosclerotic plaques: the PARADIGM study. *JACC Cardiovasc Imaging.* (2018) 11:1475–84. doi: 10.1016/j.jcmg.2018.04.015
10. Chan KL, Teo K, Dumesnil JG Ni A, Tam J. Effect of lipid lowering with rosuvastatin on progression of aortic stenosis: results of the aortic stenosis progression observation: Measuring effects of rosuvastatin (Astronomer) trial. *Circulation.* (2010) 121:306–14. doi: 10.1161/CIRCULATIONAHA.109.900027
11. Ray KK, Stoekenbroek RM, Kallend D, Nishikido T, Leiter LA, Landmesser U, et al. Effect of 1 or 2 doses of inclisiran on low-density lipoprotein cholesterol levels: one-year follow-up of the orion-1 randomized clinical trial. *JAMA Cardiol.* (2019) 4:1067–75. doi: 10.1001/jamacardio.2019.3502
12. Schwartz GG, Steg PG, Szarek M, Bhatt DL, Bittner VA, Diaz R, et al. Alirocumab and cardiovascular outcomes after acute coronary syndrome. *N Engl J Med.* (2018) 379:2097–107. doi: 10.1056/NEJMoa1801174
13. Sabatine MS, Giugliano RP, Keech AC, Honarpour N, Wiviott SD, Murphy SA, et al. Evolocumab and clinical outcomes in patients with cardiovascular disease. *N Engl J Med.* (2017) 376:1713–22. doi: 10.1056/NEJMoa1615664
14. Perrot N, Valerio V, Moschetta D, Boekholdt SM, Dina C, Chen HY, et al. Genetic and in vitro inhibition of PCSK9 and calcific aortic valve stenosis. *JACC Basic to Transl Sci.* (2020) 5:649–61. doi: 10.1016/j.jacbts.2020.05.004
15. Guasch-Ferré M, Babio N, Martínez-González MA, Corella D, Ros E, Martín-Peláez S, et al. Dietary fat intake and risk of cardiovascular disease and all-cause mortality in a population at high risk of cardiovascular disease. *Am J Clin Nutr.* (2015) 102:1563–73. doi: 10.3945/ajcn.115.116046
16. Praagman J, De Jonge EAL, Kiefte-De Jong JC, Beulens JWJ, Sluijs I, Schoufour JD, et al. Dietary saturated fatty acids and coronary heart disease risk in a Dutch middle-Aged and elderly population. *Arterioscler Thromb Vasc Biol.* (2016) 36:2011–8. doi: 10.1161/ATVBAHA.116.307578
17. Donis N, Jiang Z, D'Emal C, Dulgheru R, Giera M, Blomberg N, et al. Regular dietary intake of palmitate causes vascular and valvular calcification in a rabbit model. *Front Cardiovasc Med.* (2021) 8:1–11. doi: 10.3389/fcvm.2021.692184
18. Darby SC, Ewertz M, McGale P, Bennet AM, Blom-Goldman U, Brønnum D, et al. Risk of ischemic heart disease in women after radiotherapy for breast cancer. *N Engl J Med.* (2013) 368:987–98. doi: 10.1056/NEJMoa1209825
19. Galper SL Yu JB, Mauch PM, Strasser JF, Silver B, LaCasce A, Marcus KJ, et al. Clinically significant cardiac disease in patients with Hodgkin lymphoma treated with mediastinal irradiation. *Blood.* (2011) 117:412–8. doi: 10.1182/blood-2010-06-291328
20. Desai MY, Windecker S, Lancellotti P, Bax JJ, Griffin BP, Cahlon O, et al. Prevention, diagnosis, and management of radiation-associated cardiac disease: JACC scientific expert panel. *J Am Coll Cardiol.* (2019) 74:905–27. doi: 10.1016/j.jacc.2019.07.006
21. Donis N, Oury C, Moonen M, Lancellotti P. Treating cardiovascular complications of radiotherapy: a role for new pharmacotherapies. *Expert Opin Pharmacother.* (2018) 19:431–42. doi: 10.1080/14656566.2018.1446080
22. Anders S, Huber W. Differential expression analysis for sequence count data. *Genome Biol.* (2010) 11. doi: 10.1186/gb-2010-11-10-r106
23. Craig DB, Kannan S, Dombkowski AA. Augmented annotation and orthologue analysis for oryctolagus cuniculus: better bunny. *BMC Bioinform.* (2012) 13. doi: 10.1186/1471-2105-13-84
24. Sangar V, Blankenberg DJ, Altman N, Lesk AM. Quantitative sequence-function relationships in proteins based on gene ontology. *BMC Bioinform.* (2007) 8:1–15. doi: 10.1186/1471-2105-8-294
25. Xiao Y, Hsiao TH, Suresh U, Chen HIH, Wu X, Wolf SE, et al. novel significance score for gene selection and ranking. *Bioinformatics.* (2014) 30:801–7. doi: 10.1093/bioinformatics/btr671
26. Fan J, Kitajima S, Watanabe T, Xu J, Zhang J, Liu E, et al. Rabbit models for the study of human atherosclerosis: from pathophysiological mechanisms to translational medicine. *Pharmacol Ther.* (2015) 146:104–19. doi: 10.1016/j.pharmthera.2014.09.009
27. Tsukada T, Rosenfeld M, Ross R, Gown AM. Immunocytochemical analysis of cellular components in atherosclerotic lesions. Use of monoclonal antibodies with the Watanabe and fat-fed rabbit. *Arteriosclerosis.* (1986) 6:601–13. doi: 10.1161/01.ATV.6.6.601
28. Koniari I, Mavrilas D, Papadaki H, Karanikolas M, Mandellou M, Papalois A, et al. Structural and biomechanical alterations in rabbit thoracic aortas are associated with the progression of atherosclerosis. *Lipids Health Dis.* (2011) 10:125. doi: 10.1186/1476-511X-10-125
29. Herrmann J, Lerman LO, Mukhopadhyay D, Napoli C, Lerman A. Angiogenesis in atherogenesis. *Arterioscler Thromb Vasc Biol.* (2006) 26:1948–57. doi: 10.1161/01.ATV.0000233387.90257.9b
30. Basatemur GL, Jørgensen HF, Clarke MCH, Bennett MR, Mallat Z. Vascular smooth muscle cells in atherosclerosis. *Nat Rev Cardiol.* (2019) 16:727–44. doi: 10.1038/s41569-019-0227-9
31. von Hundelshausen P, Schmitt MMN. Platelets and their chemokines in atherosclerosis-clinical applications. *Front Physiol.* (2014) 5:1–17. doi: 10.3389/fphys.2014.00294
32. El-Khatib LA, De Feijter-Rupp H, Janoudi A, Fry L, Kehdi M, Abela GS. Cholesterol induced heart valve inflammation and injury: Efficacy of cholesterol lowering treatment. *Open Hear.* (2020) 7:1–7. doi: 10.1136/openhrt-2020-001274
33. Dye BK, Butler C, Lincoln J. Smooth muscle α-actin expression in mitral valve interstitial cells is important for mediating extracellular matrix remodeling. *J Cardiovasc Dev Dis.* (2020) 7:32. doi: 10.3390/jcdd7030032
34. Gaul DS, Stein S, Matter CM. Neutrophils in cardiovascular disease. *Eur Heart J.* (2017) 38:1702–4. doi: 10.1093/eurheartj/ehx244
35. Kopytek M, Kolasa-Trela R, Zabczyk M, Undas A, Natorska J. NETosis is associated with the severity of aortic stenosis: links with inflammation. *Int J Cardiol.* (2019) 286:121–6. doi: 10.1016/j.ijcard.2019.03.047
36. Ho YC, Lai YC, Lin HY, Ko MH, Wang SH, Yang SJ, et al. Low cardiac dose and neutrophil-to-lymphocyte ratio predict overall survival in inoperable esophageal squamous cell cancer patients after chemoradiotherapy. *Sci Rep.* (2021) 11:1702–4. doi: 10.1038/s41598-021-86019-2
37. Alhamdi Y, Abrams ST, Cheng Z, Jing S, Su D, Liu Z, et al. Circulating histones are major mediators of cardiac injury in patients with sepsis. *Crit Care Med.* (2015) 43:2094–103. doi: 10.1097/CCM.0000000000001162
38. Silk E, Zhao H, Weng H, Ma D. The role of extracellular histone in organ injury. *Cell Death Dis.* (2017) 8:1–11. doi: 10.1038/cddis.2017.52
39. Roshan MHK, Tambo A, Pace NP. The role of TLR2, TLR4, and TLR9 in the pathogenesis of atherosclerosis. *Int J Inflam.* (2016) 2016:1532832. doi: 10.1155/2016/1532832
40. Ekaney ML, Otto GP, Sossdorf M, Sponholz C, Boehringer M, Loesche W, et al. Impact of plasma histones in human sepsis and their contribution to cellular injury and inflammation. *Crit Care.* (2014) 18:1–9. doi: 10.1186/s13054-014-0543-8
41. Silvestre-roig C, Braster Q, Wichapong K, Lee EY, Teulon JM, Berrebeh N, et al. Externalized histone H4 orchestrates chronic inflammation by inducing lytic cell death. *Nature.* (2019) 569:236–240. doi: 10.1038/s41586-019-1167-6
42. Haritha VH, George A, Shaji B V, Anie Y. NET-associated citrullinated histones promote LDL aggregation and foam cell formation *in vitro*. *Exp Cell Res.* (2020) 396:112320. doi: 10.1016/j.yexcr.2020.112320
43. Sachais BS, Turrentine T, McKenna JMD, Rux AH, Rader D, Kowalska MA. Elimination of platelet factor 4 (PF4) from

platelets reduces atherosclerosis in C57Bl/6 and apoE-/- mice. *Thromb Haemost.* (2007) 98:1108–13. doi: 10.1160/TH07-04-0271

Conflict of Interest: MH and DP were employed by Belgian Volition SRL. JT was employed by Volition America.

The remaining authors declare that the research was conducted in the absence of any commercial or financial relationships that could be construed as a potential conflict of interest.

Publisher's Note: All claims expressed in this article are solely those of the authors and do not necessarily represent those of their affiliated organizations, or those of the publisher, the editors and the reviewers. Any product that may be evaluated in this article, or claim that may be made by its manufacturer, is not guaranteed or endorsed by the publisher.

frontiers | Frontiers in Cardiovascular Medicine

MINI REVIEW
published: 14 April 2022
doi: 10.3389/fcvm.2022.886266

The Evolving Story of Multifactorial Chylomicronemia Syndrome

Martine Paquette[1] *and Sophie Bernard*[1,2]*

[1] Genetic Dyslipidemias Clinic, Montreal Clinical Research Institute, Montreal, QC, Canada, [2] Division of Endocrinology, Department of Medicine, Université de Montréal, Montreal, QC, Canada

Multifactorial chylomicronemia syndrome (MCS or type V hyperlipoproteinemia) is the most frequent cause of severe hypertriglyceridemia and is associated with an increased risk of acute pancreatitis, cardiovascular disease, and non-alcoholic steatohepatitis. The estimated prevalence of MCS in the North American population is 1:600–1:250 and is increasing due to the increasing prevalence of obesity, metabolic syndrome, and type 2 diabetes. Differentiating between familial chylomicronemia syndrome and MCS is crucial due to their very different treatments. In recent years, several cohort studies have helped to differentiate these two conditions, and recent evidence suggests that MCS itself is a heterogeneous condition. This mini-review will summarize recent literature on MCS, with a specific focus on the genetic determinants of the metabolic risk and the latest developments concerning the pharmacological and non-pharmacological treatment options for these patients. Possible research directions in this field will also be discussed.

Keywords: multifactorial chylomicronemia syndrome, hypertriglyceridemia, genetic, diet, pancreatitis, cardiovascular disease

OPEN ACCESS

Edited by:
Catherine Martel,
Université de Montréal, Canada

Reviewed by:
Wenxin Song,
University of California, Los Angeles, United States

***Correspondence:**
Sophie Bernard
sophie.bernard@ircm.qc.ca

Specialty section:
This article was submitted to Lipids in Cardiovascular Disease, a section of the journal Frontiers in Cardiovascular Medicine

Received: *28 February 2022*
Accepted: *24 March 2022*
Published: *14 April 2022*

Citation:
Paquette M and Bernard S (2022) The Evolving Story of Multifactorial Chylomicronemia Syndrome. Front. Cardiovasc. Med. 9:886266. doi: 10.3389/fcvm.2022.886266

INTRODUCTION

Severe hypertriglyceridemia (HTG) is defined as a fasting triglycerides (TG) concentration of ≥10 mmol/L (>885 mg/dL). At this threshold of TG, a pathological accumulation of circulating chylomicrons (chylomicronemia) is almost always present in the plasma (1). Multifactorial chylomicronemia syndrome (MCS) (OMIM #144650), previously known as "type V hyperlipoproteinemia" according to the Fredrickson classification or "late-onset chylomicronaemia," is by far the most common form of chylomicronemia and severe HTG. Although the exact frequency of MCS in the general population is not precisely known, the prevalence of severe HTG in North America has been estimated to be between 1:600 and 1:250 (2–4). In order to develop MCS, an underlying genetic susceptibility for impaired TG metabolism must be present (5). The full expression of the MCS phenotype is then triggered by the presence of secondary factors such as a diet rich in fats and simple carbohydrates, reduced activity levels, obesity, metabolic syndrome, alcohol intake, and uncontrolled diabetes (6). In these patients, both chylomicrons and very low-density lipoproteins (VLDLs) are increased in circulation due to impairment of lipoprotein lipase (LPL) activity as well as hepatic overproduction of VLDLs and their reduced clearance. Following blood sampling, centrifugation, and overnight storage at 4°C, the presence of chylomicrons can be observable if a creamy supernatant layer is present on the top of the tube, whereas a cloudy and lactescent lower layer (infranatant) indicates the presence of VLDLs (7, 8). Clinically, the main manifestations associated with MCS include the presence of eruptive xanthomas, lipemia retinalis, abdominal pain, and impaired concentration

(6). Furthermore, MCS is associated with an increased risk of serious health consequences, which includes acute pancreatitis (AP), cardiovascular disease (CVD), as well as non-alcoholic fatty liver disease (NAFLD) (9).

COMPLICATIONS OF MCS

The risk of AP in MCS patients as compared to normolipidemic individuals from the general population is at least 7-fold higher (between ∼7- and 54-fold) (7, 10, 11), whereas the risk of CVD is 2- to 9-fold higher (7, 11). The presence of TG-rich lipoprotein remnants in circulation, which can penetrate the vascular wall, as well as the concomitant presence of atherogenic comorbidities such as obesity or diabetes, could explain the increased cardiovascular risk, whereas the exact mechanisms linking HTG and AP still remain poorly understood (12–14). However, patients with HTG generally present a more severe clinical course of AP, with increased morbidity and mortality (15, 16).

NAFLD is a chronic liver disease characterized by excessive fat accumulation in the liver and is considered as the hepatic component of the metabolic syndrome or a consequence of it. The prevalence of NAFLD in the general population is estimated to be around 25% (17). NAFLD can progress to non-alcoholic steatohepatitis and ultimately to cirrhosis and its complications (18). Excessive circulating TG represents one of the risk factors associated with the development of NAFLD (19–21). In a recent study, the prevalence of NAFLD in patients affected by MCS was studied for the first time using transient elastography (FibroScan). The authors observed that the prevalence of NAFLD was 74% in 19 MCS subjects, which is three times more prevalent than in the general population (22). Interestingly, the authors observed a negative correlation between liver fat accumulation and AP risk in these patients. This may suggest that if more TG accumulates in the liver, a lower quantity would be available to contribute to the pathophysiology of AP (22). However, because of the small sample size of this study, these results need to be replicated in a larger cohort of MCS patients.

DIFFERENCES BETWEEN MCS AND FCS

Familial chylomicronemia syndrome (FCS) (OMIM #238600, also known as type I hyperlipoproteinemia, LPL deficiency, or monogenic chylomicronemia) is a rare autosomal recessive disorder, also associated with severe HTG and risk of life-threatening AP. In these patients, the severe HTG in the fasting state is solely explained by the presence of chylomicrons. Compared to MCS, FCS is less common, with an estimated prevalence of 1 to 10 per million (6). Because there exists a large overlap in the phenotype of FCS and MCS, the differential diagnosis between these two conditions may be a challenge. However, making a proper diagnosis is important to guide appropriate treatment. In recent years, there has been increasing interest for studying the clinical differences between FCS and MCS patients (10, 11, 23–29). The study of Paquette et al. was the first that systematically compared the clinical and biochemical characteristics of genetically confirmed FCS patients ($n = 25$) vs. MCS patients ($n = 36$) (24). In this study, despite similar TG concentrations (19.57 mmol/L in FCS vs. 25.12 mmol/L in MCS), the severity of the disease was generally worse in FCS patients than in MCS patients, with a significantly higher prevalence of abdominal pain (63 vs. 19%), pancreatitis (60 vs. 6%), and multiple pancreatitis (48 vs. 3%). Furthermore, chylomicronemia discovery occurred at a younger age in FCS patients (11 vs. 36 years) and more frequently because of clinical complications including an episode of pancreatitis (12 vs. 3%) and the presence of abdominal pain (20 vs. 3%) than in MCS patients. In contrast, the cardiometabolic profile was better in FCS than in MCS patients. Indeed, when the number of metabolic syndrome features was studied [including body mass index (BMI) $\geq$ 27 kg/m^2, systolic blood pressure $\geq$ 130 mmHg or diastolic blood pressure $\geq$ 85 mmHg (or treatment for hypertension) and fasting glucose $\geq$ 5.6 mmol/L (or treatment for diabetes)], a lower frequency of patients presenting two or three abnormalities was observed in FCS (10%) compared with MCS (67%). In addition, the prevalence of CVD was lower in FCS than in MCS patients (0 vs. 17%), although the difference was not statistically significant. Other significant differences between groups included lower ALT, GGT, total cholesterol, HDL-C, LDL-C, and non-HDL-C in FCS compared to MCS patients (24). Several findings of this study were confirmed in other cohorts. Indeed, the frequency of pancreatitis was observed to be higher in FCS (ranging from 59 to 88%) than in MCS (ranging from 11 to 37%) (11, 25, 26, 28, 29). In the study of Belhassen et al., which is a prospective study over 10 years of follow-up (median of 9.8 years), the hazard ratio for incident AP was 3.6 in FCS as compared with MCS (11). These results are similar to those of D'Erasmo et al., who reported an incidence rate of AP in FCS three times higher than in MCS over a median follow-up period of 44 months (25). The younger age at baseline in FCS is also frequently reported, with >10 years of difference between these two conditions (11, 27, 28). Concerning the metabolic profile of these patients, a lower BMI is always observed in FCS patients when this variable is studied (11, 26–29). Indeed, FCS patients are typically within the normal BMI range, whereas the average BMI in MCS patients is mostly between 28 and 30 kg/m^2. A higher frequency of NAFLD has also been reported in MCS (74%) compared with FCS (42%) (22). However, conflicting results have been obtained concerning differences in prevalence or incidence of CVD, diabetes, and hypertension (11, 26, 28). Echoing the findings of Paquette et al. (24), others found significantly lower concentrations of total cholesterol (25), HDL-C (25–27), and LDL-C (26, 27) in FCS patients compared with MCS patients. Importantly, the apolipoprotein B (apoB) concentration in FCS patients was also found to be significantly lower than in MCS patients, with minimal overlap between groups (28, 30). Indeed,

Abbreviations: ALT, alanine aminotransferase; AP, acute pancreatitis; ApoB, apolipoprotein B; BMI, body mass index; CVD, cardiovascular disease; FCS, familial chylomicronemia syndrome; GGT, gamma-glutamyl transferase; HDL-C, high-density lipoprotein cholesterol; HTG, hypertriglyceridemia; LDL-C, low-density lipoprotein cholesterol; LPL, lipoprotein lipase; MCS, multifactorial chylomicronemia syndrome; NAFLD, nonalcoholic fatty liver disease; SNPs, single-nucleotide polymorphisms; TG, triglyceride; VLDL, very-low-density lipoprotein.

apoB cutoffs between 0.75 and 0.9 g/L have been proposed in order to differentiate FCS patients from MCS patients (28, 31). Finally, although TG concentrations are highly fluctuating, the majority of studies found a higher concentration of baseline TG or maximal TG in FCS subjects than in MCS subjects (11, 27–29).

GENETICS OF SEVERE HYPERTRIGLYCERIDEMIA

The gold standard for the differential diagnosis of FCS and MCS in patients with severe HTG remains the genetic testing using a targeted next-generation DNA sequencing panel (32). Other existing diagnostic strategies to identify FCS patients are described elsewhere (8). Whereas, the presence of homozygous or compound heterozygous rare variants in the canonical genes involved in TG metabolism (*LPL* gene or, less frequently, its modulators: *APOC2*, *GPIHBP1*, *APOA5*, and *LMF1* genes) is indicative of FCS, the molecular basis of MCS is more complex. Indeed, there are two main genetic determinants that confer susceptibility to MCS: the presence of a single deleterious rare variant in one of the five main TG genes (heterozygous) or the accumulation of several single-nucleotide polymorphisms (SNPs) associated with TG concentration (polygenic). This polygenic susceptibility to MCS is quantified using a polygenic risk score with common SNPs extracted from genome-wide association studies. Recent publications have shed light on the complex genetic architecture of this disease and on the proportion of each of the main types of genetic determinants found in the severe HTG population. In the study of Dron et al. in a cohort of 563 Caucasian patients with severe HTG, the authors found that a high polygenic risk score (comprised of 16 SNPs) was the most common genetic determinant of this trait in adults. Indeed, FCS (biallelic rare variants) was found in 1.1% of the cohort, whereas heterozygous rare variant and high polygenic risk were found in 14.4 and 32.0% of the cohort, respectively. Of note, half of the studied cohort remained genetically undefined (5). The involvement of non-canonical secondary TG genes has been suggested as one of the possible factors explaining the severe HTG in these patients with no identified genetic basis (5, 33–36). Also, multiple polygenic risk scores exist, with variable number of SNPs, which can be weighted or unweighted (37, 38). In a subsequent study from the same group, an overview of the genetic determinants of severe HTG was compared in patients from three different ancestry groups: European (n = 336), East Asian (n = 63), and Hispanic (n = 199). Whereas, the proportion of patients with high polygenic scores was similar between groups (frequency of 25.4–33.9%), the proportion of patients carrying deleterious rare variants [heterozygous (MCS) or biallelic (FCS)] differed. This proportion was the highest in the Hispanic cohort (36.7%), followed by the East Asian cohort (25.4%), and the European cohort (14.3%) (39). However, it should be kept in mind that TG-associated SNPs included in polygenic scores are mainly from European-based genome-wide association studies. In some isolated populations, a founder effect is present for specific deleterious rare variants, which increases the prevalence of heterozygous carriers. For example, in the French Canadian population, there exists an enrichment in two *LPL* variants [p.(Gly215Glu) and p.(Pro234Leu)]. Accordingly, the reported prevalence of MCS patients carrying a rare variant in this population is higher than expected in Caucasian patients (30, 40).

RISK STRATIFICATION AND HETEROGENEITY OF MCS

Although there is now a better understanding of the clinical and biochemical differences between FCS and MCS patients, the phenotype heterogeneity among MCS patients remains poorly studied. In a recent publication, the clinical differences between MCS patients with (positive-MCS) vs. without (negative-MCS) a rare deleterious variant in the five canonical genes involved in TG metabolism have been studied for the first time (30). The main observation of this study is that the positive-MCS group (n = 22) had an intermediate phenotype severity between the FCS (n = 28) and negative-MCS (n = 53) groups. Indeed, there was a significant difference between the three groups concerning the prevalence of abdominal pain (59% in FCS, 36% in positive-MCS, and 15% in negative-MCS), pancreatitis (61% in FCS, 41% in positive-MCS, and 9% in negative-MCS), and multiple pancreatitis (46% in FCS, 23% in positive-MCS, and 6% in negative-MCS). However, when the MCS groups were compared, the age of the first pancreatitis was not different (41 years in positive-MCS and 48 years in negative-MCS), and there was no difference concerning the prevalence of CVD. Interestingly, while the baseline TG concentration was similar between positive-MCS (10.55 mmol/L) and negative-MCS (10.33 mmol/L), the maximal recorded TG value was higher in positive-MCS (41.03 mmol/L) than in negative-MCS (19.50 mmol/L). Importantly, while the lower apoB concentration in FCS patients as compared with MCS patients has been well-documented in previous studies, this study showed for the first time that the apoB value was also significantly lower in the positive-MCS group (0.80 g/L) compared to the negative-MCS group (1.10 g/L). Of note, among MCS patients, an apoB value $<$ 1 g/L was associated with a $\sim$5-fold increased risk of pancreatitis. This cutoff was therefore suggested in order to identify higher-risk individuals among patients with severely elevated TG concentrations and to prioritize them for genetic screening. In this cohort, strong predictors of pancreatitis were the presence of a rare variant, GGT $\geq$45 U/L, maximal TG value $\geq$40 mmol/L, and fructose consumption $\geq$4% of daily energy intake. One limitation of this study is that no polygenic score has been assessed. Therefore, the proportion of patients in the negative-MCS group having a high polygenic risk as compared to those that are genetically undefined is not known (30).

In a study of 103 Chinese subjects with TG above 5.65 mmol/l and without secondary causes of HTG, patients with history of AP presented a higher frequency of rare variants in the canonical genes involved in TG metabolism than those with no history of AP. However, for several of these subjects, the variant in question was a variant of uncertain significance (36). Interestingly, the maximal TG value was also significantly

different between subjects with history of AP (16.6 mmol/L) and those with no history of AP (11.3 mmol/L) (36).

TREATMENT

The main goal in the treatment of MCS patients is to reduce the TG concentration below the threshold of 5.6 mmol/L (500 mg/dL) in order to prevent AP (41, 42). The secondary focus of treatment is then to reduce the cardiovascular risk. The first-line treatment for these patients is to manage secondary factors associated with HTG such as physical inactivity, obesity, metabolic syndrome, alcohol intake, and uncontrolled diabetes, as well as pharmacological treatment with fibrates. One of the mechanisms by which fibrates lower TG concentrations is by increasing LPL-mediated lipolysis. Therefore, this drug is generally effective in MCS patients, in which LPL activity is not completely impaired, but it is poorly effective in FCS patients, in which a marked reduction or complete loss of LPL activity is present. In the study of Paquette et al. including 75 MCS patients with a mean baseline TG > 10 mmol/L, fibrate use was associated with a ≥30% TG reduction in 83% of the cohort and a ≥50% TG reduction in 69% of the cohort (30). In contrast, none of the FCS patients ever achieved a TG reduction of more than 30% using fibrate (30). Despite the generally good response to fibrate therapy observed in MCS patients, the efficacy of fibrate is highly heterogeneous among these patients. Therefore, the treatment target of 5.6 mmol/L to reduce the risk of AP is not often achieved. Furthermore, even if fibrates are recommended for the treatment of severe HTG, no study has specifically demonstrated that fibrates use was associated with AP risk reduction, and thus far, clinical trials showed little or no cardiovascular benefit of adding a fibrate to statin therapy (43). In FCS patients, the principal therapeutic modality remains the very low-fat diet, in which fat should be limited to 10–30 g/day or 10–15% of total energy intake. The limited intake of long-chain fatty acids is required to reduce the formation of chylomicrons and maintain adequate TG concentrations. However, this approach is very restrictive, and compliance with such a diet over a lifetime is extremely difficult (44, 45). In MCS patients, both VLDLs and chylomicrons are present in excess in the circulation and contribute to the severe HTG phenotype. While reduction of dietary fat prevents the excessive formation of chylomicrons, reduction of simple carbohydrates is associated with reduced VLDL production by the liver (46). The best dietary approach to lower the TG concentration and to prevent AP in MCS patients is still unknown. A recent study by Fantino et al. investigated for the first time in a randomized crossover design the effect of two different diets on TG concentrations in MCS participants (47). After 3 weeks on each diet, fasting TG decreased by 55% following the low-fat diet (fat: 20%, carbohydrates: 60%) and by 48% following the low-carbohydrate diet (carbohydrates: 35%, fat: 45%), without any change in body weight or in total cholesterol, HDL-C, LDL-C, and apoB. Interestingly, in a subgroup analysis including solely subjects carrying a rare variant in the *LPL* gene (positive-MCS), a more pronounced TG decrease was observed following the low-fat diet [71% (−11.97 mmol/L)] than following a low-carbohydrate diet [59% (−8.93 mmol/L)]. Therefore, this study is clinically important since it demonstrated that MCS patients can be effectively treated by either low-fat or low-carbohydrate diets if they are closely monitored by a specialized dietician, achieving a TG decrease that is comparable to the decrease obtained with fibrates. However, this study included only 12 participants, so validation of these results in a larger cohort is required. Furthermore, it is not known whether following these diets over a long-term period would result in a decreased risk of AP (47). Importantly, in some patients, a 50% decrease in TG concentration is not sufficient to reach the treatment target of 5.6 mmol/L or for TG normalization (TG ≤ 1.7 mmol/L). Fortunately, new therapies for the treatment of hypertriglyceridemia are emerging, and some of them show promising results in patients with severe HTG. These emerging therapies include molecules targeting apoC-III (volanesorsen, AKCEA-APOCIII-LRx, and AROAPOC3) (48, 49), molecules targeting ANPTL3 (evinacumab and AROANG3) (50), and ω-3 krill oil (51).

CONCLUSION AND FUTURE DIRECTIONS

Recent studies have helped to better characterize MCS and the metabolic complications associated with this disease. In the past few years, differences between both chylomicronemia syndromes (FCS and MCS) have been better characterized. A novelty in our understanding of MCS is the heterogeneity in the genetic susceptibility profiles leading to distinct phenotype severity. Indeed, recent studies showed that MCS susceptibility is predominantly polygenic, rather than being caused by a single rare causal variant in the five canonical genes involved in TG metabolism. However, this latter etiology is associated with a more severe form of MCS, with increased risk of life-threatening AP. Furthermore, measurement of apoB in patients with severe HTG could be a pertinent first step to identify higher-risk individuals. Despite these new findings, the factors that explain the heterogeneity in the risk of AP in MCS patients remain poorly understood, and more studies are required in this field. It has been demonstrated that both low-fat and low-carbohydrate diets are associated with TG reduction of ∼50% in these patients, allowing flexibility in the implementation of lifestyle interventions that may encourage better compliance. However, future studies in MCS patients should aim at investigating whether following these diets over a long-term period would result in a decreased risk of adverse outcomes such as AP, development of NAFLD, or cardiovascular events. In addition, the difference in the response to different diets or interventions according to the type of genetic predisposition should be investigated. This review highlights the importance of performing a genetic screening in patients with severe HTG in order to improve risk stratification and to identify potential candidates for new biologic therapies. However, several challenges surrounding the genetic characterization of these patients remain, such as the question of accessibility and cost. Furthermore, a large part of the severe HTG population is still genetically

undefined or carries variants of uncertain significance. It would be interesting to investigate if the use of omnigenic scores would result in an improved genetic characterization of MCS patients.

AUTHOR CONTRIBUTIONS

MP and SB: writing and editing. Both authors contributed to the article and approved the submitted version.

REFERENCES

1. Brahm A, Hegele RA. Hypertriglyceridemia. *Nutrients.* (2013) 5:981–1001. doi: 10.3390/nu5030981
2. Johansen CT, Kathiresan S, Hegele RA. Genetic determinants of plasma triglycerides. *J Lipid Res.* (2011) 52:189–206. doi: 10.1194/jlr.R009720
3. Ford ES, Li C, Zhao G, Pearson WS, Mokdad AH. Hypertriglyceridemia and its pharmacologic treatment among US adults. *Arch Intern Med.* (2009) 169:572–8. doi: 10.1001/archinternmed.2008.599
4. Berberich AJ, Ouédraogo AM, Shariff SZ, Hegele RA, Clemens KK. Incidence, predictors and patterns of care of patients with very severe hypertriglyceridemia in Ontario, Canada: a population-based cohort study. *Lipids Health Dis.* (2021) 20:98. doi: 10.1186/s12944-021-01517-6
5. Dron JS, Wang J, Cao H, McIntyre AD, Iacocca MA, Menard JR, et al. Severe hypertriglyceridemia is primarily polygenic. *J Clin Lipidol.* (2019) 13:80–8. doi: 10.1016/j.jacl.2018.10.006
6. Brahm AJ, Hegele RA. Chylomicronaemia–current diagnosis and future therapies. *Nat Rev Endocrinol.* (2015) 11:352–62. doi: 10.1038/nrendo.2015.26
7. Tremblay K, Méthot J, Brisson D, Gaudet D. Etiology and risk of lactescent plasma and severe hypertriglyceridemia. *J Clin Lipidol.* (2011) 5:37–44. doi: 10.1016/j.jacl.2010.11.004
8. Baass A, Paquette M, Bernard S, Hegele RA. Familial chylomicronemia syndrome: an under-recognized cause of severe hypertriglyceridaemia. *J Intern Med.* (2020) 287:340–8. doi: 10.1111/joim.13016
9. Goldberg RB, Chait A, A. Comprehensive update on the chylomicronemia syndrome. *Front Endocrinol.* (2020) 11:593931. doi: 10.3389/fendo.2020.593931
10. Warden BA, Minnier J, Duell PB, Fazio S, Shapiro MD. Chylomicronemia syndrome: familial or not? *J Clin Lipidol.* (2020) 14:201–6. doi: 10.1016/j.jacl.2020.01.014
11. Belhassen M, Van Ganse E, Nolin M, Bérard M, Bada H, Bruckert E, et al. 10-Year comparative follow-up of familial versus multifactorial chylomicronemia syndromes. *J Clin Endocrinol Metab.* (2021) 106:e1332–42. doi: 10.1210/clinem/dgaa838
12. Nordestgaard BG, Varbo A. Triglycerides and cardiovascular disease. *Lancet.* (2014) 384:626–35. doi: 10.1016/S0140-6736(14)61177-6
13. Valdivielso P, Ramírez-Bueno A, Ewald N. Current knowledge of hypertriglyceridemic pancreatitis. *Eur J Intern Med.* (2014) 25:689–94. doi: 10.1016/j.ejim.2014.08.008
14. Ewald N, Hardt PD, Kloer HU. Severe hypertriglyceridemia and pancreatitis: presentation and management. *Curr Opin Lipidol.* (2009) 20:497–504. doi: 10.1097/MOL.0b013e3283319a1d
15. Bálint ER, Fur G, Kiss L, Németh DI, Soós A, Hegyi P, et al. Assessment of the course of acute pancreatitis in the light of aetiology: a systematic review and meta-analysis. *Sci Rep.* (2020) 10:17936. doi: 10.1038/s41598-020-74943-8
16. Kiss L, Fur G, Mátrai P, Hegyi P, Iványi E, Cazacu IM, et al. The effect of serum triglyceride concentration on the outcome of acute pancreatitis: systematic review and meta-analysis. *Sci Rep.* (2018) 8:14096. doi: 10.1038/s41598-018-32337-x
17. Younossi ZM, Koenig AB, Abdelatif D, Fazel Y, Henry L, Wymer M. Global epidemiology of nonalcoholic fatty liver disease-Meta-analytic assessment of prevalence, incidence, and outcomes. *Hepatology.* (2016) 64:73–84. doi: 10.1002/hep.28431
18. Argo CK, Caldwell SH. Epidemiology and natural history of non-alcoholic steatohepatitis. *Clin Liver Dis.* (2009) 13:511–31. doi: 10.1016/j.cld.2009.07.005
19. Marchesini G, Brizi M, Bianchi G, Tomassetti S, Bugianesi E, Lenzi M, et al. Nonalcoholic fatty liver disease: a feature of the metabolic syndrome. *Diabetes.* (2001) 50:1844–50. doi: 10.2337/diabetes.50.8.1844
20. Kotronen A, Yki-Järvinen H. Fatty liver: a novel component of the metabolic syndrome. *Arterioscler Thromb Vasc Biol.* (2008) 28:27–38. doi: 10.1161/ATVBAHA.107.147538
21. Bedogni G, Miglioli L, Masutti F, Tiribelli C, Marchesini G, Bellentani S. Prevalence of and risk factors for nonalcoholic fatty liver disease: the Dionysos nutrition and liver study. *Hepatology.* (2005) 42:44–52. doi: 10.1002/hep.20734
22. Maltais M, Brisson D, Gaudet D. Non-alcoholic fatty liver in patients with chylomicronemia. *J Clin Med.* (2021) 10:669. doi: 10.3390/jcm10040669
23. Moulin P, Dufour R, Averna M, Arca M, Cefalù AB, Noto D, et al. Identification and diagnosis of patients with familial chylomicronaemia syndrome (FCS): expert panel recommendations and proposal of an "FCS score". *Atherosclerosis.* (2018) 275:265–72. doi: 10.1016/j.atherosclerosis.2018.06.814
24. Paquette M, Bernard S, Hegele RA, Baass A. Chylomicronemia: differences between familial chylomicronemia syndrome and multifactorial chylomicronemia. *Atherosclerosis.* (2019) 283:137–42. doi: 10.1016/j.atherosclerosis.2018.12.019
25. D'Erasmo L, Di Costanzo A, Cassandra F, Minicocci I, Polito L, Montali A, et al. Spectrum of mutations and long-term clinical outcomes in genetic chylomicronemia syndromes. *Arterioscler Thromb Vasc Biol.* (2019) 39:2531–41. doi: 10.1161/ATVBAHA.119.313401
26. O'Dea LSL, MacDougall J, Alexander VJ, Digenio A, Hubbard B, Arca M, et al. Differentiating familial chylomicronemia syndrome from multifactorial severe hypertriglyceridemia by clinical profiles. *J Endocr Soc.* (2019) 3:2397–410. doi: 10.1210/js.2019-00214
27. Rioja J, Ariza MJ, García-Casares N, Coca-Prieto I, Arrobas T, Muñiz-Grijalvo O, et al. Evaluation of the chylomicron-TG to VLDL-TG ratio for type I hyperlipoproteinemia diagnostic. *Eur J Clin Invest.* (2020) 50:e13345. doi: 10.1111/eci.13345
28. Tremblay K, Gaudet D, Khoury E, Brisson D. Dissection of clinical and gene expression signatures of familial versus multifactorial chylomicronemia. *J Endocr Soc.* (2020) 4:bvaa056. doi: 10.1210/jendso/bvaa056
29. Ariza MJ, Rioja J, Ibarretxe D, Camacho A, Díaz-Díaz JL, Mangas A, et al. Molecular basis of the familial chylomicronemia syndrome in patients from the national dyslipidemia registry of the spanish atherosclerosis society. *J Clin Lipidol.* (2018) 12:1482–92.e3. doi: 10.1016/j.jacl.2018.07.013
30. Paquette M, Amyot J, Fantino M, Baass A, Bernard S. Rare variants in triglycerides-related genes increase pancreatitis risk in multifactorial chylomicronemia syndrome. *J Clin Endocrinol Metab.* (2021) 106:e3473–82. doi: 10.1210/clinem/dgab360
31. de Graaf J, Couture P, Sniderman A. A diagnostic algorithm for the atherogenic apolipoprotein B dyslipoproteinemias. *Nat Clin Pract Endocrinol Metab.* (2008) 4:608–18. doi: 10.1038/ncpendmet0982
32. Hegele RA, Dron JS. 2019 George lyman duff memorial lecture: three decades of examining DNA in patients with dyslipidemia. *Arterioscler Thromb Vasc Biol.* (2020) 40:1970–81. doi: 10.1161/ATVBAHA.120.313065
33. Dron JS, Dilliott AA, Lawson A, McIntyre AD, Davis BD, Wang J, et al. Loss-of-function CREB3L3 variants in patients with severe hypertriglyceridemia. *Arterioscler Thromb Vasc Biol.* (2020) 40:1935–41. doi: 10.1161/ATVBAHA.120.314168
34. Glodowski M, Christen S, Saxon DR, Hegele RA, Eckel RH. Novel PPARG mutation in multiple family members with chylomicronemia. *J Clin Lipidol.* (2021) 15:431–4. doi: 10.1016/j.jacl.2021.03.006
35. Gill PK, Dron JS, Hegele RA. Genetics of hypertriglyceridemia and atherosclerosis. *Curr Opin Cardiol.* (2021) 36:264–71. doi: 10.1097/HCO.0000000000000839
36. Jin JL, Sun D, Cao YX, Zhang HW, Guo YL, Wu NQ, et al. Intensive genetic analysis for Chinese patients with very high triglyceride levels: Relations of

mutations to triglyceride levels and acute pancreatitis. *EBioMedicine.* (2018) 38:171–7. doi: 10.1016/j.ebiom.2018.11.001
37. Paquette M, Baass A. Polygenic risk scores for cardiovascular disease prediction in the clinical practice: are we there? *Atherosclerosis.* (2022) 340:46–7. doi: 10.1016/j.atherosclerosis.2021.11.030
38. Dron JS, Hegele RA. The evolution of genetic-based risk scores for lipids and cardiovascular disease. *Curr Opin Lipidol.* (2019) 30:71–81. doi: 10.1097/MOL.0000000000000576
39. Gill PK, Dron JS, Dilliott AA, McIntyre AD, Cao H, Wang J, et al. Ancestry-specific profiles of genetic determinants of severe hypertriglyceridemia. *J Clin Lipidol.* (2021) 15:88–96. doi: 10.1016/j.jacl.2020.11.007
40. Gagné C, Brun LD, Julien P, Moorjani S, Lupien PJ. Primary lipoprotein-lipase-activity deficiency: clinical investigation of a French Canadian population. *CMAJ.* (1989) 140:405–11.
41. Scherer J, Singh VP, Pitchumoni CS, Yadav D. Issues in hypertriglyceridemic pancreatitis: an update. *J Clin Gastroenterol.* (2014) 48:195–203. doi: 10.1097/01.mcg.0000436438.60145.5a
42. Christian JB, Arondekar B, Buysman EK, Johnson SL, Seeger JD, Jacobson TA. Clinical and economic benefits observed when follow-up triglyceride levels are less than 500 mg/dL in patients with severe hypertriglyceridemia. *J Clin Lipidol.* (2012) 6:450–61. doi: 10.1016/j.jacl.2012.08.007
43. Ginsberg HN, Elam MB, Lovato LC, Crouse JR 3rd, Leiter LA, Linz P, et al. Effects of combination lipid therapy in type 2 diabetes mellitus. *N Engl J Med.* (2010) 362:1563–74. doi: 10.1056/NEJMoa1001282
44. Whitfield-Brown L, Hamer O, Ellahi B, Burden S, Durrington P. An investigation to determine the nutritional adequacy and individuals experience of a very low fat diet used to treat type V hypertriglyceridaemia. *J Hum Nutr Diet.* (2009) 22:232–8. doi: 10.1111/j.1365-277X.2009.00945.x
45. Davidson M, Stevenson M, Hsieh A, Ahmad Z, Roeters van Lennep J, Crowson C, et al. The burden of familial chylomicronemia syndrome: results from the global IN-FOCUS study. *J Clin Lipidol.* (2018) 12:898–907.e2. doi: 10.1016/j.jacl.2018.04.009
46. Parks EJ. Effect of dietary carbohydrate on triglyceride metabolism in humans. *J Nutr.* (2001) 131:2772S—4. doi: 10.1093/jn/131.10.2772S
47. Fantino M, Paquette M, Blais C, Saint-Pierre N, Bourque L, Baass A, et al. Both low-fat and low-carbohydrate diets reduce triglyceride concentration in subjects with multifactorial chylomicronemia syndrome: a randomized crossover study. *Nutr Res.* (2022) 101:43–52. doi: 10.1016/j.nutres.2022.02.001
48. Gouni-Berthold I, Alexander VJ, Yang Q, Hurh E, Steinhagen-Thiessen E, Moriarty PM, et al. Efficacy and safety of volanesorsen in patients with multifactorial chylomicronaemia (COMPASS): a multicentre, double-blind, randomised, placebo-controlled, phase 3 trial. *Lancet Diabetes Endocrinol.* (2021) 9:264–75. doi: 10.1016/S2213-8587(21)00046-2
49. D'Erasmo L, Gallo A, Di Costanzo A, Bruckert E, Arca M. Evaluation of efficacy and safety of antisense inhibition of apolipoprotein C-III with volanesorsen in patients with severe hypertriglyceridemia. *Expert Opin Pharmacother.* (2020) 21:1675–84. doi: 10.1080/14656566.2020.1787380
50. Ahmad Z, Pordy R, Rader DJ, Gaudet D, Ali S, Gonzaga-Jauregui C, et al. Inhibition of angiopoietin-like protein 3 with evinacumab in subjects with high and severe hypertriglyceridemia. *J Am Coll Cardiol.* (2021) 78:193–5. doi: 10.1016/j.jacc.2021.04.091
51. Mozaffarian D, Maki KC, Bays HE, Aguilera F, Gould G, Hegele RA, et al. Effectiveness of a novel ω-3 krill oil agent in patients with severe hypertriglyceridemia: a randomized clinical trial. *JAMA Netw Open.* (2022) 5:e2141898. doi: 10.1001/jamanetworkopen.2021.41898

Conflict of Interest: SB received research grants from Akcea, Fondation Leducq and Fondation Yvan Morin. She has participated in clinical research protocols from Akcea, Amgen, Ionis Pharmaceuticals, Inc., The Medicines Company, Novartis, Pfizer and Sanofi. She has served on advisory boards for Akcea, Amgen, HLS Therapeutics, Novartis, Novo Nordisk and Sanofi, and received honoraria for symposia from Akcea, Amgen, Novo Nordisk and Sanofi.

The remaining author declares that the research was conducted in the absence of any commercial or financial relationships that could be construed as a potential conflict of interest.

Publisher's Note: All claims expressed in this article are solely those of the authors and do not necessarily represent those of their affiliated organizations, or those of the publisher, the editors and the reviewers. Any product that may be evaluated in this article, or claim that may be made by its manufacturer, is not guaranteed or endorsed by the publisher.

frontiers | Frontiers in Cardiovascular Medicine

OPINION
published: 26 April 2022
doi: 10.3389/fcvm.2022.895031

High Density Lipoprotein-Based Therapeutics: Novel Mechanism of Probucol in Foam Cells

Anouar Hafiane[1]*, *Annalisa Ronca*[2], *Robert S. Kiss*[1] and *Elda Favari*[2]

[1] Research Institute of the McGill University Health Center, Montreal, QC, Canada, [2] Department of Food and Drug, University of Parma, Parma, Italy

Keywords: probucol, cellular cholesterol efflux, atherosclerosis, foam cells/macrophages, HDL

Edited by:
Wilfried Le Goff, Institut National de la Santé et de la Recherche Médicale (INSERM), France

Reviewed by:
Maki Tsujita, Nagoya City University, Japan

***Correspondence:**
Anouar Hafiane
anouar.hafiane@mail.mcgill.ca

Specialty section:
This article was submitted to Lipids in Cardiovascular Disease, a section of the journal Frontiers in Cardiovascular Medicine

Received: *12 March 2022*
Accepted: *29 March 2022*
Published: *26 April 2022*

Citation:
Hafiane A, Ronca A, Kiss RS and Favari E (2022) High Density Lipoprotein-Based Therapeutics: Novel Mechanism of Probucol in Foam Cells. Front. Cardiovasc. Med. 9:895031. doi: 10.3389/fcvm.2022.895031

Since the 1970's, high density lipoprotein (HDL) has been an active research topic due to epidemiological studies, such as the Framingham study and many others, that established the inverse association between HDL cholesterol (HDL-C) levels and the prevalence of coronary heart disease (CHD) (1). The deceptive results of HDL-based therapies (inhibitors of cholesteryl ester transfer protein, niacin, and apolipoprotein A-I (apoA-I) infusion therapies), and Mendelian randomization approaches do not fully support a causal association between HDL-C and cardiovascular protection (2). Thus, the role of HDL in health and disease is more complex than anticipated (3). Consequently, there has been a paradigm shift in the study of HDL as a therapeutic target, from the measurement of HDL concentration to the evaluation of HDL function (i.e., cholesterol efflux capacity) (4). Growing evidence proposes that cardiovascular morbid conditions alter the HDL composition and roles transforming it from healthy and functional into pro-atherogenic and dysfunctional (5). A key player in the HDL metabolic pathway that has been substantially explored by various agonists is the ATP-binding cassette transporter A1 (ABCA1) defined as the rate-limiting factor in the formation of HDL (6). This transporter mediates cellular cholesterol and phospholipid removal to generate nascent HDL (nHDL). The most extensively studied function of HDL is the ability to promote net cellular cholesterol efflux. However, the regulation of ABCA1 receptor expression is complex and poorly understood and the physiological and clinical relevance of such a treatment remains uncertain. In the current issue of BBA Advances, we report the findings of our cellular studies on a new mechanism in foam cell macrophages that is ABCA1-independent, and revealed through the use of probucol (7). Although clinical trials were stopped (8), probucol is still being investigated for its effect on the inhibition of atherosclerosis initiation *in vitro* and in animal models. Of interest, probucol trials still ongoing suggest potential benefits on CHD on top of conventional therapy (9). Basically, probucol is known to act as an ABCA1 inhibitor (10), although the method of addition of probucol to cells or animals may explain some of the differences observed in the inhibitory activity. We show that probucol treated THP-1 foam cells are still able to induce the release of cholesterol-containing small nHDL particles with a diameter of more than 7 nm in an ABCA1-independent manner. In support, we demonstrate that ABCA1 expression is the same in non-foam and foam cells, despite different efflux levels. Quantitative data show that probucol only partially inhibits the transfer of cholesterol into nHDL particles. Interestingly, the release of these probucol-nHDL were active in HDL biogenesis, supporting the contention that these particles are potentially atheroprotective, especially when macrophage-derived cholesterol is involved (**Table 1**). Indeed, the ABCA1-independent activity influencing the total accessible plasma membrane cholesterol level that remains in foam cells is consistent with the concept that lipids within nHDL originate from specific domains in the plasma membrane. A previous study by Yamamoto et al. demonstrated that probucol enhanced

TABLE 1 | Summary of potential mechanisms of pharmacologic action of probucol.

Mechanism	Model	References
Inhibits ABCA1 cholesterol efflux activity	THP-1 and J774 cells	(11, 12)
ABCA1-independent activity in foam cells	THP-1 cells	(7)
Modification in lipid droplets morphology		
Increases LDL catabolism independent of the LDL receptor	Human fibroblasts	(13)
Probucol-Oxidized Products: Spiroquinone and diphenoquinone	RAW264.7 cells	(14)
Inhibit binding of lipid free apoA-I to the cells	Human fibroblast WI-38 HepG2	(15–17)
Protects ABCA1 from calpain-mediated degradation	THP-1 cells	(11)
Decreases micro-particles containing cholesterol release (50–250 nm)	THP-1, BHK, HEPG2 cells	(18)
Reduces xanthomas and atheromatous vascular lesions	UE-12 and THP-1 cells Tendon xanthomas	(19)
Inhibits cellular cholesterol efflux in cells	J774 mouse macrophages	(12)
Increases HDL biogenesis	THP-1 cells	(11)
Prevents foam cell formation	THP-1 cells	(19)
Activates nHDL formation in foam cells	THP-1 cells	(7)
Selective reduction in HDL2 particles size of FH patients*	FH patient's plasma	(19)
Prevents the oxidative modification of LDL	Rabbit aortic endothelial cells	(20)
Increases plasma LCAT, CETP activities, and apoE concentration**	FH patient's plasma	(21)
Improve HDL function (anti-inflammatory and anti-oxidant)	New Zealand white rabbits	(22)

ABCA1, ATP-binding cassette transporter A1; THP-1, Tamm–Horsfall protein 1; LDL, low density lipoprotein; nHDL, nascent high density lipoprotein; ApoA-I, apolipoprotein A-I; BHK, baby hamster kidney cells; LCAT, lecithin-cholesterol acyltransferase; CETP, cholesteryl ester transfer protein; FH, familial hypercholesterolemia.

**Smaller HDL particles may be biologically more active and beneficial to the reverse cholesterol transport from peripheral tissue to the liver (19).*

***This was viewed as consistent with a postulated increase in reverse cholesterol transport via the remnant pathway (23).*

the release of cholesterol from foam cells but with no description of ABCA1's role (11, 14–16, 19). Despite a paradox surrounding the lipid lowering effect of probucol (**Table 1**), these findings align with data supporting the potential antiatherogenic role of probucol. Indeed, previous studies indicated positive effects of probucol on atherosclerosis treatments *in vitro* and *in vivo* (19, 24, 25), however some clinical data indicated negative effects of probucol (26). In addition, a role of probucol was observed in reducing micro-particles release mainly those rich in cholesterol with size range from various cell lines (50–250 nm) (**Table 1**) (18). Use of probucol unveiled a novel and specific pathway in foam cells where functional cholesterol efflux and formation of nHDL is enhanced in the absence of ABCA1 activity. This activity was not observed in non-foam cells. Moreover, probucol incorporation significantly influences lipid droplet morphology and size (7). This is relevant to lipids droplets roles in mammalian innate immunity, triglyceride synthesis, and mitochondrial dynamics (27, 28). These observations will clarify the mechanisms by which HDL can be protective especially in foam cells. However, the physiological and clinical importance of such approaches remains to elucidated, and substantial additional preclinical work will be required. Exploring new HDL generating pathways that enhance cholesterol efflux is a prospect of a completely novel strategy to raising plasma HDL concentration for CHD prevention that might succeed where other approaches have failed. However, because of the unsatisfactory track record of HDL-based therapies, further research is imperative before renewing our enthusiasm for HDL as a target for therapy. Despite the fact that we have not the ability of probucol to enhance an ABCA1-independent pathway, we suggest the possibility to use probucol as a tool to probe intracellular cholesterol trafficking to inhibit ABCA1. Overall, this may provide substantial evidence for a revised model of cholesterol trafficking in macrophages foam cells. In our opinion this is a new argument in HDL metabolism among cardiovascular researchers if probucol has clinical significance. There is compelling purposes to believe that this old controversial medication has much more to offer than previously known.

AUTHOR CONTRIBUTIONS

AH conceptualized, wrote, edited, and revised the manuscript. AR, RK, and EF edited and revised the manuscript. All authors approved the submitted version.

FUNDING

AH received support by Postdoctoral Fellowships from the Canadian Institutes of Health Research (CIHR, RN408399 – 430975).

REFERENCES

1. Gordon T, Castelli WP, Hjortland MC, Kannel WB, Dawber TR. High density lipoprotein as a protective factor against coronary heart disease. The Framingham study. *Am J Med.* (1977) 62:707–14. doi: 10.1016/0002-9343(77)90874-9
2. Frikke-Schmidt R, Nordestgaard BG, Stene MC, Sethi AA, Remaley AT, Schnohr P, et al. Association of loss-of-function mutations in the ABCA1

gene with high-density lipoprotein cholesterol levels and risk of ischemic heart disease. *J Am Med Assoc.* (2008) 299:2524–32. doi: 10.1001/jama.299.21.2524
3. Ndrepepa G. High-density lipoprotein: a double-edged sword in cardiovascular physiology and pathophysiology. *J Lab Precision Med.* (2021) 6:32. doi: 10.21037/jlpm-21-32
4. Sacks FM, Jensen MK. From high-density lipoprotein cholesterol to measurements of function: prospects for the development of tests for high-density lipoprotein functionality in cardiovascular disease. *Arterioscler Thromb Vasc Biol.* (2018) 38:487–99. doi: 10.1161/ATVBAHA.117.307025
5. Chiesa ST, Charakida M. High-density lipoprotein function and dysfunction in health and disease. *Cardiovasc Drugs Ther.* (2019) 33:207–19. doi: 10.1007/s10557-018-06846-w
6. Bielicki JK. ABCA1 agonist peptides for the treatment of disease. *Curr Opin Lipidol.* (2016) 27:40–6. doi: 10.1097/MOL.0000000000000258
7. Hafiane A, Pisaturo A, Ronca A, Incerti M, Kiss RS, Favari E. Probucol treatment is associated with an ABCA1-independent mechanism of cholesterol efflux to lipid poor apolipoproteins from foam cell macrophages. *BBA Adv.* (2021) 1:100003. doi: 10.1016/j.bbadva.2021.100003
8. Miida T, Seino U, Miyazaki O, Hanyu O, Hirayama S, Saito T, et al. Probucol markedly reduces HDL phospholipids and elevated prebeta1-HDL without delayed conversion into alpha-migrating HDL: putative role of angiopoietin-like protein 3 in probucol-induced HDL remodeling. *Atherosclerosis.* (2008) 200:329–35. doi: 10.1016/j.atherosclerosis.2007.12.031
9. Yamashita S, Arai H, Bujo H, Masuda D, Ohama T, Ishibashi T, et al. Probucol trial for secondary prevention of atherosclerotic events in patients with coronary heart disease (prospective). *J Atheroscler Thromb.* (2021) 28:103–23. doi: 10.5551/jat.55327
10. Yamamoto S, Tanigawa H, Li X, Komaru Y, Billheimer JT, Rader DJ. Pharmacologic suppression of hepatic ATP-binding cassette transporter 1 activity in mice reduces high-density lipoprotein cholesterol levels but promotes reverse cholesterol transport. *Circulation.* (2011) 124:1382–90. doi: 10.1161/CIRCULATIONAHA.110.009704
11. Arakawa R, Tsujita M, Iwamoto N, Ito-Ohsumi C, Lu R, Wu CA, et al. Pharmacological inhibition of ABCA1 degradation increases HDL biogenesis and exhibits antiatherogenesis. *J Lipid Res.* (2009) 50:2299–305. doi: 10.1194/jlr.M900122-JLR200
12. Favari E, Zanotti I, Zimetti F, Ronda N, Bernini F, Rothblat GH. Probucol inhibits ABCA1-mediated cellular lipid efflux. *Arterioscler Thromb Vasc Biol.* (2004) 24:2345–50. doi: 10.1161/01.ATV.0000148706.15947.8a
13. Basu SK, Goldstein JL, Anderson GW, Brown MS. Degradation of cationized low density lipoprotein and regulation of cholesterol metabolism in homozygous familial hypercholesterolemia fibroblasts. *Proc Natl Acad Sci USA.* (1976) 73:3178–82. doi: 10.1073/pnas.73.9.3178
14. Yakushiji E, Ayaori M, Nishida T, Shiotani K, Takiguchi S, Nakaya K, et al. Probucol-oxidized products, spiroquinone and diphenoquinone, promote reverse cholesterol transport in mice. *Arterioscler Thromb Vasc Biol.* (2016) 36:591–7. doi: 10.1161/ATVBAHA.115.306376
15. Tsujita M, Wu CA, Abe-Dohmae S, Usui S, Okazaki M, Yokoyama S. On the hepatic mechanism of HDL assembly by the ABCA1/apoA-I pathway. *J Lipid Res.* (2005) 46:154–62. doi: 10.1194/jlr.M400402-JLR200
16. Wu CA, Tsujita M, Hayashi M, Yokoyama S. Probucol inactivates ABCA1 in the plasma membrane with respect to its mediation of apolipoprotein binding and high density lipoprotein assembly and to its proteolytic degradation. *J Biol Chem.* (2004) 279:30168–74. doi: 10.1074/jbc.M403765200
17. Tsujita M, Yokoyama S. Selective inhibition of free apolipoprotein-mediated cellular lipid efflux by probucol. *Biochemistry.* (1996) 35:13011–20. doi: 10.1021/bi960734h
18. Hafiane A, Genest J. ATP binding cassette A1 (ABCA1) mediates microparticle formation during high-density lipoprotein (HDL) biogenesis. *Atherosclerosis.* (2017) 257:90–9. doi: 10.1016/j.atherosclerosis.2017.01.013
19. Yamamoto A, Hara H, Takaichi S, Wakasugi J, Tomikawa M. Effect of probucol on macrophages, leading to regression of xanthomas and atheromatous vascular lesions. *Am J Cardiol.* (1988) 62:31b-6b. doi: 10.1016/S0002-9149(88)80048-1
20. Parthasarathy S, Young SG, Witztum JL, Pittman RC, Steinberg D. Probucol inhibits oxidative modification of low density lipoprotein. *J Clin Invest.* (1986) 77:641–4. doi: 10.1172/JCI112349
21. Adlouni A, El Messal M, Saïle R, Parra H, Fruchart J, Ghalim N. Probucol promotes reverse cholesterol transport in heterozygous familial hypercholesterolemia. Effects on apolipoprotein AI-containing lipoprotein particles. *Atherosclerosis.* (2000) 152:433–40. doi: 10.1016/S0021-9150(99)00493-1
22. Zhong J-K, Guo Z-G, Li C, Wang Z-K, Lai W-Y, Tu Y. Probucol alleviates atherosclerosis and improves high density lipoprotein function. *Lipids Health Dis.* (2011) 10:210. doi: 10.1186/1476-511X-10-210
23. McPherson R, Hogue M, Milne RW, Tall AR, Marcel YL. Increase in plasma cholesteryl ester transfer protein during probucol treatment. Relation to changes in high density lipoprotein composition. *Arteriosclerosis Thrombosis.* (1991) 11:476–81. doi: 10.1161/01.ATV.11.3.476
24. Yamamoto A, Takaichi S, Hara H, Nishikawa O, Yokoyama S, Yamamura T, et al. Probucol prevents lipid storage in macrophages. *Atherosclerosis.* (1986) 62:209–17. doi: 10.1016/0021-9150(86)90095-X
25. Kita T, Nagano Y, Yokode M, Ishii K, Kume N, Ooshima A, et al. Probucol prevents the progression of atherosclerosis in Watanabe heritable hyperlipidemic rabbit, an animal model for familial hypercholesterolemia. *Proc Natl Acad Sci USA.* (1987) 84:5928–31. doi: 10.1073/pnas.84.16.5928
26. Yokoyama S, Yamamoto A, Kurasawa T. A little more information about aggravation of probucol-induced HDL-reduction by clofibrate. *Atherosclerosis.* (1988) 70:179–81. doi: 10.1016/0021-9150(88)90114-1
27. Bosch M, Sánchez-Álvarez M, Fajardo A, Kapetanovic R, Steiner B, Dutra F, et al. Mammalian lipid droplets are innate immune hubs integrating cell metabolism and host defense. *Science.* (2020) 370:aay8085. doi: 10.1126/science.aay8085
28. Benador IY, Veliova M, Mahdaviani K, Petcherski A, Wikstrom JD, Assali EA, et al. Mitochondria bound to lipid droplets have unique bioenergetics, composition, and dynamics that support lipid droplet expansion. *Cell Metabol.* (2018) 27:869–85.e6. doi: 10.1016/j.cmet.2018.03.003

Conflict of Interest: The authors declare that the research was conducted in the absence of any commercial or financial relationships that could be construed as a potential conflict of interest.

frontiers | Frontiers in Cardiovascular Medicine

ORIGINAL RESEARCH
published: 10 May 2022
doi: 10.3389/fcvm.2022.859567

Comparison of Low-Density Lipoprotein Cholesterol (LDL-C) Goal Achievement and Lipid-Lowering Therapy in the Patients With Coronary Artery Disease With Different Renal Functions

*Shuang Zhang, Zhi-Fan Li, Hui-Wei Shi, Wen-Jia Zhang, Yong-Gang Sui, Jian-Jun Li, Ke-Fei Dou, Jie Qian and Na-Qiong Wu**

Cardiometabolic Center, National Center for Cardiovascular Diseases, Fuwai Hospital, Chinese Academy of Medical Science & Peking Union Medical College, Beijing, China

OPEN ACCESS

Edited by:
Yiliang Chen,
Medical College of Wisconsin, United States

Reviewed by:
Yafeng Li,
The Fifth Hospital of Shanxi Medical University, China
Fang Li,
Columbia University Irving Medical Center, United States

***Correspondence:**
Na-Qiong Wu
fuwainaqiongwu@163.com

Specialty section:
This article was submitted to Lipids in Cardiovascular Disease, a section of the journal Frontiers in Cardiovascular Medicine

Received: *21 January 2022*
Accepted: *08 April 2022*
Published: *10 May 2022*

Citation:
Zhang S, Li Z-F, Shi H-W, Zhang W-J, Sui Y-G, Li J-J, Dou K-F, Qian J and Wu N-Q (2022) Comparison of Low-Density Lipoprotein Cholesterol (LDL-C) Goal Achievement and Lipid-Lowering Therapy in the Patients With Coronary Artery Disease With Different Renal Functions. Front. Cardiovasc. Med. 9:859567. doi: 10.3389/fcvm.2022.859567

Aim: The aim of this study was to evaluate the relationship between renal function and low-density lipoprotein cholesterol (LDL-C) goal achievement and compare the strategy of lipid-lowering therapy (LLT) among the patients with coronary artery disease (CAD) with different renal functions.

Methods: In this study, we enrolled 933 Chinese patients with CAD from September 2020 to June 2021 admitted to the Cardiometabolic Center of Fuwai Hospital in Beijing consecutively. All individuals were divided into two groups based on their estimated glomerular filtration rate (eGFR). The multiple logistical regression analysis was performed to identify and compare the independent factors which impacted LDL-C goal achievement in the two groups after at least 3 months of treatment.

Results: There were 808 subjects with eGFR $\geq$ 60 ml/min/1.73 m^2 who were divided into Group 1 (G1). A total of 125 patients with eGFR $<$ 60 ml/min/1.73 m^2 were divided into Group 2 (G2). The rate of LDL-C goal attainment (LDL-C $<$ 1.4 mmol/L) was significantly lower in G2 when compared with that in G1 (24.00% vs. 35.52%, $P = 0.02$), even though there was no significant difference in the aspect of LLT between the two groups (high-intensity LLT: 82.50% vs. 85.60% $P = 0.40$). Notably, in G1, the proportion of LDL-C goal achievement increased with the intensity of LLT (23.36% vs. 39.60% vs. 64.52% in the subgroup under low-/moderate-intensity LLT, or high-intensity LLT without proprotein convertase subtilisin/kexin type 9 (PCSK9) inhibitor (PCSK9i), or high-intensity LLT with PCSK9i, respectively, $P < 0.005$). In addition, in G2, there was a trend that the rate of LDL-C goal achievement was higher in the subgroup under high-intensity LLT (26.60% in the subgroup under high-intensity LLT without PCSK9i and 25.00% in the subgroup under high-intensity LLT with PCSK9i) than that under low-/moderate-intensity LLT (15.38%, $P = 0.49$). Importantly, after multiple regression analysis, we found that eGFR $<$ 60 ml/min/1.73 m^2 [odds ratio (OR) 1.81; 95%CI, 1.15–2.87; $P = 0.01$] was an

independent risk factor to impact LDL-C goal achievement. However, the combination strategy of LLT was a protective factor for LDL-C goal achievement independently (statin combined with ezetimibe: OR 0.42; 95%CI 0.30–0.60; $P < 0.001$; statin combined with PCSK9i: OR 0.15; 95%CI 0.07–0.32; $P < 0.001$, respectively).

Conclusion: Impaired renal function (eGFR < 60 ml/min/1.73 m^2) was an independent risk factor for LDL-C goal achievement in the patients with CAD. High-intensity LLT with PCSK9i could improve the rate of LDL-C goal achievement significantly. It should be suggested to increase the proportion of high-intensity LLT with PCSK9i for patients with CAD, especially those with impaired renal function.

Keywords: coronary artery disease, renal function, LDL-C, goal achievement, lipid-lowing therapy

INTRODUCTION

In the past decades, the global prevalence of arteriosclerotic cardiovascular disease (ASCVD) has increased considerably; especially, coronary artery disease (CAD) is the leading cause of mortality and morbidity worldwide. Lipid-lowering therapy (LLT) plays an important role in the treatment of CAD by reducing plasma low-density lipoprotein cholesterol (LDL-C) levels (1). Statin is the cornerstone of LLT. Furthermore, ezetimibe and proprotein convertase subtilisin/kexin type 9 (PCSK9) inhibitors (PCSK9i) are important non-statin lipid-lowering choices.

As the chronic disease, chronic kidney disease (CKD) is a gradual loss of renal function over years and is characterized by an estimated glomerular filtration rate (eGFR) of <60 ml/min/1.73 m^2 (1, 2). The burden of CKD is substantial worldwide. More than 10% of the population were affected by the CKD and the death rate caused by CKD will increase to get 14 per 100,000 people by 2030 (2). CKD has close ties with chronic inflammation, increased oxidative stress and dyslipidemia, and these abnormalities elevate the cardiovascular risk (2, 3). With the eGFR declines and kidney disease progresses from CKD stage Group 1 (G1) to stage Group 5 (G5), the proportion of patients with CKD who die from the cardiovascular disease will increase. Atherosclerotic cardiovascular events represent the most cause of death in patients with CKD (2–5). Renal dysfunction is closely related to dyslipidemia (1, 4). Dyslipidemia in CKD is characterized by hypertriglyceridemia and low high-density lipoprotein (HDL), which is major risk factors for CAD. In the early stages of renal dysfunction, patients with CKD may develop dyslipidemia. Dyslipidemia progresses with deterioration of renal function (4). Unfortunately, previous studies have showed that the rate of LDL-C goal achievement (LDL-C < 1.8 mmol/L) was low in the patients with ASCVD (1). Moreover, the latest ESC/EAS guideline recommended that all patients with ASCVD should control their LDL-C level more strictly, lower than 1.4 mmol/L, and reduction ≥ 50% from baseline (6). Currently, there were limited studies focusing on the relationship between the renal function and the rate of LDL-C goal achievement in patients with CAD at the era of PCSK9 inhibitors. The aim of our study was to identify if the renal function is the independent risk factor to impact the selection of high-intensity LLT (especially high-intensity LLT with PCSK9i)or LDL-C goal achievement in real clinical practice.

METHODS

Study Design and Patient Selection

This study was a prospective, observational cohort study. We enrolled 933 patients with CAD consecutively in the Cardiometabolic Center of Fuwai Hospital (Beijing, China) from September 2020 and June 2021. The inclusion criteria included: 1) coronary angiography showing at least one coronary artery (left anterior descending artery, left circumflex artery, or right coronary artery) stenosis ≥50% and 2) detailed medical records and laboratory data. The exclusion criteria included: 1) severe hepatic dysfunction (aspartate aminotransferase [AST] or/and alanine aminotransferase [ALT] > 3 times the upper limit of normal, 2) life expectancy < 3 months, 3) severe blood system disease, systematic inflammatory disease, and malignant disease, 4) contraindication to any LLT, 5) severe renal dysfunction, including CKD Stages 4–5 or dialysis, and 6) receiving some medicines, such as cyclosporine treatment for CKD, which could influence serum concentration of lipid-lowering medicines.

All participants were divided into two groups, and the patients with eGFR ≥ 60 ml/min/1.73 m^2 were in Group 1 (G1) and those with eGFR < 60 ml/min/1.73 m^2 were in Group 2 (G2). Hypertension was diagnosed by systolic blood pressure (SBP) ≥ 140 mmHg and/or diastolic blood pressure (DBP) ≥ 90 mmHg or receiving antihypertensive therapy. If the fasting plasma glucose was at least 7.0 mmol/L or the patient's 2-h plasma glucose from the oral glucose tolerance test was at least 11.1 mmol/L, or those receiving hypoglycemic treatment, the patients were considered diabetes mellitus (DM). The high-intensity LLT was defined as high-intensity statins (rosuvastatin 20 mg per day or atorvastatin 40–80 mg per day), any-dose statin plus ezetimibe, any-dose statin plus PCSK9i with (or without) ezetimibe, and ezetimibe with PCSK9i or PCSK9i monotherapy, while low-/moderate-intensity LLT was defined as low/moderate statin monotherapy or ezetimibe monotherapy.

Laboratory Tests

All patients' plasma samples were collected in the morning after overnight fasting. Plasma levels of lipid profile (e.g., total cholesterol [TC], LDL-C, triglyceride [TG], HDL-C, apoA, and apoB) were measured by an automatic biochemistry analyzer (Hitachi 7150, Tokyo, Japan). The serum Lp(a) levels were measured through an immune-turbidimetry assay (LASAY Lp(a) auto; SHIMA Laboratories, Tokyo, Japan).

Follow-Up

The patients were followed up in 3 months of intervals through telephone or clinical interview. The discontinuation of LLT means that the patients did not take lipid-lowering medicine for >30 days.

Statistical Analysis

The Kolmogorov–Smirnov test was used to test the distribution pattern. Continuous variables (mean ± SD) and medians with interquartile ranges between the two groups were compared using the unpaired Student's *t*-test or the Mann–Whitney *U* test. Categorical variables (frequencies) were compared using chi-square statistics or the Fisher exact test. The univariate and multiple logistic regression models were constructed to calculate adjusted odds ratios (OR) and 95% confidence intervals (CIs) for the factors that impact LDL-C target achievement. All statistical testing was 2-sided at a significance level of 0.05. Analyses were performed using the R language statistical software (version 4.0.4, Feather Spray; The R Foundation for Statistical Computing, Vienna, Austria).

RESULTS

Patient Characteristics

The demographic and clinical characteristics of 933 patients are presented in **Table 1**. In G1, there were 808 patients with eGFR $\geq$ 60 ml/min/1.73 m^2. In addition, 125 patients with eGFR < 60 ml/min/1.73 m^2 were divided into G2. In the whole participants, the average age was 58.4 ± 10.1 years, 74.91% of patients were men, and the mean eGFR was 76.0 (65.0–86.0) ml/min/1.73 m^2. However, the patients in G2 were older (63.45 ± 8.84 vs. 57.6 ± 9.99 years, $P < 0.0001$) and there were only few male patients in G2 (58.4% vs. 77.48%, $P < 0.0001$). In G2, there tended to be more comorbidities, such as hypertension (76.0% vs. 57.67%, $P < 0.0001$), DM (40.8% vs. 27.72%, $P = 0.004$), and peripheral vascular disease (6.40% vs. 2.48%, $P = 0.03$). Current smoking was prevalent in G1 (41.34% vs. 28.0%, $P = 0.01$). As for the lipid profiles, TG was significantly higher in G2 [1.66 (1.19–2.30) mmol/L vs. 1.45 (1.05–2.06) mmol/L, $P = 0.01$]. There were no significant differences in TC, HDL-C, and LDL-C levels in both the groups.

Strategy of LLT at the Baseline and Follow-Up Period

In **Table 2**, high-intensity LLT (low-/moderate-intensity statin + ezetimibe) was the most common strategy at baseline (78.09% in G1 vs. 80.06% in G2) and during the follow-up (66.71% in G1 vs. 74.40% in G2) period. There was no significant difference in strategies of LLT between the two groups at baseline ($P = 0.41$, **Figure 1**) and at follow-up period ($P = 0.11$, **Figure 1**). In addition, PCSK9i application was relatively low in both groups at baseline (3.77% in G1 vs. 3.20% in G2) and during the follow-up period (3.83% in G1 vs. 3.2% in G2). Moreover, at baseline, atorvastatin was the most common prescription in statins (48.32%), followed by rosuvastatin (32.98%) (**Figure 2**). Very low proportions (1.07%) of subjects were under LLT with high-intensity statin monotherapy.

The average LDL-C level during the follow-up period was higher in G2 than in G1 (1.91 ± 0.68 mmol/L in G2 vs. 1.71 ± 0.68 mmol/L in G1, $P = 0.0022$). The percentage of LDL-C target achievement (<1.4 mmol/L) was 35.52% in G1 and 24.00% in G2, respectively ($P = 0.02$, **Table 3**).

The proportion of high-intensity LLT strategy had a trend to be higher in G2 than that in G1 during the follow-up period (78.20% without PCSK9i and 3.20% including PCSK9i in G2 vs. 68.45% without PCSK9i and 3.20% including PCSK9i in G1, $P = 0.11$). In addition, the proportion of high-intensity LLT was significantly lower during the follow-up period than that at baseline in G1 (78.88% without PCSK9i and 3.77% including PCSK9i at baseline vs. 68.45% without PCSK9i and 3.20% including PCSK9i during follow-up in G1, $P < 0.005$). However, the proportion of high-intensity LLT did not significantly change in G2 during the follow-up period than that at baseline (81.77% without PCSK9i and 3.83% including PCSK9i at baseline vs. 78.20% without PCSK9i and 3.20% including PCSK9i during follow-up, $P = 0.14$) (**Figure 3**).

Attainment of LDL-C Goal During the Follow-Up Period

In **Table 3**, it summarized the percentage of patients achieving LDL-C target and lipid profiles during the follow-up period. After ≥3 months of LLT treatment, the rate of LDL-C < 1.4 mmol/L increased up to 33.99%. However, the rate of LDL-C goal achievement was lower in G2 compared with that in G1 (24.00% vs. 35.52%, $P = 0.02$). The average LDL-C level in G2 was higher than that in G1 during the follow-up period (1.91 ± 0.68 mmol/L vs. 1.71 ± 0.68 mmol/L, $P = 0.0022$).

The patients with the high-intensity LLT are more prone to achieve the LDL-C goal (high-intensity LLT with PCSK9i: 60.0%; high-intensity LLT without PCSK9i: 37.7%; low-/moderate-intensity LLT: 22.50%, $P < 0.005$). In G1, the proportion of LDL-C goal achievement (LDL-C < 1.4 mmol/L) increased with the intensity of LLT (23.36% vs. 39.60% vs. 64.52% in the subgroup under low-/moderate-intensity LLT, or high-intensity LLT without PCSK9i, or high-intensity LLT with PCSK9i, respectively, $P < 0.005$). In addition, in G2, there was a trend that the rate of LDL-C goal achievement was higher in the subgroup under high-intensity LLT (26.60% in the subgroup under high-intensity LLT without PCSK9i, 25.00% in the subgroup under high-intensity LLT with PCSK9i) than that under low-/moderate-intensity LLT (15.38%), even though the difference was not statistically significant ($P = 0.49$, **Figure 3**).

TABLE 1 | The baseline characteristics of total participants including G1 and G2.

Characteristics	Total (n = 933)	G1 (n = 808)	G2 (n = 125)	P-value
Male	699 (74.91)	626 (77.48)	73 (58.40)	<0.0001
Age	58.4 ± 10.10	57.60 ± 9.99	63.45 ± 8.84	<0.0001
BMI,kg/m^2	26.06 ± 3.15	25.99 ± 3.15	26.49 ± 3.09	0.10
SBP,mm Hg	136.91 ± 17.19	136.79 ± 17.09	137.68 ± 17.93	0.59
DBP,mm Hg	78.87 ± 10.54	79.01 ± 10.57	77.95 ± 10.34	0.30
History of PCI	256 (27.43)	215 (26.61)	41 (32.80)	0.18
History of CABG	11 (1.17)	8 (0.99)	3 (2.40)	0.36
History of MI	106 (11.36)	87 (10.77)	19 (15.20)	0.19
PAD	28 (3.0)	20 (2.48)	8 (6.40)	0.03
Stroke	55 (5.89)	50 (6.19)	5 (4.00)	0.45
Hypertension	561 (60.12)	466 (57.67)	95 (76.00)	<0.0001
Hyperlipidemia	631 (67.63)	537 (66.46)	94 (75.20)	0.07
DM	275 (29.47)	224 (27.72)	51 (40.80)	0.004
Current smoking	369 (39.55)	334 (41.34)	35 (28.00)	0.01
History of CAD	95 (10.18)	85 (10.52)	10 (8.00)	0.48
LVEF	62.09 ± 5.84	62.27 ± 5.41	60.92 ± 8.03	0.02
GLU,mmol/L	7.03 ± 2.72	6.90 ± 2.53	7.89 ± 3.63	0.0001
Scr,umol/L	86.76 ± 19.97	82.89 ± 13.19	111.69 ± 33.74	<0.0001
Bun,mmol/L	5.89 ± 1.55	5.74 ± 1.47	6.84 ± 1.69	<0.0001
TG, mmol/L	1.48 (1.07–2.08)	1.45 (1.05–2.06)	1.66 (1.19–2.30)	0.01
TC, mmol/L	4.05 ± 1.07	4.03 ± 1.06	4.15 ± 1.11	0.26
HDL, mmol/L	1.15 ± 0.31	1.15 ± 0.31	1.16 ± 0.34	0.72
LDL, mmol/L	2.31 ± 0.88	2.30 ± 0.87	2.39 ± 0.95	0.26
LDL<1.4mmol/L	108 (11.58)	94 (11.63)	14 (11.20)	1.00
LDL<1.8mmol/L	274 (29.36)	243 (30.07)	31 (24.80)	0.27
eGFR,ml/min/1.73m^2	76.0 (65.0–86.0)	94.2 (75.9–112.49)	54.13 (53.11–55.15)	<0.0001
Lp (a),mg/L	183.99 (77.10–399.10)	190.17 (78.36–403.54)	164.52 (70.26–397.24)	0.49
hs-crp,mg/L	2.01 ± 2.64	1.97 ± 2.62	2.30 ± 2.81	0.20
apoA,g/L	1.23 ± 0.24	1.22 ± 0.24	1.26 ± 0.23	0.15
apoB,g/L	0.73 (0.59–0.89)	0.73 (0.58–0.88)	0.74 (0.62–0.90)	0.37
nt-proBNP	207.22 ± 524.83	180.60 ± 425.06	378.42 ± 925.84	0.0001
HbA1C,%	6.59 ± 1.65	6.53 ± 1.61	7.05 ± 1.84	0.0011
Medications at baseline				
Statins	667 (71.49)	570 (70.54)	97 (77.60)	0.13
Aspirin	671 (71.92)	579 (71.66)	92 (73.60)	0.73
Clopidogrel	301 (32.26)	257 (31.81)	44 (35.20)	0.51
β-blockers	381 (40.84)	330 (40.84)	51 (40.80)	1
Nitrate	325 (34.83)	278 (34.41)	47 (37.60)	0.55
Calcium channel blockers	159 (17.04)	125 (15.47)	34 (27.20)	0
ACEI/ARB	193 (20.69)	161 (19.93)	32 (25.60)	0.18
Diuretic	10 (1.07)	8 (0.99)	2 (1.60)	0.88

BMI, body mass index; CABG, coronary artery bypass graft; PCI, percutaneous coronary intervention; MI, myocardial infarction; SBP, systolic blood pressure; DBP, diastolic blood pressure; DM, diabetes mellitus; LVEF, left ventricular ejection fraction; eGFR estimated glomerular filtration rate; TC, total cholesterol; TG, triglyceride; HDL-C, high-density lipoprotein; LDL-C, low-density lipoprotein; hs-CRP, high-sensitivity C-reactive protein; Scr, serum creatinine; Bun, blood urea nitrogen; apoA; NT-proBNP, N-terminal pro-brain natriuretic peptide; Lp(a), lipoprotein(a); Continuous variables are presented as mean ± SD or medians with interquartile ranges. Categorical variables are presented as proportions.

Factors That Impact LDL-C Goal Achievement

After multivariate logistic regression analysis, previous percutaneous coronary intervention (OR 0.55; 95%CI 0.39–0.77; $P < 0.001$), admission for acute coronary syndrome (ACS) (OR 0.65; 95%CI 0.46–0.91; $P = 0.01$), LLT including statin combination with ezetimibe (OR 0.42; 95%CI 0.3–0.6; $P < 0.001$), and LLT including statin and/or ezetimibe combination with PCSK9i (OR 0.15; 95CI% 0.07–0.32; $P < 0.001$) were all significantly associated with LDL-C goal achievement. In addition, DM (OR 1.50; 95%CI 1.09–2.02; $P = 0.001$), female patients (OR 1.66; 95%CI 1.13–2.44; $P = 0.009$) were significantly

TABLE 2 | Comparison of the lipid-lowering therapy (LLT) strategies between the two groups at baseline and follow-up period.

	Total ($n = 933$)	G1 ($n = 808$)	G2 ($n = 125$)
Baseline, *n* (%)			
Low/moderate intensity LLT			
Low/moderate intensity statin alone	149 (15.97)	132 (16.34)	17 (13.60)
Ezetimibe alone	8 (0.87)	7 (0.87)	1 (0.80)
High intensity LLT			
Low/moderate intensity statin+Ezetimibe	733 (78.56)	631 (78.09)	102 (81.60)
Moderate intensity statin+Ezetimibe+PCSK9i	27 (2.89)	25 (3.09)	2 (1.60)
High intensity statin+Ezetimibe	7 (0.75)	6 (0.74)	1 (0.80)
Moderate intensity statin+PCSK9i	4 (0.43)	2 (0.25)	2 (1.60)
High intensity statin+Ezetimibe+PCSK9i	2 (0.21)	2 (0.25)	0 (0.00)
High intensity statin	1 (0.16)	1 (0.18)	0 (0.00)
Ezetimibe+PCSK9i	1 (0.16)	1 (0.18)	0 (0.00)
Follow-up, *n* (%)			
Low/moderate intensity LLT			
Low/moderate intensity statin alone	225 (24.12)	200 (24.75)	25 (20.00)
Ezetimibe alone	15 (1.61)	14 (1.73)	1 (0.80)
High intensity LLT			
Low/moderate intensity statin+Ezetimibe	632 (67.74)	539 (66.71)	93 (74.40)
Low/moderate intensity statin+Ezetimibe+PCSK9i	25 (2.68)	23 (2.85)	2 (1.60)
High intensity statin+Ezetimibe	9 (0.96)	8 (0.99)	1 (0.80)
Low/moderate intensity statin+PCSK9i	8 (0.86)	6 (0.74)	2 (1.60)
PCSK9i alone	1 (0.11)	1 (0.12)	0 (0.00)
High intensity statin	1 (0.11)	1 (0.12)	0 (0.00)
High intensity statin+Ezetimibe+PCSK9i	1 (0.11)	1 (0.12)	0 (0.00)
Discontinuation of any LLT, n (%)	16 (1.71)	15 (1.86)	1 (0.80)

LLT, lipid-lowering therapy; PCSK9i, PCSK9 inhibitor. Continuous variables are presented as mean ± SD or medians with interquartile ranges. Categorical variables are presented as proportions.

associated with LDL-C goal achievement. Importantly, eGFR < 60 ml/min/1.73 m^2 (OR 1.81; 95%CI 1.15–2.87; $P = 0.01$) was also significantly associated with LDL-C goal achievement (**Table 4**).

DISCUSSION

In this prospective observational study, we analyzed the factors impacting LDL-C < 1.4 mmol/L goal achievement in Chinese patients with CAD and different renal function statuses. Although in the whole participants, the rate of LDL-C < 1.4 mmol/L goal achievement reached 33.99% during the follow-up period from 11.57% at baseline; however, the rate of LDL-C < 1.4 mmol/L goal achievement was significantly lower in G2 than that in G1 (24.00% vs. 35.52%, $P = 0.02$). At the same time, we found that impaired renal function (eGFR < 60 ml/min/1.73 m^2) was independently associated with LDL-C < 1.4 mmol/L goal achievement (OR 1.81; 95%CI 1.15–2.87; $P = 0.01$). From a mendelian randomization, there is a stepwise increased risk of CKD with a higher LDL-C level (hazard ratio [HR] 1.05; 95CI% 0.97-1.13; $P < 0.001$) (7). LDL-C and CKD are independent risk factors for cardiovascular events (1). Given the present research results, LDL-C goal achievement might be a challenge for CAD patients with impaired renal functions.

Based on the latest ESC/EAS guideline about the lipid management, LDL-C goal is <1.4 mmol/L and reduction ≥ 50% from the baseline for all the patients with ASCVD (6). Renal function has been well recognized to be associated with CAD and dyslipidemia (1). Concerning to lipid management in the CAD patients with impaired renal function, our findings are consistent with the results of previous studies and highlight a treatment gap between clinical practice and guideline commendation. In the previous study, it had been found that the patients with advanced CKD were less likely to achieve LDL-C target (8, 9). In a prospective cohort study CKD-REIN (NCT03381950), among high-risk patients, 45% of those on statin and/or ezetimibe achieved the LDL-C treatment target (<2.6 mmol/L). Among very high-risk patients, the percentage at goal (<1.8 mmol/L) was 38% for CKD stage G3 and 29% for stage G4/G5. There was a trend toward the higher achievement of LDL-C targets with increasing LLT intensity (adjusted OR for moderate vs. low intensity 1.20; 95%CI 0.92–1.56; high vs. low intensity 1.46; 1.02–2.09; P trend = 0.036). In the CKD-REIN study, many patients with CKD stages G3–G5 who were eligible for LLT were not treated, and those on LLT rarely achieved LDL-C targets (8). Kuznik et al. reported that the percentage of LLT increased with

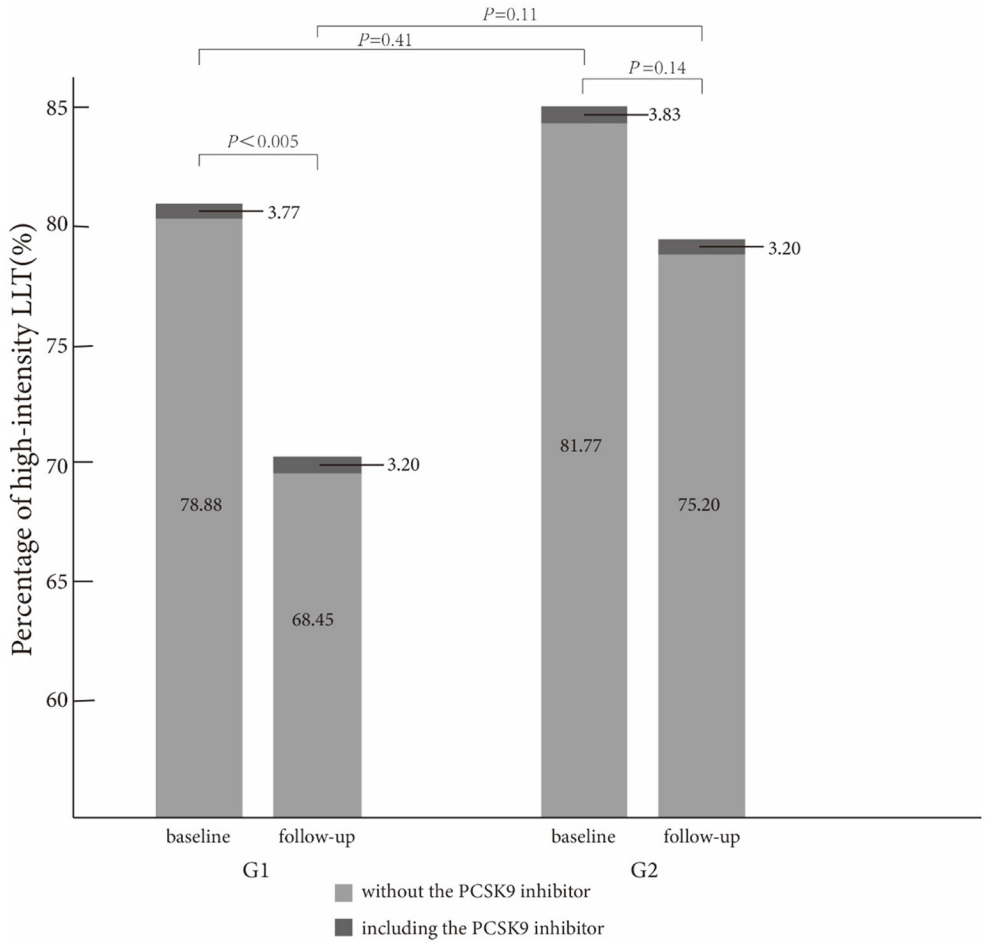

FIGURE 1 | Comparison of high-intensity lipid-lowering therapy strategies between the two groups at baseline and follow-up.

CKD stage and the rate of LDL-C < 100 mg/dL increased with CKD stage among the patients with below CKD Stage 3b, but the target rate decreased in Stage 4 (10). However, Lin et al. conducted a multi-center study (T-SPARCLE) that enrolled 3,057 individuals and 26.76% of patients with CKD. Those without CKD had a similar equivalent statin potency with the CKD group. Although the result showed that more CKD population achieved the LDL-C goal, there were no statistical significances between the CKD and non-CKD groups (55.75% vs. 54.71%, $P > 0.05$) (11). In the 2001–2010 National Health and Nutritional Examination Survey (NHANES), the use of lipid-lowering agents increased with CKD stage, from 18.1% (Stage 1) to 44.8% (Stage 4). LDL-C goal attainment increased from 35.8% (Stage 1) to 52.8% (Stage 3b) but decreased in Stage 4 (50.7%). From this survey, it was found that individuals with CKD had a high prevalence of CV-related comorbidities. However, attainment of LDL-C goals was low regardless of disease stage (10). In Taiwan CKD care programs conducted by nephrologists-based team from 2006 to 2013, they set 10 goals with treatment target ranges based on the guideline. In this program, they found that the all-goals attainment rate increased from 59.4% at baseline to 60.5% in year 3, with an especially significant improvement for LDL-C (from 46.8% to 67.0%). From the program, they concluded that goal attainment and disease progression were influence by CKD stage. A high goal achievement rate was associated with better preservation of residual renal function (9). Since the previous studies have mainly explored the primary prevention of high-risk patients with CKD, our data concentrated on the second prevention of patients with CAD with various renal functions. From our study, the renal function exerts an adverse impact on the lipid management in patients with CAD. Patients with impaired renal function should be paid more attention.

The proportion of high-intensity LLT strategy had a trend to be higher in G2 than that in G1 during the follow-up period in our study. However, there was no statistically significant difference in the aspect of LLT strategy in both the groups (78.20% without PCSK9i and 3.20% including PCSK9i in G2 vs. 68.45% without PCSK9i and 3.20% including PCSK9i in G1, $P = 0.11$). In addition, we found that the proportion of high-intensity LLT was significantly lower during the follow-up period than that at baseline in G1 (78.88% without PCSK9i and 3.77% including PCSK9i at baseline vs. 68.45% without PCSK9i and

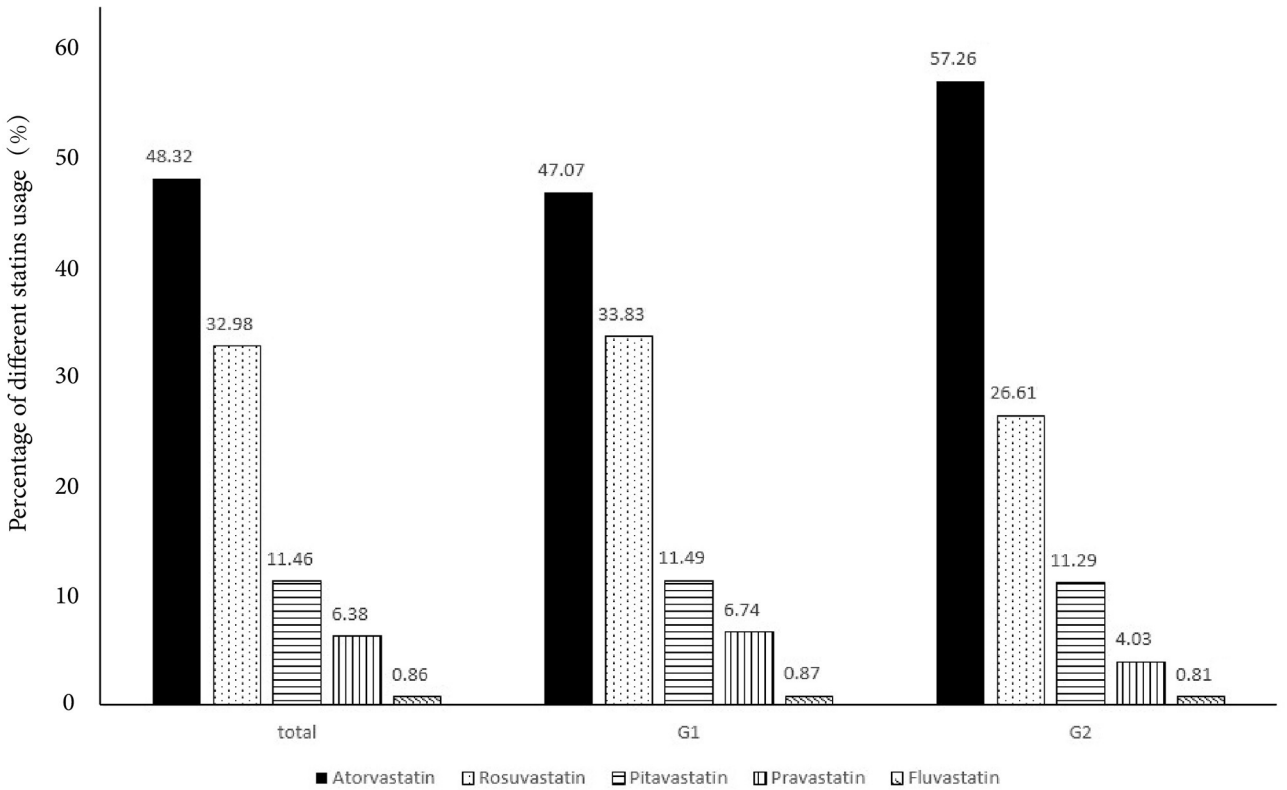

FIGURE 2 | The percentage of different statins used in total and different groups.

TABLE 3 | Comparison of the lipid profile at the follow-up period between the two groups.

	Total (n = 933)	G1 (n = 808)	G2 (n = 125)	P-value
TG, mmol/L	1.19 (0.88–1.70)	1.17 (0.86–1.69)	1.33 (1.03–1.78)	0.01*
TC, mmol/L	3.35 ± 0.95	3.34 ± 0.97	3.47 ± 0.85	0.16
HDL-C, mmol/L	1.14 ± 0.28	1.15 ± 0.28	1.11 ± 0.26	0.17
LDL-C, mmol/L	1.74 ± 0.68	1.71 ± 0.68	1.91 ± 0.68	0.0022*
LDL-C<1.4mmol/L, (%)	317 (33.98)	287 (35.52)	30 (24.00)	0.02*

*TC, total cholesterol; TG, triglyceride; HDL-C, high-density lipoprotein; LDL-C, low-density lipoprotein; *indicated the difference between the two groups is statistically significant, P < 0.05. Continuous variables are presented as mean ± SD or medians with interquartile ranges. Categorical variables are presented as proportions.*

3.20% including PCSK9i during follow-up, $P < 0.005$). However, the proportion of high-intensity LLT did not significantly change in G2 during the follow-up period than that at baseline (81.77% without PCSK9i and 3.83% including PCSK9i at baseline vs. 78.20% without PCSK9i and 3.20% including PCSK9i during follow-up, $P = 0.14$). From our study, high-intensity LLT was independently associated with LDL-C goal achievement. High-intensity LLT, such as statin plus ezetimibe, could make it more likely to achieve LDL-C target (OR 0.42; 95%CI 0.3–0.6; $P < 0.001$). It was similar that high-intensity LLT, such as statin or ezetimibe combined with PCSK9i, could also achieve LDL-C goal more likely (OR 0.15; 95CI% 0.07–0.32; $P < 0.001$). Massy et al. also reported that the combination therapy of LLT recommended by the guidelines could make more patients with CKD to achieve LDL-C goal (8). From the long-term result, Bae et al. reported a median follow-up of 4.2 years, and the combined groups always had the lower LDL-C levels ($P = 0.025$) (12). In this study, the patients under high-intensity LLT were more prone to achieve LDL-C goal, especially under LLT with PCSK9i (22.50% vs. 37.70% vs. 60.00% in the subgroup under low-/moderate-intensity LLT, or high-intensity LLT without PCSK9i, or high-intensity LLT with PCSK9i, respectively, $P < 0.005$). It was remarkable that although 68.70% of individuals were under high-intensity LLT with or without PCSK9i, the rate of LDL-C goal achievement (LDL-C < 1.4 mmol/L) was only 33.99%. The potential cause was a very low rate of PCSK9i application (only 3.69% and 3.76% at baseline and follow-up, respectively). Similarly, the previous cross-sectional studies have also reported

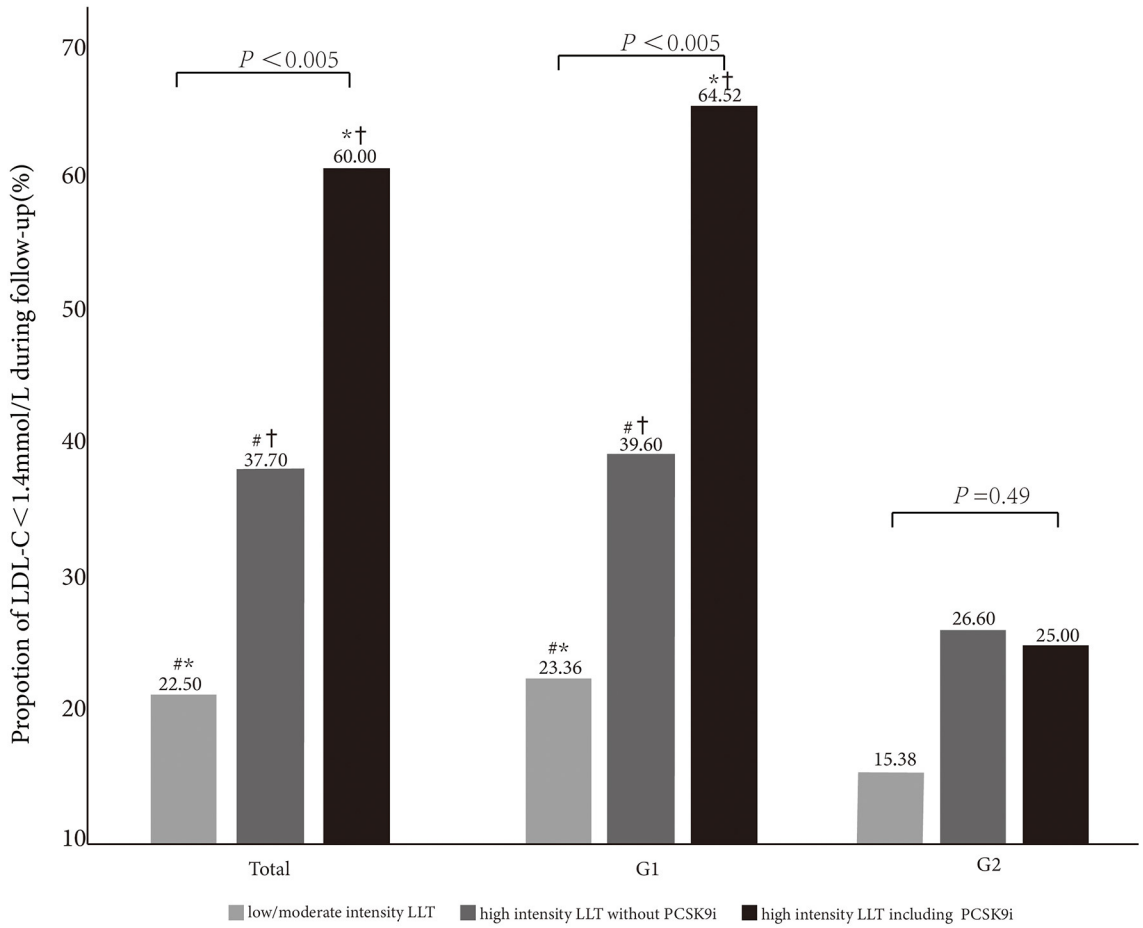

FIGURE 3 | Comparison of LDL-C < 1.4 mmol/L goal achievement under different LLT strategies in total and subgroups (G1 and G2). *, #, †indicate <0.05 between the groups.

small proportions of PCSK9i in a real-world application (13, 14). From our study, we speculated that high-intensity LLT without PCSK9i was not so enough to achieve a high rate of LDL-C goal achievement. According to the guideline, it is sound to use the PCSK9i after statin combined with ezetimibe (6). PCSK9i application might help more patients to achieve LDL-C < 1.4 mmol/L. Actually, our result showed the percentage of PCSK9i kept similar between the baseline and follow-up (baseline 3.69% vs. follow-up 3.76%). Insufficient attention had been paid to the groups with eGFR < 60 ml/min/1.73 m^2 about the lipid management. It might be considerable to prescribe PCSK9i for them more, especially for the patients with impaired renal function.

Except for the effectiveness on lowering LDL-C, LLT also exerts the protective effect on renal function. From the network meta-analysis, statins could lead to a 0.61 (95CI% 0.27–0.95) ml/min/1.73 m^2 slower annual eGFR decline. When it comes to the efficacy among different statins, there are no substantial differences (15). According to the *post-hoc* analyses from several trials, atorvastatin could improve renal function (16, 17). Statin combination with ezetimibe also had positive effects on renal function (18). The renal safety of ezetimibe had been proven by the Study of Heart and Renal Protection (SHARP) trial, which used simvastatin 20 mg plus ezetimibe 10 mg reduced atherosclerotic events in advanced patients with CKD. Compared with the statins, the combination group was prone to preserve renal function ($P < 0.001$) and had less renal events (HR 0.58; 95CI% 0.35–0.95; $P = 0.032$) (19). PCSK9i are currently the most effective lipid-lowering drugs in clinical practice, which could reduce LDL-C level by 50–70% and improve the rate of LDL-C goal achievement significantly (20, 21). The FOURIER trial investigated the influence of evolocumab on the patients with different kidney functions. As for the effect of LDL-C lowering and clinical efficacy and safety of evolocumab, it is consistent across different renal function groups and more effective to reduce the rate of adverse events in the advanced CKD group (20). Alirocumab had a similar effect as evolocumab (21). Based on the current evidence, for the patients with CAD with impaired renal function, it was more difficult to achieve LDL-C goal and it needs to optimize the application of high-intensity LLT, especially improving the proportion of PCSK9i application in order to accomplish a higher rate of LDL-C goal achievement.

TABLE 4 | Factors impacting achieving LDL-C < 1.4 mmol/L goal for patients treated with LLT.

	Univariate logistic regression			Multivariate logistic regression		
	OR	**95 CI%**	***P*-value**	**OR**	**95 CI%**	***P*-value**
Age	0.85	0.63–1.14	0.28			
Female	1.69	1.21–2.35	0.002*	1.66	1.13–2.44	0.009*
History of PCI	0.67	0.49–0.92	0.01*	0.55	0.39–0.77	<0.001
History of CABG	1.63	0.49–5.38	0.42			
History of MI	1.10	0.72–1.67	0.67			
ACS	0.71	0.52–0.98	0.03*	0.65	0.46–0.91	0.01*
PAD	1.08	0.49–2.37	0.84			
Hypertension	0.84	0.64–1.11	0.22			
DM	0.77	0.57–1.03	0.08	1.50	1.09–2.02	0.01*
smoking	1.31	1.00-1.73	0.05	0.99	0.72–1.36	0.95
eGFR<60 ml/min/1.73 m^2	1.74	1.23–2.70	0.01*	1.81	1.15–2.87	0.01*
BMI>30	1.00	0.65–1.53	1.00			
lipid-lowering therapy						
Monotherapy (statins)	Ref.			Ref.		
Combination with ezemitibe	0.52	0.37–0.74	<0.001*	0.42	0.30–0.60	<0.001*
Combination with PCSK9i	0.21	0.10–0.44	<0.001*	0.15	0.07–0.32	<0.001*

*BMI, body mass index; CABG, coronary artery bypass graft; PCI, percutaneous coronary intervention; MI, myocardial infarction; eGFR estimated glomerular filtration rate; DM, diabetes mellitus; ACS, admission for acute coronary syndrome; *indicated P < 0.05.*

Another possible contributing factor for the low rate of LDL-C goal achievement was medication adherence. In our study, LLT strategy was adjusted in 105 patients during the follow-up period when compared with that at discharge and among them, 102 patients switched from statin combination with ezetimibe to moderate-intensity statin monotherapy. In previous studies, the long-term adherence to statins was poor (22). Santoleri et al. showed that an overall adherence rate of ezetimibe was low when compared with statins during the 8-year follow-up period, and a higher percentage of discontinuation of ezetimibe than statins annually (23). In addition to patient self-discontinuation, 4% of patients discontinued ezetimibe because of physicians' suggestion. The physicians' lipid management knowledge had a great influence on the rate of LDL-C goal achievement (24).

There are some limitations in this study. First, it was a single-center observational study; although confounding variables have been statistically excluded, there might be unobserved risk factors. Second, the follow-up period in our study was relatively short; thus, the long-term effect of different renal functions and different LLTs on LDL-C goal achievement in patients with CAD remained uncertain. Third, the sample size was small. Finally, when it comes to the adherence, we did not take a more accurate way to assess the medication using situation except for patients' self-report during the follow-up period.

In summary, in our study, impaired renal function (eGFR < 60 ml/min/1.73 m^2) was an independent risk factor for LDL-C goal achievement in the patients with CAD. High-intensity LLT with PCSK9i could improve the rate of LDL-C goal achievement significantly. It should be suggested to increase the proportion of high-intensity LLT with PCSK9i for patients with CAD, especially those with impaired renal function.

DATA AVAILABILITY STATEMENT

The raw data supporting the conclusions of this article will be made available by the authors, without undue reservation.

ETHICS STATEMENT

The studies involving human participants were reviewed and approved by Fuwai hospital Ethics Committees. The patients/participants provided their written informed consent to participate in this study. Written informed consent was obtained from the individual(s) for the publication of any potentially identifiable images or data included in this article.

AUTHOR CONTRIBUTIONS

NQW: conception/design. YGS, WJZ, JJL, JQ, and KFD: provision of study materials. SZ, HWS, and ZFL: collection and/or assembly of data. SZ: data analysis, interpretation, and manuscript writing. All authors contributed to the article and approved the submitted version.

FUNDING

This study was supported by the CAMS Innovation Fund for Medical Sciences (CIFMS) (2021-I2M-1-008).

REFERENCES

1. Ferro CJ, Mark PB, Kanbay M, Sarafidis P, Heine GH, Rossignol P, et al. Lipid management in patients with chronic kidney disease. *Nat Rev Nephrol.* (2018) 14:727–49. doi: 10.1038/s41581-018-0072-9
2. Webster AC, Nagler EV, Morton RL, Masson P. Chronic Kidney Disease. *Lancet.* (2017) 389:1238–52. doi: 10.1016/S0140-6736(16)32064-5
3. Gai Z, Wang T, Visentin M, Kullak-Ublick GA, Fu X, Wang Z. Lipid accumulation and chronic kidney disease. *Nutrients.* (2019) 11:722. doi: 10.3390/nu11040722
4. Hager MR, Narla AD, Tannock LR. Dyslipidemia in patients with chronic kidney disease. *Rev Endocr Metab Disord.* (2017) 18:29–40. doi: 10.1007/s11154-016-9402-z
5. Lamprea-Montealegre JA, Staplin N, Herrington WG, Haynes R, Emberson J, Baigent C, et al. Apolipoprotein B, triglyceride-rich lipoproteins, and risk of cardiovascular events in persons with CKD. *Clin J Am Soc Nephrol.* (2020) 15:47–60. doi: 10.2215/CJN.07320619
6. Mach F, Baigent C, Catapano AL, Koskinas KC, Casula M, Badimon L, et al. 2019 ESC/EAS Guidelines for the management of dyslipidaemias: lipid modification to reduce cardiovascular risk. *Eur Heart J.* (2020) 41:111–88. doi: 10.15829/1560-4071-2020-3826
7. Emanuelsson F, Nordestgaard BG, Tybjærg-Hansen A, Benn M. Impact of LDL cholesterol on microvascular vs. macrovascular disease: a mendelian randomization study. *J Am Coll Cardiol.* (2019) 74:1465–76. doi: 10.1016/j.jacc.2019.07.037
8. Massy ZA, Ferrières J, Bruckert E, Lange C, Liabeuf S, Velkovski-Rouyer M, et al. Achievement of low-density lipoprotein cholesterol targets in CKD. *Kidney Int Rep.* (2019) 4:1546–54. doi: 10.1016/j.ekir.2019.07.014
9. Wang Y, Lee YT, Lee WC, Ng HY, Wu CH, Lee CT. Goal attainment and renal outcomes in patients enrolled in the chronic kidney disease care program in Taiwan: a 3-year observational study. *Int J Qual Health Care.* (2019) 31:252–60. doi: 10.1093/intqhc/mzy161
10. Kuznik A, Mardekian J, Tarasenko L. Evaluation of cardiovascular disease burden and therapeutic goal attainment in US adults with chronic kidney disease: an analysis of national health and nutritional examination survey data, 2001-2010. *BMC Nephrol.* (2013) 14:132. doi: 10.1186/1471-2369-14-132
11. Lin TH, Chuang SY, Chu CY, Lee WH, Hsu PC, Su HM, et al. The impact of chronic kidney disease on lipid management and goal attainment in patients with atherosclerosis diseases in Taiwan. *Int J Med Sci.* (2014) 11:381–8. doi: 10.7150/ijms.7069
12. Bae J, Hong N, Lee BW, Kang ES, Cha BS, Lee YH. Comparison of renal effects of ezetimibe-statin combination vs. statin monotherapy: a propensity-score-matched analysis. *J Clin Med.* (2020) 9:798. doi: 10.3390/jcm9030798
13. De Luca L, Arca M, Temporelli PL, Meessen J, Riccio C, Bonomo P, et al. Current lipid lowering treatment and attainment of LDL targets recommended by ESC/EAS guidelines in very high-risk patients with established atherosclerotic cardiovascular disease: Insights from the START registry. *Int J Cardiol.* (2020) 316:229–35. doi: 10.1016/j.ijcard.2020.05.055
14. Allahyari A, Jernberg T, Hagström E, Leosdottir M, Lundman P, Ueda P. Application of the 2019 ESC/EAS dyslipidaemia guidelines to nationwide data of patients with a recent myocardial infarction: a simulation study. *Eur Heart J.* (2020) 41:3900–9. doi: 10.1093/eurheartj/ehaa034
15. Esmeijer K, Dekkers OM, de Fijter JW, Dekker FW, Hoogeveen EK. Effect of different types of statins on kidney function decline and proteinuria: a network meta-analysis. *Sci Rep.* (2019) 9:16632. doi: 10.1038/s41598-019-53064-x
16. Amarenco P, Callahan A. 3rd, Campese VM, Goldstein LB, Hennerici MG, Messig M, et al. Effect of high-dose atorvastatin on renal function in subjects with stroke or transient ischemic attack in the SPARCL trial. Stroke. (2014) 45:2974–82. doi: 10.1161/STROKEAHA.114.005832
17. Vogt L, Bangalore S, Fayyad R, Melamed S, Hovingh GK, DeMicco DA, et al. Atorvastatin has a dose-dependent beneficial effect on kidney function and associated cardiovascular outcomes: *post hoc* analysis of 6 double-blind randomized controlled trials. *J Am Heart Assoc.* (2019) 8:e010827. doi: 10.1161/JAHA.118.010827
18. Lin YC, Lai TS, Wu HY, Chou YH, Chiang WC, Lin SL, et al. Effects and safety of statin and ezetimibe combination therapy in patients with chronic kidney disease: a systematic review and meta-analysis. *Clin Pharmacol Ther.* (2020) 108:833–43. doi: 10.1002/cpt.1859
19. Baigent C, Landray MJ, Reith C, Emberson J, Wheeler DC, Tomson C, et al. The effects of lowering LDL cholesterol with simvastatin plus ezetimibe in patients with chronic kidney disease (study of heart and renal protection): a randomised placebo-controlled trial. *Lancet.* (2011) 377:2181–92. doi: 10.1016/j.ymed.2011.08.055
20. Charytan DM, Sabatine MS, Pedersen TR, Im K, Park JG, Pineda AL, et al. Efficacy and safety of evolocumab in chronic kidney disease in the FOURIER trial. *J Am Coll Cardiol.* (2019) 73:2961–70. doi: 10.1016/j.jacc.2019.03.513
21. Toth PP, Dwyer JP, Cannon CP, Colhoun HM, Rader DJ, Upadhyay A, et al. Efficacy and safety of lipid lowering by alirocumab in chronic kidney disease. *Kidney Int.* (2018) 93:1397–408. doi: 10.1016/j.kint.2017.12.011
22. Talic S, Marquina C, Ofori-Asenso R, Petrova M, Liew D, Owen AJ, et al. Switching, persistence and adherence to statin therapy: a retrospective cohort study using the Australian national pharmacy data. *Cardiovasc Drugs Ther.* (2021). doi: 10.1007/s10557-021-07199-7. [Epub ahead of print].
23. Santoleri F, Romagnoli A, Costantini A. Adherence and persistence in the use of statins and ezetimibe over 8 years in a real-life study. *Curr Med Res Opin.* (2021) 37:2061–66. doi: 10.1080/03007995.2021.1980777
24. Laufs U, Karmann B, Pittrow D. Atorvastatin treatment and LDL cholesterol target attainment in patients at very high cardiovascular risk. *Clin Res Cardiol.* (2016) 105:783–90. doi: 10.1007/s00392-016-0991-z

Conflict of Interest: The authors declare that the research was conducted in the absence of any commercial or financial relationships that could be construed as a potential conflict of interest.

frontiers | Frontiers in Cardiovascular Medicine

REVIEW
published: 27 May 2022
doi: 10.3389/fcvm.2022.928566

Glycosylation of HDL-Associated Proteins and Its Implications in Cardiovascular Disease Diagnosis, Metabolism and Function

*Eduardo Z. Romo and Angela M. Zivkovic**

Department of Nutrition, University of California, Davis, Davis, CA, United States

High-density lipoprotein (HDL) particles, long known for their critical role in the prevention of cardiovascular disease (CVD), were recently identified to carry a wide array of glycosylated proteins, and the importance of this glycosylation in the structure, function and metabolism of HDL are starting to emerge. Early studies have demonstrated differential glycosylation of HDL-associated proteins in various pathological states, which may be key to understanding their etiological role in these diseases and may be important for diagnostic development. Given the vast array and specificity of glycosylation pathways, the study of HDL-associated glycosylation has the potential to uncover novel mechanisms and biomarkers of CVD. To date, no large studies examining the relationships between HDL glycosylation profiles and cardiovascular outcomes have been performed. However, small pilot studies provide promising preliminary evidence that such a relationship may exist. In this review article we discuss the current state of the evidence on the glycosylation of HDL-associated proteins, the potential for HDL glycosylation profiling in CVD diagnostics, how glycosylation affects HDL function, and the potential for modifying the glycosylation of HDL-associated proteins to confer therapeutic value.

Keywords: glycosylation, high-density lipoprotein (HDL), O-glycosylation, N-glycosylation, ApoA-I, APOC3, APOE

OPEN ACCESS

Edited by:
Mary G. Sorci-Thomas, Medical College of Wisconsin, United States

Reviewed by:
Gunther Marsche, Medical University of Graz, Austria
Daisy Sahoo, Medical College of Wisconsin, United States

****Correspondence:***
Angela M. Zivkovic
amzivkovic@ucdavis.edu

Specialty section:
This article was submitted to Lipids in Cardiovascular Disease, a section of the journal Frontiers in Cardiovascular Medicine

Received: *25 April 2022*
Accepted: *09 May 2022*
Published: *27 May 2022*

Citation:
Romo EZ and Zivkovic AM (2022) Glycosylation of HDL-Associated Proteins and Its Implications in Cardiovascular Disease Diagnosis, Metabolism and Function. Front. Cardiovasc. Med. 9:928566. doi: 10.3389/fcvm.2022.928566

INTRODUCTION

It has been established across multiple cohorts that high density lipoproteins (HDL) are atheroprotective (1–4). HDL are complex, heterogeneous nanoparticles, with various subclasses, comprised of numerous functional proteins and lipids (5), and have more recently been shown to be highly glycosylated (6) and structurally and compositionally variable in various physiological and pathological states (7, 8). Owing to this high heterogeneity, HDL particles have diverse biological functions including immunomodulatory, anti-inflammatory, antioxidant, antithrombotic, and anti-proteolytic functions among others, which are dependent on their composition (9–13). Protein and lipid composition, as well as particle structure and size, are important known factors driving differences in HDL functional capacity. The role of glycosylation in the differential functionality of HDL particles has only recently started to emerge.

Protein glycosylation is generally an enzymatically driven post-translational modification of newly biosynthesized proteins that occurs in the endoplasmic reticulum and Golgi apparatus

where sugars are attached to proteins by N- or O-linkages, forming glycans (14). N-glycans are attached to a nitrogen atom on the asparagine moiety of the protein whereas O-glycans are bound to the oxygen atom of either threonine or serine (15). Glycans contribute to various biological capacities including protein folding, receptor binding, enzyme activity, and physical properties by lending charge to the protein, and are vastly particular to the type, extent, and specific site of glycosylation (15–19). Protein glycosylation functions as a biological language and is important for biological particle self- and non- self-recognition, molecule transport, and endocytosis (20). In the last 8 years since it was first demonstrated that HDL are highly glycosylated, and specifically sialylated particles (6) (**Figure 1**), there has been a steady increase in the evidence pointing to an important connection between the glycosylation of HDL-associated proteins, and the overall functionality of HDL particles. In this review paper we will discuss the current state of the evidence on the glycosylation of HDL-associated proteins, specifically, where we stand in terms of development of cardiovascular disease (CVD) diagnostics using HDL-glycosylation profiling, how glycosylation of HDL proteins affects HDL function, and the potential for modifying the glycosylation of HDL-associated proteins to confer therapeutic value.

HDL GLYCOSYLATION PROFILING FOR DIAGNOSTIC PURPOSES

One of the problems with HDL particle analysis for diagnostic purposes has been the extreme complexity of these particles and the lack of resolution of older measurement tools. For example, although high HDL-cholesterol (HDL-C) concentrations have been found to be protective against CVD, several large recent studies demonstrated that the relationship between HDL-C concentration and adverse health outcomes tends to follow a U-shaped curve, with both low HDL-C and very high HDL-C being associated with increased cardiovascular (CV) events (21–23). Clearly, it is not simply the measurement of the total amount of cholesterol carried within HDL that is diagnostic, but rather some other aspect of HDL that is critical, whether it be compositional, structural, or functional.

For more sophisticated measurements of HDL structure, composition, and function, it is imperative to first isolate the HDL particles and purify them from other potentially contaminating components. Because HDL particles are so small (7–12 nm in diameter) as to overlap with many plasma proteins in terms of their size (e.g., ferritin), and because they are close in density to other lipoprotein particles and even extracellular vesicles, they are difficult to isolate and purify. According to multiple proteomic studies HDL could carry as few as 12 key proteins or up to an excess of 200 proteins (24, 25) depending on how they are isolated (24, 26, 27). Various methods, and combinations of these methods, have been used to isolate HDL including ultracentrifugation, size exclusion chromatography, immunoaffinity precipitation, and asymmetrical flow field flow fractionation. More recently, methods combining these different approaches have been used to improve the overall yield and purity of HDL particles while preserving their structural and functional integrity (28–30), including an optimized, validated method using sequential flotation density ultracentrifugation followed by size exclusion chromatography which yields highly purified HDL fractions (5).

Once HDL particles are isolated, the analysis of their glycosylation status can be performed. Pioneering work in lipoprotein glycobiology establishing analytical methods for profiling the glycome of HDL particles revealed for the first time that HDL has both N- and O-linked glycosylation and is distinctly highly sialylated (6). Glycosylation analysis is a complex chemical approach traditionally using mass spectrometry combined with various extraction methods such as enzymatic digestion, chemical cleavage, and liquid chromatography (31–35). HDL glycosylation can be profiled in several ways: (1) the glycans can be enzymatically or chemically cleaved, followed by mass spectrometry (6), (2) site-specific glycoprofiling can be performed by tandem mass spectrometry analysis of protease-digested samples (6, 36, 37), and (3) hydrophilic interaction liquid chromatography profiling can be performed, which uses a combination of the three main types of liquid chromatography for separation and profiling of glycan-containing peaks (38, 39).

To date, no large studies examining the relationships between HDL glycosylation profiles and CVD outcomes have been performed. However, small pilot studies provide promising preliminary evidence that such a relationship may exist. For example, in a small pilot study performed by our group, differences in HDL glycan composition were able to differentiate between individuals at equal risk for CVD based on clinical parameters (i.e., total cholesterol, low-density lipoprotein-cholesterol (LDL-C), HDL-C, etc.) who were found to have arterial occlusion vs. not (37). The role of HDL glycosylation in CV health is starting to be recognized as a promising new research field (40). Larger cohort studies investigating the relationships between HDL glycoprofiles and CV outcomes across factors including age, sex, and ethnicity are needed, and have the potential to add greatly to our ability to detect individuals at risk for CVD earlier when disease prevention measures are the most likely to be effective.

HOW GLYCOSYLATION OF HDL PROTEINS AFFECTS HDL FUNCTION

Most of the known HDL-associated proteins are glycosylated, and only a few are found to be non-glycosylated. In **Table 1** we provide information on the N- and/or O-glycosylation status, sites of attachment, and number of unique glycans attached for several HDL proteins for which this information has been confirmed by extensive MS/MS analysis. Whereas, here are many putative sites for O-glycosylation (i.e., any Ser or Thr residue) on any given protein, whether O-glycans are actually attached must be confirmed by advanced MS analysis. Thus, although several HDL-associated proteins, such as ApoC-I have Ser or Thr residues that could in theory be O-glycosylated, in **Table 1** we report only those that have been demonstrated to

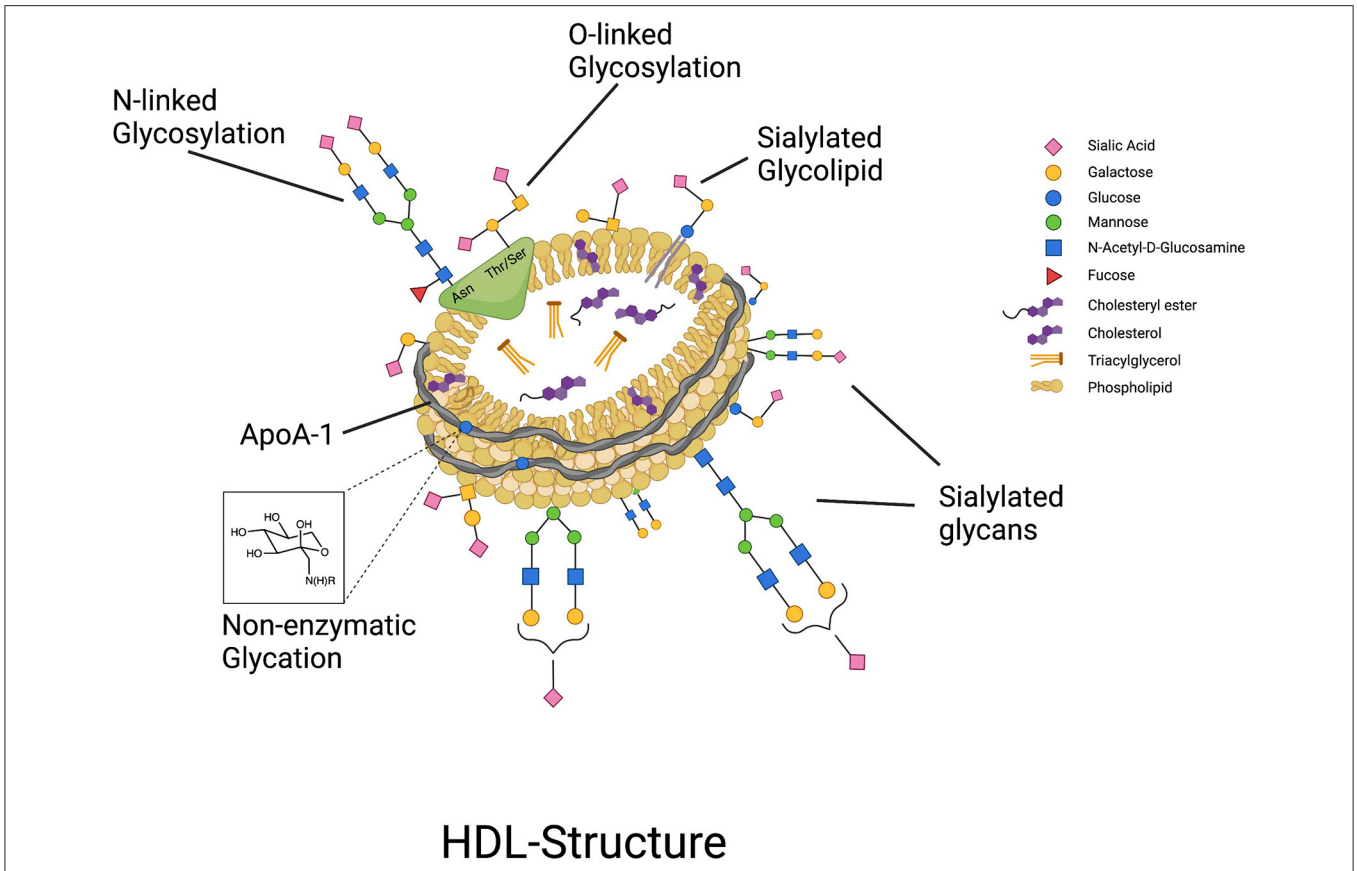

FIGURE 1 | HDL particles are highly glycosylated, containing both glycoproteins that can be N- and O-glycosylated, and glycolipids, with glycan groups added enzymatically through highly regulated cellular processes. In contrast, non-enzymatic glycation of proteins such as ApoA-I can occur under conditions of hyperglycemia.

beO-glycosylated by MS measurement of isolated HDL fractions derived from a starting volume of 500 uL of plasma. It is possible that some proteins (e.g., PLTP) are present at such low abundance in isolated HDL that their glycoforms fall below the limits of detection. Thus, to further investigate the glycosylation status of these low-abundance HDL proteins future experiments involving enrichment for these proteins will be required. Other proteins, such as ApoA-I, have been reported to be glycosylated in the literature, however, we do not include it in **Table 1** because based on detailed MS analysis the O-glycosylation could not be confirmed. In the following section we review what is currently known about the impact of glycosylation of several key HDL-associated on overall HDL metabolism and function, for which there is currently information. As the field evolves this list will doubtless grow and a more comprehensive picture of the extent and diversity of glycans attached to HDL-associated proteins will emerge.

Apolipoprotein A-I

ApoA-I, the major structural, defining HDL apoprotein accounting for around 70% of total HDL protein mass, plays a key role in lipid and cholesterol metabolism and is highly associated with cardioprotection (42). Despite ApoA-I being reported to possibly be glycosylated (43–45) extensive mass spectrometry-based (MS)-based profiling demonstrated that there is no evidence of ApoA-I glycosylation (25). ApoA-I does not have the consensus sequence for N-glycosylation (AsnXxxSer/Thr/Cys, where Xxx can be any amino acid except proline), and whereas O-glycosylation is possible on any serine or threonine residue, detailed analysis of isolated HDL has not yielded any confirmed O-glycosylated peptides on ApoA-I. It is possible that ApoA-I O-glycosylation can occur in certain conditions or disease states, however MS-based analysis has never confirmed the existence of this to date. ApoA-I can, however, be non-enzymatically or chemically glycated (44), which has been found to be deleterious for its function.

Apolipoprotein A-II

ApoA-II is the second most abundant HDL apoprotein, representing as much as 20% of total protein mass (42), and has been shown to have important implications for CV health though results were historically inconsistent and controversial. For instance one early study showed that low serum ApoA-II was a marker of atheroprotection in patients with non-insulin-dependent-diabetes mellitus (46) but conversely another study showed that elevated levels of ApoA-II were proatherogenic

TABLE 1 | Glycosylation status of HDL-associated proteins with confirmed glycosylation sites.

Protein	N-glycans	O-glycans	Sites of attachment
Alpha-1-antichymotrypsin (AACT)	8	0	Asn106, Asn127, Asn271
Alpha-1-antitrypsin (A1AT)	18	0	Asn70, Asn107, Asn271
Alpha-1B-glycoprotein (A1BG)	1	0	Asn179
Alpha-2-HS-glycoprotein (FETUA or A2HSG)	17	2	Asn156, Asn176, Thr346
Apolipoprotein A-II (APOA2)	0	4	Ser35, Ser88, Thr95
Apolipoprotein C-III (APOC3)	0	21	Thr94
Apolipoprotein D (APOD)	28	0	Asn65, Asn98
Apolipoprotein E (APOE)	0	40	Ser215, Thr307/Ser308*, Ser76/Thr83*, Ser129/Thr130*, Thr194, Ser197, Ser263, Thr289/Ser290* Ser296 (25, 41)
Apolipoprotein F (APOF)	0	3	Ser269, Thr273/Thr27*
Apolipoprotein M (APOM)	9	0	Asn135
Clusterin (CLUS or APOJ)	10	0	Asn86, Asn291, Asn374
Complement C1s subcomponent (C1S)	2	0	Asn174
Complement C3 (C3)	4	0	Asn85
Hemopexin (HPX)	6	0	Asn187, Asn453, Asn240/Asn246*
Heparin cofactor 2 (HCF2)	2	0	Asn49
Kininogen-1 (KNG1)	4	0	Asn169, Asn205
Lecithin-cholesterol acyltransferase (LCAT)	1	0	Asn108
Serum amyloid A-4 (SAA4)	7	0	Asn94
Serum paraoxonase/arylesterase 1 (PON1)	8	0	Asn253, Asn324

Proteins included in this table include only those with glycosylation sites confirmed to actually express glycans at those sites by mass spectrometry analysis of isolated HDL fractions from a starting volume of 500 uL of plasma, as described in (25). HDL-associated proteins that have been reported to be glycosylated previously, and/or have putative sites but that either could not be confirmed by mass spectrometry or are present at low abundance such that they fall under the limit of detection, are not reported in this table.
[*]For these sites, the site of attachment could not be disambiguated thus both possible attachment sites are reported.

(47). However, more recently a large prospective study ($n = 912$) showed that ApoA-II was indeed inversely associated with future risk for coronary artery disease (CAD) and was exerting antiatherogenic properties (48). ApoA-II binds to phospholipid transfer protein (PLTP) on HDL (49), suggesting that it plays an important role in the remodeling of HDL particles. ApoA-II contributes to structural properties of HDL (50) and its presence on HDL enhances ATP-binding cassette transporter-1 (ABCA-1)-mediated efflux, suggesting that ApoA-II can contribute to structural changes in ApoA-I, and improve functionality of the HDL particle (51). Like ApoA-I, ApoA-II does not contain the consensus sequence for N-linked glycosylation, however it has been shown to be O-glycosylated (25, 52). The glycosylation of ApoA-II contributes to its association affinities since sialylated ApoA-II preferentially associates with smaller HDL whereas non-sialylated ApoA-II associates with all sizes of HDL (53). In a recent study in patients who were equally at risk for CAD based on traditional biomarkers and who were then diagnosed as either having CAD or not using diagnostic coronary arteriography, ApoA-II was significantly lower in CAD patients compared to patients without CAD (7). In children given a lipid rich dietary supplementation there was no difference in ApoA-II glycosylation between groups, but the analysis did confirm that ApoA-II indeed had multiple glycoforms (25). It is currently unknown what the role of glycosylation in ApoA-II function is, and whether the extent of sialylation drives the binding of ApoA-II to smaller HDL particles or whether higher sialylation is reflective of a particular pathway of metabolism that is linked with the production of small particles.

Apolipoprotein C-III

ApoC-III is a critical metabolic protein whose glycosylation status has long been known to be an important determinant of its function. ApoC-III is a small (8 kDa) O-glycosylated apoprotein whose glycans can be capped with 0, 1, or 2 sialic acids and thus is often denoted as, ApoC-III_0, ApoC-III_1, and ApoC-III_2 accordingly. Because of the negative charge conferred by the sialic acids the ApoC-III glycoforms have differential migration on gel (18), which enabled the study of its glycosylation much earlier than more advanced MS-based tools became available. ApoC-III is synthesized in the liver and intestine and found on very-low-density-lipoproteins (VLDL), chylomicrons, LDL and HDL and is a multifunctional protein whose primary functions are to hinder apolipoprotein E (ApoE) mediated hepatic uptake of lipoproteins, and to inhibit lipoprotein lipase, a key enzyme that catalyzes the hydrolysis of triacylglycerols from lipoproteins to free fatty acids and monoacylglycerol fragments (54). ApoC-III has gained considerable attention due to its relationship with CV health and the strong correlation with ApoC-III overexpression and CVD due to its involvement in hypertriglyceridemia (55, 56).

Though the association between elevated ApoC-III concentration and CVD has been established for some time, the focus has been primarily on the role of ApoC-III in VLDL metabolism, however, recently a relationship between

ApoC-III and HDL has emerged. For example, CVD patients have increased HDL ApoC-III content (57, 58). Changes in sialyation in the more common glycoforms of ApoC-III have been observed in multiple conditions including uremia, obesity, kidney disease, cancers and diabetes (8, 59–62). The enzyme from the GalNAc-transferase family Golgi-localized polypeptide N-acetyl-D-galactosamine-transferase 2 isozyme (GALNT2) initiates the first step in the O-glycosylation of ApoC-III, as well as several other lipoprotein-associated targets including ApoE, PLTP, and angiopoietin-like 3 (ANGPTL3) (63). Loss of function of GALNT2 was found to be associated with extremely low HDL concentrations (64), highlighting the importance of O-glycosylation of critical apoproteins and related proteins involved in lipoprotein remodeling in HDL metabolism. Elevated circulating levels of triglycerides (TG) are a risk factor for CVD (65) which is positively correlated with circulating ApoC-III concentrations (66, 67). High-throughput mass spectrometric immunoassay found that increased plasma TG levels were associated with higher ratio of ApoC-III_1 over ApoC-III_2 (68). Importantly, it is already well-known that the sialylation state of ApoC-III associated with LDL particles is responsible for its binding affinity to cell surface receptors, with ApoC-III_2 being preferentially cleared by heparan sulfate proteoglycans and conversely ApoC-III_1 being more effectively cleared by the LDL receptor and other receptors in the LDL receptor family (69). It is currently unknown whether and how the sialylation state of ApoC-III associated with HDL particles influences the binding of those HDL to cell surface receptors.

The glycosylation of ApoC-III is more complex than was previously thought. In addition to the known glycosite at position Alanine-74 (Ala)-74 (70) and the three possible non-sialylated and sialylated glycans attached at this site (6), our group identified a total of 20 glycoforms most of which were fucosylated and nearly half were sialylated (15). Interestingly, 13 unique glycoforms of ApoC-III were significantly enriched in HDL particles compared to serum, with the HDL-associated glycoforms being more highly sialylated (15). These findings suggest that either ApoC-III glycosylation state modifies its affinity for a specific lipoprotein class, or that the metabolism of ApoC-III and its exchange between the circulating lipoproteins is reflected in its glycosylation. Research is needed to better understand the mechanisms driving these intriguing findings about the links between ApoC-III glycosylation and its association with HDL vs. the ApoB containing lipoproteins, and the unique role of ApoC-III in HDL particle metabolism.

In a recent study comparing the site-specific glycosylation of ApoC-III in patients across the spectrum from healthy, to those with metabolic syndrome to diabetic patients with chronic kidney disease on hemodialysis, ApoC-III was differentially glycosylated in patients with metabolic syndrome and diabetic hemodialysis compared to controls (37). Patients with chronic kidney disease who were on hemodialysis and patients with metabolic syndrome had HDL that were significantly more enriched in ApoC-III especially in di-sialylated ApoC-III (ApoC-III_2) compared to the control group (37). Importantly, HDL ApoC-III glycosylation was able to distinguish between HDL that suppressed vs. increased IL-6 secretion by monocytes stimulated with lipopolysaccharide (LPS), when clinical biomarkers such as total cholesterol, LDL cholesterol, C-reactive protein (CRP), glucose and blood pressure were not discriminatory in this immunomodulatory ability (37). These intriguing preliminary findings suggest that ApoC-III glycosylation may play an important role in directing the immunomodulatory capacity of HDL particles.

Apolipoprotein E

ApoE may well be one of the most influential proteins in lipoprotein biology, and in metabolic health overall. Genome-wide association studies across multiple geographic regions have irrefutably identified APOE, which directs lipoprotein metabolism both peripherally and in the central nervous system, as the single strongest genetic marker of extreme longevity across multiple, multi-ethnic cohorts (70). APOE genotype is a major risk factor for a number of age-related pathologies including CVD and Alzheimer's disease (71, 72). ApoE exists in three isoforms, ApoE2, ApoE3, and ApoE4, with ApoE4 conferring increased risk for both CVD and Alzheimer's (73–75). Importantly, it is well-known that compared to ApoE3 the ApoE4 isoform has a reduced ability to induce cholesterol efflux (76, 77), and has a higher binding affinity for VLDL than HDL particles, altering its metabolic fate (78). Unlike the intracellular fate of ApoB-100, which is largely degraded upon uptake via the LDL receptor, as much as 80% of ApoE internalized as part of VLDL particles is recycled and re-secreted as part of HDL particles (79). This recycling and re-secretion pathway is not exclusive to hepatocytes, and instead has been demonstrated to occur across a wide variety of cell types (79). Importantly, when internalized as part of TG-rich lipoproteins via receptors in the LDL receptor family, ApoE4 is more likely to be retained in the cell than recycled and re-secreted as part of HDL particles compared to ApoE3, resulting in diminished concentrations of ApoE4 in circulation and reduced cholesterol efflux (76). The endocytic vesicles involved in ApoE recycling were identified to contain sialyltransferase enzymes (80), suggesting that addition of sialic acid residues to ApoE glycan structures may be a critical step in directing ApoE from internalized TG-rich particles to re-secreted HDL particles. In support of this hypothesis, it has been found that HDL-associated ApoE is more highly sialylated than VLDL-associated ApoE (81).

ApoE was found to be glycosylated in 1979 (82), with 6 sialylated glycoforms identified (83). ApoE does not contain the consensus amino acid sequence for N-linked glycosylation, and instead is O-glycosylated with mucin-type glycans at the originally characterized site at $Threonine^{194}$ (Thr194), which is not essential for ApoE secretion (84). More recently, additional glycosylation sites have been identified, including one at Thr^{212} (85), and 3 additional sites were identified at $Serine^{290}$ (Ser^{290}), Thr^{289} and Ser^{296} in ApoE secreted by macrophages isolated from peripheral blood mononuclear cells of a single donor with ApoE3/E3 genotype (86). It was recently shown that ApoE in fact has two more glycosites, for a total of 7 mucin-type O-glycosylation sites, with glycans ranging from simple GlcNAc to biantennary structures

containing sialylation and fucosylation (87). Evidence regarding the importance of ApoE glycosylation in lipoprotein function is starting to emerge, building on the established evidence that ApoE structure impacts the metabolism of lipoproteins (41, 76). An aberrantly glycosylated variant of ApoE causes defective binding to the LDL receptor (88). ApoE is highly sialyated when associated with HDL compared to serum, and its sialylation state is involved in mediating ApoE's binding affinity to HDL vs. VLDL (81, 89). ApoE glycosylation was shown to be considerably different in cerebral spinal fluid (CSF) than in serum (90) and its extent of sialylation in CSF affects ApoE binding to amyloid beta, thus influencing the development of plaque formation and Alzheimer's disease (91) and suggesting that glycosylation of ApoE may be tissue-specific (90). Importantly, it was recently demonstrated that site-specific glycoprofiles of HDL-associated ApoE are correlated with HDL functional capacity (87), strongly suggesting that ApoE glycosylation is important for HDL function. ApoE isoform-specific glycoprofiling has not yet been performed and will likely be important in distinguishing ApoE genotype-specific effects on disease risk.

Alpha-1 Antitrypsin

A1AT is an acute phase protein mainly synthesized by the liver, which acts as a protease inhibitor, and which has been shown to increase dramatically during inflammation and has also been found to persist post infection (92). Recent work showed that statins can also induce A1AT concentrations, and that association of A1AT with HDL protects the protein and enhances its anti-proteolytic activity in the context of the highly oxidative environment of the acute phase response (93). Post translational modifications of A1AT contribute to changes in conformation that may influence its function (94). Differential glycoforms of A1AT have been reported in patients with various types of lung cancers and are used in lung cancer diagnosis (95). Sialylation variations of A1AT have also been observed in patients with COVID-19 (96).

A1AT is N-glycosylated, and its site-specific glycosylation profiles differ when associated with HDL compared to serum (15). A1AT glycosylation is critical for its secretion by monocytes (97), is differential between serum and hepatocytes (98), and has increased fucosylated biantennary glycans in the serum of hepatocellular carcinoma patients (99). The site-specific glycosylation profiles of A1AT were highly differential between diabetic chronic kidney disease patients on hemodialysis compared to patients with metabolic syndrome and healthy controls: kidney disease patients had a higher proportion of monofucosylated to non-fucosylated glycans, and a lower proportion of di-sialylated glycans on A1AT (37). In the same study, HDL particles that attenuated the amount of Interlukin-6 (IL-6) secreted by LPS-stimulated monocytes had higher amounts of A1AT as well as lower amounts of several disialylated glycans across multiple sites, suggesting A1AT and its specific glycoprofile are involved in mediating HDL immunomodulatory function (37). A disialylated A1AT glycopeptide was also positively correlated with cholesterol efflux capacity in healthy young adults (87), and in young children from Ghana (25). These findings suggest an important connection between HDL A1AT glycosylation, particularly disialylated A1AT glycans, and HDL functionality.

Alpha-2-HS-Glycoprotein

A2HSG is a hepatically derived protein found in plasma and associated with HDL particles (24). Several studies have shown that A2HSG is critically important for CV health (100–103), playing a particularly important role in preventing vascular calcification, and emerging as an independent risk factor of CVD and all-cause mortality (100). A2HSG is differentially glycosylated in patients with chronic pancreatitis and pancreatic cancer (104). Site-specific analysis of HDL-associated A2HSG revealed that it is highly sialylated and decorated with both N- and O-glycans at multiple sites (6). In patients with chronic kidney disease HDL were enriched with non-sialylated A2HSG, and non-sialylated A2HSG was enriched in HDL particles that enhanced IL-6 secretion by LPS-stimulated monocytes (37). Interestingly, A2HSG concentrations were lower in HDL compared to serum but specific glycoforms were significantly more enriched in HDL than in serum (15). Multiple A2HSG glycopeptides were positively correlated with HDL cholesterol efflux capacity and immunomodulatory capacity in healthy adults (87), and in young children in Ghana supplemented with a lipid-based nutrient supplement (25).

Lecithin-Cholesterol Acyltransferase

LCAT functions as a key enzyme in reverse cholesterol transport and HDL particle maturation by esterifying free cholesterol with a fatty acid from phosphatidylcholine (lecithin), which allows HDL particles to carry a larger cholesterol load as cholesteryl esters (CE) in the core of the particle (105). LCAT is strongly linked with CV health and disease (106). ApoA-I is a potent activator of LCAT (107). Mutations in the LCAT gene lead to altered function of the enzyme resulting in elevated levels of TG and reduced HDL-C, which can lead to atherosclerotic pathology (108). The glycosylation of LCAT has been known since the 1990's, with both N-linked and O-linked glycoforms identified (109, 110), and with important implications for LCAT function (111). The glycosylation of LCAT is critical for its structural stability and function (112). Loss of glycosylation at several sites resulted in loss of function but loss of glycosylation at site 408 increased the activity of the enzyme (113). Desialylation of LCAT by neuraminidase resulted in considerable alteration of LCAT activity, reducing cholesterol esterification and concomitantly reducing the size of HDL (114). Depending on LCAT glycotype LCAT binds preferentially to HDL or ApoB-containing lipoproteins (115). These findings provide strong evidence that LCAT glycosylation is imperative for overall lipoprotein metabolism as well as cholesterol efflux and transport globally, as well as metabolism and efflux capacity of HDL particles in particular.

Cholesterol Ester Transfer Protein

CETP is a critical mediator of lipid transfer between HDL and ApoB-containing lipoproteins, which in the context of high TG concentrations, transfers CE from HDL in exchange for

TG from ApoB-lipoproteins, thereby enriching HDL particles with TG and altering their metabolism (116, 117). Loss of function genetic mutations in CETP and lower concentrations of CETP are associated with lower LDL-C and increased HDL-C, and lower risk of CVD, which has made CETP a major pharmacological target for CVD and atherosclerosis prevention (116, 118). CETP is highly sialylated with four N-linked glycoforms (119). A major form of serum CETP lacking glycosylation at Asparagine341 (Asn341) was shown to have markedly increased functionality compared to other forms (119, 120). Defective sialylation of CETP in heavy alcohol drinkers showed a significant reduction in the function of CETP compared to controls (121). Patients with a congenital disorder of glycosylation of the glycosyltransferase enzyme beta-1,4-galactosyltransferase 1 have defectively glycosylated CETP with reduced functionality, and larger HDL than healthy controls (122). CETP is a minor component of HDL, whose function is to temporarily associate with HDL while bridging between the HDL and ApoB particle between which the exchange of lipids occurs, thus it is often missed as an HDL-associated protein depending on the HDL isolation method and sensitivity of the protein detection method (24). However, its importance in lipid metabolism and strong links with CVD make it an important protein whose content and glycosylation when associated with HDL particles is an area of focus for future studies.

Phospholipid Transfer Protein

The primary function of PLTP is to transfer phospholipids from ApoB containing TG-rich lipoproteins to HDL (123, 124). As a key modulator of HDL size, composition, and concentration PLTP has gained considerable attention for its role in the development of CVD (125). PLTP overexpression has been reported to be an independent risk factor for CAD and is associated with type II diabetes and obesity (126). Two forms of PLTP have been described that have high and low phospholipid transfer activity, which may explain the conflicting findings of the association between PLTP and pro- vs. anti-atherogenic effects (127). Higher concentrations of the low-activity PLTP type may be the driver of the pro-atherogenic effects, and PLTP glycosylation may play a critical role in the function and activity of the protein. Human PLTP has 6 N-linked and 2 O-linked glycoforms (123). Multiple earlier studies showed that tunicamycin treatment disrupts the ability of cells to secrete PTLP, suggesting glycosylation is necessary for synthesis and secretion (128, 129). A later study confirmed that inhibition of PLTP N-glycosylation affected its structural stability and markedly reduced its ability to be excreted resulting in the non-glycosylated PLTP being intracellularly degraded (125). Much like CETP, PLTP is a protein that temporarily associates with HDL particles to mediate the exchange of material between HDL and ApoB-containing lipoproteins, thus the ability to detect its presence on HDL depends on the nature of the HDL isolation method. Although PLTP is a minor constituent of HDL particles and thus measuring its glycosylation may be limited without enrichment prior to analysis, its content and glycosylation profile are likely to be important factors in overall HDL metabolism.

POTENTIAL FOR MODIFYING THE GLYCOSYLATION OF HDL-ASSOCIATED PROTEINS TO CONFER THERAPEUTIC VALUE

Given the growing evidence that HDL glycosylation may be critically involved in both metabolism and function, with implications for both CVD diagnosis and treatment, the potential for HDL-based therapeutics targeting HDL glycosylation is compelling. Strategies to reduce CVD risk and prevent or reverse CVD by increasing the concentration of HDL particles have been largely disappointing. Increasing the number of HDL particles through pharmacological means (e.g., CETP inhibitors, niacin), has met with some success, however the ability to further reduce residual CVD risk following LDL-lowering with statins has been difficult to achieve (130, 131). Several additional HDL modifying therapies, including injection with reconstituted HDL particles, ApoA-I, as well as extracorporeal HDL lipid depletion, where HDL particles are removed from plasma, exogenously delipidated, and then reinfused, have similarly met with modest success despite promising results in animal trials (132, 133). Thus, novel therapeutic approaches to increase not just the concentration but also the function of HDL particles remain an important area of research. The potential for dietary and pharmacological strategies to improve HDL function via modulation of HDL glycoprofiles is tantalizing given the growing evidence of the importance of HDL glycosylation in its function. Several recent studies show promising results for the modification of HDL glycosylation through diet. Whereas, the glycosylation of HDL-associated ApoE was not affected by a short-term intervention with Mediterranean vs. fast food diet, the glycosylation of HDL-associated ApoC-III was significantly altered in just 4 days (87). Specifically, disialylated ApoC-III ($ApoC\text{-}III_2$) was increased after the Mediterranean diet whereas nonsialylated ApoC-III ($ApoC\text{-}III_0$) was increased after 4 days of consuming a diet enriched in saturated fat and simple sugars and depleted in fiber (87). These alterations were associated with HDL cholesterol efflux capacity as well as immunomodulatory capacity (ability to suppress cytokine secretion in stimulated monocytes) (87). In young children in Ghana supplemented with a lipid nutrient supplement, HDL glycopeptides that were altered by the supplement were correlated with HDL cholesterol efflux capacity (25). There is also evidence that targeting GALNT2 activity may be a viable strategy to alter the glycosylation of HDL-associated proteins and thus increase HDL concentration and function (64, 134). While this research area is very new, early tantalizing evidence provides support for the idea that the alteration of HDL glycoprofiles via dietary or pharmacological interventions may be a viable strategy for improving the functional capacity of HDL particles and thus improving CV outcomes.

CONCLUSION

While the study of HDL glycosylation is still in a nascent state, emerging evidence suggests that differential glycoprofiles

of HDL-associated proteins may be diagnostic and may reveal new mechanisms in lipoprotein-mediated aspects of CVD. In order to uncover glycan-based disease biomarkers newly developed glycan analytical methods need to be applied to large, comprehensively characterized, and preferably genotyped cohorts with known CV outcomes. Basic cell and molecular biology studies are also needed to better understand how glycosylation affects HDL metabolism and function, so that the potential for modifying the glycosylation of HDL-associated proteins through intervention to confer therapeutic value can be realized. In the last 10 years there has been progress toward developing the fundamental methodologies for both the isolation of HDL from plasma and the analysis of HDL glycosylation especially using MS. This field is now ripe for major discoveries utilizing these tools in the areas of glycan-based HDL CVD biomarkers, novel CVD disease mechanisms, and ultimately, novel HDL-based therapeutics for cardioprotection.

AUTHOR CONTRIBUTIONS

ER and AZ had significant contribution to the content, design, and preparation of this manuscript. Both authors have reviewed and approved the submission of this document.

FUNDING

The project described was supported by the National Institute of Aging of the NIH (R01AG062240, UH3CA241694) and the USDA National Institute of Food and Agriculture, Hatch project (CA-D-NUT-2242-H). The content is solely the responsibiltiy of the authors and does not necessarily represent the official views of the NIH.

REFERENCES

1. Kannel WB, Castelli WP, McNamara PM. Serum lipid fractions and risk of coronary heart disease. The Framingham study. *Minn Med.* (1969) 52:1225–30. doi: 10.1378/chest.56.1.43
2. Gordon DJ, Probstfield JL, Garrison RJ, Neaton JD, Castelli WP, Knoke JD, et al. High-density lipoprotein cholesterol and cardiovascular disease. Four prospective American studies. *Circulation.* (1989) 79:8–15. doi: 10.1161/01.CIR.79.1.8
3. Miller GJ, Miller NE. Plasma-high-density-lipoprotein concentration and development of ischæmic heart-disease. *The Lancet*. (1975) 305:16–9. doi: 10.1016/S0140-6736(75)92376-4
4. Kim DS, Burt AA, Rosenthal EA, Ranchalis JE, Eintracht JF, Hatsukami TS, et al. HDL-3 is a superior predictor of carotid artery disease in a case-control cohort of Participants. *J Am Heart Assoc.* (1725) 3:e000902. doi: 10.1161/JAHA.114.000902
5. Zheng JJ, Agus JK, Hong BV, Tang X, Rhodes CH, Houts HE, et al. Isolation of HDL by sequential flotation ultracentrifugation followed by size exclusion chromatography reveals size-based enrichment of HDL-associated proteins. *Sci Rep*. (2021) 11:16086. doi: 10.1038/s41598-021-95451-3
6. Huang J, Lee H, Zivkovic AM, Smilowitz JT, Rivera N, German JB, et al. Glycomic analysis of high density lipoprotein shows a highly sialylated particle. *J Proteome Res*. (2014) 13:681–91. doi: 10.1021/pr4012393
7. Krishnan S, Huang J, Lee H, Guerrero A, Berglund L, Anuurad E, et al. Combined high-density lipoprotein proteomic and glycomic profiles in patients at risk for coronary artery disease. *J Proteome Res*. (2015) 14:5109–18. doi: 10.1021/acs.jproteome.5b00730
8. Savinova OV, Fillaus K, Jing L, Harris WS, Shearer GC. Reduced apolipoprotein glycosylation in patients with the metabolic syndrome. *PLoS ONE.* (2014) 9:e104833. doi: 10.1371/journal.pone.0104833
9. Sanllorente A, Castañer O, Lassale C, Almanza-Aguilera E, Elosua R, Vila J, et al. High-density lipoprotein functional traits and coronary artery disease in a general population: a case–cohort study. *Eur J Prev Cardiol*. (2022) 29:e47–9. doi: 10.1093/eurjpc/zwaa149
10. Eren E, Yilmaz N, Aydin O. High density lipoprotein and it's dysfunction. *Open Biochem J.* (2012) 6:78–93. doi: 10.2174/1874091X01206010078
11. Liu D, Ji L, Zhang D, Tong X, Pan B, Liu P, et al. Nonenzymatic glycation of high-density lipoprotein impairs its anti-inflammatory effects in innate immunity. *Diabetes Metab Res Rev.* (2012) 28:186–95. doi: 10.1002/dmrr.1297
12. Van Lenten BJ, Wagner AC, Nayak DP, Hama S, Navab M, Fogelman AM. High-density lipoprotein loses its anti-inflammatory properties during acute influenza a infection. *Circulation*. (2001) 103:2283–8. doi: 10.1161/01.CIR.103.18.2283
13. Tölle M, Huang T, Schuchardt M, Jankowski V, Prüfer N, Jankowski J, et al. High-density lipoprotein loses its anti-inflammatory capacity by accumulation of pro-inflammatory-serum amyloid A. *Cardiovasc Res.* (2012) 94:154–62. doi: 10.1093/cvr/cvs089
14. Maverakis E, Kim K, Shimoda M, Gershwin ME, Patel F, Wilken R, et al. Glycans in the immune system and the altered glycan theory of autoimmunity: a critical review. *J Autoimmun.* (2015) 0:1–13. doi: 10.1016/j.jaut.2014.12.002
15. Kailemia MJ, Wei W, Nguyen K, Beals E, Sawrey-Kubicek L, Rhodes C, et al. Targeted measurements of O- and N-glycopeptides show that proteins in high density lipoprotein particles are enriched with specific glycosylation compared to plasma. *J Proteome Res.* (2018) 17:834–45. doi: 10.1021/acs.jproteome.7b00604
16. Liu YS, Guo XY, Hirata T, Rong Y, Motooka D, Kitajima T, et al. N-Glycan–dependent protein folding and endoplasmic reticulum retention regulate GPI-anchor processing. *J Cell Biol.* (2017) 217:585–99. doi: 10.1083/jcb.201706135
17. Ermonval M, Duvet S, Zonneveld D, Cacan R, Buttin G, Braakman I. Truncated N-glycans affect protein folding in the ER of CHO-derived mutant cell lines without preventing calnexin binding. *Glycobiology*. (2000) 10:77–87. doi: 10.1093/glycob/10.1.77
18. Mauger JF, Couture P, Bergeron N, Lamarche B. Apolipoprotein C-III isoforms: kinetics and relative implication in lipid metabolism. *J Lipid Res*. (2006) 47:1212–8. doi: 10.1194/jlr.M500455-JLR200
19. Krautter F, Iqbal AJ. Glycans and glycan-binding proteins as regulators and potential targets in leukocyte recruitment. *Front Cell Dev Biol*. (2021) 9:624082. doi: 10.3389/fcell.2021.624082
20. Varki A. Biological roles of glycans. *Glycobiology*. (2017) 27:3–49. doi: 10.1093/glycob/cww086
21. Allard-Ratick MP. *Everything in Moderation: Investigating the U-Shaped Link Between HDL Cholesterol and Adverse Outcomes*. (2019). Available online at: https://www.uscjournal.com/articles/everything-moderation-investigating-u-shaped-link-between-hdl-cholesterol-and-adverse (accessed April 17, 2022).
22. Lorkowski SW, Smith JD. HDL is not dead yet. *Biomedicines*. (2022) 10:128. doi: 10.3390/biomedicines10010128
23. Yang HS, Jeong HJ, Kim H, Hwang HK, Hur M, Lee S. Sex-specific U-shaped relationships between high-density lipoprotein cholesterol levels and 10-year major adverse cardiovascular events: a nationwide cohort study of 5.7 million South Koreans. *Ann Lab Med*. (2022) 42:415–27. doi: 10.3343/alm.2022.42.4.415
24. Davidson WS, Shah AS, Sexmith H, Gordon SM. The HDL proteome watch: compilation of studies leads to new insights on HDL function. *Biochim Biophys Acta Mol Cell Biol Lipids.* (2022) 1867:159072. doi: 10.1016/j.bbalip.2021.159072

25. Hong BV, Zhu C, Wong M, Sacchi R, Rhodes CH, Kang JW, et al. Lipid-based nutrient supplementation increases high-density lipoprotein (HDL) cholesterol efflux capacity and is associated with changes in the HDL glycoproteome in children. *ACS Omega.* (2021) 6:32022–31. doi: 10.1021/acsomega.1c04811
26. Vaisar t. Proteomics investigations of HDL, challenges and promise. *Curr Vasc Pharmacol.* (2012) 10:410–21. doi: 10.2174/157016112800812755
27. Heinecke JW. The HDL proteome: a marker–and perhaps mediator–of coronary artery disease. *J Lipid Res.* (2009) 50(Suppl):S167–71. doi: 10.1194/jlr.R800097-JLR200
28. Vickers KC, Palmisano BT, Shoucri BM, Shamburek RD, Remaley AT. MicroRNAs are transported in plasma and delivered to recipient cells by high-density lipoproteins. *Nat Cell Biol.* (2011) 13:423–33. doi: 10.1038/ncb2210
29. Michell DL, Allen RM, Landstreet SR, Zhao S, Toth CL, Sheng Q, et al. Isolation of High-density lipoproteins for Non-coding Small RNA quantification. *J Vis Exp.* (2016) 54488. doi: 10.3791/54488
30. Holzer M, Kern S, Birner-Grünberger R, Curcic S, Heinemann A, Marsche G. Refined purification strategy for reliable proteomic profiling of HDL2/3: impact on proteomic complexity. *Sci Rep*. (2016) 6:38533. doi: 10.1038/srep38533
31. Hua S, Nwosu CC, Strum JS, Seipert RR, An HJ, Zivkovic AM, et al. Site-specific protein glycosylation analysis with glycan isomer differentiation. *Anal Bioanal Chem*. (2012) 403:1291–302. doi: 10.1007/s00216-011-5109-x
32. Ruhaak LR, Xu G, Li Q, Goonatilleke E, Lebrilla CB. Mass spectrometry approaches to glycomic and glycoproteomic analyses. *Chem Rev*. (2018) 118:7886–930. doi: 10.1021/acs.chemrev.7b00732
33. Xie Y, Chen S, Li Q, Sheng Y, Alvarez MR, Reyes J, et al. Glycan–protein cross-linking mass spectrometry reveals sialic acid-mediated protein networks on cell surfaces. *Chem Sci*. (2021) 12:8767–77. doi: 10.1039/D1SC00814E
34. Kim T, Xie Y, Li Q, Artegoitia VM, Lebrilla CB, Keim NL, et al. Diet affects glycosylation of serum proteins in women at risk for cardiometabolic disease. *Eur J Nutr.* (2021) 60:3727–41. doi: 10.1007/s00394-021-02539-7
35. Banazadeh A, Veillon L, Wooding KM, Zabet M, Mechref Y. Recent advances in mass spectrometric analysis of glycoproteins. *Electrophoresis.* (2017) 38:162–89. doi: 10.1002/elps.201600357
36. Nwosu CC, Seipert RR, Strum JS, Hua SS, An HJ, Zivkovic AM, et al. Simultaneous and extensive site-specific N- and O-glycosylation analysis in protein mixtures. *J Proteome Res*. (2011) 10:2612–24. doi: 10.1021/pr2001429
37. Krishnan S, Shimoda M, Sacchi R, Kailemia MJ, Luxardi G, Kaysen GA, et al. HDL glycoprotein composition and site-specific glycosylation differentiates between clinical groups and affects IL-6 secretion in lipopolysaccharide-stimulated monocytes. *Sci Rep.* (2017) 7:43728. doi: 10.1038/srep43728
38. Buszewski B, Noga S. Hydrophilic interaction liquid chromatography (HILIC)—a powerful separation technique. *Anal Bioanal Chem*. (2012) 402:231–47. doi: 10.1007/s00216-011-5308-5
39. Zvintzou E, Lhomme M, Chasapi S, Filou S, Theodoropoulos V, Xapapadaki E, et al. Pleiotropic effects of apolipoprotein C3 on HDL functionality and adipose tissue metabolic activity. *J Lipid Res.* (2017) 58:1869–83. doi: 10.1194/jlr.M077925
40. Gudelj I, Lauc G. Protein N-glycosylation in cardiovascular diseases and related risk factors. *Curr Cardiovasc Risk Rep.* (2018) 12:16. doi: 10.1007/s12170-018-0579-4
41. Okoro EU, Zhao Y, Guo Z, Zhou L, Lin X, Yang H. Apolipoprotein E4 is deficient in inducing macrophage ABCA1 expression and stimulating the Sp1 signaling pathway. *PLoS ONE.* (2012) 7:e44430. doi: 10.1371/journal.pone.0044430
42. Furtado JD, Yamamoto R, Melchior JT, Andraski AB, Gamez-Guerrero M, Mulcahy P, et al. Distinct proteomic signatures in 16 HDL (high-density lipoprotein) subspecies. *Arterioscler Thromb Vasc Biol.* (2018) 38:2827–42. doi: 10.1161/ATVBAHA.118.311607
43. Cubedo J, Padró T, Badimon L. Glycoproteome of human apolipoprotein A-I: N- and O-glycosylated forms are increased in patients with acute myocardial infarction. *Transl Res.* (2014) 164:209–22. doi: 10.1016/j.trsl.2014.03.008
44. Lapolla A, Brioschi M, Banfi C, Tremoli E, Cosma C, Bonfante L, et al. Nonenzymatically glycated lipoprotein ApoA-I in plasma of diabetic and nephropathic patients. *Ann N Y Acad Sci.* (2008) 1126:295–9. doi: 10.1196/annals.1433.005
45. Pirillo A, Svecla M, Catapano AL, Holleboom AG, Norata GD. Impact of protein glycosylation on lipoprotein metabolism and atherosclerosis. *Cardiovasc Res.* (2021) 117:1033–45. doi: 10.1093/cvr/cvaa252
46. Syvänne M, Kahri J, Virtanen KS, Taskinen MR. HDLs containing apolipoproteins A-I and A-II (LpA-I:A-II) as markers of coronary artery disease in men with non-insulin-dependent diabetes mellitus. *Circulation.* (1995) 92:364–70. doi: 10.1161/01.CIR.92.3.364
47. Alaupovic P, Mack WJ, Knight-Gibson C, Hodis HN. The role of triglyceride-rich lipoprotein families in the progression of atherosclerotic lesions as determined by sequential coronary angiography from a controlled clinical trial. *Arterioscler Thromb Vasc Biol.* (1997) 17:715–22. doi: 10.1161/01.ATV.17.4.715
48. Birjmohun RS, Dallinga-Thie GM, Kuivenhoven JA, Stroes ESG, Otvos JD, Wareham NJ, et al. Apolipoprotein A-II is inversely associated with risk of future coronary artery disease. *Circulation.* (2007) 116:2029–35. doi: 10.1161/CIRCULATIONAHA.107.704031
49. Pussinen PJ, Jauhiainen M, Metso J, Pyle LE, Marcel YL, Fidge NH, et al. Binding of phospholipid transfer protein (PLTP) to apolipoproteins A-I and A-II: location of a PLTP binding domain in the amino terminal region of apoA-I. *J Lipid Res.* (1998) 39:152–61. doi: 10.1016/S0022-2275(20)34211-5
50. Gao X, Yuan S, Jayaraman S, Gursky O. Role of apolipoprotein A-II in the structure and remodeling of human high-density lipoprotein (HDL): protein conformational ensemble on HDL. *Biochemistry.* (2012) 51:4633–41. doi: 10.1021/bi300555d
51. Melchior JT, Street SE, Andraski AB, Furtado JD, Sacks FM, Shute RL, et al. Apolipoprotein A-II alters the proteome of human lipoproteins and enhances cholesterol efflux from ABCA1. *J Lipid Res.* (2017) 58:1374–85. doi: 10.1194/jlr.M075382
52. Jin Y, Manabe T. Direct targeting of human plasma for matrix-assisted laser desorption/ionization and analysis of plasma proteins by time of flight-mass spectrometry. *Electrophoresis.* (2005) 26:2823–34. doi: 10.1002/elps.200410421
53. Remaley AT, Wong AW, Schumacher UK, Meng MS, Brewer HB, Hoeg JM. O-linked glycosylation modifies the association of apolipoprotein A-II to high density lipoproteins. *J Biol Chem.* (1993) 268:6785–90. doi: 10.1016/S0021-9258(18)53318-4
54. Norata GD, Tsimikas S, Pirillo A, Catapano AL. Apolipoprotein C-III: from pathophysiology to pharmacology. *Trends Pharmacol Sci*. (2015) 36:675–87. doi: 10.1016/j.tips.2015.07.001
55. Taskinen MR, Borén J. Why is apolipoprotein CIII emerging as a novel therapeutic target to reduce the burden of cardiovascular disease? *Curr Atheroscler Rep.* (2016) 18:59. doi: 10.1007/s11883-016-0614-1
56. Dittrich J, Beutner F, Teren A, Thiery J, Burkhardt R, Scholz M, et al. Plasma levels of apolipoproteins C-III, A-IV, and E are independently associated with stable atherosclerotic cardiovascular disease. *Atherosclerosis*. (2019) 281:17–24. doi: 10.1016/j.atherosclerosis.2018.11.006
57. Vaisar T, Mayer P, Nilsson E, Zhao XQ, Knopp R, Prazen BJ. HDL in humans with cardiovascular disease exhibits a proteomic signature. *Clin Chim Acta*. (2010) 411:972–9. doi: 10.1016/j.cca.2010.03.023
58. Jensen MK, Rimm EB, Furtado JD, Sacks FM. Apolipoprotein C-III as a potential modulator of the association between HDL-cholesterol and incident coronary heart disease. *J Am Heart Assoc.* (2012) 1:jah3-e000232. doi: 10.1161/JAHA.111.000232
59. Kornak U, Reynders E, Dimopoulou A, van Reeuwijk J, Fischer B, Rajab A, et al. Impaired glycosylation and cutis laxa caused by mutations in the vesicular H+-ATPase subunit ATP6V0A2. *Nat Genet*. (2008) 40:32–4. doi: 10.1038/ng.2007.45
60. Juntti-Berggren L, Refai E, Appelskog I, Andersson M, Imreh G, Dekki N, et al. Apolipoprotein CIII promotes Ca2+-dependent beta cell death in type 1 diabetes. *Proc Natl Acad Sci U S A*. (2004) 101:10090–4. doi: 10.1073/pnas.0403551101
61. Harvey SB, Zhang Y, Wilson-Grady J, Monkkonen T, Nelsestuen GL, Kasthuri RS, et al. O-Glycoside biomarker of apolipoprotein C3: responsiveness to obesity, bariatric surgery, and therapy with metformin, to chronic or severe liver disease and to mortality in severe sepsis and graft vs. host disease. *J Proteome Res.* (2009) 8:603–12. doi: 10.1021/pr800751x

62. Ueda K, Fukase Y, Katagiri T, Ishikawa N, Irie S, Sato TA, et al. Targeted serum glycoproteomics for the discovery of lung cancer-associated glycosylation disorders using lectin-coupled ProteinChip arrays. *Proteomics.* (2009) 9:2182–92. doi: 10.1002/pmic.200800374
63. Zilmer M, Edmondson AC, Khetarpal SA, Alesi V, Zaki MS, Rostasy K, et al. Novel congenital disorder of O-linked glycosylation caused by GALNT2 loss of function. *Brain.* (2020) 143:1114–26. doi: 10.1093/brain/awaa063
64. Khetarpal SA, Schjoldager KT, Christoffersen C, Raghavan A, Edmondson AC, Reutter HM, et al. Loss of function of GALNT2 lowers high density lipoproteins in humans, nonhuman primates, and rodents. *Cell Metab.* (2016) 24:234–45. doi: 10.1016/j.cmet.2016.07.012
65. Dallinga-Thie GM, Kroon J, Borén J, Chapman MJ. Triglyceride-rich lipoproteins and remnants: targets for therapy? *Curr Cardiol Rep.* (2016) 18:67. doi: 10.1007/s11886-016-0745-6
66. van Capelleveen JC, Moens SJB, Yang X, Kastelein JJP, Wareham NJ, Zwinderman AH, et al. Apolipoprotein C-III levels and incident coronary artery disease risk: the EPIC-norfolk prospective population study. *Arterioscler Thromb Vasc Biol.* (2017) 37:1206–12. doi: 10.1161/ATVBAHA.117.309007
67. Jørgensen AB, Frikke-Schmidt R, Nordestgaard BG, Tybjærg-Hansen A. Loss-of-function mutations in APOC3 and risk of ischemic vascular disease. *N Engl J Med.* (2014) 371:32–41. doi: 10.1056/NEJMoa1308027
68. Koska J, Yassine H, Trenchevska O, Sinari S, Schwenke DC, Yen FT, et al. Disialylated apolipoprotein C-III proteoform is associated with improved lipids in prediabetes and type 2 diabetes1. *J Lipid Res.* (2016) 57:894–905. doi: 10.1194/jlr.P064816
69. Kegulian NC, Ramms B, Horton S, Trenchevska O, Nedelkov D, Graham MJ, et al. ApoC-III glycoforms are differentially cleared by hepatic triglyceride-rich lipoprotein receptors. *Arterioscler Thromb Vasc Biol.* (2019) 39:2145–56. doi: 10.1161/ATVBAHA.119.312723
70. Roghani A, Zannis VI. Mutagenesis of the glycosylation site of human ApoCIII. O-linked glycosylation is not required for ApoCIII secretion and lipid binding. *J Biol Chem.* (1988) 263:17925–32. doi: 10.1016/S0021-9258(19)81305-4
71. Egert S, Rimbach G, Huebbe P. ApoE genotype: from geographic distribution to function and responsiveness to dietary factors. *Proc Nutr Soc.* (2012) 71:410–24. doi: 10.1017/S0029665112000249
72. Corder EH, Saunders AM, Strittmatter WJ, Schmechel DE, Gaskell PC, Small GW, et al. Gene dose of apolipoprotein E type 4 allele and the risk of Alzheimer's disease in late onset families. *Science.* (1993) 261:921–3. doi: 10.1126/science.8346443
73. Marais AD. Apolipoprotein E in lipoprotein metabolism, health and cardiovascular disease. *Pathology.* (2019) 51:165–76. doi: 10.1016/j.pathol.2018.11.002
74. Mahoney-Sanchez L, Belaidi AA, Bush AI, Ayton S. The complex role of apolipoprotein E in Alzheimer's disease: an overview and update. *J Mol Neurosci.* (2016) 60:325–35. doi: 10.1007/s12031-016-0839-z
75. Deane R, Sagare A, Hamm K, Parisi M, Lane S, Finn MB, et al. apoE isoform–specific disruption of amyloid β peptide clearance from mouse brain. *J Clin Invest.* (2008) 118:4002–13. doi: 10.1172/JCI36663
76. Heeren J, Grewal T, Laatsch A, Becker N, Rinninger F, Rye KA, et al. Impaired recycling of apolipoprotein E4 is associated with intracellular cholesterol accumulation. *J Biol Chem.* (2004) 279:55483–92. doi: 10.1074/jbc.M409324200
77. Minagawa H, Gong JS, Jung CG, Watanabe A, Lund-Katz S, Phillips MC, et al. Mechanism underlying apolipoprotein E (ApoE) isoform-dependent lipid efflux from neural cells in culture. *J Neurosci Res.* (2009) 87:2498–508. doi: 10.1002/jnr.22073
78. Mamotte CDS, Sturm M, Foo JI, van Bockxmeer FM, Taylor RR. Comparison of the LDL-receptor binding of VLDL and LDL from apoE4 and apoE3 homozygotes. *Am J Physiol Endocrin Metab.* (1999) 276:E553–7. doi: 10.1152/ajpendo.1999.276.3.E553
79. Röhrl C, Stangl H. HDL endocytosis and resecretion. *Biochim Biophys Acta.* (2013) 1831:1626–33. doi: 10.1016/j.bbalip.2013.07.014
80. Heeren J, Beisiegel U, Grewal T. Apolipoprotein E recycling. *Arterioscler Thromb Vasc Biol.* (2006) 26:442–8. doi: 10.1161/01.ATV.0000201282.64751.47
81. Marmillot P, Rao MN, Liu QH, Lakshman MR. Desialylation of human apolipoprotein E decreases its binding to human high-density lipoprotein and its ability to deliver esterified cholesterol to the liver. *Metabolism.* (1999) 48:1184–92. doi: 10.1016/S0026-0495(99)90136-1
82. Jain RS, Quarfordt SH. The carbohydrate content of apolipoprotein E from human very low density lipoproteins. *Life Sci.* (1979) 25:1315–23. doi: 10.1016/0024-3205(79)90397-7
83. Zannis VI. vanderSpek J, Silverman D. Intracellular modifications of human apolipoprotein E. *J Biol Chem.* (1986) 261:13415–21. doi: 10.1016/S0021-9258(18)67033-4
84. Wernette-Hammond ME, Lauer SJ, Corsini A, Walker D, Taylor JM, Rall SC. Glycosylation of human apolipoprotein E: the carbohydrate attachment site is threonine 194. *J Biol Chem.* (1989) 264:9094–101. doi: 10.1016/S0021-9258(18)81907-X
85. Mancone C, Amicone L, Fimia GM, Bravo E, Piacentini M, Tripodi M, et al. Proteomic analysis of human very low-density lipoprotein by two-dimensional gel electrophoresis and MALDI-TOF/TOF. *Proteomics.* (2007) 7:143–54. doi: 10.1002/pmic.200600339
86. Lee Y, Kockx M, Raftery MJ, Jessup W, Griffith R, Kritharides L. Glycosylation and sialylation of macrophage-derived human apolipoprotein E analyzed by SDS-PAGE and mass spectrometry. *Mol Cell Proteomics.* (2010) 9:1968–81. doi: 10.1074/mcp.M900430-MCP200
87. Zhu C, Wong M, Li Q, Sawrey-Kubicek L, Beals E, Rhodes CH, et al. Site-specific glycoprofiles of HDL-associated ApoE are correlated with HDL functional capacity and unaffected by short-term diet. *J Proteome Res.* (2019) 18:3977–84. doi: 10.1021/acs.jproteome.9b00450
88. Fazio S, Horie Y, Weisgraber K, Havekes L, Rall S. Preferential association of apolipoprotein E Leiden with very low density lipoproteins of human plasma. *J Lipid Res.* (1993) 34:447–53. doi: 10.1016/S0022-2275(20)40736-9
89. Ghosh P, Hale EA, Mayur K, Seddon J, Lakshman MR. Effects of chronic alcohol treatment on the synthesis, sialylation, and disposition of nascent apolipoprotein E by peritoneal macrophages of rats. *Am J Clin Nutr.* (2000) 2:190–8. doi: 10.1093/ajcn/72.1.190
90. Flowers SA, Grant OC, Woods RJ, Rebeck GW. O-glycosylation on cerebrospinal fluid and plasma apolipoprotein E differs in the lipid-binding domain. *Glycobiology.* (2020) 30:74–85. doi: 10.1093/glycob/cwz084
91. Sugano M, Yamauchi K, Kawasaki K, Tozuka M, Fujita K, Okumura N, et al. Sialic acid moiety of apolipoprotein E3 at Thr194 affects its interaction with β-amyloid1–42 peptides. *Clinica Chimica Acta.* (2008) 388:123–9. doi: 10.1016/j.cca.2007.10.024
92. McCarthy C, Saldova R, Wormald MR, Rudd PM, McElvaney NG, Reeves EP. The role and importance of glycosylation of acute phase proteins with focus on alpha-1 antitrypsin in acute and chronic inflammatory conditions. *J Proteome Res.* (2014) 13:3131–43. doi: 10.1021/pr500146y
93. Gordon SM, McKenzie B, Kemeh G, Sampson M, Perl S, Young NS, et al. Rosuvastatin alters the proteome of high density lipoproteins: generation of alpha-1-antitrypsin enriched particles with anti-inflammatory properties. *Mol Cell Proteomics.* (2015) 14:3247–57. doi: 10.1074/mcp.M115.054031
94. Lechowicz U, Rudzinski S, Jezela-Stanek A, Janciauskiene S, Chorostowska-Wynimko J. Post-translational modifications of circulating alpha-1-antitrypsin protein. *Int J Mol Sci.* (2020) 21:9187. doi: 10.3390/ijms21239187
95. Liang Y, Ma T, Thakur A, Yu H, Gao L, Shi P, et al. Differentially expressed glycosylated patterns of α-1-antitrypsin as serum biomarkers for the diagnosis of lung cancer. *Glycobiology.* (2015) 25:331–40. doi: 10.1093/glycob/cwu115
96. McElvaney OJ, McEvoy NL, McElvaney OF, Carroll TP, Murphy MP, Dunlea DM, et al. Characterization of the inflammatory response to severe COVID-19 illness. *Am J Respir Crit Care Med.* (2020) 202:812–21. doi: 10.1164/rccm.202005-1583OC
97. Gross V, vom Berg D, Kreuzkamp J, Ganter U, Bauer J, Würtemberger G, et al. Biosynthesis and secretion of M- and Z-type alpha 1-proteinase inhibitor by human monocytes Effect of inhibitors of glycosylation and of oligosaccharide processing on secretion and function. *Biol Chem Hoppe Seyler.* (1990) 371:231–8. doi: 10.1515/bchm3.1990.371.1.231
98. Jeppsson JO, Larsson C, Eriksson S. Characterization of α1-antitrypsin in the inclusion bodies from the liver in α1-antitrypsin deficiency. *N Engl J Med.* (1975) 293:576–9. doi: 10.1056/NEJM197509182931203

99. Saitoh A, Aoyagi Y, Asakura H. Structural analysis on the sugar chains of human α1-antitrypsin: presence of fucosylated biantennary glycan in hepatocellular carcinoma. *Arch Biochem Biophys*. (1993) 303:281–7. doi: 10.1006/abbi.1993.1284
100. Ketteler M, Bongartz P, Westenfeld R, Wildberger JE, Mahnken AH, Böhm R, et al. Association of low fetuin-A (AHSG) concentrations in serum with cardiovascular mortality in patients on dialysis: a cross-sectional study. *Lancet*. (2003) 361:827–33. doi: 10.1016/S0140-6736(03)12710-9
101. Ketteler M, Schlieper G, Floege J. Calcification and cardiovascular health. *Hypertension*. (2006) 47:1027–34. doi: 10.1161/01.HYP.0000219635.51844.da
102. Jahnen-Dechent W, Heiss A, Schäfer C, Ketteler M, Towler DA. Fetuin-A Regulation of calcified matrix metabolism. *Circ Res*. (2011) 108:1494–509. doi: 10.1161/CIRCRESAHA.110.234260
103. Ix JH, Barrett-Connor E, Wassel CL, Cummins K, Bergstrom J, Daniels LB, et al. The associations of fetuin-A with subclinical cardiovascular disease in community-dwelling persons: the rancho bernardo study. *J Am Coll Cardiol*. (2011) 58:2372–9. doi: 10.1016/j.jacc.2011.08.035
104. Sarrats A, Saldova R, Pla E, Fort E, Harvey DJ, Struwe WB, et al. Glycosylation of liver acute-phase proteins in pancreatic cancer and chronic pancreatitis. *Proteomics Clin Appl*. (2010) 4:432–48. doi: 10.1002/prca.200900150
105. Sorci-Thomas MG, Bhat S, Thomas MJ. Activation of lecithin:cholesterol acyltransferase by HDL ApoA-I central helices. *Clin Lipidol*. (2009) 4:113–24. doi: 10.2217/17584299.4.1.113
106. Yokoyama K, Tani S, Matsuo R, Matsumoto N. Association of lecithin-cholesterol acyltransferase activity and low-density lipoprotein heterogeneity with atherosclerotic cardiovascular disease risk: a longitudinal pilot study. *BMC Cardiovasc Disord*. (2018) 18:224. doi: 10.1186/s12872-018-0967-1
107. Manthei KA, Patra D, Wilson CJ, Fawaz MV, Piersimoni L, Shenkar JC, et al. Structural analysis of lecithin:cholesterol acyltransferase bound to high density lipoprotein particles. *Commun Biol*. (2020) 3:1–11. doi: 10.1038/s42003-019-0749-z
108. Hovingh GK, Hutten BA, Holleboom AG, Petersen W, Rol P, Stalenhoef A, et al. Compromised LCAT function is associated with increased atherosclerosis. *Circulation*. (2005) 112:879–84. doi: 10.1161/CIRCULATIONAHA.105.540427
109. Lacko AG, Reason AJ, Nuckolls C, Kudchodkar BJ, Nair MP, Sundarrajan G, et al. Characterization of recombinant human plasma lecithin: cholesterol acyltransferase (LCAT): N-linked carbohydrate structures and catalytic properties. *J Lipid Res*. (1998) 39:807–20. doi: 10.1016/S0022-2275(20)32568-2
110. Schindler PA, Settineri CA, Collet X, Fielding CJ, Burlingame AL. Site-specific detection and structural characterization of the glycosylation of human plasma proteins lecithin: cholesterol acyltransferase and apolipoprotein D using HPLC/electrospray mass spectrometry and sequential glycosidase digestion. *Protein Sci*. (1995) 4:791–803. doi: 10.1002/pro.5560040419
111. Miller KR, Wang J, Sorci-Thomas M, Anderson RA, Parks JS. Glycosylation structure and enzyme activity of lecithin: cholesterol acyltransferase from human plasma, HepG2 cells, and baculoviral and Chinese hamster ovary cell expression systems. *J Lipid Res*. (1996) 37:551–61. doi: 10.1016/S0022-2275(20)37598-2
112. Kosman J, Jonas A. Deletion of specific glycan chains affects differentially the stability, local structures, and activity of lecithin-cholesterol acyltransferase*. *J Biol Chem*. (2001) 276:37230–6. doi: 10.1074/jbc.M104326200
113. O K, Hill JS, Wang X, McLeod R, Pritchard PH. Lecithin: cholesterol acyltransferase: role of N-linked glycosylation in enzyme function. *Biochem J*. (1993) 294:879–84. doi: 10.1042/bj2940879
114. Sukhorukov V, Gudelj I, Pučić-Baković M, Zakiev E, Orekhov A, Kontush A, et al. Glycosylation of human plasma lipoproteins reveals a high level of diversity, which directly impacts their functional properties. *Biochimica et Biophysica Acta (BBA) – Mol Cell Biol Lipids*. (2019) 1864:643–53. doi: 10.1016/j.bbalip.2019.01.005
115. Carlson LA, Holmquist L. Evidence for deficiency of high density lipoprotein lecithin: cholesterol acyltransferase activity (alpha-LCAT) in fish eye disease. *Acta Med Scand*. (1985) 218:189–96. doi: 10.1111/j.0954-6820.1985.tb08846.x
116. Barter PJ, Brewer HB, Chapman MJ, Hennekens CH, Rader DJ, Tall AR. Cholesteryl ester transfer protein. *Arterioscler Thromb Vasc Biol*. (2003) 23:160–7. doi: 10.1161/01.ATV.0000054658.91146.64
117. Ikewaki K, Rader DJ, Sakamoto T, Nishiwaki M, Wakimoto N, Schaefer JR, et al. Delayed catabolism of high density lipoprotein apolipoproteins A-I and A-II in human cholesteryl ester transfer protein deficiency. *J Clin Invest*. (1993) 92:1650–8. doi: 10.1172/JCI116750
118. Holmes MV, Davey Smith G. Revealing the effect of CETP inhibition in cardiovascular disease. *Nat Rev Cardiol*. (2017) 14:635–6. doi: 10.1038/nrcardio.2017.156
119. Stevenson SC, Wang S, Deng L, Tall AR. Human plasma cholesteryl ester transfer protein consists of a mixture of two forms reflecting variable glycosylation at asparagine 341. *Biochemistry*. (1993) 32:5121–6. doi: 10.1021/bi00070a021
120. Tall A. Plasma cholesteryl ester transfer protein. *J Lipid Res*. (1993) 34:1255–74. doi: 10.1016/S0022-2275(20)36957-1
121. Liinamaa MJ, Hannuksela ML, Rämet ME, Savolainen MJ. Defective glycosylation of cholesteryl ester transfer protein in plasma from alcohol abusers. *Alcohol Alcohol*. (2006) 41:18–23. doi: 10.1093/alcalc/agh216
122. van den Boogert MAW, Crunelle CL, Ali L, Larsen LE, Kuil SD, Levels JHM, et al. Reduced CETP glycosylation and activity in patients with homozygous B4GALT1 mutations. *J Inherit Metab Dis*. (2020) 43:611–7. doi: 10.1002/jimd.12200
123. Day JR, Albers JJ, Lofton-Day CE, Gilbert TL, Ching AF, Grant FJ, et al. Complete cDNA encoding human phospholipid transfer protein from human endothelial cells. *J Biol Chem*. (1994) 269:9388–91. doi: 10.1016/S0021-9258(17)37120-X
124. Jiang XC, Bruce C. Regulation of murine plasma phospholipid transfer protein activity and mRNA levels by lipopolysaccharide and high cholesterol diet (*). *J Biol Chem*. (1995) 270:17133–8. doi: 10.1074/jbc.270.29.17133
125. Huuskonen J, Olkkonen VM, Jauhiainen M, Ehnholm C. The impact of phospholipid transfer protein (PLTP) on HDL metabolism. *Atherosclerosis*. (2001) 155:269–81. doi: 10.1016/S0021-9150(01)00447-6
126. Schlitt A, Bickel C, Thumma P, Blankenberg S, Rupprecht HJ, Meyer J, et al. High plasma phospholipid transfer protein levels as a risk factor for coronary artery disease. *Arterioscler Thromb Vasc Biol*. (2003) 23:1857–62. doi: 10.1161/01.ATV.0000094433.98445.7F
127. Krauss RM. Phospholipid transfer protein and atherosclerosis. *Circulation*. (2010) 122:452–4. doi: 10.1161/CIRCULATIONAHA.110.966572
128. Au-Young J, Fielding CJ. Synthesis and secretion of wild-type and mutant human plasma cholesteryl ester transfer protein in baculovirus-transfected insect cells: the carboxyl-terminal region is required for both lipoprotein binding and catalysis of transfer. *Proc Natl Acad Sci USA*. (1992) 89:4094–8. doi: 10.1073/pnas.89.9.4094
129. Swenson T, Simmons J, Hesler C, Bisgaier C, Tall A. Cholesteryl ester transfer protein is secreted by Hep G2 cells and contains asparagine-linked carbohydrate and sialic acid. *J Biol Chem*. (1987) 262:16271–4. doi: 10.1016/S0021-9258(18)49249-6
130. D'Andrea E, Hey SP, Ramirez CL, Kesselheim AS. Assessment of the role of niacin in managing cardiovascular disease outcomes: a systematic review and meta-analysis. *JAMA Netw Open*. (2019) 2:e192224. doi: 10.1001/jamanetworkopen.2019.2224
131. Taheri H, Filion KB, Windle SB, Reynier P, Eisenberg MJ. Cholesteryl ester transfer protein inhibitors and cardiovascular outcomes: a systematic review and meta-analysis of randomized controlled trials. *CRD*. (2020) 145:236–50. doi: 10.1159/000505365
132. Abudukeremu A, Huang C, Li H, Sun R, Liu X, Wu X, et al. Efficacy and safety of high-density lipoprotein/apolipoprotein a1 replacement therapy in humans and mice with atherosclerosis: a systematic review and meta-analysis. *Front Cardiovasc Med*. (2021) 8:700233. doi: 10.3389/fcvm.2021.700233

133. Barter PJ, Rye KA. Targeting high-density lipoproteins to reduce cardiovascular risk: what is the evidence? *Clin Ther*. (2015) 37:2716–31. doi: 10.1016/j.clinthera.2015.07.021
134. Di Paola R, Marucci A, Trischitta V. GALNT2 effect on HDL-cholesterol and triglycerides levels in humans: evidence of pleiotropy? *Nutr Metab Cardiovasc Dis*. (2017) 27:281–2. doi: 10.1016/j.numecd.2016.11.006

Conflict of Interest: The authors declare that the research was conducted in the absence of any commercial or financial relationships that could be construed as a potential conflict of interest.

Publisher's Note: All claims expressed in this article are solely those of the authors and do not necessarily represent those of their affiliated organizations, or those of the publisher, the editors and the reviewers. Any product that may be evaluated in this article, or claim that may be made by its manufacturer, is not guaranteed or endorsed by the publisher.

frontiers | Frontiers in Cardiovascular Medicine

ORIGINAL RESEARCH
published: 06 June 2022
doi: 10.3389/fcvm.2022.889985

Influence of the Human Lipidome on Epicardial Fat Volume in Mexican American Individuals

*Ana Cristina Leandro[1], Laura F. Michael[2], Marcio Almeida[1], Mikko Kuokkanen[1], Kevin Huynh[3,4], Corey Giles[3,4], Thy Duong[3], Vincent P. Diego[1], Ravindranath Duggirala[1], Geoffrey D. Clarke[5], John Blangero[1], Peter J. Meikle[3,4] and Joanne E. Curran[1]**

[1] Department of Human Genetics and South Texas Diabetes and Obesity Institute, University of Texas Rio Grande Valley School of Medicine, Brownsville, TX, United States, [2] Eli Lilly and Company, Indianapolis, IN, United States, [3] Metabolomics Laboratory, Baker Heart and Diabetes Institute, Melbourne, VIC, Australia, [4] Baker Department of Cardiometabolic Health, University of Melbourne, Parkville, VIC, Australia, [5] Department of Radiology and Research Imaging Institute, University of Texas Health Science Center, San Antonio, TX, United States

OPEN ACCESS

Edited by:
Mary G. Sorci-Thomas, Medical College of Wisconsin, United States

Reviewed by:
Matthieu Ruiz, Université de Montréal, Canada
Michael J. Thomas, Medical College of Wisconsin, United States

***Correspondence:**
Joanne E. Curran
joanne.curran@utrgv.edu

Specialty section:
This article was submitted to Lipids in Cardiovascular Disease, a section of the journal Frontiers in Cardiovascular Medicine

Received: *04 March 2022*
Accepted: *05 May 2022*
Published: *06 June 2022*

Citation:
Leandro AC, Michael LF, Almeida M, Kuokkanen M, Huynh K, Giles C, Duong T, Diego VP, Duggirala R, Clarke GD, Blangero J, Meikle PJ and Curran JE (2022) Influence of the Human Lipidome on Epicardial Fat Volume in Mexican American Individuals. Front. Cardiovasc. Med. 9:889985. doi: 10.3389/fcvm.2022.889985

Introduction: Cardiovascular disease (CVD) is the leading cause of mortality worldwide and is the leading cause of death in the US. Lipid dysregulation is a well-known precursor to metabolic diseases, including CVD. There is a growing body of literature that suggests MRI-derived epicardial fat volume, or epicardial adipose tissue (EAT) volume, is linked to the development of coronary artery disease. Interestingly, epicardial fat is also actively involved in lipid and energy homeostasis, with epicardial adipose tissue having a greater capacity for release and uptake of free fatty acids. However, there is a scarcity of knowledge on the influence of plasma lipids on EAT volume.

Aim: The focus of this study is on the identification of novel lipidomic species associated with CMRI-derived measures of epicardial fat in Mexican American individuals.

Methods: We performed lipidomic profiling on 200 Mexican American individuals. High-throughput mass spectrometry enabled rapid capture of precise lipidomic profiles, providing measures of 799 unique species from circulating plasma samples. Because of our extended pedigree design, we utilized a standard quantitative genetic linear mixed model analysis to determine whether lipids were correlated with EAT by formally testing for association between each lipid species and the CMRI epicardial fat phenotype.

Results: After correction for multiple testing using the FDR approach, we identified 135 lipid species showing significant association with epicardial fat. Of those, 131 lipid species were positively correlated with EAT, where increased circulating lipid levels were correlated with increased epicardial fat. Interestingly, the top 10 lipid species associated with an increased epicardial fat volume were from the deoxyceramide (Cer(m)) and triacylglycerol (TG) families. Deoxyceramides are atypical and neurotoxic sphingolipids. Triacylglycerols are an abundant lipid class and comprise the bulk of storage fat in tissues. Pathologically elevated TG and Cer(m) levels are related to CVD risk and, in our study, to EAT volume.

Conclusion: Our results indicate that specific lipid abnormalities such as enriched saturated triacylglycerols and the presence of toxic ceramides Cer(m) in plasma of our individuals could precede CVD with increased EAT volume.

Keywords: cardiovascular disease, lipidomic profiles, epicardial fat volume, Mexican Americans, CMRI

INTRODUCTION

Cardiovascular disease (CVD) is the leading cause of mortality worldwide and remains the leading cause of death in the US (1, 2). CVD encompasses a broad range of disorders of the cardiovascular system, including coronary heart disease, cerebrovascular disease, and peripheral artery disease. Underlying them all is atherosclerosis (ATS)—a complex disorder in which a host of different intrinsic and extrinsic processes and factors contribute to the development of lesions that eventually compromise normal vascular function (3). ATS is an inflammatory disease of the arteries associated with lipid and other metabolic alterations (4). Lipid dysregulation is a well-known precursor to metabolic diseases (MeD), including CVD. Risk factors for ATS and CVD, including age, sex, lipid levels, smoking and blood pressure, are incorporated in risk algorithms that are used to predict an individual's absolute risk for CVD in the general population (5). Although these risk factors are useful to predict disease risk in populations, their accuracy in predicting cardiovascular risk in individuals varies considerably across populations (6). Mexican Americans have a high prevalence of cardiovascular morbidity and mortality (5, 7). The high risk for CVD in this ethnic group is partly explained by a high propensity to MeD (5).

Evidence from epidemiological and lipidomic studies has shown that specific lipoproteins and their constituent lipids are important factors in the development of metabolic related disorders (8–10), including CVD (11–13). The classical lipid traits (such as HDL-C, LDL-C, and triglycerides), most commonly examined in disease risk, are complex molecules comprised of multiple lipid and protein components (14). The lipidome is the total complement of these lipid species. Even though these lipid measures are influenced by both environmental and genetic factors, genetic variation is a significant determinant with traditional plasma measures having heritability of more than 50% (15, 16). Although CVD risk is heritable and there have been a number of successes localizing QTLs that influence disease risk, the genetic basis of this risk is still relatively unknown. Quantitative endophenotypes that are related to disease liability can offer more power for gene localization/identification than dichotomous disease status and thus serve as valuable phenotypes for disease gene identification. Such endophenotypes, whose alterations precede disease, may also be useful for early risk assessment. Measures of the human lipidome represents a wealth of phenotypes that may be better predictors of disease than the traditional clinical measures (17). The biologically simpler nature of these individual species suggests that they may reside closer to the causal action of genes, making them valuable endophenotypes (18). Lipidomic studies are helping to decipher the complex interactions between lipid metabolism and MeD, and identifying pathways representing potential therapeutic targets not seen with studies of traditional lipids (19).

Intermediate phenotypes such as those derived by CMRI and lipid profiling lie closer to the genomic level and the causal action of genes. Organ-specific adiposity has renewed growing interest in that and contributes to the pathophysiology of cardiometabolic diseases (20, 21). However, the molecular changes in adipose tissue that promote these disorders are not completely understood and, in particular, the specific role of cardiac adiposity. Pericardial adipose tissue is ectopic fat in the mediastinum, which is associated with poor metabolic and cardiac health, especially in with type II diabetes mellitus (T2DM) patients (22, 23). Pericardial adipose tissue is comprised of two compartments. Epicardial adipose tissue (EAT) is defined as the visceral fat deposited between the epicardium and the pericardium. Paracardial adipose tissue (PAT) is the fat deposited on the external surface of the pericardium within the mediastinum (24). Growing evidence indicates that epicardial adipose tissue (EAT) volume is positively associated with coronary artery disease (23). The increase of EAT has been associated with different cardiovascular risk factors (25) such as type 2 diabetes mellitus, hypertension, and obesity, in isolation or as part of the MeD (26–28). Growing evidence indicates that EAT volume is positively associated with coronary artery disease (29), but the mechanisms involved in this relationship remain largely unknown. EAT is the visceral fat deposit over the heart, located between the myocardium and the visceral pericardium (21, 30). EAT is more than a simple fat storage depot. Indeed, it is now widely recognized to be an extremely active endocrine organ, producing cytokines, adipokines, and chemokines that can be either protective or harmful depending on the local microenvironment (31, 32). These functions highlight the complex cellularity and crosstalk between EAT and neighboring structures (21). EAT metabolism is uniquely regulated due to the high basal rates of fatty acid uptake, insulin-induced lipogenesis, and high fatty acid breakdown (33, 34). EAT may act as a local energy store for cardiac muscle and has a protective role against elevated levels of free fatty acid (FFA) in the coronary circulation (35). Additionally, EAT could influence coronary atherogenesis and myocardial function because there is no fibrous fascial layer to impede the diffusion of FFA and adipokines between it and the underlying vessel wall as well as the myocardium (34, 36). EAT is also actively involved in lipid and energy homeostasis, with EAT having a greater capacity for release and uptake of FFA (36–38). FFA synthesis and rates of incorporation and breakdown are significantly higher in EAT than in other fat deposits. However, the amount and type of fatty acids stored could also play a role in the onset and development of atherosclerosis (39). These metabolites serve as direct signatures of biochemical activity,

being, therefore, easier to correlate with quantitative plasma lipid phenotypes. In this context, lipidomics has become a powerful approach to mechanistically investigate how biochemistry relates to clinical phenotype (40, 41). We concentrate on EAT because it is a known adiposity-related risk factor for CVD, directly related to heart function, but has been comparatively less studied than more easily measured fat measures. However, there is a scarcity of information on the interaction of plasma lipids and CMRI EAT measures. Therefore, this study identifies plasma lipidomic species associated with CMRI-derived measures of epicardial fat, as a measure of CVD risk, in a cohort of Mexican American individuals.

MATERIALS AND METHODS

Study Participants

The SAFHS began in 1991 and was initially designed to investigate the genetics of CVD in Mexican Americans. The SAFHS enrolled large, extended Mexican Americans families residing in San Antonio, TX, and ascertainment occurred by way of the random selection of an adult Mexican American proband, without regard to disease. The enrollment procedures, inclusion and exclusion criteria, and phenotypic assessments of the study participants have been described in detail previously (7, 42). This is an ongoing investigation, which has had four phases of data collection over a 25-year period. The data and samples used in this study were collected during the first phase of data collection, occurring between 1992 and 1996. Blood samples were collected from participants on their visit day using standard procedures, and participants were fasted for 12 h. For plasma, blood was collected in a K2-EDTA vacutainer, and the plasma layer removed after centrifugation. Plasma was stored in 50 μL aliquots at −80°C and has not been thawed post-collection. In the current study, 200 individuals that have both lipidome profile measures and CMRI-derived epicardial fat data were included. Of these 200 SAFHS participants, 63% were female, and the sample was aged between 18 and 83 (46.85 ± 16.23). Informed consent was obtained from all participants before collection of samples. The study conformed to the Declaration of Helsinki, and the Institutional Review Boards of the University of Texas Health Sciences Center at San Antonio and the University of Texas Rio Grande Valley approved this study.

Epicardial Fat Tissue Measurement by Cardiac Magnetic Resonance Imaging

Cardiac imaging was performed on a 3.0 Tesla MR scanner (TIM Trio; Siemens, Erlangen, Germany) with a 6-channel anterior matrix torso coil combined with posterior spine-coil elements producing an aggregate of 12 data channels. For MRI of the abdominal aorta, an additional 6-channel anterior matrix receiver coil ensures full coverage. All subject assessment, blood collection, and imaging were performed at the Research Imaging Institute at UTHSCSA. Before each session, a standard quality control phantom was imaged. Cardiac morphology and function were determined after initial anatomical localizer images. High temporal resolution cine MR imaging with prospective gating was performed, using a balanced, steady-state free precession sequence (TR/TE = 2.44/1.22 ms, 25–30 cardiac phases, matrix 224 × 288, FOV 336 × 430 mm^2, pixel resolution 1.5 × 1.5 mm^2). Two 3-slice, cine, long-axis data sets in a left anterior oblique and a four-chamber view were acquired. A stack of contiguous short-axis slices, extending from the apex of the LV through the atria, are then acquired with repetitive end expiration breath-holds. Heart rate and EKG were monitored during the CMRI. Pericardial fat scans were obtained in diastole using a short-axis, single-shot steady-state free precession (IR-SFFP) sequence with an inversion-recovery pre-pulse (TR/TE = 2.4/1.1 ms, slice = 8.5 mm, 1.3 × 1.3 mm pixel, flip angle = 50°) that covered the complete left ventricle by long-axis stacks in a single breath-hold. The inversion time (TI) was adjusted between 180 and 280 ms to obtain optimal enhancement of the epicardial fat. The cvi42 image analysis package (Circle Cardiovascular Imaging Inc., Calgary, AB) was used for assessment of pericardial fat. Using long axis, 4-chamber images, thickness of pericardial fat was measured at the cardiac mid-ventricular level laterally. For analyses of pericardial fat, manual ROI contours were drawn to define the EAT area by the region included inside contours of the epicardium and pericardium. Summation of the pixels included in the contours was recorded and multiplied by the per-pixel dimensions to obtain an area measurement. For epicardial fat volume determination, the area subtended by the manual tracings is determined in each slice and multiplied by the slice thickness and then summed to yield the fat volume. Visceral fat was not examined in this study, it is measured in the abdomen and our imaging protocol did not capture the abdominal region.

Lipidomic Profiling

Lipidomics was performed as described previously (43) with modifications. Analysis of plasma extracts was performed on an Agilent 1290 series HPLC system coupled to an Agilent 6495C triple quadrupole mass spectrometer. Liquid chromatography was performed on a dual column system with ZORBAX eclipse plus C18 columns (2.1 × 100 × 1.8 mm, Agilent) heated to 45°C. Mass spectrometry analysis was performed in both positive and negative ion mode with dynamic scheduled multiple reaction monitoring (MRM). The running solvent consisted of solvent A: 50% H2O/30% acetonitrile/20% isopropanol (v/v/v) containing 10 mM ammonium formate and 5 μM medronic acid, and solvent B: 1% H2O/9% acetonitrile/90% isopropanol (v/v/v) containing 10 mM ammonium formate. Gradient conditions are presented in **Supplementary Table S1**, with alternating columns for sample analysis (Pump A) and equilibration (Pump B). The following mass spectrometer conditions were used: gas temperature 150°C, gas flow rate 17 L/min, nebulizer 20 psi, sheath gas temperature 200°C, capillary voltage 3,500 V and sheath gas flow 10 L/min. Isolation widths for Q1 and Q3 were set to "unit" resolution (0.7 amu). Plasma quality control (PQC) samples consisting of a pooled set of plasma samples taken from six healthy individuals and extracted alongside the study samples were incorporated into the analysis at 1 PQC per 20 plasma samples. NIST 1950 SRM sample (Sigma) was included as a reference plasma sample, at a rate of 1 per 40 samples. Relative quantification of lipid species was determined by comparison to the relevant internal standard. Lipid class total

TABLE 1 | Characteristics of the study population.

Parameters	Average	Minimum	Maximum
Sex			
Male (*n*-%)	74 (37)	–	–
Female (*n*-%)	126 (63)	–	–
Age (years old)	46.85 ± 16.23	18	83
Male	45.18 ± 17.10	19	77
Female	47.83 ± 15.62	18	83
Education (years)	12.39 ± 2.94	1	22
Height (cm)	161.96 ± 9.54	127.00	186.50
Weight (Kg)	84.44 ± 18.76	39.92	163.29
BMI	32.158 ± 6.40	17.51	51.25
Waist (cm)	101.56 ± 14.82	63.00	149.00
Systolic BP-Avg (mmHg)	125.24 ± 16.82	96.00	191.67
Diastolic BP-Avg (mmHg)	76.24 ± 11.58	40.33	142.00
Diabetes mellitus (*n*-%)	43 (21.5%)	–	–
Hypertension (*n*-%)	73 (36.5%)	–	–

n, number of participants; %, percentage; cm, centimeters; Kg, Kilograms; mmHg, millimeters of mercury.

concentrations were calculated as the sum of individual lipid species concentrations, except in the case of two lipid classes, triacylglycerol (TG) and alkyldiacylglycerol, TG(O), where we measured both neutral loss (NL) and single ion monitoring (SIM) transitions. We used the more quantitatively accurate but less structurally resolved (SIM) species concentrations for summation purposes when examining lipid totals, while their (NL) counterparts were used for associations.

Statistical Analysis

Initially, we estimated epicardial fat volume content heritability using a quantitative genetic variance component decomposition approach as implemented on SOLAR (version 8.1.1) (44). We used a linear mixed model $\Omega = 2\phi\sigma_G^2 + I\sigma_e^2$ where, Ω is the total phenotypic covariance matrix of a trait, ϕ is the matrix of kinship coefficients, I is the identity matrix, σ_G^2 is additive genetic variance, and σ_e^2 is residual environmental variance. All the models were adjusted for the following covariates: age, age^2, sex, age × sex, and age^2 × sex. We do not use medication as a covariate. This cohort is a traditionally medically underserved population and very few of them are taking lipid lowering or other relevant medications (we collect medications at all subject visits). When we correct for medications, the observed results are not qualitatively changed. Heritability was defined as the proportion of phenotypic variance explained by an additive genetic model. We tested the association of each lipid species and lipid classes with epicardial fat volume by means of LRT (Likelihood Ratio Test) comparing two models with and without the presence of a lipid class/species while allowing for residual non-independence due to underlying genetic factors which induce correlations between related individuals. Statistical significance of a given lipid association with epicardial fat was tested by constraining the regression coefficient to 0 and comparing the log-likelihoods of the constrained and unconstrained regression models to yield an LRT test that is distributed as χ^2 variate with one degree of freedom. The significant lipid classes and species were defined using a False Discovery Rate (FDR) smaller than 0.05 calculated using the empirical *p*-value distribution.

RESULTS

For this study, we had a cohort of 200 Mexican American individuals with lipidomic profiles and CMRI-derived epicardial fat volume measures. Baseline demographic and clinical status of these 200 participants is shown in **Table 1**. The mean age of the participants was 46.85 ± 16.23 years old, 74 (37%) were male, 73 (36.5%) had hypertension, and 43 (21.5%) had type 2 diabetes (T2D). Mean body mass index (BMI) was 32.158 ± 6.40 kg/m^2. There were no differences in BMI, prevalence of hypertension or T2D between men and women, however the prevalence of T2D in women was 2.5 times higher than in men.

EAT volume was evaluated with good reproducibility in our study. Average EAT volume was 7.95 ± 3.81 cm^3 in all individuals. EAT volume was not significantly different in hypertensive vs. normotensive subjects (8.85 ± 3.73 cm^3 vs. 7.45 ± 3.74 cm^3, $p = 0.6699$); nor was it significantly different between subjects with and without T2D (9.32 ± 4.0 cm^3 vs. 7.6 ± 3.65 cm^3, $p = 0.2812$). In this study, the mean EAT volume was 7.95 ± 3.81 cm^3, ranging from 0.94 to 19.88 cm^3. The age-adjusted difference in EAT volume between males and females was trending toward significance (8.0 ± 3.74 cm^3 vs. 7.92 ± 3.84 cm^3, $p = 0.0561$). After analyzing the sample by increasing age, we observed a significant increase in EAT volume with increasing age, in both males and females ($p < 2.5 \times 10^{-6}$) (**Figure 1**). There was no evidence for any interactions of sex and age. Additionally, there was no significant evidence for a non-linear relationship with age.

Quantitative genetic analysis revealed that EAT is under substantial genetic control in this population. The estimated heritability was 0.86 ± 0.16, 95% CI = (0.55, 1.0), $p = 1.8 \times 10^{-6}$. To our knowledge, this is the first study to evaluate the relative importance of additive genetic factors for this phenotype in humans.

To optimize the number of statistical tests being performed, we first conducted our analyses at the level of lipid class. We analyzed the association of 48 lipid classes listed in **Table 2** with epicardial fat volume. Using multivariable regression models performed in SOLAR and controlling the false discovery rate (FDR) using the Benjamini-Hochberg method (45–47), we found that nine lipid classes were statistically associated with EAT volume (**Table 3**). The classes were triacylglycerol (TG), hydroxylated acylcarnitine (AC-OH), deoxyceramide (Cer(m)), alkyldiacylglycerol (TG(O)), ubiquinone, diacylglyceride (DG), dihydroceramide (dhCer), phosphatidylinositol (PI) and phosphatidylglycerol (PG), respectively by lowest to highest FDR < 0.05. It is worth noting that several of the classes associated with EAT volume were previously implicated in the pathogenesis of T2D, insulin resistance and consecutively in CVD risk.

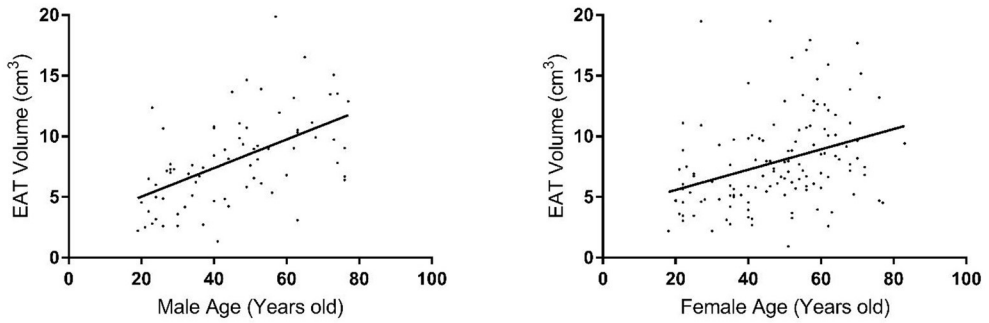

FIGURE 1 | Distribution of epicardial fat volume in males **(left plot)** and females **(right plot)** by age group.

We next examined the association of lipid species with EAT volume using SOLAR, analyzing 799 lipid species from the 48 classes. After appropriate adjustments described in methods, our plasma lipidome analyses showed that 135 lipid species belonging to 19 lipid classes were significantly associated with EAT volume with an FDR <0.05 as shown in **Figures 2**, **3**. The list of lipid species with their respective average concentration, concentration range and number of lipid species within the class with an FDR < 0.05 are shown in **Table 2**. The full list of lipid classes and species with *p*-value, beta coefficient of regression (SDU) and FDR analysis are shown in **Supplementary Tables S2, S3**, respectively.

After appropriate adjustment for the effective number of tests in our plasma lipidome analyses in SOLAR, the EAT volume was associated with the increase of 131 lipids and decrease of 4 individual lipid species. The strongest associations observed were with two deoxyceramide species Cer(m18:1/18:0) and Cer(m18:1/20:0) with beta coefficient of regression of 0.40 and 0.34 and $p = 1.63 \times 10^{-4}$ and $p = 4.44 \times 10^{-3}$, respectively. This association demonstrated, in our study, that a larger EAT volume was correlated with an increased plasma concentration of deoxyceramide. The 20 species of lipids with the most significant *p*-values are described in **Table 3** and shown in **Figure 3**. Interestingly, these lipid species belong to only 3 classes of lipids: deoxyceramide, triacylglycerol and phosphatidylinositol. In addition, only species from an extra 6 classes of lipid showed significant associations (**Table 3**). These additional species belong to the classes: hydroxylated acylcarnitine, alkyldiacylglycerol, ubiquinone, diacylglycerol, dihydroceramide, and phosphatidylglycerol. Additionally, we observed substantial heterogeneity of effects within 10 lipid classes (cholesterol ester (CE), ceramide (Cer(d)), deoxyceramide (Cer(m)), dehydrodesmosterol ester (deDE), lysophosphatidylcholine (LPC), phosphatidylcholine (PC), phosphatidylethanolamine (PE), phosphatidylinositol, sphingomyelin (SM) and lysophosphatidylinositol (LPI). Interestingly, one class (PC) showed both significant increasing (three species) and decreasing (one species) associations with EAT volume, suggesting the potential for dynamic feedback within class, most likely driven by the fatty acids.

The associations observed with the plasma lipidome measures were more significant than those observed for standard clinical lipid markers. We examined the associations of the clinical lipid measures and EAT in this sample and found the associations to be $p = 0.01$ for total cholesterol, $p = 0.008$ for calculated LDL, $p = 0.0008$ for HDL and $p = 4.32 \times 10^{-6}$ for triglyceride levels. Triglyceride levels were the only clinical lipid measure nearing the level of significance observed in the lipidome measures, particularly for the triacylglycerol (TG) species. This is to be expected as the triglyceride measure is the sum composition of all triacylglycerol species measured in our analysis. In contrast the many other species of ceramide, deoxyceramide and phospholipid species containing polyunsaturated fatty acids are not strongly correlated with clinical lipid measures and so are providing independent information about EAT. For standardized phenotypes, *p*-values are directly related to observed effect sizes (e.g., residual correlation). Therefore, the improved *p*-values directly relate to larger associations and hence greater biological significance.

DISCUSSION

Given that CVD is the leading cause of death in the US and much of the world, the identification of novel risk factors is essential to help alleviate the substantial health and economic burden. So, novel insights into biological mechanisms that predispose individuals to CVD hold the promise of a significant reduction in this considerable economic burden. It is well-known that a relationship exists between lipid variation and CVD, but the mechanisms are unclear. Modern genomic technologies can be exploited to rapidly identify genes involved in disease susceptibility. However, the cost-effectiveness of such exploratory endeavors can be greatly augmented if genetic basis to a phenotype is strongly suspected. A recent article by Blanco-Gomez et al. (48) explains nicely the complex interplay between phenotypes and disease at the global level where most major diseases are considered complex phenotypes and are the consequence of intermediate phenotypes causally related to or involved in their pathogenesis. These intermediate phenotypes can go all the way down to the tissue, transcript, and ultimately to genomic level (48). Therefore, intermediate phenotypes such as those derived by CMRI, and lipid profiling as described in this study could

TABLE 2 | Lipid classes assessed by targeted lipidomics: concentration (pmol/mL), range of concentration (maximum and minimum, pmol/mL) and associations with EAT volume.

Lipid class name	Class abbreviation	Concentration	Minimum	Maximum	No. of species	No. of species*
Acylcarnitine	AC	780.16	277.75	1,897.03	28	4
Alkenylphosphatidylcholine (P)	PC(P)	60,236.05	25,391.79	128,139.69	30	0
Alkenylphosphatidylethanolamine (P)	PE(P)	63,098.10	22,049.00	157,529.53	53	0
Alkyldiacylglycerol	TG(O)	2,225.81	526.33	17,015.81	20	12
Alkylmonoacylglycerol	DG(O)	1,931.96	442.86	5,054.66	2	0
Alkylphosphatidylcholine	PC(O)	71,020.49	35,800.19	125,404.02	34	0
Alkylphosphatidylethanolamine	PE(O)	3,595.49	1,510.84	7,742.28	14	0
Bile acid	BA	835.86	115.07	6,533.81	2	0
Ceramide	Cer(d)	18,222.47	5,289.50	35,327.51	47	8
Ceramide-1-phosphate	C1P	5.95	0.96	17.30	1	0
Cholesteryl ester	CE	3,481,161.11	1,801,143.14	6,008,721.67	27	2
Dehydrocholesterol ester	DE	18,330.58	7,819.13	61,318.78	6	1
Dehydrodemosterol ester	deDE	360.13	23.77	5,225.42	2	0
Deoxyceramide	Cer(m)	1,337.83	258.05	7,013.12	11	8
Diacylglycerol	DG	113,181.88	37,769.76	432,782.54	26	14
Dihexosylceramide	Hex2Cer	4,007.89	1,549.11	7,162.76	10	0
Dihydroceramide	dhCer	375.41	149.99	777.79	6	2
Dimethyl-cholesteryl ester	dimethyl-CE	24,635.70	7,573.76	71,080.92	4	0
Free cholesterol	COH	747,839.09	428,202.30	1,178,895.10	1	0
Free fatty acid	FFA	395,032.85	205,376.16	683,429.45	17	0
GD1 ganglioside	GD1	7.36	1.84	14.66	1	0
GM1 ganglioside	GM1	19.03	0.61	41.33	1	0
GM3 ganglioside	GM3	3,121.22	1,384.39	5,629.32	7	0
Hydroxylated acylcarnitine	AC-OH	23.52	9.22	46.06	8	5
Lysoalkenylphosphatidylcholine (P)	LPC(P)	772.16	198.42	1,508.36	6	0
Lysoalkenylphosphatidylethanolamine (P)	LPE(P)	310.79	102.04	745.05	4	0
Lysoalkylphosphatidylcholine (LAF)	LPC(O)	3,094.26	1,333.28	4,890.32	10	0
Lysophosphatidylcholine	LPC	219,759.08	115,804.17	370,825.40	61	3
Lysophosphatidylethanolamine	LPE	6,563.27	3,124.24	12,965.85	14	0
Lysophosphatidylinositol	LPI	1,519.93	844.58	2,776.85	7	2
Methyl-cholesteryl ester	methyl-CE	37,950.13	10,953.57	129,335.37	5	0
Methyl-dehydrocholesteryl ester	methyl-DE	2,929.83	622.81	9,579.89	2	0
Monohexosylceramide	HexCer	3,212.20	911.79	6,392.99	14	0
Oxidized lipids	OxSpecies	6,579.85	2,681.95	13,155.84	6	1
Phosphatidic acid	PA	76.43	40.32	164.48	5	0
Phosphatidylcholine	PC	1,737,177.86	1,048,144.69	2,398,255.66	90	4
Phosphatidylethanolamine	PE	40,484.40	15,353.48	95,420.85	37	5
Phosphatidylglycerol	PG	475.99	134.61	1,170.81	3	1
Phosphatidylinositol	PI	215,820.31	60,717.32	370,648.86	27	9
Phosphatidylinositol monophosphate	PIP1	628.26	85.24	1,380.75	1	0
Phosphatidylserine	PS	6,981.00	354.86	23,312.22	7	0
Sphingomyelin	SM	342,792.34	190,455.47	557,621.10	47	2
Sphingosine	Sph	494.68	214.47	1,108.70	1	0
Sphingosine-1-phosphate	S1P	2,072.79	1,120.77	4,252.17	4	0
Sulfatide	SHexCer	565.90	269.16	1,082.07	6	0
Triacylglycerol (NL)	TG	1,742,464.14	450,098.99	7,784,888.83	77	51
Trihexosylcermide	Hex3Cer	1,580.81	739.32	2,721.76	6	0
Ubiquinone	Ubiquinone	2,069.76	508.35	4,924.12	1	1
Total					**799**	**135**

*Numeric values are given as average and range. No., number; P, Plasmogen; LAF, lysoplatelet activating factor. *No. with $p < 0.05$ designates the number of lipids significantly associated with EAT volume measurement at the 0.05 level of false discovery rate (FDR) under adjustment for age, sex and their interactions.*

TABLE 3 | Species and classes of lipid with the lowest false discovery rate *p*-values in our study.

Lipid classes				
Lipid classes name	**Lipid abbreviation**	***p*-value**	**Beta (SDU)**	**FDR**
Triacylglycerol	TG	3.23E-04	0.3062	6.97E-03
Alkyldiacylglycerol	TG(O)	1.07E-04	0.2620	1.24E-03
Hydroxylated acylcarnitine	AC-OH	1.28E-03	0.2415	1.34E-02
Deoxyceramide	Cer(m)	2.48E-03	0.2698	2.07E-02
Ubiquinone	Ubiquinone	3.81E-03	0.2465	2.79E-02
Diacylglycerol	DG	4.09E-03	0.2481	2.85E-02
Dihydroceramide	dhCer	5.01E-03	0.2331	3.17E-02
Phosphatidylinositol	PI	6.33E-03	0.2349	3.59E-02
Phosphatidylglycerol	PG	8.38E-03	0.2232	4.39E-02
Lipid species				
Lipid species name	**Lipid class**	***p*-value**	**Beta (SDU)**	**FDR**
Cer(m18:1/18:0)	Cer(m)	1.84E-07	0.4000	1.63E-04
Cer(m18:1/20:0)	Cer(m)	2.23E-05	0.3463	4.44E-03
TG(50:1)[NL-16:0]	TG	2.20E-05	0.3450	4.44E-03
TG(50:1)[NL-18:1]	TG	3.37E-05	0.3405	4.44E-03
TG(50:2)[NL-18:2]	TG	3.18E-05	0.3393	4.44E-03
TG(49:1)[NL-17:1]	TG	2.89E-05	0.3366	4.44E-03
TG(51:2)[NL-17:1]	TG	5.23E-05	0.3354	5.17E-03
TG(54:2)[NL-18:0	TG	6.36E-05	0.3205	5.17E-03
TG(54:6)[NL-20:4]	TG	5.45E-05	0.3069	5.17E-03
TG(53:2)[NL-17:1]	TG	8.04E-05	0.3232	5.76E-03
PI(16:0/16:1)	PI	8.46E-05	0.2901	5.76E-03
TG(51:2)[NL-17:0]	TG	1.13E-04	0.3252	6.22E-03
TG(54:5)[NL-20:4]	TG	1.12E-04	0.2972	6.22E-03
PI(16:0/20:4)	PI	1.08E-04	0.2935	6.22E-03
TG(50:2)[NL-16:1]	TG	1.54E-04	0.3199	6.66E-03
TG(50:3)[NL-16:1]	TG	1.65E-04	0.3182	6.66E-03
TG(52:1)[NL-18:1]	TG	1.64E-04	0.3117	6.66E-03
TG(48:1)[NL-16:1]	TG	1.84E-04	0.3057	6.66E-03
TG(52:2)[NL-18:2]	TG	1.88E-04	0.3028	6.66E-03
TG(50:6)[NL-20:4]	TG	1.40E-04	0.2840	6.66E-03

SDU, standard deviation units.

lie closer to the genomic level and ultimately the causal action of genes. So, the identification of novel lipid-related endophenotypes that are genetically correlated with CVD offers the potential to discover biomarkers which will quickly lead us to the identification of novel CVD treatments and ultimately preventatives.

The most common risk factors for CVD are deleterious lipid concentrations, obesity, hypertension, and smoking. Additionally, significant health disparities exist in CVD in some minority groups, in both health outcomes and quality of care. Hispanic populations have a significantly worse CVD risk profile, however the prevalence of some CVDs, such as coronary heart disease, are lower than in other ethnic groups, a phenomenon known as the Hispanic Paradox (49). Hispanic individuals face significant socioeconomic challenges, and they tend to have low rates of disease awareness and health insurance and are less likely to seek treatment. A recent American Heart Association statement on the health burden of CVD in Hispanics acknowledges insufficient understanding of Hispanic heart health and supports the need for more Hispanic CVD research (49, 50). The work of our group in Mexican American individuals, has demonstrated a role for these lipid species and the measurement of CMRI-derived phenotypes in CVD disease risk. Our results provide information that lipid measures (which are significantly associated with common complex diseases) and the use of the extended pedigrees of Mexican Americans, along with our novel lipidomic approach and CMRI-derived measures are extremely powerful and cost-effective tools for the identification of the relationship between lipid metabolism and CVD risk.

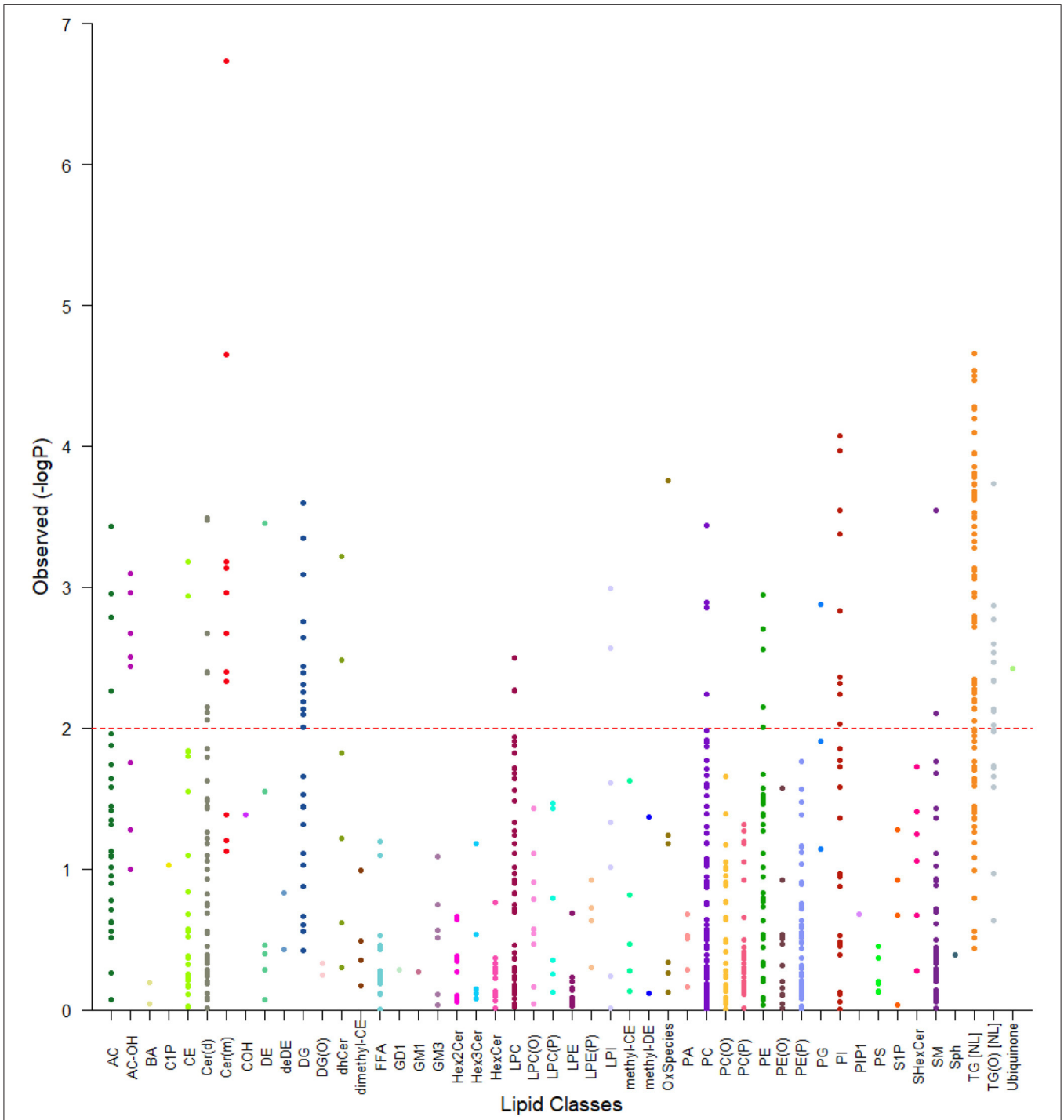

FIGURE 2 | Tornado plot of plasma lipidome associations with EAT volume. The figure shows all lipid species within their specific classes and the degree of association with EAT volume (FDR). Each dot represents a lipid species and each color a lipid class. The dotted line represents an FDR of 0.05. All species above the dotted line were considered as significantly associated with epicardial fat volume.

Heritability of coronary heart disease is estimated to be up to 60% and comes from a variety of family and twin studies (51). CMRI phenotypes, including measures of left ventricle (LV) mass, volume and function, demonstrate high heritability (LV mass heritability ranges from 15 to 84%) (52). In our study, the heritability of epicardial fat volume was 86.29% (p-$value = 1.8 \times 10^{-6} \pm 0.1617$). This is a validation that EAT volume is significantly genetically regulated and demonstrates

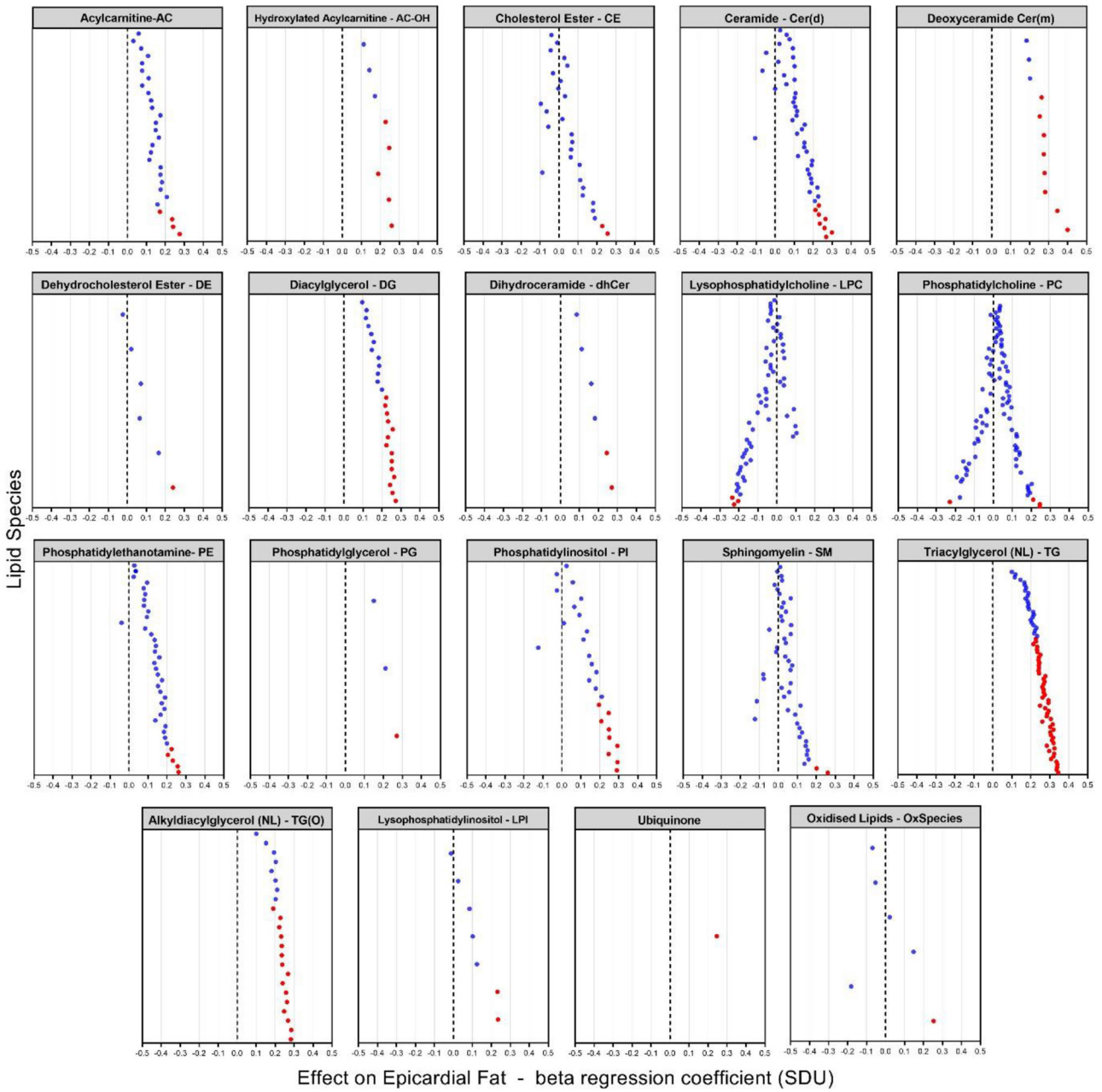

FIGURE 3 | Plasma lipidome associations with EAT volume [beta coefficient of regression (SDU)]. The figure shows significant increases and decreases in lipid levels in 19 classes of lipids with species having an FDR < 0.05 (indicated by the red dots). Each dot represents a lipid species within the specific lipid class.

the power for identification of intermediate phenotypes in CVD prevention. This study focused on cardiac imaging and lipidomic profile with the ultimate aim of identifying possible lipid phenotypes influencing CVD risk. Focusing on these intermediate phenotypes may direct us more rapidly to CVD risk gene identification.

The fundamental mechanisms potentially responsible for cardiovascular events in overweight individuals remains uncertain. Thus, it is important to ask the question whether increases in epicardial fat, as a component of obesity, may provide one of the links between obesity, coronary atherosclerosis and consequently CVD. Fat in the heart resides in three distinct depots: epicardial, pericardial and intracellular fat. Epicardial fat is located on the surface of the heart especially around the epicardial coronary vessels. It can extend into the heart and intersperse within myocardial muscle fibers (35). There is a significant direct relationship between the amount of epicardial fat and general body adiposity (visceral adiposity)

as demonstrated in clinical imaging studies by Rabkin (27, 35). Several lines of evidence support a role for epicardial fat in the pathogenesis of coronary artery disease: first, due to the close anatomic relationship between epicardial fat and coronary arteries (35, 53); second, due to the positive correlation between the amount of epicardial fat and the presence of coronary atherosclerosis (54, 55) and third, due to the ability of adipose tissue to secrete hormones and cytokines that modulate coronary artery atherothrombosis (31). Thus, epicardial fat may be an important factor responsible for cardiovascular disease in obesity (25, 33).

Genetic and epidemiological studies have greatly improved our understanding of pathophysiology underlying the complex of CVDs and have identified several risk factors. Amongst the well-recognized predisposing factors, lipid metabolism plays a central role in the development of CVDs (56, 57). Since the landmark publications from the Framingham study (58), plasma lipids have been recognized as important predictors of future CVD events (59). To assess these events, plasma lipids are routinely monitored by profiling total cholesterol, triglycerides, high-density lipoprotein cholesterol (HDL-C) and low-density lipoprotein cholesterol (LDL-C) (referred as "traditional lipids"). Efforts to understand the role of lipids in CVD pathophysiology had largely focused on these traditional lipids, and to some extent on free fatty acids and lipoproteins. However, human plasma consists of thousands of functionally and chemically diverse molecular lipid species (41, 60). Nevertheless, tremendous advancements in the field of lipidomics has facilitated these efforts to unravel the metabolic dysregulation in complex lipid-related disorders, particularly in CVDs and for the identification of predictive biomarkers beyond traditional lipids (61, 62). Lipids are of central importance for the bioenergetic metabolism of the heart and in the healthy heart, fatty acids (FAs) account for 60–90% of ATP production while glucose provides the remainder (63, 64). When damaged, the heart shifts away from lipids toward a greater reliance on glycolysis, ketone body oxidation, amino acids, and lactate as sources of energy (63, 65). This shift in cardiac metabolism and identification of the metabolic pathways involved remains a challenge and consequently so too does the translation of these metabolic findings to the clinical setting for improved or novel diagnostic/prognostic biomarkers (17). That interdependence of metabolites results in a disease signature which can be used to more precisely identify or predict disease states, which represents the closest link to the phenotype. The biologically simpler nature of these individual lipid species suggest that they may reside closer to the causal action of genes, making them valuable endophenotypes (18). Even though changes in the levels of numerous metabolites have been shown to occur in the failing heart (BCAA, lactate, ketones), specific lipid metabolites appear to consistently change in metabolomic profiles of CVD patients, namely sphingolipids, phospholipids, glycolipids, cholesterol esters, fatty acids and acylcarnitines (63).

Epidemiological and lipidomic studies has shown that specific lipoproteins and their constituent lipids are important factors in the development of metabolic related disorders (9, 10, 66) and CVD specifically (67–69). Glycerolipids are a large group of lipids accounting for a good proportion of total lipids in plasma. Triacylglycerol (TG) is the most abundant lipid class and comprises the bulk of storage fat in tissues. Monoacylglycerol (MG) and diacylglycerol (DG) represent intermediates in the biosynthesis and hydrolysis of TG and function as second messengers in signal transduction processes (70, 71). It has previously been shown that the breakdown and synthesis of triglycerides by DG and MG have a causal effect on CVD risk (13). Sphingolipids are wide range of complex lipids and constitute several hundreds of different species, including ceramides, which function as a precursor for complex sphingolipids (72, 73). Sphingolipids and their precursors, may be involved in the pathogenesis of CVD through multiple pathways including inflammation (74), atherosclerosis (75), and apoptosis (76). Kulkarni et al. have demonstrated a role for diacylglycerols, with four species (each containing palmitic acid) showing significant genetic correlations with hypertension (9). Additionally, Mamtani et al. showed consistent association of ceramides (Cer(d)) with waist circumference where levels were significantly higher in diabetics compared to non-diabetics ($p = 2.5 \times 10^{-7}$) (10). Alshehry et al. showed that monohexosylceramide (HexCer), dihexosylceramide (Hex2Cer) and lysoalkylphosphatidylcholine (LPC(O)) were associated with cardiovascular events and HexCer and Hex2Cer with cardiovascular death (68). Alshehry et al. found that five species of lipids containing polyunsaturated fatty acids (PUFAs), including phospatidylcholine (PC,) alkenylphosphatidylcholine (PC(P)) and triacylglycerol were inversely associated with CVD risk. In our results, we show that two of these lipids (PC and TG) are associated with epicardial fat volume.

It is now well-established that ceramide metabolism is altered in the context of type 2 diabetes (T2D) and obesity which are both linked to CVD (77, 78). In fact, higher plasma ceramide levels have been associated with visceral obesity, non-alcoholic fatty liver disease, and T2D, which are also predictors of CVDs (79–84). There is an interplay between the level of ceramides in the plasma/tissues and disease development. Hepatocellular ceramides stimulate fatty acid uptake (85) and decrease glucose uptake (85, 86), which enables hepatocytes to favor fatty acids over glucose as a preferred energy source and leads to NAFLD (85). In our study, eight of the 47 ceramide lipids were significantly associated with EAT volume. The most significant species within the Cer(d) class with both FDR value of 6.97x 10^{-3} was Cer(d18:1/18:0) and Cer(d19:1/18:0) (p-value 3.31 $\times$ 10^{-4}). Several studies have found these species to be associated with CVD (82–84) and that ratios of long chain ceramide species Cer(d18:1/16:0) and Cer(d18:1/18:0) were more strongly correlated with negative cardiovascular outcomes than ratios of very long chains of ceramide species Cer(d18:1/24:0) (84). The Cer(d) species associated with EAT volume in our cohort were only long chain ceramide species. Laaksonen et al. (84) found that the ratios of Cer(d18:1/24:0)/Cer(d18:1/16:0) and Cer(d18:1/24:0)/Cer(d18:1/16:0) negatively correlate with coronary heart disease and mortality, and Anroedh et al. found Cer(d18:1/20:0) to be associated with CVD event and death (87). This last lipid species was positively associated with EAT volume in our cohort with (SDU 0.3463; FDR 4.44 $\times$ 10^{-3};

p-value 2.23×10^{-5}). Another more recent study found that serum sphingolipids are markers of coronary artery disease, independent of cholesterol (88), further solidifying the strong correlation between these species and negative cardiac outcomes. These dual (positive or negative) ceramide actions may be due to manipulations of the *de novo* ceramide synthesis pathway suggesting that certain ceramide species are deleterious, whereas others are beneficial (77, 89–91). Those containing the C16 or C18 acyl chain (77, 89, 90) and a double bond (i.e., ceramides, not dihydroceramides) (92) in the sphingolipid backbone are particularly harmful. Thus, plasma ceramide levels can be used as clinical biomarkers to predict risk of cardiovascular death. Another lipid class that we found to be significantly associated with EAT volume was dihydroceramide (dhCer). This lipid is the precursor of ceramide in the *de novo* synthesis pathway. Ceramides and their derivates are involved in many, if not all, essential cellular process such cell growth, cell adhesion and migration, senescence, apoptosis, inflammation, immune system and angiogenesis (73, 93). Ceramide synthesis and accumulation are influenced by multiple factors, which include excessive supply of substrates, systemic inflammation, oxidative stress and the microbiome (94). Therefore, the many roles played by ceramides and derivates in cardiometabolic health and diseases are associated with this connection between excessive supply of lipids and inflammation (95). The ceramide family of species has been reported to have a strong correlation with CVD risk in the literature. We found that 2 of 6 measured dhCer species (dhCer(d18:0/24:1) and dhCer(d18:0/22:0)) were significantly associated with EAT volume. Other authors have reported the existence of a strong correlation between CVD and increased dihydroceramide levels. Elevated levels of dihydroceramides have been found in atherosclerotic plaques (75). The role this increase in dihydroceramides plays in plaque stability is still debatable, since the extracellular addition of dihydroceramides to human aortic smooth muscle cells did not cause apoptosis, whereas addition of ceramides did (75). One atypical sphingolipid (deoxyceramide -Cer(m)) was also associated with EAT in our study, with the two most significant FDR results. These ceramides are neurotoxic sphingolipids which are formed by the enzyme serine palmitoyltransferase (SPT). Pathologically elevated Cer(m) levels were found in patients with MetS or T2D (96–99). The mechanisms which underlie this increased Cer(m) formation in metabolic disorders is not understood. Low but detectable Cer(m) levels are generally found in plasma - also of healthy individuals. However, patients with MetS or T2D have significantly elevated plasma Cer(m) levels (98, 99). These observations may reflect an underlying interaction between the severity or control of T2D in this population and cardiovascular risk.

The glycerophospholipids, also known as phospholipids, are the major structural component of cell membranes and are involved in various biological processes including inflammation (72). It has been shown that there is a marked difference in the lipidome of adipose tissues depending on their epicardial or subcutaneous origin (SAT) (21). Barchuk et al. found a specific enrichment in sphingolipids, phosphatidylcholine (PC), phosphatidylethanolamine (PE), and phosphatidylethanolamine plasmalogens (PE(P)) in EAT compared with SAT. They observed that EAT was rich in PC and in PE. Our results corroborate this finding, identifying a total of 127 different species of PC and PE, accounting for almost 16% of total lipid profile. From those, a total of nine lipids (4 PC and 5 PE) were associated with EAT in our cohort. Barchuk et al. (21) also observed a specific lipidomic signature of EAT in coronary artery disease (CAD) patients, identifying 97 lipid species that discriminated patients with and without CAD. They also observed that patients with CAD exhibited more ceramides, diacylglycerides, monoacylglycerides, and less unsaturated triacylglycerols in their EAT. This group also found that that the EAT lipidome was independent to that of SAT, possibly indicating a specific high metabolic activity, or a beige associated phenotype. Although we did not evaluate cardiovascular disease between the individuals with high EAT in our cohort, the lipid profile associated with EAT was basically the same as found by Barchuk et al., where the majority of the lipids associated with EAT were from sphingolipids (ceramides, dihydroceramides, 1-deoxy-sphingolipds, sphingomyelins) and glycerolipids (DG and TG) (21). Our results suggest that saturated fatty acids (FAs) on the TG species show strong association with EAT. The majority of the FAs on the top 28 TG species significantly associated with EAT were saturated. Stegemann et al. in a population-based study, identified a specific cluster of triacylglycerol species with saturated and monounsaturated acyl chains as most consistently associated with CVD (100). The association between saturated/monounsaturated fatty acids and cardiovascular risk was also evident in or study. Recently, Tomasova et al., found a higher content of phosphatidylcholine and decreased level of phosphatidylethanolamine (18:0/20:4) in EAT compared with SAT (101). Although our study didn't measure SAT volume for comparison with EAT, we did find high numbers of PCs and PEs associated with EAT volume, where high concentrations of these lipids was observed in individuals with high epicardial volume. These observations may reflect an underlying interaction between the severity or control of T2D and CVD risk.

These associations suggest that there are multiple factors that influence lipid homeostasis and presumably CVD risk. The effects of these lipid species on epicardial fat volume, after adjustment for established risk factors, likely reflects both environmental and genetic factors not currently considered in CVD risk.

LIMITATIONS

Some limitations of the present study need to be considered. First, our findings should be seen as indicative and need confirmation by replication in independent cohorts. All study participants were Mexican Americans, so, it is not possible to generalize these results to other ethnic groups. Future studies need to investigate the similarities and differences of lipid associations and CVD risk in different ethnic populations. Second is the limitation of all lipidomic studies where the coverage is incomplete. In this study, we used a targeted approach that has enabled us to measure 799 lipid species from 48 different lipid classes, providing a broad, but still incomplete, coverage of the lipidome. Third, the high variance associated with lipidomic measurements can reduce

the strength of observed associations. Lastly, all inferences in this study are based on cross-sectional data. The associations therefore do not automatically imply a causal role of plasma lipid species in the pathogenesis of CVD. The main goal of the study was to query the existence of potential correlations in EAT volume and specific lipid species for prediction of CVD risk.

CONCLUSION

In conclusion, using a novel integrative approach by combining plasma lipidomics and CMR imaging of epicardial fat volume, we have shown that specific lipid abnormalities correlate with cardiovascular disease risk. Our findings should be considered as preliminary and the possible role of these triacylglycerols and/or ceramides in the development or prevention of CVD warrant further investigations. On a general level, our study also provides a framework for linking plasma lipidomic markers not only with clinical endpoints, but also with the more subtle intermediate phenotypes, as derived from medical imaging of potential pathophysiological relevance.

DATA AVAILABILITY STATEMENT

The original contributions presented in the study are included in the article/**Supplementary Material**, further inquiries can be directed to the corresponding author/s.

ETHICS STATEMENT

The studies involving human participants were reviewed and approved by both the Institutional Review Board at University of Texas Health Science Center San Antonio and the Institutional Review Board at University of Texas Rio Grande Valley. The patients/participants provided their written informed consent to participate in this study.

AUTHOR CONTRIBUTIONS

LM, JB, and JC contributed to the conception and design of the study. AL organized the study data, performed descriptive statistics, generated tables and figures, and wrote the first draft of the manuscript. RD was responsible for the recruitment of the SAFHS participants in the study. GC performed the cardiac MRI acquisition and calculation of EAT volume. KH, CG, and TD performed lipidomic profiling and quantification of lipid species and classes. PM was responsible for overseeing the lipidomic profiling, interpretation of the data, and wrote sections of the manuscript. JB directs the SAFHS cohort and was responsible for overseeing the statistical analysis and wrote sections of the manuscript. MA, MK, and VD were responsible for the statistical analyses in SOLAR and for generating some of the figures. JC directed the study and wrote sections of the manuscript. All authors contributed to manuscript revision, read, and approved the submitted version.

FUNDING

This work was supported in part by National Institutes of Health (NIH) grants P01 HL045522 (SAFHS data collection), R01 HL140681 (lipid profiling), R37 MH059490 (analytical methods and software used), R01 EB015611 (analytical methods and software used), Eli Lilly and Company (cardiac imaging) and a grant from the Valley Baptist Legacy Foundation for Project THRIVE (biorepository). This work was conducted in part in facilities constructed under the support of NIH grant C06 RR020547. PM was supported by a L3 Investigator grant from the National Health and Medical Research Council of Australia (2009965). KH was supported by a National Health and Medical Research Council of Australia investigator grant (1197190). The funders were not involved in the study design, collection, analysis, interpretation of data, the writing of this article or the decision to submit it for publication.

ACKNOWLEDGMENTS

The authors thank and acknowledge the participants of the San Antonio Family Heart Study for their continued involvement in our research programs. We thank Katherine Truax, Marcelo Leandro, and Johnathon Waggoner from the Department of Human Genetics and South Texas Diabetes and Obesity Institute, UTRGV for laboratory assistance and Scott Mc Ahren from Eli Lilly for assistance with study quality control.

SUPPLEMENTARY MATERIAL

The Supplementary Material for this article can be found online at: https://www.frontiersin.org/articles/10.3389/fcvm.2022.889985/full#supplementary-material

REFERENCES

1. Benjamin EJ, Virani SS, Callaway CW, Chamberlain AM, Chang AR, Cheng S, et al. Heart disease and stroke statistics-2018 update: a report from the American Heart Association. *Circulation.* (2018) 137:e67–492. doi: 10.1161/CIR.0000000000000558
2. Olvera Lopez E, Ballard BD, Jan A. *Cardiovascular Disease*. Treasure Island, FL: StatPearls (2022).
3. Barquera S, Pedroza-Tobias A, Medina C, Hernandez-Barrera L, Bibbins-Domingo K, Lozano R, et al. Global overview of the epidemiology of atherosclerotic cardiovascular disease. *Arch Med Res.* (2015) 46:328–38. doi: 10.1016/j.arcmed.2015.06.006
4. Berger JS, Jordan CO, Lloyd-Jones D, Blumenthal RS. Screening for cardiovascular risk in asymptomatic patients. *J Am Coll Cardiol.* (2010) 55:1169–77. doi: 10.1016/j.jacc.2009.09.066
5. Reynolds K, He J. Epidemiology of the metabolic syndrome. *Am J Med Sci.* (2005) 330:273–9. doi: 10.1097/00000441-200512000-00004
6. Forouhi NG, Sattar N, CVD. risk factors and ethnicity–a homogeneous relationship? *Atheroscler Suppl.* (2006) 7:11–9. doi: 10.1016/j.atherosclerosissup.2006.01.003

7. Mitchell BD, Kammerer CM, Blangero J, Mahaney MC, Rainwater DL, Dyke B, et al. Genetic and environmental contributions to cardiovascular risk factors in Mexican Americans. The San Antonio Family Heart Study. *Circulation.* (1996) 94:2159–70. doi: 10.1161/01.CIR.94.9.2159
8. Kulkarni H, Meikle PJ, Mamtani M, Weir JM, Almeida M, Diego V, et al. Plasma lipidome is independently associated with variability in metabolic syndrome in Mexican American families. *J Lipid Res.* (2014) 55:939–46. doi: 10.1194/jlr.M044065
9. Kulkarni H, Meikle PJ, Mamtani M, Weir JM, Barlow CK, Jowett JB, et al. Plasma lipidomic profile signature of hypertension in Mexican American families: specific role of diacylglycerols. *Hypertension.* (2013) 62:621–6. doi: 10.1161/HYPERTENSIONAHA.113.01396
10. Mamtani M, Meikle PJ, Kulkarni H, Weir JM, Barlow CK, Jowett JB, et al. Plasma dihydroceramide species associate with waist circumference in Mexican American families. *Obesity.* (2014) 22:950–6. doi: 10.1002/oby.20598
11. Jorgensen AB, Frikke-Schmidt R, West AS, Grande P, Nordestgaard BG, Tybjaerg-Hansen A. Genetically elevated non-fasting triglycerides and calculated remnant cholesterol as causal risk factors for myocardial infarction. *Eur Heart J.* (2013) 34:1826–33. doi: 10.1093/eurheartj/ehs431
12. Varbo A, Benn M, Tybjaerg-Hansen A, Jorgensen AB, Frikke-Schmidt R, Nordestgaard BG. Remnant cholesterol as a causal risk factor for ischemic heart disease. *J Am Coll Cardiol.* (2013) 61:427–36. doi: 10.1016/j.jacc.2012.08.1026
13. Do R, Willer CJ, Schmidt EM, Sengupta S, Gao C, Peloso GM, et al. Common variants associated with plasma triglycerides and risk for coronary artery disease. *Nat Genet.* (2013) 45:1345–52. doi: 10.1038/ng.2795
14. Sniderman AD, Couture P, Martin SS, DeGraaf J, Lawler PR, Cromwell WC, et al. Hypertriglyceridemia and cardiovascular risk: a cautionary note about metabolic confounding. *J Lipid Res.* (2018) 59:1266–75. doi: 10.1194/jlr.R082271
15. Weissglas-Volkov D, Pajukanta P. Genetic causes of high and low serum HDL-cholesterol. *J Lipid Res.* (2010) 51:2032–57. doi: 10.1194/jlr.R004739
16. Bosse Y, Perusse L, Vohl MC. Genetics of LDL particle heterogeneity: from genetic epidemiology to DNA-based variations. *J Lipid Res.* (2004) 45:1008–26. doi: 10.1194/jlr.R400002-JLR200
17. Wong G, Barlow CK, Weir JM, Jowett JB, Magliano DJ, Zimmet P, et al. Inclusion of plasma lipid species improves classification of individuals at risk of type 2 diabetes. *PLoS ONE.* (2013) 8:e76577. doi: 10.1371/journal.pone.0076577
18. Curran JE, Meikle PJ, Blangero J. New approaches for the discovery of lipidrelated genes. *Clin Lipidol.* (2011) 6:495–500. doi: 10.2217/clp.11.45
19. Meikle PJ, Summers SA. Sphingolipids and phospholipids in insulin resistance and related metabolic disorders. *Nat Rev Endocrinol.* (2017) 13:79–91. doi: 10.1038/nrendo.2016.169
20. Despres JP. Body fat distribution and risk of cardiovascular disease: an update. *Circulation.* (2012) 126:1301–13. doi: 10.1161/CIRCULATIONAHA.111.067264
21. Barchuk M, Dutour A, Ancel P, Svilar L, Miksztowicz V, Lopez G, et al. Untargeted lipidomics reveals a specific enrichment in plasmalogens in epicardial adipose tissue and a specific signature in coronary artery disease. *Arterioscler Thromb Vasc Biol.* (2020) 40:986–1000. doi: 10.1161/ATVBAHA.120.313955
22. Iacobellis G, Ribaudo MC, Assael F, Vecci E, Tiberti C, Zappaterreno A, et al. Echocardiographic epicardial adipose tissue is related to anthropometric and clinical parameters of metabolic syndrome: a new indicator of cardiovascular risk. *J Clin Endocrinol Metab.* (2003) 88:5163–8. doi: 10.1210/jc.2003-030698
23. Colom C, Vilades D, Perez-Cuellar M, Leta R, Rivas-Urbina A, Carreras G, et al. Associations between epicardial adipose tissue, subclinical atherosclerosis and high-density lipoprotein composition in type 1 diabetes. *Cardiovasc Diabetol.* (2018) 17:156. doi: 10.1186/s12933-018-0794-9
24. Sacks HS, Fain JN. Human epicardial adipose tissue: a review. *Am Heart J.* (2007) 153:907–17. doi: 10.1016/j.ahj.2007.03.019
25. Iacobellis G, Leonetti F. Epicardial adipose tissue and insulin resistance in obese subjects. *J Clin Endocrinol Metab.* (2005) 90:6300–2. doi: 10.1210/jc.2005-1087
26. Wang CP, Hsu HL, Hung WC Yu TH, Chen YH, Chiu CA, et al. Increased epicardial adipose tissue (EAT) volume in type 2 diabetes mellitus and association with metabolic syndrome and severity of coronary atherosclerosis. *Clin Endocrinol (Oxf).* (2009) 70:876–82. doi: 10.1111/j.1365-2265.2008.03411.x
27. Rabkin SW. The relationship between epicardial fat and indices of obesity and the metabolic syndrome: a systematic review and meta-analysis. *Metab Syndr Relat Disord.* (2014) 12:31–42. doi: 10.1089/met.2013.0107
28. Gruzdeva O, Borodkina D, Uchasova E, Dyleva Y, Barbarash O. Localization of fat depots and cardiovascular risk. *Lipids Health Dis.* (2018) 17:218. doi: 10.1186/s12944-018-0856-8
29. Kim SH, Chung JH, Kwon BJ, Song SW, Choi WS. The associations of epicardial adipose tissue with coronary artery disease and coronary atherosclerosis. *Int Heart J.* (2014) 55:197–203. doi: 10.1536/ihj.13-303
30. Gaborit B, Sengenes C, Ancel P, Jacquier A, Dutour A. Role of epicardial adipose tissue in health and disease: a matter of fat? *Compr Physiol.* (2017) 7:1051–82. doi: 10.1002/cphy.c160034
31. Mazurek T, Zhang L, Zalewski A, Mannion JD, Diehl JT, Arafat H, et al. Human epicardial adipose tissue is a source of inflammatory mediators. *Circulation.* (2003) 108:2460–6. doi: 10.1161/01.CIR.0000099542.57313.C5
32. Iacobellis G. Local and systemic effects of the multifaceted epicardial adipose tissue depot. *Nat Rev Endocrinol.* (2015) 11:363–71. doi: 10.1038/nrendo.2015.58
33. Fitzgibbons TP, Czech MP. Epicardial and perivascular adipose tissues and their influence on cardiovascular disease: basic mechanisms and clinical associations. *J Am Heart Assoc.* (2014) 3:e000582. doi: 10.1161/JAHA.113.000582
34. Marchington JM, Mattacks CA, Pond CM. Adipose tissue in the mammalian heart and pericardium: structure, foetal development and biochemical properties. *Comp Biochem Physiol B.* (1989) 94:225–32. doi: 10.1016/0305-0491(89)90337-4
35. Rabkin SW. Epicardial fat: properties, function and relationship to obesity. *Obes Rev.* (2007) 8:253–61. doi: 10.1111/j.1467-789X.2006.00293.x
36. Wisneski JA, Gertz EW, Neese RA, Mayr M. Myocardial metabolism of free fatty acids. Studies with 14C-labeled substrates in humans. *J Clin Invest.* (1987) 79:359–66. doi: 10.1172/JCI112820
37. Friedman JM. Obesity in the new millennium. *Nature.* (2000) 404:632–4. doi: 10.1038/35007504
38. Shulman GI. Cellular mechanisms of insulin resistance. *J Clin Invest.* (2000) 106:171–6. doi: 10.1172/JCI10583
39. Pezeshkian M, Noori M, Najjarpour-Jabbari H, Abolfathi A, Darabi M, Darabi M, et al. Fatty acid composition of epicardial and subcutaneous human adipose tissue. *Metab Syndr Relat Disord.* (2009) 7:125–31. doi: 10.1089/met.2008.0056
40. Quehenberger O, Armando AM, Brown AH, Milne SB, Myers DS, Merrill AH, et al. Lipidomics reveals a remarkable diversity of lipids in human plasma. *J Lipid Res.* (2010) 51:3299–305. doi: 10.1194/jlr.M009449
41. Quehenberger O, Dennis EA. The human plasma lipidome. *N Engl J Med.* (2011) 365:1812–23. doi: 10.1056/NEJMra1104901
42. Olvera RL, Bearden CE, Velligan DI, Almasy L, Carless MA, Curran JE, et al. Common genetic influences on depression, alcohol, and substance use disorders in Mexican-American families. *Am J Med Genet B Neuropsychiatr Genet.* (2011) 156B:561–8. doi: 10.1002/ajmg.b.31196
43. Huynh K, Barlow CK, Jayawardana KS, Weir JM, Mellett NA, Cinel M, et al. High-throughput plasma lipidomics: detailed mapping of the associations with cardiometabolic risk factors. *Cell Chem Biol.* (2019) 26:71–84 e4. doi: 10.1016/j.chembiol.2018.10.008
44. Almasy L, Blangero J. Multipoint quantitative-trait linkage analysis in general pedigrees. *Am J Hum Genet.* (1998) 62:1198–211. doi: 10.1086/301844
45. Feser WJ, Fingerlin TE, Strand MJ, Glueck DH. Calculating average power for the Benjamini-Hochberg Procedure. *J Stat Theory Appl.* (2009) 8:325–52.
46. Ferreira JA. The Benjamini-Hochberg method in the case of discrete test statistics. *Int J Biostat.* (2007) 3:11. doi: 10.2202/1557-4679.1065
47. Benjamini Y, Hochberg Y. Controlling the false discovery rate: a practical and powerful approach to multiple testing. *J R Stat Soc Ser B.* (1995) 57:289–300. doi: 10.1111/j.2517-6161.1995.tb02031.x

48. Blanco-Gomez A, Castillo-Lluva S, Del Mar Saez-Freire M, Hontecillas-Prieto L, Mao JH, Castellanos-Martin A, et al. Missing heritability of complex diseases: enlightenment by genetic variants from intermediate phenotypes. *Bioessays.* (2016) 38:664–73. doi: 10.1002/bies.201600084
49. Balfour PC. Jr., Ruiz JM, Talavera GA, Allison MA, Rodriguez CJ. Cardiovascular Disease in Hispanics/Latinos in the United States. *J Lat Psychol.* (2016) 4:98–113. doi: 10.1037/lat0000056
50. Rodriguez CJ, Allison M, Daviglus ML, Isasi CR, Keller C, Leira EC, et al. Status of cardiovascular disease and stroke in Hispanics/Latinos in the United States: a science advisory from the American Heart Association. *Circulation.* (2014) 130:593–625. doi: 10.1161/CIR.0000000000000071
51. Wain LV. Rare variants and cardiovascular disease. *Brief Funct Genomics.* (2014) 13:384–91. doi: 10.1093/bfgp/elu010
52. Jin Y, Kuznetsova T, Bochud M, Richart T, Thijs L, Cusi D, et al. Heritability of left ventricular structure and function in Caucasian families. *Eur J Echocardiogr.* (2011) 12:326–32. doi: 10.1093/ejechocard/jer019
53. Keegan J, Gatehouse PD, Yang GZ, Firmin DN. Spiral phase velocity mapping of left and right coronary artery blood flow: correction for through-plane motion using selective fat-only excitation. *J Magn Reson Imaging.* (2004) 20:953–60. doi: 10.1002/jmri.20208
54. Ward MR, Jeremias A, Hibi K, Herity NA, Lo ST, Filardo SD, et al. The influence of plaque orientation (pericardial or myocardial) on coronary arterial remodeling. *Atherosclerosis.* (2001) 154:179–83. doi: 10.1016/S0021-9150(00)00459-7
55. Prati F, Arbustini E, Labellarte A, Sommariva L, Pawlowski T, Manzoli A, et al. Eccentric atherosclerotic plaques with positive remodelling have a pericardial distribution: a permissive role of epicardial fat? A three-dimensional intravascular ultrasound study of left anterior descending artery lesions. *Eur Heart J.* (2003) 24:329–36. doi: 10.1016/S0195-668X(02)00426-8
56. O'Donnell MJ, Xavier D, Liu L, Zhang H, Chin SL, Rao-Melacini P, et al. Risk factors for ischaemic and intracerebral haemorrhagic stroke in 22 countries (the INTERSTROKE study): a case-control study. *Lancet.* (2010) 376:112–23. doi: 10.1016/S0140-6736(10)60834-3
57. Yusuf S, Joseph P, Rangarajan S, Islam S, Mente A, Hystad P, et al. Modifiable risk factors, cardiovascular disease, and mortality in 155 722 individuals from 21 high-income, middle-income, and low-income countries (PURE): a prospective cohort study. *Lancet.* (2020) 395:795–808. doi: 10.1016/S0140-6736(19)32008-2
58. Kannel WB, Dawber TR, Friedman GD, Glennon WE, McNamara PM. Risk Factors in Coronary Heart Disease. An Evaluation of Several Serum Lipids as Predictors of Coronary Heart Disease; the Framingham Study. *Ann Intern Med.* (1964) 61:888–99. doi: 10.7326/0003-4819-61-5-888
59. Arnett DK, Blumenthal RS, Albert MA, Buroker AB, Goldberger ZD, Hahn EJ, et al. 2019 ACC/AHA Guideline on the Primary Prevention of Cardiovascular Disease: A Report of the American College of Cardiology/American Heart Association Task Force on Clinical Practice Guidelines. *Circulation.* (2019) 140:e596–646. doi: 10.1161/CIR.0000000000000678
60. Dennis EA. Lipidomics joins the omics evolution. *Proc Natl Acad Sci USA.* (2009) 106:2089–90. doi: 10.1073/pnas.0812636106
61. Shevchenko A, Simons K. Lipidomics: coming to grips with lipid diversity. *Nat Rev Mol Cell Biol.* (2010) 11:593–8. doi: 10.1038/nrm2934
62. Tabassum R, Ramo JT, Ripatti P, Koskela JT, Kurki M, Karjalainen J, et al. Genetic architecture of human plasma lipidome and its link to cardiovascular disease. *Nat Commun.* (2019) 10:4329. doi: 10.1038/s41467-019-11954-8
63. McGranaghan P, Kirwan JA, Garcia-Rivera MA, Pieske B, Edelmann F, Blaschke F, et al. Lipid metabolite biomarkers in cardiovascular disease: discovery and biomechanism translation from human studies. *Metabolites.* (2021) 11:621. doi: 10.3390/metabo11090621
64. Neubauer S. The failing heart–an engine out of fuel. *N Engl J Med.* (2007) 356:1140–51. doi: 10.1056/NEJMra063052
65. Karwi QG, Uddin GM, Ho KL, Lopaschuk GD. Loss of metabolic flexibility in the failing heart. *Front Cardiovasc Med.* (2018) 5:68. doi: 10.3389/fcvm.2018.00068
66. Kulkarni H, Meikle PJ, Mamtani M, Weir JM, Barlow CK, Jowett JB, et al. Variability in associations of phosphatidylcholine molecular species with metabolic syndrome in Mexican-American families. *Lipids.* (2013) 48:497–503. doi: 10.1007/s11745-013-3781-7
67. Bellis C, Kulkarni H, Mamtani M, Kent JW. Jr., Wong G, Weir JM, et al. Human plasma lipidome is pleiotropically associated with cardiovascular risk factors and death. *Circ Cardiovasc Genet.* (2014) 7:854–63. doi: 10.1161/CIRCGENETICS.114.000600
68. Alshehry ZH, Mundra PA, Barlow CK, Mellett NA, Wong G, McConville MJ, et al. Plasma lipidomic profiles improve on traditional risk factors for the prediction of cardiovascular events in type 2 diabetes mellitus. *Circulation.* (2016) 134:1637–50. doi: 10.1161/CIRCULATIONAHA.116.023233
69. Cadby G, Melton PE, McCarthy NS, Giles C, Mellett NA, Huynh K, et al. Heritability of 596 lipid species and genetic correlation with cardiovascular traits in the Busselton Family Heart Study. *J Lipid Res.* (2020) 61:537–45. doi: 10.1194/jlr.RA119000594
70. Coleman RA, Lee DP. Enzymes of triacylglycerol synthesis and their regulation. *Prog Lipid Res.* (2004) 43:134–76. doi: 10.1016/S0163-7827(03)00051-1
71. Prentki M, Madiraju SR. Glycerolipid metabolism and signaling in health and disease. *Endocr Rev.* (2008) 29:647–76. doi: 10.1210/er.2008-0007
72. Stephenson DJ, Hoeferlin LA, Chalfant CE. Lipidomics in translational research and the clinical significance of lipid-based biomarkers. *Transl Res.* (2017) 189:13–29. doi: 10.1016/j.trsl.2017.06.006
73. Hannun YA, Obeid LM. Sphingolipids and their metabolism in physiology and disease. *Nat Rev Mol Cell Biol.* (2018) 19:175–91. doi: 10.1038/nrm.2017.107
74. Maceyka M, Spiegel S. Sphingolipid metabolites in inflammatory disease. *Nature.* (2014) 510:58–67. doi: 10.1038/nature13475
75. Edsfeldt A, Duner P, Stahlman M, Mollet IG, Asciutto G, Grufman H, et al. Sphingolipids contribute to human atherosclerotic plaque inflammation. *Arterioscler Thromb Vasc Biol.* (2016) 36:1132–40. doi: 10.1161/ATVBAHA.116.305675
76. Tirodkar TS, Voelkel-Johnson C. Sphingolipids in apoptosis. *Exp Oncol.* (2012) 34:231–42.
77. Turpin SM, Nicholls HT, Willmes DM, Mourier A, Brodesser S, Wunderlich CM, et al. Obesity-induced CerS6-dependent C16:0 ceramide production promotes weight gain and glucose intolerance. *Cell Metab.* (2014) 20:678–86. doi: 10.1016/j.cmet.2014.08.002
78. Kuzmenko DI, Klimentyeva TK. Role of ceramide in apoptosis and development of insulin resistance. *Biochemistry.* (2016) 81:913–27. doi: 10.1134/S0006297916090017
79. Raichur S, Brunner B, Bielohuby M, Hansen G, Pfenninger A, Wang B, et al. The role of C16:0 ceramide in the development of obesity and type 2 diabetes: CerS6 inhibition as a novel therapeutic approach. *Mol Metab.* (2019) 21:36–50. doi: 10.1016/j.molmet.2018.12.008
80. Boini KM, Xia M, Koka S, Gehr TW Li PL. Sphingolipids in obesity and related complications. *Front Biosci.* (2017) 22:96–116. doi: 10.2741/4474
81. Kasumov T, Li L, Li M, Gulshan K, Kirwan JP, Liu X, et al. Ceramide as a mediator of non-alcoholic Fatty liver disease and associated atherosclerosis. *PLoS ONE.* (2015) 10:e0126910. doi: 10.1371/journal.pone.0126910
82. Havulinna AS, Sysi-Aho M, Hilvo M, Kauhanen D, Hurme R, Ekroos K, et al. Circulating ceramides predict cardiovascular outcomes in the population-based FINRISK 2002 cohort. *Arterioscler Thromb Vasc Biol.* (2016) 36:2424–30. doi: 10.1161/ATVBAHA.116.307497
83. Hilvo M, Vasile VC, Donato LJ, Hurme R, Laaksonen R. Ceramides and ceramide scores: clinical applications for cardiometabolic risk stratification. *Front Endocrinol.* (2020) 11:570628. doi: 10.3389/fendo.2020.570628
84. Laaksonen R, Ekroos K, Sysi-Aho M, Hilvo M, Vihervaara T, Kauhanen D, et al. Plasma ceramides predict cardiovascular death in patients with stable coronary artery disease and acute coronary syndromes beyond LDL-cholesterol. *Eur Heart J.* (2016) 37:1967–76. doi: 10.1093/eurheartj/ehw148
85. Poss AM, Summers SA. Too much of a good thing? An evolutionary theory to explain the role of ceramides in NAFLD. *Front Endocrinol.* (2020) 11:505. doi: 10.3389/fendo.2020.00505
86. Chavez JA, Knotts TA, Wang LP Li G, Dobrowsky RT, Florant GL, et al. A role for ceramide, but not diacylglycerol, in the antagonism of insulin signal transduction by saturated fatty acids. *J Biol Chem.* (2003) 278:10297–303. doi: 10.1074/jbc.M212307200
87. Anroedh S, Hilvo M, Akkerhuis KM, Kauhanen D, Koistinen K, Oemrawsingh R, et al. Plasma concentrations of molecular lipid species

predict long-term clinical outcome in coronary artery disease patients. *J Lipid Res.* (2018) 59:1729–37. doi: 10.1194/jlr.P081281
88. Poss AM, Maschek JA, Cox JE, Hauner BJ, Hopkins PN, Hunt SC, et al. Machine learning reveals serum sphingolipids as cholesterol-independent biomarkers of coronary artery disease. *J Clin Invest.* (2020) 130:1363–76. doi: 10.1172/JCI131838
89. Hla T, Kolesnick R. C16:0-ceramide signals insulin resistance. *Cell Metab.* (2014) 20:703–5. doi: 10.1016/j.cmet.2014.10.017
90. Turpin-Nolan SM, Hammerschmidt P, Chen W, Jais A, Timper K, Awazawa M, et al. CerS1-derived C18:0 ceramide in skeletal muscle promotes obesity-induced insulin resistance. *Cell Rep*. (2019) 26:1–10 e7. doi: 10.1016/j.celrep.2018.12.031
91. Raichur S, Wang ST, Chan PW Li Y, Ching J, Chaurasia B, et al. CerS2 haploinsufficiency inhibits beta-oxidation and confers susceptibility to diet-induced steatohepatitis and insulin resistance. *Cell Metab.* (2014) 20:687–95. doi: 10.1016/j.cmet.2014.09.015
92. Chaurasia B, Tippetts TS, Mayoral Monibas R, Liu J, Li Y, Wang L, et al. Targeting a ceramide double bond improves insulin resistance and hepatic steatosis. *Science.* (2019) 365:386–92. doi: 10.1126/science.aav3722
93. Tan-Chen S, Guitton J, Bourron O, Le Stunff H, Hajduch E. Sphingolipid metabolism and signaling in skeletal muscle: from physiology to physiopathology. *Front Endocrinol.* (2020) 11:491. doi: 10.3389/fendo.2020.00491
94. Green CD, Maceyka M, Cowart LA, Spiegel S. Sphingolipids in metabolic disease: the good, the bad, and the unknown. *Cell Metab.* (2021) 33:1293–306. doi: 10.1016/j.cmet.2021.06.006
95. Chaurasia B, Talbot CL, Summers SA. Adipocyte ceramides-the nexus of inflammation and metabolic disease. *Front Immunol.* (2020) 11:576347. doi: 10.3389/fimmu.2020.576347
96. Fridman V, Zarini S, Sillau S, Harrison K, Bergman BC, Feldman EL, et al. Altered plasma serine and 1-deoxydihydroceramide profiles are associated with diabetic neuropathy in type 2 diabetes and obesity. *J Diabetes Complications.* (2021) 35:107852. doi: 10.1016/j.jdiacomp.2021.107852
97. Mwinyi J, Bostrom A, Fehrer I, Othman A, Waeber G, Marti-Soler H, et al. Plasma 1-deoxysphingolipids are early predictors of incident type 2 diabetes mellitus. *PLoS ONE.* (2017) 12:e0175776. doi: 10.1371/journal.pone.0175776
98. Othman A, Rutti MF, Ernst D, Saely CH, Rein P, Drexel H, et al. Plasma deoxysphingolipids: a novel class of biomarkers for the metabolic syndrome? *Diabetologia.* (2012) 55:421–31. doi: 10.1007/s00125-011-2384-1
99. Othman A, Saely CH, Muendlein A, Vonbank A, Drexel H, von Eckardstein A, et al. Plasma 1-deoxysphingolipids are predictive biomarkers for type 2 diabetes mellitus. *BMJ Open Diabetes Res Care.* (2015) 3:e000073. doi: 10.1136/bmjdrc-2014-000073
100. Stegemann C, Pechlaner R, Willeit P, Langley SR, Mangino M, Mayr U, et al. Lipidomics profiling and risk of cardiovascular disease in the prospective population-based Bruneck study. *Circulation.* (2014) 129:1821–31. doi: 10.1161/CIRCULATIONAHA.113.002500
101. Tomasova P, Cermakova M, Pelantova H, Vecka M, Kratochvilova H, Lips M, et al. Minor lipids profiling in subcutaneous and epicardial fat tissue using LC/MS with an optimized preanalytical phase. *J Chromatogr B Analyt Technol Biomed Life Sci.* (2019) 1113:50–9. doi: 10.1016/j.jchromb.2019.03.006

Conflict of Interest: LM was employed by Eli Lilly and Company.

The remaining authors declare that the research was conducted in the absence of any commercial or financial relationships that could be construed as a potential conflict of interest.

Publisher's Note: All claims expressed in this article are solely those of the authors and do not necessarily represent those of their affiliated organizations, or those of the publisher, the editors and the reviewers. Any product that may be evaluated in this article, or claim that may be made by its manufacturer, is not guaranteed or endorsed by the publisher.

frontiers | Frontiers in Cardiovascular Medicine

REVIEW
published: 24 June 2022
doi: 10.3389/fcvm.2022.937071

Glycation and a Spark of ALEs (Advanced Lipoxidation End Products) – Igniting RAGE/Diaphanous-1 and Cardiometabolic Disease

Lakshmi Arivazhagan[1], *Raquel López-Díez*[1], *Alexander Shekhtman*[2], *Ravichandran Ramasamy*[1] *and Ann Marie Schmidt*[1]*

[1] *Diabetes Research Program, Department of Medicine, New York University Grossman School of Medicine, New York, NY, United States,* [2] *Department of Chemistry, The State University of New York at Albany, Albany, NY, United States*

OPEN ACCESS

Edited by:
Nathalie Pamir, Oregon Health and Science University, United States

Reviewed by:
Manuela Calin, Institute of Cellular Biology and Pathology (ICBP), Romania
Ina Nemet, Cleveland Clinic, United States

***Correspondence:**
Ann Marie Schmidt
annmarie.schmidt@nyulangone.org

Specialty section:
This article was submitted to Lipids in Cardiovascular Disease, a section of the journal Frontiers in Cardiovascular Medicine

Received: *05 May 2022*
Accepted: *30 May 2022*
Published: *24 June 2022*

Citation:
Arivazhagan L, López-Díez R, Shekhtman A, Ramasamy R and Schmidt AM (2022) Glycation and a Spark of ALEs (Advanced Lipoxidation End Products) – Igniting RAGE/Diaphanous-1 and Cardiometabolic Disease. Front. Cardiovasc. Med. 9:937071. doi: 10.3389/fcvm.2022.937071

Obesity and non-alcoholic fatty liver disease (NAFLD) are on the rise world-wide; despite fervent advocacy for healthier diets and enhanced physical activity, these disorders persist unabated and, long-term, are major causes of morbidity and mortality. Numerous fundamental biochemical and molecular pathways participate in these events at incipient, mid- and advanced stages during atherogenesis and impaired regression of established atherosclerosis. It is proposed that upon the consumption of high fat/high sugar diets, the production of receptor for advanced glycation end products (RAGE) ligands, advanced glycation end products (AGEs) and advanced lipoxidation end products (ALEs), contribute to the development of foam cells, endothelial injury, vascular inflammation, and, ultimately, atherosclerosis and its consequences. RAGE/Diaphanous-1 (DIAPH1) increases macrophage foam cell formation; decreases cholesterol efflux and causes foam cells to produce and release damage associated molecular patterns (DAMPs) molecules, which are also ligands of RAGE. DAMPs stimulate upregulation of Interferon Regulatory Factor 7 (IRF7) in macrophages, which exacerbates vascular inflammation and further perturbs cholesterol metabolism. Obesity and NAFLD, characterized by the upregulation of AGEs, ALEs and DAMPs in the target tissues, contribute to insulin resistance, hyperglycemia and type two diabetes. Once in motion, a vicious cycle of RAGE ligand production and exacerbation of RAGE/DIAPH1 signaling ensues, which, if left unchecked, augments cardiometabolic disease and its consequences. This Review focuses on RAGE/DIAPH1 and its role in perturbation of metabolism and processes that converge to augur cardiovascular disease.

Keywords: RAGE axis, glycation, lipoxidation, cardiometabolic disease, obesity, non-alcoholic fatty liver disease, lipid metabolism

INTRODUCTION

The receptor for advanced glycation end products (RAGE), a member of the immunoglobulin (Ig) superfamily of cell surface molecules, was discovered on account of its ability to bind the advanced glycation end products, or AGEs. The extracellular domains of RAGE are composed of one Variable (V)-type Ig domain followed by two Constant (C)-type Ig domains (1, 2). The key to understanding the breadth of RAGE activities emerged from multiple investigations that highlighted roles for RAGE as a multi-ligand receptor. In addition to the AGEs ligands, RAGE binds multiple members of the S100/calgranulin family; amphoterin (also called high mobility group box 1 or HMGB1); amyloid beta peptide; lysophosphatidic acid (LPA); phosphatidylserine (PS); and Mac-1, as examples (1, 2). The cytoplasmic tail of RAGE binds to the formin, Diaphanous-1 (DIAPH1) (3), and this interaction was shown in cultured cells to be important for RAGE signaling. Specifically, when the key amino acids in the RAGE cytoplasmic tail responsible for binding to DIAPH1 were mutated (R5/Q6), which correspond to R366/Q367 in the full-length RAGE, to alanine residues, binding to DIAPH1 and ligand-induced cellular signaling were reduced (4).

Beyond these discoveries, RAGE also binds ligands relevant to lipid moieties and evidence is mounting that the RAGE axis regulates transcriptional programs that significantly affect lipid metabolism. This Review will consider these lipid-associated ligands of RAGE and how these ligand families, through RAGE, are importantly involved in the pathogenesis of atherosclerosis, obesity and associated liver diseases.

LIPID-ASSOCIATED LIGANDS OF RAGE

Advanced Lipoxidation End Products

In addition to the classical sugar-mediated modifications that yield the AGEs, advanced lipoxidation end products (ALEs) also bind to RAGE. ALEs are produced through the reaction of amino acids (such as lysine) with lipoxidation products; examples of which include 4-hydroxy-trans-2-nonenal (HNE), acrolein (ACR) and malondialdehyde (MDA) (5). These species were recently shown to bind to RAGE particularly through the RAGE extracellular VC1 domain structural unit (5, 6). A chief signal transduction-stimulating ligand of RAGE, carboxymethyllysine or CML-AGE (7), may be formed both by glycoxidation and lipoxidation reactions (8). A unifying mechanism by which AGE/ALE mediates cellular stress through RAGE is *via* the generation of reactive oxygen species (ROS) (9).

It is important to note that ALEs, just like AGEs, interact with distinct receptors besides RAGE. For example, in the kidney, where ALE interaction with Galectin-3 is important for the uptake and removal of ALEs, in contrast, upon ALE interaction with RAGE, ALEs activate pro-inflammatory pathways that are linked to the development of fibrotic and inflammatory injuries in the kidney tissue (10). In addition to ALEs, other studies have shown that RAGE binds distinct lipid-related species.

Lysophosphatidic Acid

LPA is a circulating phospholipid that acts through classical G-protein coupled receptors (GPCRs) to mediate a range of biological responses in diverse cell types (11); LPA also binds to RAGE. Through surface plasmon resonance (SPR) and nuclear magnetic resonance (NMR) studies, LPA was found to bind to the V-type Ig domain of RAGE (12). In vascular smooth muscle cells (SMCs), incubation with LPA resulted in activation of signal transduction pathways.

It was previously shown that LPA enhances the implantation and metastasis of RAGE-expressing ID8 cells, a murine epithelial ovarian cancer cell line (13). *In vivo,* upon injection of ID8 cells into C57BL/6 mice, LPA is required for the development of tumor growth and metastasis. In LPA-treated mice injected with ID8 cells, treatment with soluble (s) RAGE or performance of these studies in *Ager* null vs. wild-type mice resulted in a significant reduction in tumor cell burden and metastasis (12). It is notable that tumors were not fully eliminated in these sRAGE-treated or *Ager* null mice, consistent with the expression of non-RAGE receptors for LPA on these tumor cells.

It is noteworthy that distinct studies implicated LPA-RAGE interaction in lung, mammary and ovarian tumors (14, 15). Other studies suggested roles for LPA-RAGE in stroke (16) and upon exposure to World Trade Center particulate matter, the released LPA induced inflammation in macrophages, at least in part through RAGE (17).

Phosphatidylserine

Insights into potentially homeostatic roles for RAGE were uncovered through studies reporting that RAGE bound the glycerophospholipid, phosphatidylserine (PS), which plays key roles in the process of apoptosis (18). In binding experiments, by surface plasmon resonance (SPR), RAGE bound PS (K_D, 563 nM) and demonstrated very slight binding to phosphatidylglycerol. No binding of RAGE was demonstrated in the cases of diacylglycerol (DAG), phosphatidic acid (PA), phosphatidylinositol (PI), phosphatidylethanolamine (PE), phosphatidylcholine (PC) or sphingomyelin (SM) (18). Using confocal microscopy imaging and fluorescence resonance energy transfer (FRET) techniques, it was shown that RAGE co-localized with PS on apoptotic thymocytes, at least in part in pseudopod structures (18). *In vivo* experiments in mouse models supported the relevance of RAGE-PS binding, as both sRAGE and deficiency of *Ager* in mice were shown to impair macrophage phagocytosis (18). Although it is notable in these studies that the biophysical basis of RAGE binding selectively to PS was not probed; that is, why RAGE did not bind to PE, PC, or PA. For example, the results provide insight into the degree of meticulous specificity of RAGE-dependent processes in the context of lipid-stimulated biological signaling mechanisms.

Collectively, these studies describing examples of lipid-related ligands of RAGE, such as the ALEs, LPA and PS opened the doors to understanding that non-peptide/non-protein biochemical species were able to bind to RAGE. Given the vast roles for lipids as key components of cell membranes and as critical components of signal transduction rafts, and their fundamental roles in cholesterol and triglyceride metabolism with implications

for human obesity and cardiovascular diseases, as examples, these findings define important roles for RAGE in human pathobiologies. In the section to follow, the links between RAGE and foam cell biology will be considered.

FOAM CELL FORMATION: IMPLICATIONS FOR THE RAGE PATHWAY

Modified Lipids, Foam Cell Formation and the Effects of Diabetes

In the process of atherogenesis, apolipoprotein B (ApoB)-containing lipoproteins, such as low-density lipoprotein (LDL), and the remnant lipoproteins including very low-density lipoprotein (VLDL), intermediate density lipoprotein (IDL) and chylomicron remnants, may traverse the endothelial cell (EC) barrier into the vascular intima, and, especially in sites of dense extracellular matrix (ECM), these particles may become trapped (19, 20). Biochemical processes in this microenvironment significantly affect the nature of these lipids, such as oxidation, proteolysis, lipolysis and inflammation, as examples (21). Once formed, these lipid-modified species may be recognized and taken up by macrophages, leading to the production of foam cells; processes that begin early in life (22). It is also reported that smooth muscle cells also host these modified lipids and contribute to the pool of foam cells (23).

In diabetes, additional biochemical processes are spurred through the presence of increased concentrations of glucose, leading to activation of the Maillard reaction and the production of glycation-modified lipids (24). The principal amino acid residue in Apo-B 100 that undergoes glycation is lysine; lysine residues are important for recognition by the LDL receptor (LDLR); hence, it is not surprising that glycation promotes an increase in the half-life of glycated LDL in human diabetic vs. non-diabetic plasma (25). Additional pathways that modify lipids and are relevant in the diabetic environment include the effects of carbonyl stress, which lead to the production of ALEs, which were reviewed above and noted as ligands of RAGE; and through increased inflammatory processes observed in the vessel wall and mediated through myeloperoxidase and additional oxidative stress programs (24).

In the sections to follow, the links between lipid modifications, foam cells and the components of the AGE-RAGE pathway are considered.

AGE Receptors and Foam Cell Biology

The first clues suggesting that the RAGE pathway might play roles in foam cell formation emerged from a series of studies reporting that in addition to RAGE, the ligand AGEs also bound scavenger type receptors known to play roles in uptake of oxidized (ox) LDL. For example, CD36 binds both AGEs and oxLDL (26). Other studies reported that scavenger receptors Scavenger Receptor A (SR-A), SR-B1 and Lectin like oxLDL receptor (LOX-1) for oxLDL also bound AGEs (27). A number of studies reported that AGEs, at least in part through RAGE, increased macrophage uptake of oxLDL and increased the levels of macrophage cholesterol esters, leading to the formation of lipid-laden macrophages, also called "foam cells" (28).

RAGE/DIAPH1 and Foam Cell Formation

Numerous studies have implicated the ligand-RAGE pathway to foam cell formation and have identified putative mediating downstream pathways. AGEs were shown to mediate uptake of oxLDL through upregulation of *Cdk5* (cyclin dependent kinase 5) and *Cd36* in macrophages. These mechanisms required AGE-RAGE-mediated generation of oxidative stress, as inhibition of oxidative stress using N-acetyl-cysteine (NAC) and RAGE aptamers blocked AGE-mediated upregulation of *Cdk5* and *Cd36,* and, consequently blocked AGE-mediated foam cell formation (29). Other studies implicated the RAGE ligand S100A12 (30) in foam cell formation at least in part through CD36, RAGE and toll like receptor 4 (TLR4)-dependent mechanisms (31). Furthermore, AGE-RAGE-dependent roles in smooth muscle cells (SMCs) were also implicated in foam cell formation as a specific AGE, CML-AGE stimulated SMC lipid uptake and foam cell formation, along with the transdifferentiation of these cells into macrophage-like cells, at least in part via RAGE (32).

Roles for RAGE and DIAPH1 in these processes were demonstrated through studies using a new class of RAGE-DIAPH1 antagonists (33, 34). Specifically, these small molecules bind to the cytoplasmic tail of RAGE and block the RAGE tail interaction with DIAPH1; this has been illustrated directly using *in vitro* binding assays as well as FRET assays (34). A representative small molecule antagonist of RAGE/DIAPH1 was shown to suppress uptake of oxLDL and foam cell formation in wild-type RAGE-expressing macrophages (35). In parallel, it was shown that in macrophages, the small molecule RAGE/DIAPH1 antagonist blocked AGE-mediated RAC1 activity, activation of NF-kB, production of proinflammatory cytokines and cellular migration (35).

In addition to roles for RAGE in foam cell formation, evidence indicates that the RAGE pathway contributes to reduction in both macrophage cholesterol efflux and to *in vivo* reverse cholesterol transport. These processes together with ligand-RAGE-dependent increased foam cell formation, may synergize to contribute to atherosclerosis. In the sections to follow, roles for RAGE in efflux of cholesterol are considered.

MACROPHAGE CHOLESTEROL EFFLUX AND REVERSE CHOLESTEROL TRANSPORT AND THE RAGE PATHWAY

Evidence from human subjects suggests that one of the mechanisms by which diabetes may accelerate atherosclerosis is through suppression of serum cholesterol efflux capacity and impaired reverse cholesterol transport (36, 37). These findings have been recapitulated in animal models of type 1 diabetes in which it was shown that macrophage-to-feces reverse cholesterol transport was impaired (38). Support for roles for RAGE and its ligands in these processes emerged from multiple *in vitro* and *in vivo* analyses.

The first reports linking RAGE to cholesterol efflux pathways were highlighted in human primary macrophages in which *in vitro*-prepared AGE albumin was shown to reduce mRNA and protein expression of ABCG1 (ATP binding cassette transporter G1), but not ABCA1 (ATP binding cassette transporter A1) (39). Roles for RAGE were established through the suppressive effects of anti-RAGE antibodies on AGE albumin functions. It was also noted in that study that at the functional level, AGE albumin reduced macrophage cholesterol efflux to High Density Lipoprotein (HDL) but not to Apolipoprotein A1 (ApoA1). Interestingly, that work showed that the effects of AGE albumin were independent of the LXR (Liver X Receptor) pathway (39).

Subsequent studies employed bone marrow -derived macrophages (BMDMs) from wild-type or *Ager* (the gene encoding RAGE)-deficient mice and showed that macrophage cholesterol efflux to both HDL and ApoA1 was suppressed upon *Ager* deletion, in parallel with reduced levels of *Abcg1* and *Abca1* mRNA and ABCG1 and ABCA1 protein (40). In *in vitro* studies using human THP1 macrophage like cells, the effects of RAGE on regulation of these transporters were traced to peroxisome proliferator activated receptor-gamma (PPAR-gamma)-dependent mechanisms and not to LXR pathways (40). Using macrophages from diabetic wild-type or *Ager* null mice, it was shown that macrophage reverse cholesterol transport to plasma, liver and feces was reduced in diabetic mice *via* RAGE (40).

Beyond *in vitro*-prepared AGEs, isolated AGE albumin from human type 1 or type 2 diabetic plasma vs. control non-diabetic plasma was also demonstrated to reduce macrophage cholesterol efflux to human THP1 cells or to wild type BMDMs *via* RAGE (41). In that study, human diabetic AGE albumin regulated macrophage inflammatory and pro-oxidative gene expression *via* RAGE (41). Beyond AGEs, other RAGE ligands were also shown to reduce macrophage cholesterol efflux; for example, S100B, S100A8/A9 and S100A12 also played roles in these processes (42, 43).

Finally, it has also been suggested that statin drugs may act, in part, by reducing AGE-mediated suppression of cholesterol efflux. For example, rosuvastatin blocks AGE-mediated reduction in macrophage cholesterol efflux through blockade of AGE-induced oxidative stress (44). In other studies, in THP1 macrophages, treatment with atorvastatin increased cholesterol efflux and expression of the transporter ABCG1, phenomena which were found to be reduced by AGEs treatment. In addition, treatment with atorvastatin reduced RAGE expression in macrophages as well (45).

Collectively, these findings using mouse and human cells as well as mice and human subject-derived AGE albumin implicate the RAGE pathway in key macrophage properties that contribute to foam cell formation and failure of resolution in atherosclerosis especially in diabetes but in the non-diabetic state as well. In this context, recent research has uncovered new mechanisms by which RAGE/DIAPH1 might contribute to regulation of cholesterol metabolism through the regulation of Interferon Regulatory Factor 7 (IRF7).

THE RAGE PATHWAY, ATHEROSCLEROSIS AND REGULATION OF IRF7

Although extensive reports implicated RAGE in the development/progression of atherosclerosis (non-diabetes and diabetes) in mouse models (46–59), little was known about potential roles for RAGE/DIAPH1 in the regression of atherosclerosis, particularly in diabetes.

To test roles for RAGE in regression of diabetic atherosclerosis, a murine model of aortic arch transplantation was performed. In that model, mice devoid of the *Ldlr* were rendered diabetic with streptozotocin and then fed a Western diet. Upon development of atherosclerosis, aortic arches were surgically interpositioned into the vasculature of the recipient diabetic wild-type, *Ager* null or *Diaph1* null mice (60). Compared to wild-type diabetic recipient mice, diabetic mice devoid of *Ager* or *Diaph1* displayed accelerated regression of atherosclerosis with smaller atherosclerotic lesion areas, reduced lesional neutral lipid staining (Oil Red O) and reduced macrophage content per lesion area ($CD68^+$ cells).

In order to identify the underlying mechanisms, donor diabetic *Ldlr* null aortic arches (CD45.2) were transplanted into the above recipient mice (CD45.1) (60). At five days after transplantation, flow cytometry experiments revealed that there were no differences in the percent recipient CD45.1 vs. donor CD45.2 of the $CD11B^+/F4/80^+$ macrophage lesional content by recipient genotype (wild-type vs. *Ager* null), but that there were trends to higher recipient $CD45.1/CD68^+$ macrophage content in the aortic arch lesions transplanted into the *Ager* null vs. the WT diabetic recipient mice. Overall, these findings were consistent with earlier work that demonstrated that the majority of the aortic arch lesional macrophages during the regression process are accounted for by newly recruited cells from the recipient mice (60, 61) and it was further demonstrated that expression or deficiency of *Ager* did not affect the relative contributions of donor vs. recipient macrophages in the regression environment.

On account of the ability to discern donor CD45.2 vs. recipient macrophages CD45.1 in the atherosclerotic plaques in this experimental paradigm, bulk RNA-sequencing was performed on sorted macrophages from the distinct groups of diabetic mice. Bioinformatics analysis revealed downregulation of three pathways in the *Ager* null vs. wild-type recipient macrophages that were linked to the interferon signaling, specifically interferon alpha/beta signaling and gamma signaling (60). In contrast, the fourth pathway identified by this analysis revealed a significant increase in "glycolysis" pathway in *Ager* null vs. wild-type recipient macrophages. Further analysis of the differentially-expressed genes uncovered that *Irf7* mRNA was significantly lower in the *Ager* null vs. wild-type recipient CD45.1 macrophages.

In *in vitro* studies, BMDMs were treated with serum from Western diet–fed Ldlr null mice, which is enriched in RAGE ligand DAMPs, or with isolated RAGE ligand CML-AGE; compared to wild-type BMDMs, those devoid of *Ager* demonstrated lower levels of Irf7 mRNA in the presence of

these RAGE ligands. Through these studies, roles for *Irf7* in regulation of cholesterol metabolism and inflammation in macrophages were also identified. BMDMs were grown in the serum from Western diet-fed mice devoid of the *Ldlr*. Compared with scrambled siRNA, Irf7 knockdown resulted in significant upregulation of genes linked to cholesterol efflux (Abca1 and Abcg1), and increased expression of Nr1h2 (LXRβ), Nr1h3 (LXRα), and Srebp1 and Scap. Significant reductions in Cd36 were observed in Irf7-knockdown vs. scramble siRNA–treated cells as well. In parallel, BMDMs exposed to Western diet–fed Ldlr null mice serum in the presence of Irf7 knockdown displayed lower levels of cholesterol. Finally, compared with scrambled siRNA, Irf7 knockdown resulted in upregulation of Arg1 and Il10 and reduction in Tnfa, Nos2, Il6, and Ccl2 (60). Collectively, these findings linked RAGE to regulation of IRF7 and uncovered intriguing roles for RAGE/IRF7 in cholesterol metabolism and inflammation. Future studies will need to address the full range and implication of these findings to the response to viral infection, atherosclerosis, and obesity, as examples of disorders in which key roles for "immunometabolism" have been suggested. Experiments designed to test these hypotheses and relationships are underway.

In this report describing roles for RAGE in atherosclerosis regression in diabetes, unexpected differences in circulating lipids were also noted. Specifically, compared to diabetic wild-type recipient mice in the aorta transplantation model, diabetic mice devoid of *Ager* or devoid of *Diaph1* demonstrated modest but significantly lower levels of total cholesterol with no differences in triglyceride levels (60). Although the mechanisms underlying these intriguing observations are yet to be discovered, they are under intensive investigation at this time.

In the final sections of this review, roles for RAGE in disrupted lipid metabolism in obesity and non-alcoholic fatty liver disease (NAFLD) have been identified and will be considered.

ABERRANT LIGAND-RAGE INTERACTION AND LIPID DYSREGULATION: IMPLICATIONS FOR THE PATHOGENESIS OF OBESITY

RAGE Expression and Actions in Adipocytes

Although initial work upon the discovery of RAGE focused largely on the impact of its expression in vascular cells, immune cells, cardiomyocytes and neurons, as examples, ongoing investigations illustrated that RAGE was also expressed on adipocytes. In studies in 3T3-L1 adipocyte-like cells, a range of AGEs exerted maladaptive effects *via* RAGE (62). First, it was shown that AGEs derived from glucose, glyceraldehyde, or glycolaldehyde inhibited the differentiation of 3T3-L1 cells. Second, these AGEs suppressed glucose uptake in the presence or absence of insulin. These effects of AGEs were prevented by treatment of the cells with antibodies against AGEs or against RAGE. The RAGE-dependent downstream mechanisms in these pathways were traced to oxidative stress, as treatment of the 3T3-L1 adipocytes with N-acetylcysteine blocked the effects of AGEs on these metabolic consequences (62). Third, it was shown that AGE treatment of 3T3-L1 adipocytes also induced upregulation of monocyte chemoattractant protein 1 (MCP1), thereby identifying a mechanism to stimulate pro-inflammatory effects in AGE-treated adipocytes.

In other studies in a human preadipocyte cell line, SW872 cells, secretion of HMGB1 was demonstrated, which led to the production of IL6. In those cells, a direct role for HMGB1 in the production of IL6 was shown by treatment with recombinant HMGB1, which stimulated production of IL6 (63). The effects of recombinant HMGB1 on regulation of IL6 production were dependent on RAGE and not on TLR2 or TLR4. Others showed that AGE-RAGE in adipocytes was linked to outcomes such as matrix metalloproteinase (MMP) activity (64) and induction of insulin resistance through regulation of GLUT4 activities (65).

Links to DIAPH1 in regulation of adipocyte functions were also demonstrated in other recently reported work. Specifically, visceral adipocytes were retrieved from human subjects with and without diabetes and were examined in both 2-dimensional (2D) and 3D-ECM systems. These authors reported that AGE content was higher in the diabetic vs. nondiabetic adipocytes. In studying potential effects of AGEs, glycated collagen one and AGE-modified ECM materials were shown to regulate glucose uptake, and upregulate expression of *AGER* and *CD36* in the adipocytes as well as expression of RHO GTPase signaling mediators including DIAPH1 (66). Interestingly, in this system, inhibition of DIAPH1, but not RAGE or CD36, reduced AGE-ECM-mediated inhibition of glucose uptake in the adipocytes (66). Although not directly tested in that work, it is possible that the direct links between DIAPH1 and actin cytoskeleton dynamics were responsible for DIAPH1's impact on AGE-ECM properties in adipocytes.

These concepts linking RAGE to obesity have been tested in animal models of high fat diet feeding or in genetically obese and diabetic mice, and will be considered in the sections to follow.

RAGE in Murine Models of Obesity

Numerous reports have tested the role of RAGE in mice fed a high fat diet (60% fat content). Mice bearing global or bone marrow-specific deletion of *Ager* displayed significant protection from diet-induced obesity and adiposity (67). In parallel, mice globally devoid of *Ager* and fed a high fat diet also displayed improved glucose and insulin tolerance. Interestingly, these studies showed that mice bearing global deletion of *Ager* demonstrated higher energy expenditure compared to wild-type mice fed the high fat diet. To more specifically probe the role of RAGE in energy expenditure, mice bearing adipocyte-specific deletion of *Ager* were studied in settings that would evoke a definitive metabolic response. Compared to the wild-type *Ager*-bearing control animals, mice devoid of adipocyte *Ager* demonstrated superior metabolic recovery after fasting, a 4°C cold challenge, or high-fat feeding. Using both *in vivo* and *in vitro* methodologies, that work illustrated that RAGE-dependent mechanisms included suppression of protein kinase A (PKA)-mediated phosphorylation of its major targets, hormone-sensitive lipase (HSL) and p38 mitogen-activated protein (MAP) kinase, upon β-adrenergic receptor stimulation (68) and that

these processes reduced the expression and activity of uncoupling protein 1 (UCP1) and, therefore, the associated thermogenic programs (68).

It is important to note that a distinct publication suggested that mice devoid of *Ager* displayed increased weight gain on a high fat diet (60% kcal fat) vs. *Ager*-expressing control mice (69). Although it is not possible to discern the reasons for the varied findings between the studies, it is possible that the genetic background of the mice, the mode of breeding of the mice, as well as other factors within the environment and the health status of the vivarium, may have differed between the studies. Furthermore, it is notable that beyond global deletion of *Ager*, the studies described above also employed bone marrow or adipocyte-specific deletion of *Ager* (in which protection from diet-induced obesity was shown). In that work, treatment of wild-type C57BL/6 mice with soluble RAGE who were fed a high fat diet also demonstrated significant reductions in gain of body mass vs. the vehicle-treated controls (67).

Studies in human subjects are being conducted to accrue correlations between the RAGE pathway and human obesity and overweight states. Relationships between RAGE ligands and RAGE expression in adipocytes and other cell types relevant to metabolic dysfunction suggest that it is logical to test contributory and mediating roles for this pathway in human obesity.

RAGE/DIAPH1 and Human Obesity

A typical means by which RAGE is assessed *in vivo* in human subjects is through the measurement of sRAGE; total sRAGE is composed of both a cell surface cleaved form of the receptor, which represents about 80% of total sRAGE and the soluble product of an mRNA splice variant of *AGER* that results in production of endogenous secretory or esRAGE (70). There are multiple examples of clinical settings relevant to obesity in which sRAGEs were measured. First, studies compared levels of sRAGE in patients with obesity vs. healthy controls and found that sRAGE levels were lower in patients with obesity vs. healthy weight persons (71). After bariatric surgery and weight loss, it was found that the levels of sRAGE rose. Correlation models were performed and yielded the following insights: the differences in levels of sRAGE were associated with the differences in 1 and 2 h post-prandial glucose, differences in fasting insulin, differences in 2 h post-prandial insulin levels, differences in homeostatic model assessment-insulin resistance (HOMA-IR) model and the differences in levels of triglyceride. In the multivariate model, the differences in 1 and 2 h post-prandial glucose, the differences in 2 h post-prandial insulin and differences in HOMA-IR predicted the differences in sRAGE. Hence, these studies suggested that the differences in levels of sRAGE were coupled to measures of glucose and insulin tolerance. Other studies in patients undergoing bariatric surgery also queried if differences in levels of sRAGE were observed. Patients with obesity were randomized to either bariatric surgery or medical weight loss and levels of sRAGE were observed pre-surgery and at 6 months post-surgery. In the patients undergoing bariatric surgery, but not in the medical weight loss group, higher baseline levels of sRAGE were associated with better weight loss outcomes (72).

Distinct studies also examined the levels of RAGE ligands, particularly CML-AGE in obese adipose tissues. In human obese vs. lean adipose tissue, even in the absence of diabetes, higher levels of CML-AGE and RAGE expression were observed (73). To explain the lower plasma levels of CML-AGE in patients with obesity vs. lean state, a model was developed in mice with genetically mediated diabetes (*db/db* mice); the results of studies in this model suggested that plasma levels of CML-AGE were lower in obesity on account of trapping of the RAGE ligand in the obese (high RAGE-expressing) adipose tissue. Furthermore, upon more in-depth analyses, it was shown that the decreased plasma levels of CML-AGE in patients with obesity were strongly associated with insulin resistance (73).

Studies reported from the Northern Manhattan Study (NOMAS) examined a diverse group of human subjects and reported that median sRAGE levels were significantly lower in subjects who had elevated waist circumference, blood pressure, and fasting glucose, but that no relationship was observed between levels of sRAGE and elevated triglycerides or reduced HDL levels that were also noted in these subjects (74). Strikingly, when the NOMAS investigators performed additional stratification and interaction analyses, they uncovered the key finding that the association of sRAGE levels with metabolic syndrome factors was more prominent in Hispanic vs. White persons and that there was no association with the components of the metabolic syndrome in Black persons (74). These results thus indicate that more research is required in order to determine potential mechanisms underlying these findings, and if racial background should be considered in the interpretation of studies tracking sRAGE levels in cardiometabolic diseases and therapeutic approaches.

Finally, recent work has addressed the potential relationships between *AGER* and *DIAPH1* expression and metabolic health in patients with obesity. The mRNA expression of these genes and multiple other genes involved in glycation and inflammation was studied in human omental and subcutaneous adipose tissue in patients with obesity. The key findings from that study further cemented the relationship between *AGER* and *DIAPH1*; it was reported that only in subcutaneous but not omental adipose tissues, the mRNA expression of *AGER* significantly correlated with that of *DIAPH1* (75). Only in subcutaneous but not omental adipose tissue, genes linked to the AGE-RAGE-DIAPH1 axis strongly correlated with markers of inflammation and adipogenesis and, intriguingly, in subcutaneous but not omental adipose tissue, the mRNA expression of *AGER* was found to correlate significantly with HOMA-IR (75). Whereas, some of these associations, particularly to inflammation markers and HOMA-IR might have been expected to be uncovered between *AGER* and *DIAPH1* in omental adipose tissue, this was not the case. These interesting findings pinpoint future directions for more in-depth study of RAGE/DIAPH1 biology in the subcutaneous adipose tissue depot. As non-alcoholic fatty liver disease (NAFLD) commonly accompanies obesity and is associated with excess lipid content in the liver, potential roles for the RAGE pathway in this setting have been tested as well and will be reviewed in the section to follow.

THE RAGE PATHWAY AND NAFLD

Obesity is closely associated with the development of NAFLD and non-alcoholic steatohepatitis (NASH); a recent Statement published from the American Heart Association indicated that the majority of patients presenting with NAFLD also suffer with obesity, as no more than 20% of NAFLD cases in the United States and Europe were observed in lean persons (76, 77).

Associations between the RAGE pathway and NAFLD have been suggested by multiple studies showing the hepatic and plasma/serum levels of RAGE ligands AGEs, ALEs, S100 and HMGB1, were enhanced in NAFLD vs. healthy controls (78–82). RAGE is expressed on multiple cell types in the liver, such as hepatocytes, stellate cells, Kupffer cells, infiltrating immune cells and vascular cells (83, 84). Interestingly, in conditions in which NAFLD-type disorders occur, either through diet or genetic modification, global deletion of *Ager* is not protective against steatosis, inflammation or fibrosis (85, 86). In contrast, mice bearing deletion of hepatocyte *Ager* and fed a high-AGE diet were protected from hepatic inflammation and fibrosis through suppression of the adverse effects of RAGE-induced oxidative stress (87). In other studies, reduction of *Ager* expression by adenoviruses injection reduced hepatosteatosis and liver inflammation in aged mice (88). Thus, these studies, employing various diets, genetic models and distinct means to silence *Ager* in a NAFLD-like environment, highlight that RAGE may play adaptive vs. deleterious roles in NAFLD-like conditions, and that more research is needed to dissect cell-intrinsic and cell-cell cross-talk mechanisms in hepatic metabolic dysfunction.

Studies are underway to probe how DIAPH1 may contribute to hepatic lipid metabolism as well given its relationship to RAGE signal transduction. In first studies in mice with a type 1-like diabetes induced by streptozotocin and fed normal rodent chow, ^{1}H magnetic resonance spectroscopy and chemical

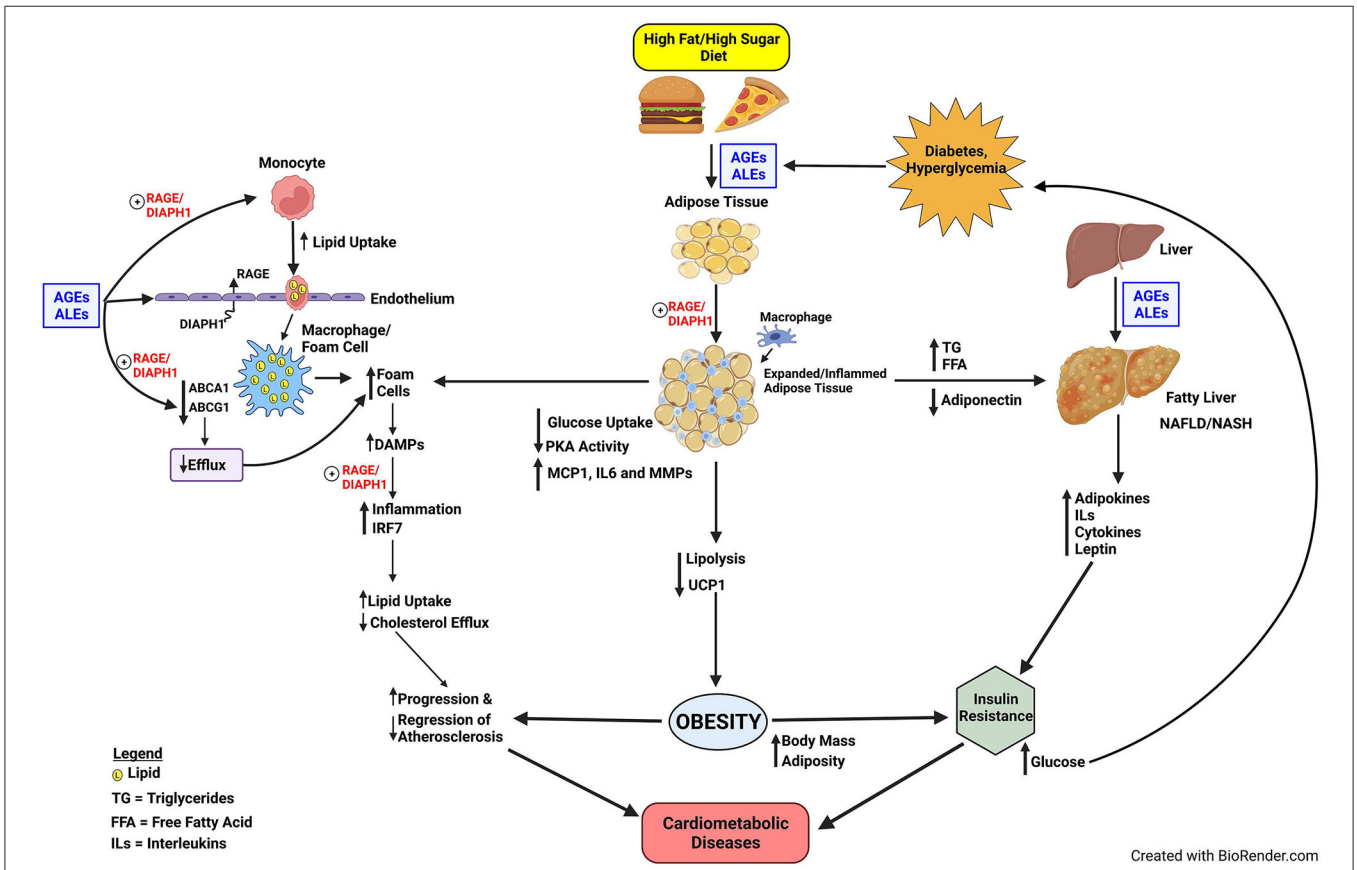

FIGURE 1 | Proposed model of RAGE/DIAPH1 in glycation and lipid metabolism and implications for cardiometabolic disease. Diets high in fats and sugars trigger the production of AGEs and ALEs, which are ligands of RAGE. In very early events in atherogenesis, the production of foam cells in monocytes/macrophages and smooth muscle cells may be facilitated by AGE/ALE signaling through RAGE/DIAPH1. Foam cells, characterized by heightened inflammation in the atherosclerotic vessel wall, produce RAGE ligand DAMPs, which perpetuate inflammatory responses *via* RAGE/DIAPH1; one consequence of which is upregulation of IRF7, which itself perturbs inflammation and cholesterol metabolism pathways and processes that exacerbate progression of atherosclerosis and delay its regression. AGEs and ALEs also accumulate in obese adipose tissue and liver, the latter especially relevant to the pathogenesis of NAFLD. Obesity and NAFLD contribute to the development of insulin resistance, and, therefore, the potential for development of hyperglycemia and processes that amplify AGE/ALE production and their vicious cycle of cellular stress. The optimal means to divert RAGE-DIAPH1 binding and downstream signaling is under intensive investigation and is hypothesized to reduce cardiometabolic risk and its consequences.

shift-encoded magnetic resonance imaging techniques revealed that compared to wild-type mice, mice globally devoid of *Diaph1* displayed significant reductions in hepatic and cardiac triglyceride content (89). These findings suggest that DIAPH1 contributes to lipid metabolism and potential roles for RAGE in these processes and the precise mediating mechanisms are under intensive investigation.

SUMMARY

Disorders of glucose and lipid metabolism are central to the pathogenesis of cardiometabolic diseases and the increased risk for obesity, NAFLD/NASH, atherosclerosis, heart attacks, strokes, and peripheral vascular diseases; processes which may culminate in severe complications such as heart failure, irreversible neurological damage and dementia, and amputations of digits and limbs. Although the RAGE axis was discovered on account of the ability of the AGEs to bind and signal *via* this receptor, soon after its identification, its role in transducing the signals triggered by ALEs expanded the implications of RAGE pathobiologies to those mediated by pathological lipid species. Furthermore, the discoveries that RAGE bound non-AGE and non-ALE ligands expanded our understanding of the biology of RAGE and implicated this receptor in inflammation, lipid signaling and activation of the innate immune system (**Figure 1**).

Well beyond the implications for roles in the pathological consequences of sugar-modified molecules, the above cited studies recount how the RAGE pathway contributes in multiple cell types, tissues and organs to disordered lipid metabolism. In foam cells, the RAGE pathway imbues multiple hits to these cells, favoring their overall accumulation of lipids through increased uptake and decreased efflux mechanisms. The results of studies in foam cells highlighted that the RAGE pathway regulates seminal transcriptional events, and in some cases, in unique ways. For example, although the regulation of the expression of cholesterol transporters has been importantly ascribed to Liver X Receptor (LXR) pathways, RAGE-dependent downregulation of *ABCA1* and *ABCG1* was LXR-independent, and accounted for, at least in part, by PPARG.

The surprising discovery that RAGE ligands also regulated expression of IRF7 has opened new doors to probing if RAGE plays important roles in response to viral infections and the understanding that RAGE is a receptor for multiple classes of DAMPs emitted from the cytoplasm or damaged mitochondria. IRF7 has been described as a master regulator of the type 1 interferon response (90). It is fascinating that like RAGE, IRF7 signaling is also associated with MyD88 and NF-kB signaling, triggered in part by mediators such as TLR9 (91), which is also a RAGE ligand (92, 93). These discoveries support intriguing associations through which the RAGE pathway intersects with COVID19 and its important risk factors, such as obesity, diabetes and advanced aging – all conditions in which AGEs, ALEs and DAMPs are exuberantly produced (94–98).

Furthermore, although the RAGE pathway was long implicated in diabetes and diabetic complications, the RAGE ligands AGEs and ALEs accumulate in obese non-diabetic adipose tissues and may be "trapped" in the tissue by higher levels of RAGE expression, when compared to adipose tissue from lean non-diabetic subjects (73). Unanticipated roles for RAGE ligands in regulation of adipocyte glucose uptake; inflammation; and PKA activities, which mediate lipolysis and regulation of UCP1 and thermogenesis, have broadened our understanding of RAGE and suggested perhaps natural functions of the receptor. Specifically, is it plausible that RAGE functions in an energy conservation pathway to regulate PKA activities in adipocytes; in time of starvation, RAGE acts as a barometer to gauge the need for and regulate energy expenditure? However, in states of overnutrition, retention of these RAGE innate functions supports obesity and its metabolic sequelae. Similarly, in diabetes and obesity, perturbation to the liver may trigger the production of NAFLD and its implications for raising cardiometabolic risk (76). Although roles for RAGE in NAFLD may be more complex and involve both adaptive and maladaptive cellular consequences, it is plausible that prevention and treatment of the underlying causes, such as obesity, may assuage NAFLD-like conditions and reduce cardiovascular risk (**Figure 1**).

The observations that RAGE plays roles in diet-induced obesity and NAFLD have important implications for the development of insulin and glucose intolerance, thereby bringing roles for the RAGE pathway in cardiometabolic dysfunction to full circle. Through insulin resistance, hyperglycemia and oxidative stress may ensue, thereby triggering production of new AGEs/ALEs, more cellular stress, thereby begetting more DAMPs, and, thus, sustaining and reinforcing the cycle proposed in **Figure 1**.

Is this RAGE-dependent cycle of cardiometabolic stress interruptible? Numerous studies have underscored that the RAGE ligands may bind on multiple and discrete domains of the extracellular V, C1, and C2-type Ig domains (99, 100). On account of these findings by multiple research groups, it is plausible that targeting the RAGE-DIAPH1 interaction may represent a superior approach to capture the signaling impact of the multiple RAGE ligands through blocking downstream events; in this context, administration of the chemical probe, RAGE229, which binds to the cytoplasmic domain of RAGE and blocks interaction with DIAPH1, to mice blocks delayed type hypersensitivity inflammation, cardiac ischemia (diabetic mice), type 1 and type 2-diabetes like kidney disease and improves wound healing in mice with type 2-like diabetes (33, 34). Time will tell if stopping the cycle of RAGE/DIAPH1-dependent dysregulation of glucose and lipid metabolism, through this small molecule approach, may be translated to benefit for human subjects.

AUTHOR CONTRIBUTIONS

AMS, LA, RL-D, AS, and RR contributed to the writing of the manuscript and edited the final version. AMS wrote

the first draft and edited the final manuscript. All authors contributed to the article and approved the submitted version.

FUNDING

This research was funded by U.S. Public Health Service: 5P01HL146367, 1R24DK103032, 1R01DK122456-01A1, 1P01HL131481-01A1, 5R01HL132516, and 5R01DK109675. U.S. Department of Defense: W81XWH-17-1-0201 and W81XWH-17-1-0202. Support was also provided from the Diabetes Research Program, NYU Grossman School of Medicine.

ACKNOWLEDGMENTS

The authors gratefully acknowledge the expert assistance of Latoya Woods of the Diabetes Research Program, Department of Medicine, NYU Grossman School of Medicine, in the preparation of this manuscript.

REFERENCES

1. Shekhtman A, Ramasamy R, Schmidt AM. Glycation & the RAGE axis: targeting signal transduction through DIAPH1. *Expert Rev Proteomics.* (2017) 14:147–56. doi: 10.1080/14789450.2017.1271719
2. Ramasamy R, Yan SF, Schmidt AM. The diverse ligand repertoire of the receptor for advanced glycation endproducts and pathways to the complications of diabetes. *Vascul Pharmacol.* (2012) 57:160–7. doi: 10.1016/j.vph.2012.06.004
3. Hudson BI, Kalea AZ, Del Mar Arriero M, Harja E, Boulanger E, D'Agati V, et al. Interaction of the RAGE cytoplasmic domain with diaphanous-1 is required for ligand-stimulated cellular migration through activation of Rac1 and Cdc42. *J Biol Chem.* (2008) 283:34457–68. doi: 10.1074/jbc.M801465200
4. Rai V, Maldonado AY, Burz DS, Reverdatto S, Yan SF, Schmidt AM, et al. Signal transduction in receptor for advanced glycation end products (RAGE): solution structure of C-terminal rage (ctRAGE) and its binding to mDia1. *J Biol Chem.* (2012) 287:5133–44. doi: 10.1074/jbc.M111.277731
5. Mol M, Degani G, Coppa C, Baron G, Popolo L, Carini M, et al. Advanced lipoxidation end products (ALEs) as RAGE binders: Mass spectrometric and computational studies to explain the reasons why. *Redox Biol.* (2019) 23:101083. doi: 10.1016/j.redox.2018.101083
6. Degani G, Altomare AA, Colzani M, Martino C, Mazzolari A, Fritz G, et al. capture method based on the VC1 domain reveals new binding properties of the human receptor for advanced glycation end products (RAGE). *Redox Biol.* (2017) 11:275–85. doi: 10.1016/j.redox.2016.12.017
7. Kislinger T, Fu C, Huber B, Qu W, Taguchi A, Du Yan S, et al. N^{ε}-(carboxymethyl)lysine adducts of proteins are ligands for receptor for advanced glycation end products that activate cell signaling pathways and modulate gene expression. *J Biol Chem.* (1999) 274:31740–9. doi: 10.1074/jbc.274.44.31740
8. Requena JR, Fu MX, Ahmed MU, Jenkins AJ, Lyons TJ, Thorpe SR. Lipoxidation products as biomarkers of oxidative damage to proteins during lipid peroxidation reactions. *Nephrol Dial Transplant.* (1996) 11(Suppl. 5):48–53. doi: 10.1093/ndt/11.supp5.48
9. Moldogazieva NT, Mokhosoev IM. Mel'nikova TI, Porozov YB, Terentiev AA. Oxidative stress and advanced lipoxidation and glycation end products (ALEs and AGEs) in aging and age-related diseases. *Oxid Med Cell Longev.* (2019) 2019:3085756. doi: 10.1155/2019/3085756
10. Iacobini C, Menini S, Ricci C, Scipioni A, Sansoni V, Mazzitelli G, et al. Advanced lipoxidation end-products mediate lipid-induced glomerular injury: role of receptor-mediated mechanisms. *J Pathol.* (2009) 218:360–9. doi: 10.1002/path.2536
11. Smyth SS, Kraemer M, Yang L, Van Hoose P, Morris AJ. Roles for lysophosphatidic acid signaling in vascular development and disease. *Biochim Biophys Acta Mol Cell Biol Lipids.* (2020) 1865:158734. doi: 10.1016/j.bbalip.2020.158734
12. Rai V, Touré F, Chitayat S, Pei R, Song F, Li Q, et al. Lysophosphatidic acid targets vascular and oncogenic pathways via RAGE signaling. *J Exp Med.* (2012) 209:2339–50. doi: 10.1084/jem.20120873
13. Roby KF, Taylor CC, Sweetwood JP, Cheng Y, Pace JL, Tawfik O, et al. Development of a syngeneic mouse model for events related to ovarian cancer. *Carcinogenesis.* (2000) 21:585–91. doi: 10.1093/carcin/21.4.585
14. Ray R, Jangde N, Singh SK, Sinha S, Rai V. Lysophosphatidic acid-RAGE axis promotes lung and mammary oncogenesis via protein kinase B and regulating tumor microenvironment. *Cell Commun Signal.* (2020) 18:170. doi: 10.1186/s12964-020-00666-y
15. Tian M, Tang Y, Huang T, Liu Y, Pan Y. Amelioration of human peritoneal mesothelial cell co-culture-evoked malignant potential of ovarian cancer cells by acacetin involves LPA release-activated RAGE-PI3K/AKT signaling. *Cell Mol Biol Lett.* (2021) 26:51. doi: 10.1186/s11658-021-00296-3
16. Sapkota A, Park SJ, Choi JW. Receptor for advanced glycation end products is involved in LPA(5)-mediated brain damage after a transient ischemic stroke. *Life.* (2021) 11:80. doi: 10.3390/life11020080
17. Lam R, Haider SH, Crowley G, Caraher EJ, Ostrofsky DF, Talusan A, et al. Synergistic effect of WTC-particulate matter and lysophosphatidic acid exposure and the role of RAGE: in-vitro and translational assessment. *Int J Environ Res Public Health.* (2020) 17:4318. doi: 10.3390/ijerph17124318
18. He M, Kubo H, Morimoto K, Fujino N, Suzuki T, Takahasi T, et al. Receptor for advanced glycation end products binds to phosphatidylserine and assists in the clearance of apoptotic cells. *EMBO Rep.* (2011) 12:358–64. doi: 10.1038/embor.2011.28
19. Borén J, Williams KJ. The central role of arterial retention of cholesterol-rich apolipoprotein-B-containing lipoproteins in the pathogenesis of atherosclerosis: a triumph of simplicity. *Curr Opin Lipidol.* (2016) 27:473–83. doi: 10.1097/MOL.0000000000000330
20. Williams KJ, Tabas I. The response-to-retention hypothesis of early atherogenesis. *Arterioscler Thromb Vasc Biol.* (1995) 15:551–61. doi: 10.1161/01.ATV.15.5.551
21. Spickett CM. Formation of oxidatively modified lipids as the basis for a cellular epilipidome. *Front Endocrinol.* (2020) 11:e602771. doi: 10.3389/fendo.2020.602771
22. Stary HC. Macrophage foam cells in the coronary artery intima of human infants. *Ann N Y Acad Sci.* (1985) 454:5–8. doi: 10.1111/j.1749-6632.1985.tb11839.x
23. Cookson FB. The origin of foam cells in atherosclerosis. *Br J Exp Pathol.* (1971) 52:62–9.
24. Bonilha I, Hajduch E, Luchiari B, Nadruz W, Le Goff W, Sposito AC. The reciprocal relationship between LDL metabolism and type 2 diabetes mellitus. *Metabolites.* (2021) 11:807. doi: 10.3390/metabo11120807
25. Tames FJ, Mackness MI, Arrol S, Laing I, Durrington PN. Non-enzymatic glycation of apolipoprotein B in the sera of diabetic and non-diabetic subjects. *Atherosclerosis.* (1992) 93:237–44. doi: 10.1016/0021-9150(92)90260-N
26. Ohgami N, Nagai R, Ikemoto M, Arai H, Miyazaki A, Hakamata H, et al. CD36, serves as a receptor for advanced glycation endproducts (AGE). *J Diabetes Complications.* (2002) 16:56–9. doi: 10.1016/S1056-8727(01)00208-2
27. Horiuchi S, Sakamoto Y, Sakai M. Scavenger receptors for oxidized and glycated proteins. *Amino Acids.* (2003) 25:283–92. doi: 10.1007/s00726-003-0029-5
28. Xu L, Wang YR Li PC, Feng B. Advanced glycation end products increase lipids accumulation in macrophages through upregulation of receptor of advanced glycation end products: increasing uptake, esterification and decreasing efflux of cholesterol. *Lipids Health Dis.* (2016) 15:161. doi: 10.1186/s12944-016-0334-0

29. Yashima H, Terasaki M, Sotokawauchi A, Matsui T, Mori Y, Saito T, et al. Axis stimulates oxidized LDL uptake into macrophages through cyclin-dependent kinase 5-CD36 pathway via oxidative stress generation. *Int J Mol Sci.* (2020) 21:9263. doi: 10.3390/ijms21239263
30. Hofmann MA, Drury S, Fu C, Qu W, Taguchi A, Lu Y, et al. RAGE mediates a novel proinflammatory axis: a central cell surface receptor for S100/calgranulin polypeptides. *Cell.* (1999) 97:889–901. doi: 10.1016/S0092-8674(00)80801-6
31. Farokhzadian J, Mangolian Shahrbabaki P, Bagheri V. S100A12-CD36 axis: a novel player in the pathogenesis of atherosclerosis? *Cytokine.* (2019) 122:154104. doi: 10.1016/j.cyto.2017.07.010
32. Bao Z, Li L, Geng Y, Yan J, Dai Z, Shao C, et al. Advanced glycation end products induce vascular smooth muscle cell-derived foam cell formation and transdifferentiate to a macrophage-like state. *Mediators Inflamm.* (2020) 2020:6850187. doi: 10.1155/2020/6850187
33. Manigrasso MB, Pan J, Rai V, Zhang J, Reverdatto S, Quadri N, et al. Small molecule inhibition of ligand-stimulated RAGE-DIAPH1 signal transduction. *Sci Rep.* (2016) 6:22450. doi: 10.1038/srep22450
34. Manigrasso MB, Rabbani P, Egaña-Gorroño L, Quadri N, Frye L, Zhou B, et al. Small-molecule antagonism of the interaction of the RAGE cytoplasmic domain with DIAPH1 reduces diabetic complications in mice. *Sci Transl Med*. (2021) 13:eabf7084. doi: 10.1126/scitranslmed.abf7084
35. Leerach N, Munesue S, Harashima A, Kimura K, Oshima Y, Kawano S, et al. signaling antagonist suppresses mouse macrophage foam cell formation. *Biochem Biophys Res Commun.* (2021) 555:74–80. doi: 10.1016/j.bbrc.2021.03.139
36. Shiu SW, Zhou H, Wong Y, Tan KC. Endothelial lipase and reverse cholesterol transport in type 2 diabetes mellitus. *J Diabetes Investig.* (2010) 1:111–6. doi: 10.1111/j.2040-1124.2010.00016.x
37. Zhou H, Shiu SW, Wong Y, Tan KC. Impaired serum capacity to induce cholesterol efflux is associated with endothelial dysfunction in type 2 diabetes mellitus. *Diab Vasc Dis Res.* (2009) 6:238–43. doi: 10.1177/1479164109344934
38. Freark de Boer J, Annema W, Schreurs M, van der Veen JN, van der Giet M, Nijstad N, et al. Type I diabetes mellitus decreases in vivo macrophage-to-feces reverse cholesterol transport despite increased biliary sterol secretion in mice. *J Lipid Res.* (2012) 53:348–57. doi: 10.1194/jlr.M018671
39. Isoda K, Folco EJ, Shimizu K, Libby P. AGE-BSA decreases ABCG1 expression and reduces macrophage cholesterol efflux to HDL. *Atherosclerosis.* (2007) 192:298–304. doi: 10.1016/j.atherosclerosis.2006.07.023
40. Daffu G, Shen X, Senatus L, Thiagarajan D, Abedini A, Hurtado Del Pozo C, et al. suppresses ABCG1-mediated macrophage cholesterol efflux in diabetes. *Diabetes.* (2015) 64:4046–60. doi: 10.2337/db15-0575
41. Machado-Lima A, López-Díez R, Iborra RT, Pinto RS, Daffu G, Shen X, et al. RAGE mediates cholesterol efflux impairment in macrophages caused by human advanced glycated albumin. *Int J Mol Sci.* (2020) 21:7265. doi: 10.3390/ijms21197265
42. Chellan B, Yan L, Sontag TJ, Reardon CA, Hofmann Bowman MA. IL-22 is induced by S100/calgranulin and impairs cholesterol efflux in macrophages by downregulating ABCG1. *J Lipid Res.* (2014) 55:443–54. doi: 10.1194/jlr.M044305
43. Kumar P, Raghavan S, Shanmugam G, Shanmugam N. Ligation of RAGE with ligand S100B attenuates ABCA1 expression in monocytes. *Metabolism.* (2013) 62:1149–58. doi: 10.1016/j.metabol.2013.02.006
44. Ishibashi Y, Matsui T, Takeuchi M, Yamagishi S. Rosuvastatin blocks advanced glycation end products-elicited reduction of macrophage cholesterol efflux by suppressing NADPH oxidase activity via inhibition of geranylgeranylation of Rac-1. *Horm Metab Res.* (2011) 43:619–24. doi: 10.1055/s-0031-1283148
45. Xu L, Wang YR Li PC, Feng B. Atorvastatin blocks advanced glycation end products induced reduction in macrophage cholesterol efflux mediated with ATP-binding cassette transporters G 1. *Circ J.* (2019) 83:1954–64. doi: 10.1253/circj.CJ-19-0153
46. Park L, Raman KG, Lee KJ, Lu Y, Ferran LJ Jr. Chow WS, Stern D suppression of accelerated diabetic atherosclerosis by the soluble receptor for advanced glycation endproducts. *Nat Med.* (1998) 4:1025–31. doi: 10.1038/2012
47. Bucciarelli LG, Wendt T, Qu W, Lu Y, Lalla E, Rong LL, et al. blockade stabilizes established atherosclerosis in diabetic apolipoprotein E-null mice. *Circulation.* (2002) 106:2827–35. doi: 10.1161/01.CIR.0000039325.03698.36
48. Lin RY, Choudhury RP, Cai W, Lu M, Fallon JT, Fisher EA, et al. Dietary glycotoxins promote diabetic atherosclerosis in apolipoprotein E-deficient mice. *Atherosclerosis.* (2003) 168:213–20. doi: 10.1016/S0021-9150(03)00050-9
49. Wendt T, Harja E, Bucciarelli L, Qu W, Lu Y, Rong LL, et al. modulates vascular inflammation and atherosclerosis in a murine model of type 2 diabetes. *Atherosclerosis.* (2006) 185:70–7. doi: 10.1016/j.atherosclerosis.2005.06.013
50. Harja E, Bu DX, Hudson BI, Chang JS, Shen X, Hallam K, et al. Vascular and inflammatory stresses mediate atherosclerosis via RAGE and its ligands in apoE-/- mice. *J Clin Invest.* (2008) 118:183–94. doi: 10.1172/JCI32703
51. Bro S, Flyvbjerg A, Binder CJ, Bang CA, Denner L, Olgaard K, et al. Neutralizing antibody against receptor for advanced glycation end products (RAGE) reduces atherosclerosis in uremic mice. *Atherosclerosis.* (2008) 201:274–80. doi: 10.1016/j.atherosclerosis.2008.01.015
52. Soro-Paavonen A, Watson AM, Li J, Paavonen K, Koitka A, Calkin AC, et al. Receptor for advanced glycation end products (RAGE) deficiency attenuates the development of atherosclerosis in diabetes. *Diabetes.* (2008) 57:2461–9. doi: 10.2337/db07-1808
53. Sun L, Ishida T, Yasuda T, Kojima Y, Honjo T, Yamamoto Y, et al. mediates oxidized LDL-induced pro-inflammatory effects and atherosclerosis in non-diabetic LDL receptor-deficient mice. *Cardiovasc Res.* (2009) 82:371–81. doi: 10.1093/cvr/cvp036
54. Bu DX, Rai V, Shen X, Rosario R, Lu Y, D'Agati V, et al. Activation of the ROCK1 branch of the transforming growth factor-beta pathway contributes to RAGE-dependent acceleration of atherosclerosis in diabetic ApoE-null mice. *Circ Res.* (2010) 106:1040–51. doi: 10.1161/CIRCRESAHA.109.201103
55. Ueno H, Koyama H, Shoji T, Monden M, Fukumoto S, Tanaka S, et al. Receptor for advanced glycation end-products (RAGE) regulation of adiposity and adiponectin is associated with atherogenesis in apoE-deficient mouse. *Atherosclerosis.* (2010) 211:431–6. doi: 10.1016/j.atherosclerosis.2010.04.006
56. Morris-Rosenfeld S, Blessing E, Preusch MR, Albrecht C, Bierhaus A, Andrassy M, et al. Deletion of bone marrow-derived receptor for advanced glycation end products inhibits atherosclerotic plaque progression. *Eur J Clin Invest.* (2011) 41:1164–71. doi: 10.1111/j.1365-2362.2011.02514.x
57. Li Y, Liu S, Zhang Z, Xu Q, Xie F, Wang J, et al. mediates accelerated diabetic vein graft atherosclerosis induced by combined mechanical stress and AGEs via synergistic ERK activation. *PLoS One.* (2012) 7:e35016. doi: 10.1371/journal.pone.0035016
58. Koulis C, Kanellakis P, Pickering RJ, Tsorotes D, Murphy AJ, Gray SP, et al. Role of bone-marrow- and non-bone-marrow-derived receptor for advanced glycation end-products (RAGE) in a mouse model of diabetes-associated atherosclerosis. *Clin Sci.* (2014) 127:485–97. doi: 10.1042/CS20140045
59. Uekita H, Ishibashi T, Shiomi M, Koyama H, Ohtsuka S, Yamamoto H, et al. Integral role of receptor for advanced glycation end products (RAGE) in nondiabetic atherosclerosis. *Fukushima J Med Sci.* (2019) 65:109–21. doi: 10.5387/fms.2019-12
60. Senatus L, López-Díez R, Egaña-Gorroño L, Liu J, Hu J, Daffu G, et al. Impairs murine diabetic atherosclerosis regression and implicates IRF7 in macrophage inflammation and cholesterol metabolism. *JCI Insight.* (2020) 5:e137289. doi: 10.1172/jci.insight.137289
61. Rahman K, Vengrenyuk Y, Ramsey SA, Vila NR, Girgis NM, Liu J, et al. Inflammatory Ly6C^{hi} monocytes and their conversion to M2 macrophages drive atherosclerosis regression. *J Clin Invest.* (2017) 127:2904–15. doi: 10.1172/JCI75005
62. Unoki H, Bujo H, Yamagishi S, Takeuchi M, Imaizumi T, Saito Y. Advanced glycation end products attenuate cellular insulin sensitivity by increasing the generation of intracellular reactive oxygen species in adipocytes. *Diabetes Res Clin Pract.* (2007) 76:236–44. doi: 10.1016/j.diabres.2006.09.016
63. Nativel B, Marimoutou M, Thon-Hon VG, Gunasekaran MK, Andries J, Stanislas G, et al. Soluble HMGB1 is a novel adipokine stimulating IL-6 secretion through RAGE receptor in SW872 preadipocyte cell line: contribution to chronic inflammation in fat tissue. *PLoS One.* (2013) 8:e76039. doi: 10.1371/journal.pone.0076039

64. Mahmoud AM, Ali MM. High glucose and advanced glycation end products induce CD147-Mediated MMP activity in human adipocytes. *Cells.* (2021) 10:2098. doi: 10.3390/cells10082098
65. Chilelli NC, Faggian A, Favaretto F, Milan G, Compagnin C, Dassie F, et al. *In vitro* chronic glycation induces AGEs accumulation reducing insulin-stimulated glucose uptake and increasing GLP1R in adipocytes. *Am J Physiol Endocrinol Metab.* (2021) 320:e976–88. doi: 10.1152/ajpendo.00156.2020
66. Strieder-Barboza C, Baker NA, Flesher CG, Karmakar M, Neeley CK, Polsinelli D, et al. Advanced glycation end-products regulate extracellular matrix-adipocyte metabolic crosstalk in diabetes. *Sci Rep.* (2019) 9:19748. doi: 10.1038/s41598-019-56242-z
67. Song F, Hurtado del Pozo C, Rosario R, Zou YS, Ananthakrishnan R, Xu X, et al. RAGE regulates the metabolic and inflammatory response to high-fat feeding in mice. *Diabetes.* (2014) 63:1948–65. doi: 10.2337/db13-1636
68. Hurtado Del Pozo C, Ruiz HH, Arivazhagan L, Aranda JF, Shim C, Daya P, et al. A receptor of the immunoglobulin superfamily regulates adaptive thermogenesis. *Cell Rep*. (2019) 28:773.e7–91.e7. doi: 10.1016/j.celrep.2019.06.061
69. Leuner B, Max M, Thamm K, Kausler C, Yakobus Y, Bierhaus A, et al. Influences obesity in mice. Effects of the presence of RAGE on weight gain, AGE accumulation, and insulin levels in mice on a high fat diet Z. *Gerontol Geriatr.* (2012) 45:102–8. doi: 10.1007/s00391-011-0279-x
70. Schmidt AM. Soluble RAGEs - Prospects for treating & tracking metabolic and inflammatory disease. *Vascul Pharmacol.* (2015) 72:1–8. doi: 10.1016/j.vph.2015.06.011
71. Brix JM, Höllerl F, Kopp HP, Schernthaner GH, Schernthaner G. The soluble form of the receptor of advanced glycation endproducts increases after bariatric surgery in morbid obesity. *Int J Obes.* (2012) 36:1412–7. doi: 10.1038/ijo.2012.107
72. Parikh M, Chung M, Sheth S, McMacken M, Zahra T, Saunders JK, et al. Randomized pilot trial of bariatric surgery versus intensive medical weight management on diabetes remission in type 2 diabetic patients who do NOT meet NIH criteria for surgery and the role of soluble RAGE as a novel biomarker of success. *Ann Surg.* (2014) 260:617–22; discussion 22–4. doi: 10.1097/SLA.0000000000000919
73. Gaens KH, Goossens GH, Niessen PM, van Greevenbroek MM, van der Kallen CJ, Niessen HW, et al. N^{ε}-(carboxymethyl)lysine-receptor for advanced glycation end product axis is a key modulator of obesity-induced dysregulation of adipokine expression and insulin resistance. *Arterioscler Thromb Vasc Biol.* (2014) 34:1199–208. doi: 10.1161/ATVBAHA.113.302281
74. Hudson BI, Dong C, Gardener H, Elkind MS, Wright CB, Goldberg R, et al. Serum levels of soluble receptor for advanced glycation end-products and metabolic syndrome: the Northern Manhattan Study. *Metabolism.* (2014) 63:1125–30. doi: 10.1016/j.metabol.2014.05.011
75. Ruiz HH, Nguyen A, Wang C, He L, Li H, Hallowell P, et al. AGE/RAGE/DIAPH1 axis is associated with immunometabolic markers and risk of insulin resistance in subcutaneous but not omental adipose tissue in human obesity. *Int J Obes.* (2021) 45:2083–94. doi: 10.1038/s41366-021-00878-3
76. Duell PB, Welty FK, Miller M, Chait A, Hammond G, Ahmad Z, et al. Nonalcoholic fatty liver disease and cardiovascular risk: a scientific statement from the American Heart Association. *Arterioscler Thromb Vasc Biol.* (2022) 42:e168–85. doi: 10.1161/ATV.0000000000000153
77. Younossi Z, Anstee QM, Marietti M, Hardy T, Henry L, Eslam M, et al. Global burden of NAFLD and NASH: trends, predictions, risk factors and prevention. *Nat Rev Gastroenterol Hepatol.* (2018) 15:11–20. doi: 10.1038/nrgastro.2017.109
78. Teng F, Jiang J, Zhang J, Yuan Y, Li K, Zhou B, et al. The S100 calcium-binding protein A11 promotes hepatic steatosis through RAGE-mediated AKT-mTOR signaling. *Metabolism.* (2021) 117:154725. doi: 10.1016/j.metabol.2021.154725
79. Pereira E, Araujo BP, Rodrigues KL, Silvares RR, Martins CSM, Flores EEI, et al. Simvastatin improves microcirculatory function in non-alcoholic fatty liver disease and downregulates oxidative and ALE-RAGE stress. *Nutrients.* (2022) 14:716. doi: 10.3390/nu14030716
80. Petriv N, Neubert L, Vatashchuk M, Timrott K, Suo H, Hochnadel I, et al. Increase of α-dicarbonyls in liver and receptor for advanced glycation end products on immune cells are linked to nonalcoholic fatty liver disease and liver cancer. *Oncoimmunology.* (2021) 10:1874159. doi: 10.1080/2162402X.2021.1874159
81. Gaens KH, Niessen PM, Rensen SS, Buurman WA, Greve JW, Driessen A, et al. Endogenous formation of N^{ε}-(carboxymethyl)lysine is increased in fatty livers and induces inflammatory markers in an in vitro model of hepatic steatosis. *J Hepatol.* (2012) 56:647–55. doi: 10.1016/j.jhep.2011.07.028
82. Chandrashekaran V, Seth RK, Dattaroy D, Alhasson F, Ziolenka J, Carson J, et al. HMGB1-RAGE pathway drives peroxynitrite signaling-induced IBD-like inflammation in murine nonalcoholic fatty liver disease. *Redox Biol.* (2017) 13:8–19. doi: 10.1016/j.redox.2017.05.005
83. Hyogo H, Yamagishi S. Advanced glycation end products (AGEs) and their involvement in liver disease. *Curr Pharm Des.* (2008) 14:969–72. doi: 10.2174/138161208784139701
84. Yamagishi S-I, Matsui T. Role of receptor for advanced glycation end products (RAGE) in liver disease. *Eur J Med Res.* (2015) 20:15. doi: 10.1186/s40001-015-0090-z
85. Wouters K, Cento AS, Gaens KH, Teunissen M, Scheijen JLJM, Barutta F, et al. Deletion of RAGE fails to prevent hepatosteatosis in obese mice due to impairment of other AGEs receptors and detoxifying systems. *Sci Rep*. (2021) 11:17373. doi: 10.1038/s41598-021-96859-7
86. Bijnen M, Beelen N, Wetzels S, Gaar JV, Vroomen M, Wijnands E, et al. Deficiency does not affect non-alcoholic steatohepatitis and atherosclerosis in Western type diet-fed Ldlr(-/-) mice. *Sci Rep.* (2018) 8:15256. doi: 10.1038/s41598-018-33661-y
87. Dehnad A, Fan W, Jiang JX, Fish SR, Li Y, Das S, et al. AGER1 downregulation associates with fibrosis in nonalcoholic steatohepatitis and type 2 diabetes. *J Clin Invest.* (2020) 130:4320–30. doi: 10.1172/JCI133051
88. Wan J, Wu X, Chen H, Xia X, Song X, Chen S, et al. Aging-induced aberrant RAGE/PPARα axis promotes hepatic steatosis via dysfunctional mitochondrial β oxidation. *Aging Cell.* (2020) 19:e13238. doi: 10.1111/acel.13238
89. Menon RG, Martel D, Quadri N, Detremmerie C, Frye L, Schmidt AM, et al. Assessment of cardiac and liver metabolite changes in diabetic and DIAPH1 knockout mice using 1H-MRS and chemical-shift encoded MRI. *Proc. Intl. Soc. Mag. Reson. Med.* (2020) 28.
90. Honda K, Yanai H, Negishi H, Asagiri M, Sato M, Mizutani T, et al. IRF-7 is the master regulator of type-I interferon-dependent immune responses. *Nature.* (2005) 434:772–7. doi: 10.1038/nature03464
91. Honda K, Ohba Y, Yanai H, Negishi H, Mizutani T, Takaoka A, et al. Spatiotemporal regulation of MyD88-IRF-7 signaling for robust type-I interferon induction. *Nature.* (2005) 434:1035–40. doi: 10.1038/nature03547
92. Bertheloot D, Naumovski AL, Langhoff P, Horvath GL, Jin T, Xiao TS, et al. Enhances TLR responses through binding and internalization of RNA. *J Immunol.* (2016) 197:4118–26. doi: 10.4049/jimmunol.1502169
93. Tian J, Avalos AM, Mao SY, Chen B, Senthil K, Wu H, et al. Toll-like receptor 9-dependent activation by DNA-containing immune complexes is mediated by HMGB1 and RAGE. *Nat Immunol.* (2007) 8:487–96. doi: 10.1038/ni1457
94. Wick KD, Siegel L, Neaton JD, Oldmixon C, Lundgren J, Dewar RL, et al. Has potential pathogenetic and prognostic value in nonintubated hospitalized patients with COVID-19. *JCI Insight.* (2022) 7:e157499. doi: 10.1172/jci.insight.157499
95. Jessop F, Schwarz B, Scott D, Roberts LM, Bohrnsen E, Hoidal JR, et al. Impairing RAGE signaling promotes survival and limits disease pathogenesis following SARS-CoV-2 infection in mice. *JCI Insight.* (2022) 7:e155896. doi: 10.1172/jci.insight.155896
96. Birts CN, Wilton DC. Age, obesity and hyperglycaemia: Activation of innate immunity initiates a series of molecular interactions involving anionic surfaces leading to COVID-19 morbidity and mortality. *Med Hypotheses.* (2021) 155:110646. doi: 10.1016/j.mehy.2021.110646
97. Sellegounder D, Zafari P, Rajabinejad M, Taghadosi M, Kapahi P. Advanced glycation end products (AGEs) and its receptor, RAGE, modulate age-dependent COVID-19 morbidity and mortality. A review and hypothesis. *Int Immunopharmacol.* (2021) 98:107806. doi: 10.1016/j.intimp.2021.107806
98. Roy D, Ramasamy R, Schmidt AM. Journey to a receptor for advanced glycation end products connection in severe acute respiratory syndrome coronavirus 2 infection: with stops along the way in the lung, heart, blood vessels, and adipose tissue. *Arterioscler Thromb Vasc Biol.* (2021) 41:614–27. doi: 10.1161/ATVBAHA.120.315527

99. Bongarzone S, Savickas V, Luzi F, Gee AD. Targeting the Receptor for Advanced Glycation Endproducts (RAGE): a medicinal chemistry perspective. *J Med Chem.* (2017) 60:7213–32. doi: 10.1021/acs.jmedchem.7b00058
100. Leclerc E, Fritz G, Vetter SW, Heizmann CW. Binding of S100 proteins to RAGE: an update. *Biochim Biophys Acta.* (2009) 1793:993–1007. doi: 10.1016/j.bbamcr.2008.11.016

Conflict of Interest: RR, AS, and AMS have patents and patent applications through NYU Grossman School of Medicine that have been submitted/published that are related to some of the work reviewed in this manuscript.

The remaining authors declare that the research was conducted in the absence of any commercial or financial relationships that could be construed as a potential conflict of interest.

Publisher's Note: All claims expressed in this article are solely those of the authors and do not necessarily represent those of their affiliated organizations, or those of the publisher, the editors and the reviewers. Any product that may be evaluated in this article, or claim that may be made by its manufacturer, is not guaranteed or endorsed by the publisher.

frontiers | Frontiers in Cardiovascular Medicine

REVIEW
published: 30 June 2022
doi: 10.3389/fcvm.2022.901408

Inhibition of Vascular Inflammation by Apolipoprotein A-IV

*Kate Shearston[1], Joanne T. M. Tan[2,3], Blake J. Cochran[1] and Kerry-Anne Rye[1]**

[1] Lipid Research Group, Faculty of Medicine, School of Medical Sciences, University of New South Wales, Sydney, NSW, Australia, [2] Vascular Research Centre, Lifelong Health Theme, South Australian Health and Medical Research Institute, Adelaide, SA, Australia, [3] Adelaide Medical School, The University of Adelaide, Adelaide, SA, Australia

Background: Apolipoprotein (apo) A-IV, the third most abundant apolipoprotein in human high density lipoproteins (HDLs), inhibits intestinal and systemic inflammation. This study asks if apoA-IV also inhibits acute vascular inflammation.

Methods: Inflammation was induced in New Zealand White rabbits by placing a non-occlusive silastic collar around the common carotid artery. A single 1 mg/kg intravenous infusion of lipid-free apoA-IV or saline (control) was administered to the animals 24 h before collar insertion. The animals were euthanised 24 h post-collar insertion. Human coronary artery cells (HCAECs) were pre-incubated with reconstituted HDLs containing apoA-IV complexed with phosphatidylcholine, (A-IV)rHDLs, then activated by incubation with tumour necrosis factor (TNF)-α. Cell surface vascular cell adhesion molecule-1 (VCAM-1) and intercellular adhesion molecule-1 (ICAM-1) in the TNF-α-activated HCAECs was quantified by flow cytometry. VCAM-1, ICAM-1 and 3β-hydroxysteroid-Δ24 reductase (DHCR24) mRNA levels were quantified by real time PCR.

Results: Apolipoprotein ApoA-IV treatment significantly decreased collar-induced endothelial expression of VCAM-1, ICAM-1 and neutrophil infiltration into the arterial intima by 67.6 ± 9.9% ($p < 0.01$), 75.4 ± 6.9% ($p < 0.01$) and 74.4 ± 8.5% ($p < 0.05$), respectively. It also increased endothelial expression of DHCR24 by 2.6-fold ($p < 0.05$). Pre-incubation of HCAECs with (A-IV)rHDLs prior to stimulation with TNF-α inhibited VCAM-1 and ICAM-1 protein levels by 62.2 ± 12.1% and 33.7 ± 5.7%, respectively. VCAM-1 and ICAM-1 mRNA levels were decreased by 55.8 ± 7.2% and 49.6 ± 7.9%, respectively, while DHCR24 mRNA expression increased by threefold. Transfection of HCAECs with DHCR24 siRNA attenuated the anti-inflammatory effects of (A-IV)rHDLs. Pre-incubation of TNF-α-activated HCAECs with (A-IV)rHDLs also inhibited nuclear translocation of the p65 subunit of nuclear factor-κB (NF-κB), and decreased IκBα phosphorylation.

Conclusion: These results indicate that apoA-IV inhibits vascular inflammation *in vitro* and *in vivo* by inhibiting NF-κB activation in a DHCR24-dependent manner.

Keywords: apolipoprotein A-IV, inflammation, high-density lipoproteins, endothelial cells, nuclear factor-kappaB, 3β-hydroxysteroid-Δ24 reductase

Abbreviations: Apo, apolipoprotein; VCAM-1, vascular cell adhesion molecule 1; ICAM-1, intercellular adhesion molecule 1; DHCR24, 3β-hydroxysteroid-Δ24 reductase; HCAECs, human coronary artery endothelial cells; TNF-α, tumour necrosis factor alpha; IκBα, I kappaB alpha; NF-κB, nuclear factor-kappaB; NZW, New Zealand White.

OPEN ACCESS

Edited by:
Mary G. Sorci-Thomas, Medical College of Wisconsin, United States

Reviewed by:
Majken K. Jensen, Harvard University, United States
Xiaofeng Yang, Temple University, United States

****Correspondence:***
Kerry-Anne Rye
k.rye@unsw.edu.au

Specialty section:
This article was submitted to Lipids in Cardiovascular Disease, a section of the journal Frontiers in Cardiovascular Medicine

Received: *21 March 2022*
Accepted: *25 May 2022*
Published: *30 June 2022*

Citation:
Shearston K, Tan JTM, Cochran BJ and Rye K-A (2022) Inhibition of Vascular Inflammation by Apolipoprotein A-IV. Front. Cardiovasc. Med. 9:901408. doi: 10.3389/fcvm.2022.901408

INTRODUCTION

High-density lipoproteins (HDLs), and the main HDL apolipoprotein, apoA-I, have potent anti-inflammatory properties *in vitro* and *in vivo* (1–3). HDLs mediate these effects by inhibiting key steps in activation of the nuclear factor-κB (NF-κB) pathway, including nuclear translocation of the p65 subunit of NF-κB in multiple cell types (4–6). We have also reported that the anti-inflammatory properties of HDLs and apoA-I are related to their ability to increase expression of the anti-apoptotic and antioxidant enzyme, 3β-hydroxysteroid-Δ24 reductase (DHCR24) and induce the potentially cardioprotective enzyme, heme oxygenase-1 (5, 7).

Apolipoprotein A-IV, the third most abundant apolipoprotein in human HDLs, is a 46 kDa protein that is synthesised in the small intestine. It effluxes cholesterol from peripheral cells, including cholesterol-loaded macrophages, in the first step of the potentially anti-atherogenic reverse cholesterol transport pathway (8, 9), participates in the biogenesis of HDLs in an ATP binding cassette transporter A1- and lecithin:cholesterol acyltransferase-dependent manner (10) and has plaque stabilising properties (11).

ApoA-IV is a satiety factor and promotes thermogenesis in brown adipose tissue (12–14). It has anti-diabetic (15–17), antioxidant (18), anti-atherosclerotic (19, 20), anti-apoptotic (21) and anti-thrombotic properties (22) and inhibits intestinal inflammation and pro-inflammatory cytokine expression in animal models, as well as allergy-driven inflammation in humans and mice (20, 23, 24). The anti-inflammatory properties of apoA-IV are potentially clinically relevant and they have recently been identified as an independent risk marker of reduced inflammation in chronic kidney disease (25).

The present study asks if apoA-IV can inhibit acute vascular inflammation in New Zealand White (NZW) rabbits and, if so, whether it targets the same NF-κB- and DHCR24-related pathways as reported previously for HDLs and apoA-I. The results establish that extremely small amounts of apoA-IV markedly inhibit the vascular inflammation that is induced in these animals following insertion of a non-occlusive periarterial carotid collar. We also performed *in vitro* studies which established that the underlying mechanism of this anti-inflammatory effect is related, at least in part, to increased endothelial expression of DHCR24, and inhibition of NF-κB activation.

MATERIALS AND METHODS

Animals

Male New Zealand White rabbits (approximately 2.5 kg) were obtained from the Institute of Medical and Veterinary Sciences (Gilles Plains, SA, Australia) and maintained on a normal chow diet. All procedures were approved by the Sydney South West Area Health Service Animal Welfare Committee (Project No. 2009/019A). The animals (n = 6/group) were randomised to receive a single intravenous (iv) infusion of either saline, lipid-free apoA-I [8 mg/kg (0.3 μmol/kg), positive control], or lipid-free apoA-IV [1 mg/kg, 0.02 μmol/kg)] into the left marginal ear vein 24 h before placing a non-occlusive, peri-arterial collar around the left common carotid artery (1). Prior to the procedure, the animals were sedated with subcutaneous acetylpromazine (0.5 mL/kg), then anaesthetised with inhaled isoflurane (4–5% for induction and 1.5–2% for maintenance). The animals were euthanised 24 h post-collar insertion and collared and non-collared carotid arteries were extracted for immunohistochemical analysis.

Isolation of Apolipoprotein A-I and Rabbit High Density Lipoproteins

High density lipoproteins were isolated from pooled samples of autologously donated human plasma (Healthscope Pathology, Adelaide, SA, Australia) by sequential ultracentrifugation ($1.063 < d < 1.21$ g/mL) and delipidated using standard techniques (26). The resulting apoHDL was chromatographed on a Q-Sepharose Fast-Flow column and apoA-I was isolated as described (27, 28). The apoA-I preparations were judged to be >95% pure by electrophoresis on SDS-polyacrylamide PhastGels (GE Healthcare, Chicago, IL, United States) and Coomassie Blue staining.

For isolation of rabbit HDLs, plasma was adjusted to 1.25 g/mL with solid KBr and ultracentrifuged at 55,000 rpm for 16 h at 4°C, in a 70 Ti fixed angle rotor in an Optima LE-80K Ultracentrifuge (Beckman-Coulter Inc, Brea, CA, United States). The $d < 1.25$ g/mL fraction (600 μL) was injected onto two Superdex 200 columns connected in series to an AKTA FPLC system (GE Healthcare). The HDLs were eluted at a flow rate of 0.3 mL/min.

Expression of Apolipoprotein A-IV

Apolipoprotein A-IV was cloned into the pET14b vector (with integral His-tag; Merck, Darmstadt, Germany), transformed into BL21 (pLysS) cells (Promega, Madison, WI, United States) and grown in Luria-Bertani (LB) culture media with ampicillin for selection of pET14b transformants. When the OD^{600} reached 0.6–0.8, protein expression was induced by incubation for 4 h with isopropyl β-D-1-thiogalactopyranoside (IPTG, 0.8 mM, Applichem, Darmstadt, Germany). The cells were pelleted, lysed with Bugbuster (Merck) and dialysed against 20 mM phosphate buffer containing 6 M urea, 0.3 M NaCl, and 20 mM imidazole (pH 8.0), then loaded onto 5 pre-equilibrated His-trap FF columns (5 mL, GE Healthcare) connected in series. ApoA-IV was eluted at 5 mL/min for 15 min with 20 mM phosphate buffer containing 6 M urea, 0.3 M NaCl and 500 mM imidazole (1–100% gradient) (pH 8.0). The apoA-IV was dialysed into TBS prior to removing the His-tag by incubation for 5 h at room temperature with thrombin (2 U/mg apoA-IV). The reaction was stopped by addition of Phosphatase Inhibitor Cocktail 2 (1 mL, Sigma-Aldrich, St Louis, MO, United States). The apoA-IV was dialysed into 20 mM Tris (pH 8.5), adjusted to 6 M with solid, deionised urea and loaded onto a pre-equilibrated Q-Sepharose Fast Flow column (GE Healthcare). ApoA-IV was eluted from the column at a flow rate of 3 mL/min with 20 mM Tris containing 6 M urea and a gradient of 0.5 M

NaCl (pH 8.5): 0–40% for 5 min, 40–48% for 15 min, 48–70% for 15 min. The apoA-IV was dialysed against endotoxin-free PBS and added to 1% Triton X-114 (v/v) at 4°C for 30 min to remove residual endotoxin, then incubated at 37°C for 10 min and centrifuged (5,200 × *g*) for 1 h. The aqueous layer (containing apoA-IV) was removed, and the process repeated three times. Residual Triton X-114 was removed from the apoA-IV by incubation for 2 h at 4°C with Bio beads (Bio-Rad, Hercules, CA, United States). The apoA-IV was concentrated (Amicon Ultra -15 centrifugal filter, Billerica, MA, United States) and filtered (0.22 μM). Endotoxin levels were tested using an EndoSafe PTS-Reader and 0.1–10 EU/mL PTS cartridges (Charles River, Wilmington, MA, United States) and found to be <0.5 EU/mL.

Preparation of Discoidal Reconstituted HDLs

Discoidal rHDLs containing palmitoyl-2-linoleoyl-*sn*-glycero-3-phosphatidylcholine (PLPC, Avanti Polar Lipids, Alabaster, AL, United States) and apoA-I [initial PLPC/apoA-I molar ratio 100/1, (A-Ir)HDLs] or apoA-IV [initial PLPC/apoA-IV molar ratio 150/1, (A-IV)rHDLs] were prepared by the cholate dialysis method (29). The rHDLs were dialysed extensively against endotoxin-free PBS before use. Particle sizes were determined by non-denaturing gradient gel electrophoresis (30). Cross-linking with the homo-bifunctional cross-linking agent bis (sulfosuccinimidylsuccinate) (BS) was performed as described (31, 32).

Cell Culture

Human coronary artery endothelial cells (HCAECs, passages 2 to 6) were maintained in MesoEndo media (Cell Applications, San Diego, CA, United States). The cells, in either 12-well (1×10^5 cells/well for mRNA quantification) or 6-well plates (2×10^5 cells/well for protein extraction) were pre-incubated for 16 h with discoidal (A-I)rHDLs, discoidal (A-IV)rHDLs, isolated rabbit HDLs or PBS. After removal of the rHDLs or HDLs, the cells were incubated for 5 h at 37°C with TNF-α (final concentration 0.2 ng/mL), then subjected to flow cytometry or total RNA isolation. For measurement of the p65 subunit of NF-κB and IκBα, the cells were incubated with TNF-α (final concentration 0.2 ng/mL) for 20 min.

Knockdown of 3β-Hydroxysteroid-Δ24 Reductase

Human coronary artery endothelial cells (0.5×10^5 cells/well) were plated into 24-well plates and transfected at 37°C for 7 h with either DHCR24 siRNA (Santa Cruz, Dallas, TX, United States; sc-60531) or scrambled control siRNA (Santa Cruz; sc-37007) using 15 pmol of siRNA.

Flow Cytometry

Human coronary artery endothelial cells were plated into 24-well (0.5×10^5 cells/well) and incubated at 4°C for 30 min with an ICAM-1 antibody (1:5; CD54 FITC, Beckman-Coulter), a VCAM-1 antibody (1:500; CD106 PeCy5 510C9, BD Bioscience, Franklin Lakes NJ, United States) or PBS containing 10% (v/v) heat-inactivated fetal bovine serum (FBS). An isotype control (PECy5 mouse IgG1, BD Bioscience and IgG1 FITC, Beckman-Coulter) was used to confirm the specificity of the fluorescent labelling. Cells incubated in the absence of TNF-α were used to ascertain background expression of ICAM-1 and VCAM-1.

Western Blotting

Human coronary artery endothelial cells were rinsed with PBS and nuclear and cytoplasmic extracts were prepared (NE-PER, Pierce, Rockford, Ill). The extracted proteins were quantified (BCA assay), loaded onto 3–14% Bis-Tris gels (Life Technologies, Carlsbad, CA, United States), electrophoresed for 45 min, transferred to nitrocellulose membranes and blocked with 10% (w/v) skim milk. Phosphorylated and total IκBα, the p65 subunit of NF-κB and β-actin were detected with mouse anti-human IκBα (1:1000, Cell Signalling), rabbit anti-human phospho-IκBα (1:1000, Cell Signalling Technology, Danvers, MA, United States), rabbit anti-human p65 (1:500, Santa Cruz Biotechnology, Dallas, TX, United States) and mouse anti-human β-actin (1:3000) monoclonal antibodies (Abcam, Cambridge, United Kingdom). Goat anti-rabbit or goat anti-mouse IgG-HRP (Santa-Cruz) were used as secondary antibodies. The membranes were developed using ECL Plus (GE Healthcare) and imaged with a Chemidoc imager (Bio-Rad).

Plasma Lipid and Lipoprotein Analysis

All analyses were carried out in triplicate on a Hitachi 902 autoanalyser (Roche Diagnostics, Mannheim, Germany). Protein concentrations were measured using the bicinchoninic acid assay (33). Phospholipid and unesterified cholesterol concentrations were measured enzymatically (34, 35). Total cholesterol concentrations were measured using commercial kits (Roche Diagnostics). ApoA-I was measured immunoturbidometrically using a goat anti-human apoA-I antibody (Calbiochem, San Diego, CA, United States) (36). ApoA-IV was quantified using a commercially available ELISA kit (Millipore, Burlington, MA, United States).

Immunohistochemistry

Carotid artery sections were dehydrated and embedded in paraffin, sectioned (5 μm), and mounted on glass slides. The sections were then incubated overnight at 37°C prior to antigen retrieval (Target Retrieval Buffer (pH 9.0), Dako, Glostrup, Denmark). After blocking endogenous peroxidase activity with Peroxidase block (Envision Mouse Kit, Dako), the sections were incubated with 10% (v/v) rabbit serum to block non-specific binding and stained with mouse anti-rabbit CD18 (1:200; AbD Serotec, Raleigh, NC, United States), mouse anti-rabbit VCAM-1 (1:200), mouse anti-rabbit ICAM-1 (1:200) (provided Dr M. Cybulsky, University of Toronto) monoclonal antibodies or a goat anti-human polyclonal antibody against DHCR24 (1:200) (Santa-Cruz). The sections were rinsed, incubated with appropriate HRP-conjugated secondary antibodies (Envision

Mouse Kit, Dako), then incubated with 3,3-diaminobenzidine solution (Envision Mouse Kit, Dako) and counter-stained with Haematoxylin and Eosin. Images were obtained using a Zeiss Imager M1 microscope with an attached AxioCam MRc5 at 40 × magnification. Staining was quantified using ImageJ.[1] The threshold for positive staining was determined by a blinded observer and applied to all sections. To account for variations in carotid artery size, the number of pixels staining positive for endothelial VCAM-1 and ICAM-1 was divided by the endothelial circumference and the results were expressed as image units. CD18-positive and DHCR24-positive staining was expressed as % total intima/media cross-sectional area.

Real Time PCR

Total RNA was isolated with Trizol and reverse transcribed using an iScript cDNA synthesis kit (Bio-Rad) and a Mastercycler thermocycler (Eppendorf, Hamburg, Germany). Real time PCR was performed using iQ SYBR Green Supermix (Bio-Rad) in an iCycler iQ Real-Time thermocycler. Quantitation of gene expression was assessed by the ΔΔCt method with β-2 microglobulin (B2 M), hypoxanthine phosphoribosyltransferase 1 (HPRT-1), and β-actin as housekeeping genes. Primers are shown in **Supplementary Table 1**.

Statistical Analysis

All statistical analyses were performed using GraphPad Prism Version 5.0 d for Mac (GraphPad Software, San Diego, CA United States).[2] Significant differences between data sets were determined using a two-tailed, unpaired Student's *t*-test or one-way ANOVA with Dunnett's post-test, with $p < 0.05$ considered significant. The normality of all data was determined with the Kolmogorov-Smirnov test and $\alpha = 0.05$ considered to be normally distributed. All results are presented as mean ± SEM unless otherwise specified.

RESULTS

A Single Infusion of Lipid-Free Apolipoprotein A-IV Inhibits Peri-Arterial Collar-Induced Vascular Inflammation in New Zealand White Rabbits

A non-occlusive collar was placed around the common carotid artery of NZW rabbits (n = 6/group) 24 h after administration of a single infusion of apoA-IV (1 mg/kg iv), saline (negative control) or apoA-I (8 mg/kg, positive control). As reported previously, neutrophils ($CD18^+$ cells) were not detected in the non-collared arteries in the saline-infused animals (**Figure 1A**) (1). The arteries also had low levels of constitutive ICAM-1 (**Figure 1E**) and VCAM-1 (**Figure 1I**) expression.

The collar induced an acute inflammatory response that was accompanied by neutrophil infiltration into the intima-media (**Figure 1B**) and increased endothelial expression of ICAM-1 (**Figure 1F**) and VCAM-1 (**Figure 1J**). A single 8 mg/kg iv infusion of lipid-free apoA-I 24 h prior to collar insertion reduced collar-mediated $CD18^+$ cell infiltration from 16.4 ± 6.7% (**Figure 1B**) to 1.4 ± 0.7% of the total intima-media area (**Figure 1C**, $p < 0.01$). A single 1 mg/kg iv infusion of apoA-IV similarly decreased the area staining positive for $CD18^+$ cells from 16.4 ± 6.7% (**Figure 1B**) to 4.2 ± 1.4%, (**Figure 1D**, $p < 0.05$).

The collar-mediated increase in endothelial ICAM-1 expression was reduced from 32.1 ± 12.5 image units (**Figure 1F**) to 7.1 ± 1.2 image units (**Figure 1G**) in the animals that were infused with apoA-I, and to 7.9 ± 2.2 image units (**Figure 1H**) in the animals that were infused with apoA-IV ($p < 0.01$ for both). The collar-induced increase in endothelial VCAM-1 expression was attenuated from 11.1 ± 2.3 image units (**Figure 1J**) in the saline-infused animals to 7.7 ± 1.1 image units (**Figure 1K**) in the animals that were infused with lipid-free apoA-I, and to 3.6 ± 1.1 image units (**Figure 1L**) in the apoA-IV-infused animals, ($p < 0.01$ for both).

Insertion of a carotid collar did not alter DHCR24 protein expression in the intima-media of the saline-infused animals relative to what was observed for the non-collared arteries (**Figures 1M,N**). This is consistent with what has been reported previously (37). Expression of DHCR24 in the intima-media, by contrast, increased from 3.4 ± 0.5% (**Figure 1M**) in the collared, saline-infused animals to 10.9 ± 2.7% of the total area in the animals that were infused with apoA-I (**Figure 1O**, $p < 0.01$), and to 9.0 ± 1.4% in the animals that were infused with apoA-IV (**Figure 1P**, $p < 0.05$).

A Single Apolipoprotein A-IV Infusion Does Not Affect Plasma Lipids or High Density Lipoprotein Size and Composition

Plasma apoA-I, apoA-IV, phospholipid, unesterified cholesterol, total cholesterol and phospholipid levels did not differ between the three groups of rabbits at baseline (**Supplementary Table 2**). At 24 h post-infusion (i.e., at the time of collar insertion) plasma lipid, apoA-I and apoA-IV levels in the rabbits that received saline, apoA-IV and apoA-I were comparable. There was also no difference in plasma lipid, apoA-I and apoA-IV levels at 48 h after the infusion of apoA-IV, apoA-I or saline.

HDLs were isolated from plasma as described in section "Materials and Methods" and, given that rabbits are deficient in apoA-II, the composition of the preparations was determined based on the assumption that apoA-I is the predominant apolipoprotein (38). HDL composition did not differ significantly in the animals that were infused with saline, apoA-IV or apoA-I (**Supplementary Table 3**). This is consistent with what has been reported previously for HDLs isolated from saline- and apoA-I-infused rabbits (39). The apoA-I and apoA-IV infusions also had no effect on HDL particle size (**Supplementary Table 3**).

[1] https://imagej.nih.gov/ij/

[2] www.graphpad.com

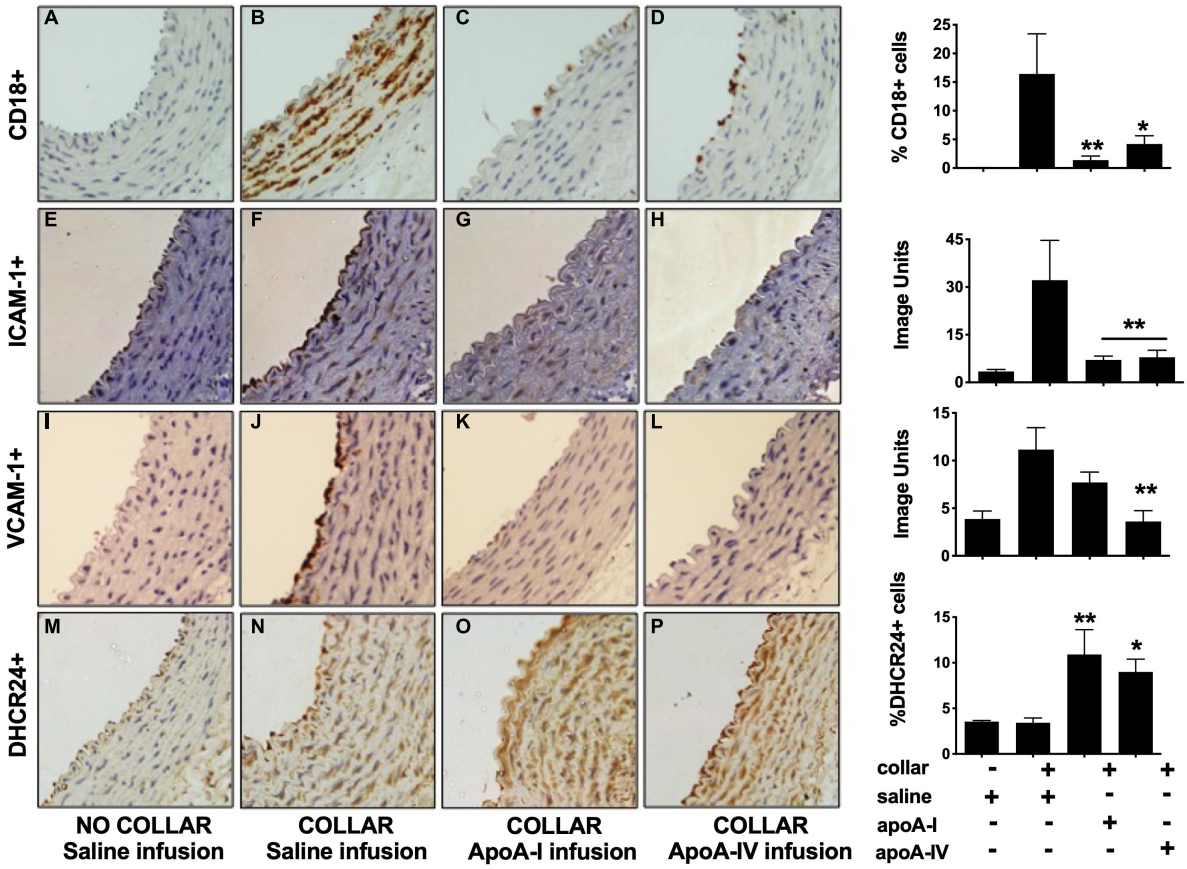

FIGURE 1 | Apolipoprotein A-IV inhibits acute vascular inflammation in NZW rabbit carotid arteries. NZW rabbits (n = 6/group) were infused iv with saline [Panels **(A,B,E,F,I,J,M,N)**], apoA-I [Panels **(C,G,K,O)**; 8 mg/kg iv] or apoA-IV [Panels **(D,H,L,P)**; 1 mg/kg iv] 24 h prior to inserting a non-occlusive peri-arterial collar around the left common carotid artery. The animals were euthanised 24 h post-collar insertion. Sections from the non-collared [Panels **(A,E,I,M)**] and the collared carotid arteries were stained for neutrophils [CD18, Panels **(B–D)**], ICAM-1 [Panels **(F–H)**], VCAM-1 [Panels **(J–L)**] and DHCR24 [Panels **(N–P)**]. Representative immunostained images as shown. *$p < 0.05$, **$p < 0.01$.

A Single Apolipoprotein A-IV Infusion Does Not Improve the Anti-inflammatory Function of High Density Lipoproteins in New Zealand White Rabbits

The anti-inflammatory properties of the HDLs that were isolated from the saline-, apoA-I- and apoA-IV-infused rabbits were also evaluated in TNF-α-activated HCAECs as described in section "Materials and Methods." The isolated HDLs did not inhibit ICAM-1 expression in TNF-α-activated HCAECs, irrespective of whether the animals were infused with saline, lipid-free apoA-I, or lipid-free apoA-IV (**Figures 2A–C**).

The isolated HDLs from the saline-, apoA- I-, and apoA-IV - infused rabbits, by contrast, inhibited VCAM-1 expression in a concentration dependent manner (**Figures 2D–F**). At an HDL protein concentration of 20 μM, the HDLs from the saline-infused rabbits decreased VCAM-1 protein levels by 42.9 ± 7.3% (**Figure 2D**, $p < 0.001$), compared to 24 ± 6.5% for the rabbits that were infused with apoA-I (**Figure 2E**, $p < 0.05$) and by 39.5 ± 6.0% for the rabbits that were infused with apoA-IV (**Figure 2F**, $p < 0.001$).

As the reduction in VCAM-1 expression was similar irrespective of whether the rabbits were infused with saline, apoA-I or apoA-IV, it was concluded that treatment with apoA-IV does not improve the anti-inflammatory function of HDLs.

(A-IV)rHDLs Inhibit Intercellular Adhesion Molecule 1 and Vascular Cell Adhesion Molecule 1 Expression in Human Coronary Artery Endothelial Cells More Effectively Than (A-I)rHDLs

Although apoA-IV inhibits intestinal inflammation and decreases atherosclerosis in mice (20, 23), it has a low affinity for lipid, with up to 98% of the total apoA-IV in fasted human plasma being present in the lipid-free form after ultracentrifugation (40). This indicates that most of the apoA-IV may have dissociated from the rabbit HDLs during the isolation procedure, thus explaining why the HDL preparations from the apoA-IV-treated rabbits inhibited VCAM-1 expression in HCAECs to the same extent as the isolated HDLs from the apoA-I-treated rabbits (**Figure 2**).

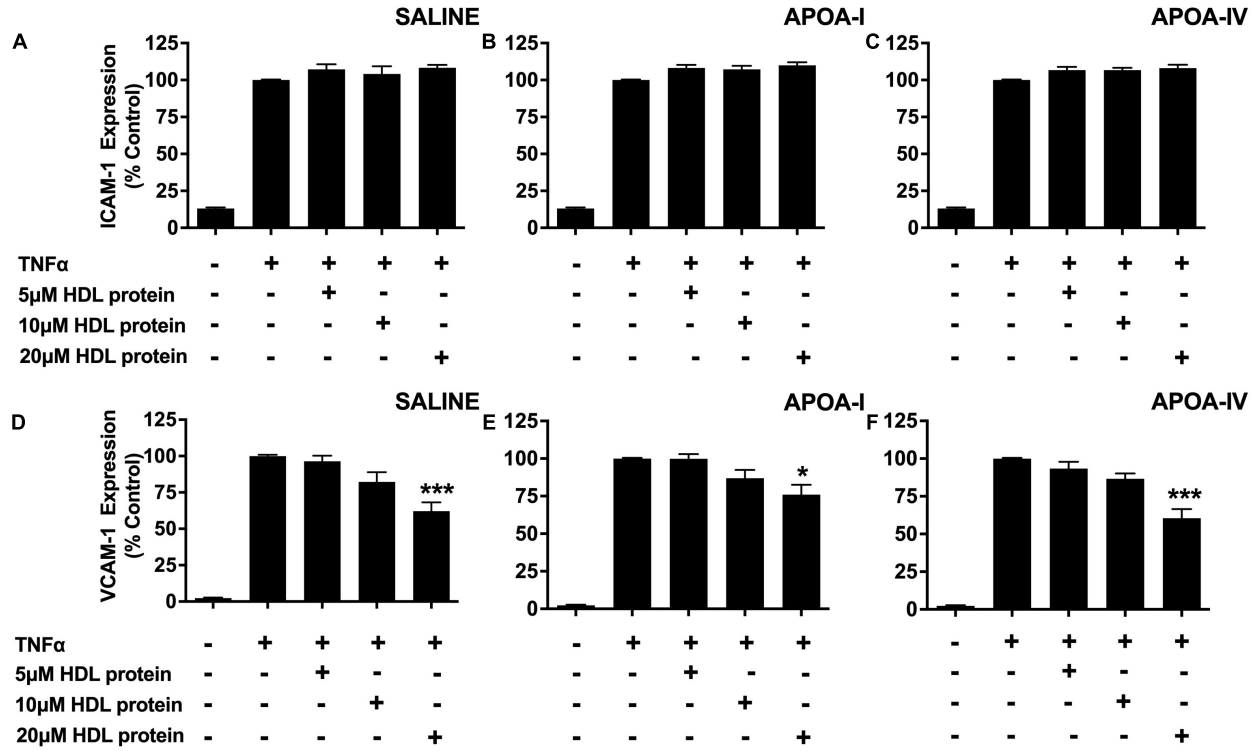

FIGURE 2 | A single apoA-IV infusion does not alter the anti-inflammatory properties of rabbit HDLs. HDLs were ultracentrifugally isolated from NZW rabbits that had been treated with saline [Panels **(A,D)**], lipid-free apoA-I [Panels **(B,E)**] or lipid-free apoA-IV [Panels **(C,F)**] as described in the legend to **Figure 1**. The isolated HDLs (final apoA-I concentration: 5, 10, or 20 μM) were incubated at 37°C for 16 h with HCAECs prior to stimulation with TNF-α (0.2 ng) for 5 h at 37°C. ICAM-1 and VCAM-1 protein expression was quantified by flow cytometry. Data points represent mean ± SEM of three independent experiments with three replicates/experiment. $^{*}p < 0.05$, $^{***}p < 0.001$.

To ascertain whether apoA-IV is able to inhibit ICAM-1 and VCAM-1 in endothelial cells *in vitro*, discoidal (A-IV)rHDLs were prepared by complexing lipid-free apoA-IV with PLPC. The discoidal (A-IV)rHDLs consisted of a major population of particles 10.9 nm in diameter and three larger, minor populations of particles (**Figure 3A**). Discoidal (A-I)rHDLs were used as a positive control and consisted predominantly of particles 8.8 and 7.4 nm in diameter (**Figure 3A**). The PLPC/apolipoprotein molar ratio of the (A-IV)rHDLs and (A-I)rHDLs were 88/1 and 54/1, respectively (**Figure 3A**). As judged by covalent cross-linking, the (A-I)rHDL and (A-IV)rHDL preparations consisted of populations of particles with two, three and four apolipoprotein molecules/particle (**Figure 3B**).

Pre-incubation of HCAECs with the discoidal (A-I)rHDLs at a final apoA-I concentration of 32 μM prior to stimulation with TNF-α, inhibited cell surface ICAM-1 levels by 50 ± 2% (**Figure 4A**) and VCAM-1 levels by 73 ± 9% (**Figure 4B**) ($p < 0.001$ for both compared to TNF-α-stimulated HCAECs). Pre-incubation of the HCAECs with discoidal (A-IV)rHDLs at a final apoA-IV concentration of 5 μM did not inhibit ICAM-1 or VCAM-1 expression significantly. Pre-incubation with discoidal (A-IV)rHDLs at a final apoA-IV concentration of 10 μM, by contrast, inhibited ICAM-1 and VCAM-1 levels by 34 ± 3% (**Figure 4A**) and 62 ± 12% respectively (**Figure 4B**) ($p < 0.001$ for both compared to TNF-α-stimulated HCAECs).

The reduction in ICAM-1 and VCAM-1 protein levels was accompanied by a decrease in their respective mRNA levels. Pre-incubation of HCAECs with discoidal (A-I)rHDLs at a final apoA-I concentration of 32 μM inhibited ICAM-1 (**Figure 4C**) and VCAM-1 mRNA levels (**Figure 4D**) by 76 ± 3% and 69 ± 12% respectively ($p < 0.001$ for both compared with TNF-α-stimulated HCAECs). Pre-incubation of HCAECs with discoidal (A-IV)rHDLs at a final apoA-IV concentration of 5 or 10 μM decreased ICAM-1 mRNA levels by 44 ± 8% and 50 ± 8%, respectively (**Figure 4C**, $p < 0.001$ for both compared with TNF-α-activated HCAECs), while VCAM-1 mRNA levels were decreased by 68 ± 9% and 55 ± 7%, respectively (**Figure 4C**) ($p < 0.001$ for both). These results are consistent with rHDLs that contain apoA-IV being more effective on a per particle basis than (A-I)rHDLs at inhibiting ICAM-1 and VCAM-1 mRNA levels and transcription in TNF-α-activated HCAECs.

Pre-incubation of HCAECs with discoidal (A-I)rHDLs (final apoA-I concentration 32 μM) prior to stimulation with TNF-α also increased DHCR24 mRNA levels by 196 ± 68% (**Figure 4E**, $p < 0.05$). This is consistent with what has been reported previously (5). Similarly, pre-incubation of TNF-α-stimulated HCAECs with discoidal (A-IV)rHDLs at final

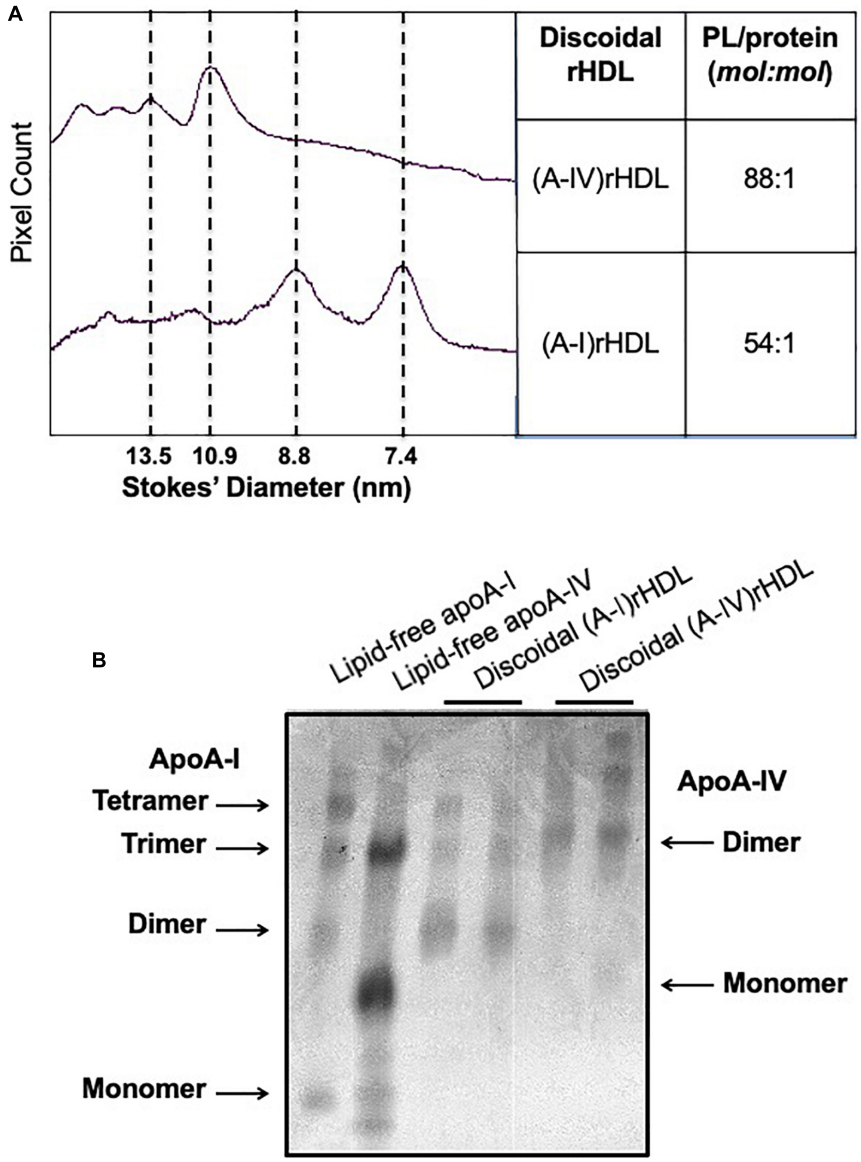

FIGURE 3 | Size and composition of discoidal (A-IV)rHDLs and discoidal (A-I)rHDLs. Discoidal (A-IV)rHDLs and (A-I)rHDLs were prepared by the cholate dialysis method and analysed in terms of size and composition [Panel **(A)**]. The discoidal rHDLs were then cross-linked with BS and their migration was compared with that of cross-linked lipid-free apoA-I and apoA-IV [Panel **(B)**].

apoA-IV concentrations of 5 or 10 μM increased DHCR24 mRNA levels by 244 ± 30% and 257 ± 44%, respectively (**Figure 4E**, $p < 0.001$ for both).

(A-IV)rHDLs Inhibit Nuclear Factor-kappaB Activation in Human Coronary Artery Endothelial Cells

To ascertain if (A-IV)rHDLs inhibit ICAM-1 and VCAM-1 expression in HCAECs *via* the canonical NF-κB pathway, nuclear p65, as well as cytoplasmic levels of total and phosphorylated IκBα were quantified in TNF-α-activated HCAECs. Incubation with TNF-α increased HCAEC nuclear p65 levels (**Figures 5A,B**). Pre-incubation of the cells with discoidal (A-I)rHDLs (final apoA-I concentration 32 μM) prior to stimulation with TNF-α, reduced nuclear p65 protein levels by 34 ± 6% compared to cells incubated with TNF-α alone (**Figures 5A,B**), ($p < 0.001$). Pre-incubation of TNF-α-stimulated HCAECs with discoidal (A-IV)rHDLs at final apoA-IV concentrations of 5 or 10 μM inhibited nuclear p65 levels by 33 ± 8% ($p < 0.01$) and 56 ± 6% ($p < 0.001$), respectively, compared to cells incubated with TNF-α alone) (**Figures 5A,B**). Cytoplasmic p65 levels were not affected by pre-incubation with discoidal (A-I)rHDLs or discoidal (A-IV)rHDLs, or by incubation with TNF-α (**Figures 5C,D**).

Incubation with TNF-α markedly increased the phosphorylated IκBα/total IκBα ratio in HCAECs (**Figures 5D,E**).

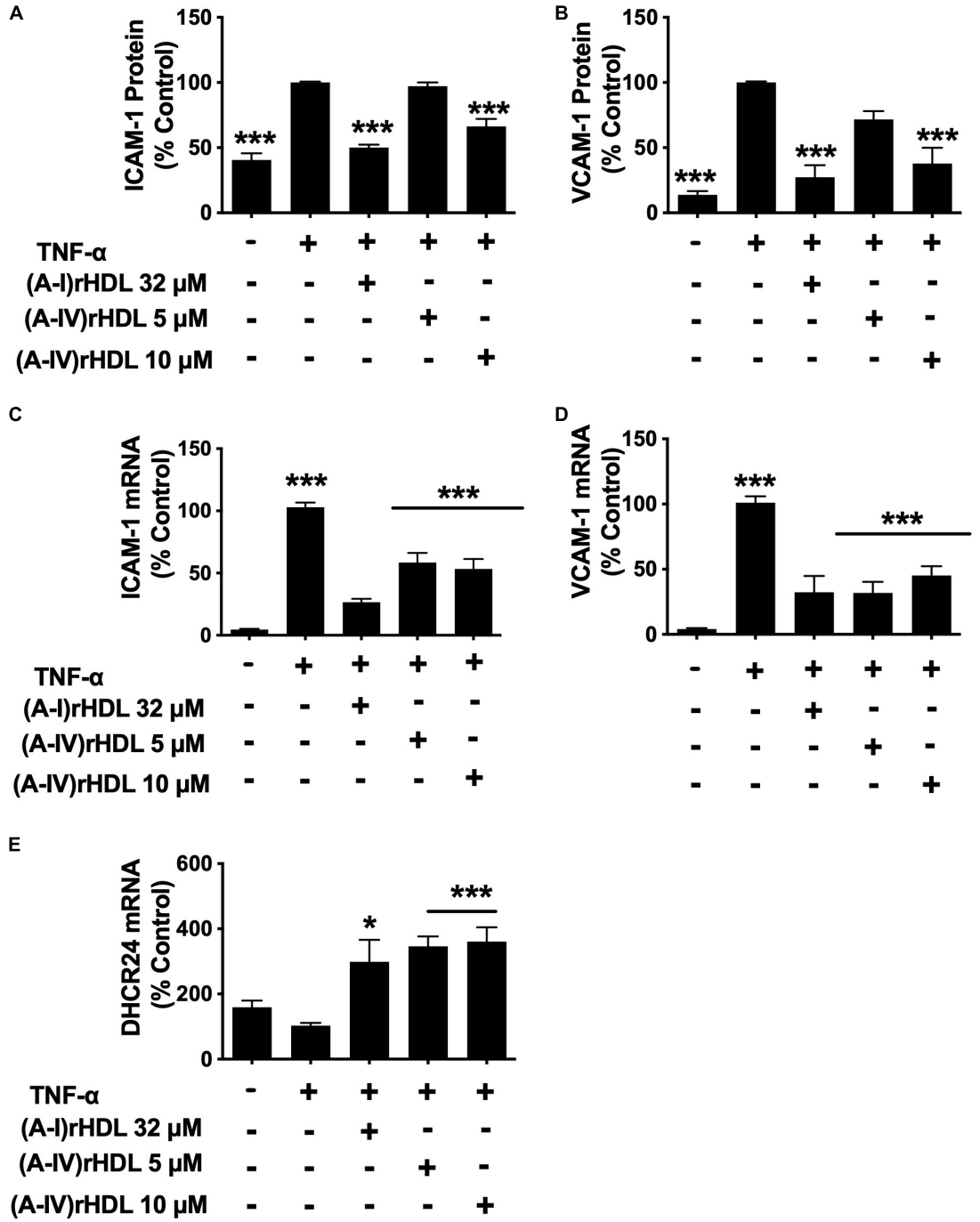

FIGURE 4 | (A-IV)rHDLs inhibit ICAM-1, VCAM-1 expression and increase DHCR24 expression in TNF-α-stimulated HCAECs. HCAECs were incubated for 16 h with (A-I)rHDLs (final apoA-I concentration 32 μM) and (A-IV)rHDLs (final apoA-IV concentrations 5 and 10 μM). The rHDLs were then removed and the cells were incubated for a further 5 h with TNF-α (final concentration 0.2 ng/mL). ICAM-1 [Panel **(A)**] and VCAM-1 [Panel **(B)**] protein expression was quantified by flow cytometry. ICAM-1 [Panel **(C)**], VCAM-1 [Panel **(D)**], and DHCR24 [Panel **(E)**] mRNA levels were quantified by qPCR. The mean ± SEM of three independent experiments, each performed in triplicate are shown. $^{*}p < 0.05$, $^{***}p < 0.005$.

Pre-incubation of HCAECs with (A-I)rHDLs prior to TNF-α-stimulation reduced the phosphorylated IκBα/total IκBα ratio by 38.1 ± 1.3% (**Figures 5D,E**, $p < 0.001$). This is consistent with what has been reported previously (4). Pre-incubation of TNF-α-stimulated HCAECs with discoidal (A-IV)rHDLs at final concentrations of 5 or 10 μM reduced the phosphorylated IκBα/total IκBα ratio by 45.0 ± 5.0% and 75.7 ± 2.4%, respectively (**Figures 5D,E**) ($p < 0.001$ for both). Taken together,

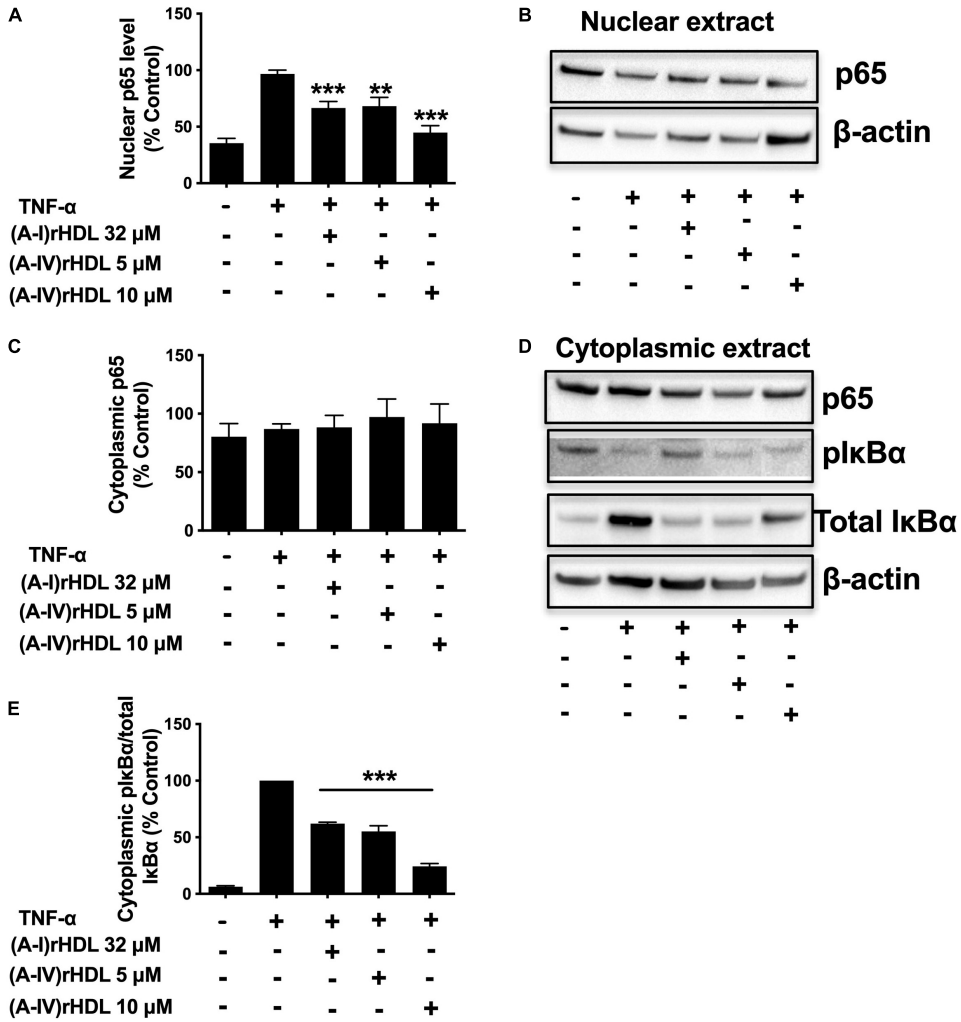

FIGURE 5 | (A-IV)rHDL inhibits NF-κB activation in TNF-α-stimulated HCAECs. HCAECs were incubated for 16 h at 37°C with (A-I)rHDLs (final apoA-I concentration 32 μM) or (A-IV)rHDLs (final A-IV concentration 5 and 10 μM). The rHDLs were removed and the cells were incubated for 20 min at 37°C with TNF-α (0.2 ng/mL). Nuclear extracts were isolated and subjected to immunoblotting using β-actin as a loading control. Nuclear p65 protein levels **(A,B)** and cytoplasmic levels of p65 and phosphorylated IκBα (pIκBα), **(C,D)** are shown. **(E)** Shows the ratio of cytoplasmic pIκBα/IκBα. Results represent mean ± SEM of three independent experiments, each performed in triplicate. $^{**}p < 0.01$, $^{***}p < 0.001$.

these results indicate that discoidal (A-IV)rHDLs decrease cytokine-induced inflammation in HCAECs by inhibiting NF-κB activation.

(A-IV)rHDLs Inhibit Intercellular Adhesion Molecule 1 and Vascular Cell Adhesion Molecule 1 Expression in Tumour Necrosis Factor Alpha Stimulated Human Coronary Artery Endothelial Cells in a 3β-Hydroxysteroid-Δ24 Reductase -Dependent Manner

Transfection of HCAECs with DHCR24 siRNA reduced DHCR24 protein and mRNA levels by 45 ± 4 ($p < 0.01$) and 93 ± 6%, respectively, relative to HCAECs transfected with scrambled siRNA (**Figure 6A**).

Incubation of the scrambled, siRNA-transfected HCAECs with TNF-α significantly increased ICAM-1 protein expression (**Figure 6B**, open bars) ($p < 0.001$). Pre-incubation of the scrambled, siRNA-transfected HCAECs with discoidal (A-I)rHDLs (final apoA-I concentration 32 μM) or discoidal (A-IV)rHDLs (final apoA-IV concentration 10 μM), prior to stimulation with TNF-α, inhibited the cytokine-induced increase in ICAM-1 expression by 26 ± 9% ($p < 0.05$) and 26 ± 4% ($p < 0.01$), respectively (**Figure 6B**, open bars). ICAM-1 expression was not inhibited in HCAECs that were transfected with DHCR24 siRNA and pre-incubated with discoidal (A-IV)rHDLs or discoidal (A-I)rHDLs prior to stimulation with TNF-α (**Figure 6B**, closed bars).

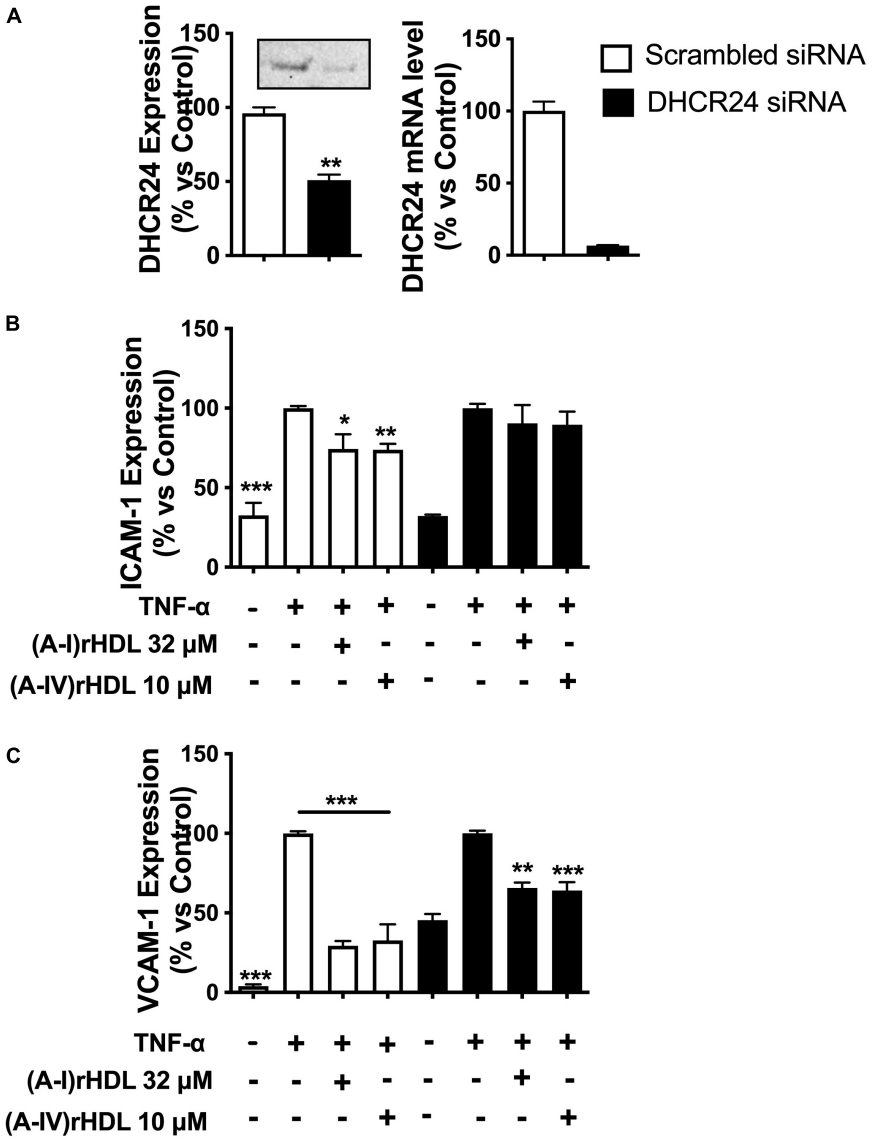

FIGURE 6 | (A-IV)rHDLs inhibit TNF-α-induced ICAM-1 and VCAM-1 expression in HCAECs in a DHCR24-dependent manner. HCAECs were transfected with DHCR24 or scrambled siRNA then pre-incubated at 37°C for 16 h with (A-I)rHDLs (final apoA-I concentration 32 μM) or (A-IV)rHDLs (final apoA-IV concentration 10 μM). The rHDLs were removed and the cells were stimulated for 5 h with TNF-α (final concentration 0.2 ng/mL). The reduction in DHCR24 protein and mRNA levels in the transfected HCAECs was quantified by Western blotting and qPCR [Panel **(A)**]. ICAM-1 [Panel **(B)**] and VCAM-1 [Panel **(C)**] protein levels were quantified in the TNF-α-activated HCAECs by flow cytometry. Results represent the mean ± SEM of three independent experiments, each performed in triplicate. $^{*}p < 0.05$, $^{**}p < 0.01$, $^{***}p < 0.001$ vs. TNF-α-stimulated cells.

Pre-incubation of scrambled siRNA-transfected-HCAECs with discoidal (A-I)rHDLs and discoidal (A-IV)rHDLs prior to stimulation with TNF-α inhibited the cytokine-induced increase in VCAM-1 expression by 71 ± 3% (**Figure 6C**, open bars) and 67 ± 10% (**Figure 6C**, open bars), respectively ($p < 0.001$ for both compared with TNF-α-stimulated cells). For HCAECs that were transfected with DHCR24 siRNA, and pre-incubated with (A-I)rHDLs prior to activation with TNF-α, the cytokine-induced increase in VCAM-1 expression was inhibited by 34 ± 3% (**Figure 6C**, $p < 0.01$), and by 36 ± 5% for the cells that were pre-incubated with (A-IV)rHDLs (**Figure 6C**, $p < 0.001$).

DISCUSSION

This study shows for the first time that apoA-IV is a more effective inhibitor of acute vascular inflammation in NZW rabbits than apoA-I. This is demonstrated by the ability of a single 1 mg/kg (2×10^{-8} mol/kg) iv injection of apoA-IV to reduce collar-induced neutrophil infiltration into the carotid artery, inhibit endothelial expression of ICAM-1 and VCAM-1 and increase expression of the anti-apoptotic and antioxidant enzyme, DHCR24, in NZW rabbits to a comparable extent as a single 8 mg/kg (28×10^{-8} mol/kg) iv injection of apoA-I

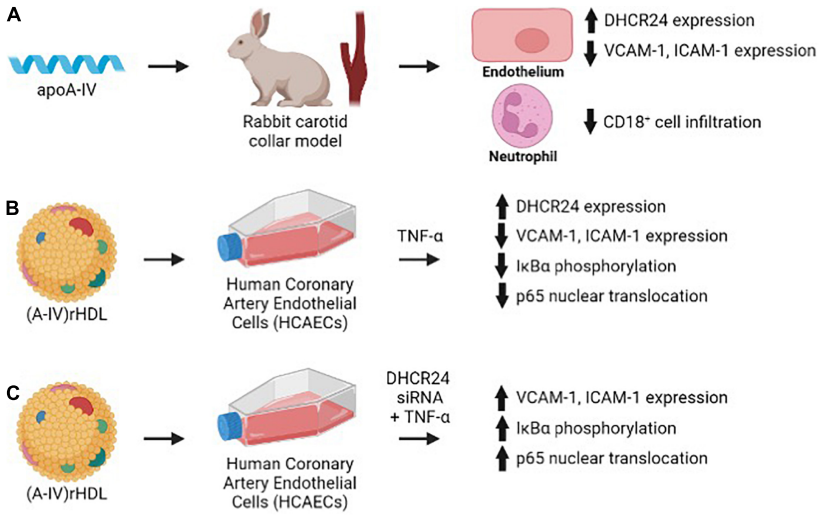

FIGURE 7 | Lipid-free and lipid-associated apoA-IV reduces acute vascular inflammation by inhibiting endothelial ICAM-1 and VCAM-1 expression **(A,B)** and NF-κB activation in a DHCR24-dependent manner **(C)**.

(**Figure 7A**) (2). The results also establish that discoidal (A-IV)rHDLs reduce ICAM-1 and VCAM-1 expression in TNF-α-activated HCAECs by inhibiting NF-κB activation in a DHCR24-dependent manner (**Figures 7B,C**).

These outcomes extend previous studies in which lipid-free apoA-IV reduced inflammation in a mouse model of colitis, inhibited histamine release from basophils in patients with allergic rhinitis and reduced TNF-α secretion from human monocytes following stimulation with lipopolysaccharide (20, 23, 41). Importantly, apoA-I was unable to recapitulate the anti-inflammatory properties of apoA-IV in any of these studies (20, 23, 41), thus identifying apoA-IV as a unique, anti-inflammatory agent with therapeutic potential.

As the HDLs that were isolated from apoA-IV-treated NZW rabbits did not inhibit cell surface ICAM-1 or VCAM-1 expression in TNF-α-activated HCAECs to a greater extent than what was observed for saline-infused NZW rabbits, the anti-inflammatory properties of apoA-IV cannot be explained in terms of improved HDL function. However, it is possible that the anti-inflammatory properties of the endogenous HDLs were improved immediately post-infusion, but that this was no longer evident at 48 h post-infusion, when the animals were euthanised prior to isolation of HDLs. This is consistent with what we have reported previously, where there was a transient improvement in the anti-inflammatory properties of HDLs isolated from rabbits at 5 min, but not at 6 h, after a single infusion of apoA-I (39). It is also possible that the association of apoA-IV with endogenous rabbit HDLs was disrupted during the ultracentrifugal isolation process, such that the isolated HDLs from the apoA-IV-treated rabbits were not selectively enriched with this apolipoprotein.

The lack of a sustained effect of apoA-IV on HDL function is further supported by the fact that turnover of this apolipoprotein in human plasma is 8.7 mg/kg/day (42), and is likely to be considerably faster than that in NZW rabbits. Given that the animals weighed 2–3 kg and apoA-IV was administered at a dose of 1 mg/kg, it follows that the amount of human apoA-IV remaining in the plasma compartment of these animals after 48 h was most likely minimal.

Structural differences between apoA-IV and apoA-I may have contributed to the superior *in vivo* anti-inflammatory properties of apoA-IV. Both apoA-IV and apoA-I contain 22 amino acid amphipathic α-helical repeats that are disrupted by conserved proline residues (43). Both apolipoproteins also contain Class Y and atypical Class A α-helices (43). However, the class Y α-helices that predominate in apoA-IV, and may contribute to its low affinity for lipid relative to apoA-I, favour partitioning into cell membranes at the level of the phospholipid head groups, rather than the phospholipid acyl chains, which is where apoA-I is located (43, 44). As studies of apoA-I mimetic peptides have indicated that their anti-inflammatory properties are enhanced by association with cell membrane phospholipid headgroups rather than acyl chains, it follows that differential partitioning may have contributed to the enhanced anti-inflammatory properties of apoA-IV relative to those of apoA-I (45–47).

One of the main aims of this study was to obtain an insight into the mechanism by which apoA-IV inhibits vascular inflammation. As lipid-free apoA-I and (A-I)rHDLs decrease expression of ICAM-1 and VCAM-1 by inhibiting NF-κB activation in a DHCR24-dependent manner (5, 39), this pathway was investigated in the current study. This was achieved be evaluating the ability of (A-IV)rHDLs to reduce the activity of IκB kinase, reduce the ratio of phosphorylated IκBα to total IκBα, and reduce nuclear localisation of the p65 subunit of NF-κB (4, 5, 48, 49).

The results of these *in vitro* studies confirmed that (A-IV)rHDLs inhibit all of these steps in the NF-κB pathway, and additionally increase expression of the anti-oxidant and

anti-apoptotic enzyme DHCR24. Interestingly apoA-IV, both in a lipid-free form *in vivo* and as a constituent of discoidal (A-IV)rHDLs *in vitro*, increased DHCR24 protein and mRNA levels at much lower concentrations than apoA-I. However, the ability of apoA-IV to inhibit VCAM-1, but not ICAM-1, *in vitro* was only partly dependent on DHCR24. This suggests that pathways other than inhibition of NF-κB must also contribute to the anti-inflammatory properties of discoidal (A-IV)rHDLs.

An alternate pathway by which discoidal (A-IV)rHDLs may inhibit inflammation in endothelial cells is *via* interaction with scavenger receptor class B type 1 (SR-B1). Discoidal (A-I)rHDLs have been reported to interact with SR-B1 and the SR-B1 adaptor protein, PDZK1, to increase DHCR24 expression and induce the cytoprotective protein, heme-oxygenase 1 (37). As lipid-free apoA-IV and discoidal (A-IV)rHDLs both interact with SR-B1 (10), it is possible that they may inhibit inflammation in endothelial cells *via* this pathway.

Another explanation for the anti-inflammatory properties of (A-IV)HDLs may be related to their ability to increase bioavailability of the vasodilator nitric oxide (NO) in endothelial cells. This possibility is related to the observation that inhibition of NO production is associated with upregulation of endothelial monocyte chemoattractant protein-1 (MCP-1) and VCAM-1 expression *via* the NF-κB pathway (50, 51). ApoA-IV-containing HDLs may therefore protect against these adverse effects by inhibiting MCP-1 and VCAM-1 expression as well as activation of NF-κB, Other mechanisms whereby (A-IV)HDLs may reduce NO bioavailability involve inhibition of the acute phase response and inhibition of oxidised LDL formation, which also reduces NO bioavailability (52–54).

It is additionally conceivable that lipid-free and lipid-associated apoA-IV have endogenous anti-oxidant properties that reduce endothelial expression of ICAM-1 and VCAM-1 (18, 19, 55, 56). This possibility is based on the observation that TNF-α generates reactive oxygen species (ROS) and upregulates ICAM-1 and VCAM-1 expression in endothelial cells (57–59) and that HDLs protect against glucose induced ROS generation in endothelial cells (60). However, whether HDLs, and apoA-IV in particular, inhibit TNF-α induced ROS endothelial production is unknown and clearly worthy of further investigation.

In conclusion, this study demonstrates for the first time that apoA-IV potently inhibits vascular inflammation *in vivo* and *in vitro* and that the mechanistic basis of this effect is driven by inhibition of NF-κB activity and upregulation of the anti-oxidant and anti-apoptotic enzyme DHCR24. One of the most important observations to emerge from this study is that very low concentrations of apoA-IV are profoundly anti-inflammatory *in vivo*. While this finding identifies apoA-IV as being of potential therapeutic interest, the full-length apolipoprotein is unlikely to be a viable treatment option for inflammatory disorders. Future studies mapping the domains of apoA-IV that are responsible for its anti-inflammatory effects could, however, be further progressed, leading to the production of peptides that mimic this function and are potentially of considerable therapeutic value.

AUTHOR CONTRIBUTIONS

KS, K-AR, and JT designed the study and interpreted the results. KS and JT performed the experiments. KS, K-AR, and BC prepared and edited the manuscript. All authors contributed to the article and approved the submitted version.

FUNDING

This work was supported by the National Health and Medical Research Council of Australia Grant (APPP482800).

SUPPLEMENTARY MATERIAL

The Supplementary Material for this article can be found online at: https://www.frontiersin.org/articles/10.3389/fcvm.2022.901408/full#supplementary-material

REFERENCES

1. Nicholls SJ, Dusting GJ, Cutri B, Bao S, Drummond GR, Rye KA, et al. Reconstituted high-density lipoproteins inhibit the acute pro-oxidant and proinflammatory vascular changes induced by a periarterial collar in normocholesterolemic rabbits. *Circulation.* (2005) 111:1543–50. doi: 10.1161/01.CIR.0000159351.95399.50
2. Puranik R, Bao S, Nobecourt E, Nicholls SJ, Dusting GJ, Barter PJ, et al. Low dose apolipoprotein A-I rescues carotid arteries from inflammation in vivo. *Atherosclerosis.* (2008) 196:240–7. doi: 10.1016/j.atherosclerosis.2007.05.008
3. Cockerill GW, Rye KA, Gamble JR, Vadas MA, Barter PJ. High-density lipoproteins inhibit cytokine-induced expression of endothelial cell adhesion molecules. *Arterioscler Thromb Vasc Biol.* (1995) 15:1987–94. doi: 10.1161/01.ATV.15.11.1987
4. Bursill CA, Castro ML, Beattie DT, Nakhla S, van der Vorst E, Heather AK, et al. High-density lipoproteins suppress chemokines and chemokine receptors in vitro and in vivo. *Arterioscler Thromb Vasc Biol.* (2010) 30:1773–8. doi: 10.1161/ATVBAHA.110.211342
5. McGrath KC, Li XH, Puranik R, Liong EC, Tan JT, Dy VM, et al. Role of 3beta-hydroxysteroid-delta 24 reductase in mediating antiinflammatory effects of high-density lipoproteins in endothelial cells. *Arterioscler Thromb Vasc Biol.* (2009) 29:877–82. doi: 10.1161/ATVBAHA.109.184663
6. Sultana A, Cochran BJ, Tabet F, Patel M, Torres LC, Barter PJ, et al. Inhibition of inflammatory signaling pathways in 3T3-L1 adipocytes by apolipoprotein A-I. *FASEB J.* (2016) 30:2324–35. doi: 10.1096/fj.201500026R
7. Li J, Song M, Qian D, Lu W, Wang J, Jiang G, et al. Decreased plasma apolipoprotein A-IV levels in patients with acute coronary syndrome. *Clin Invest Med.* (2013) 36:E207. doi: 10.25011/cim.v36i4.19954
8. Stein O, Stein Y, Lefevre M, Roheim PS. The role of apolipoprotein A-IV in reverse cholesterol transport studied with cultured cells and liposomes derived from an ether analog of phosphatidylcholine. *Biochim Biophys Acta.* (1986) 878:7–13. doi: 10.1016/0005-2760(86)90337-1
9. Okuda LS, Iborra RT, Pinto PR, Machado UF, Correa-Giannella ML, Pickford R, et al. Advanced glycated apoA-IV loses its ability to prevent the lps-induced reduction in cholesterol efflux-related gene expression in macrophages. *Mediators Inflamm.* (2020) 2020:6515401. doi: 10.1155/2020/6515401
10. Duka A, Fotakis P, Georgiadou D, Kateifides A, Tzavlaki K, von Eckardstein L, et al. ApoA-IV promotes the biogenesis of apoA-IV-containing HDL particles with the participation of ABCA1 and LCAT. *J Lipid Res.* (2013) 54:107–15. doi: 10.1194/jlr.M030114

11. Geronimo FRB, Barter PJ, Rye KA, Heather AK, Shearston KD, Rodgers KJ. Plaque stabilizing effects of apolipoprotein A-IV. *Atherosclerosis.* (2016) 251:39–46. doi: 10.1016/j.atherosclerosis.2016.04.019
12. Tso P, Chen Q, Fujimoto K, Fukagawa K, Sakata T. Apolipoprotein A-IV: a circulating satiety signal produced by the small intestine. *Obes Res.* (1995) 5:689S–95S. doi: 10.1002/j.1550-8528.1995.tb00487.x
13. Pence S, LaRussa Z, Shen Z, Liu M, Coschigano KT, Shi H, et al. Central apolipoprotein A-IV stimulates thermogenesis in brown adipose tissue. *Int J Mol Sci.* (2021) 22:1221. doi: 10.3390/ijms22031221
14. Shen L, Lo CC, Woollett LA, Liu M. Apolipoprotein A-IV exerts its anorectic action through a PI3K/Akt signaling pathway in the hypothalamus. *Biochem Biophys Res Commun.* (2017) 494:152–7. doi: 10.1016/j.bbrc.2017.10.063
15. Wang F, Kohan AB, Kindel TL, Corbin KL, Nunemaker CS, Obici S, et al. Apolipoprotein A-IV improves glucose homeostasis by enhancing insulin secretion. *Proc Natl Acad Sci USA.* (2012) 109:9641–6. doi: 10.1073/pnas.1201433109
16. Li X, Wang F, Xu M, Howles P, Tso P. ApoA-IV improves insulin sensitivity and glucose uptake in mouse adipocytes via PI3K-Akt signaling. *Sci Rep.* (2017) 7:41289. doi: 10.1038/srep41289
17. Wang F, Yang Q, Huesman S, Xu M, Li X, Lou D, et al. The role of apolipoprotein A-IV in regulating glucagon-like peptide-1 secretion. *Am J Physiol Gastrointest Liver Physiol.* (2015) 309:G680–7. doi: 10.1152/ajpgi.00075.2015
18. Ferretti G, Bacchetti T, Bicchiega V, Curatola G. Effect of human Apo AIV against lipid peroxidation of very low density lipoproteins. *Chem Phys Lipids.* (2002) 114:45–54. doi: 10.1016/S0009-3084(01)00201-8
19. Ostos MA, Conconi M, Vergnes L, Baroukh N, Ribalta J, Girona J, et al. Antioxidative and antiatherosclerotic effects of human apolipoprotein A-IV in apolipoprotein E-deficient mice. *Arterioscler Thromb Vasc Biol.* (2001) 21:1023–8. doi: 10.1161/01.ATV.21.6.1023
20. Recalde D, Ostos MA, Badell E, Garcia-Otin AL, Pidoux J, Castro G, et al. Human apolipoprotein A-IV reduces secretion of proinflammatory cytokines and atherosclerotic effects of a chronic infection mimicked by lipopolysaccharide. *Arterioscler Thromb Vasc Biol.* (2004) 24:756–61. doi: 10.1161/01.ATV.0000119353.03690.22
21. Spaulding HL, Saijo F, Turnage RH, Alexander JS, Aw TY, Kalogeris TJ. Apolipoprotein A-IV attenuates oxidant-induced apoptosis in mitotic competent, undifferentiated cells by modulating intracellular glutathione redox balance. *Am J Physiol Cell Physiol.* (2006) 290:C95–103. doi: 10.1152/ajpcell.00388.2005
22. Xu XR, Wang Y, Adili R, Ju L, Spring CM, Jin JW, et al. Apolipoprotein A-IV binds αIIbβ3 integrin and inhibits thrombosis. *Nat Commun.* (2018) 9:3608. doi: 10.1038/s41467-018-05806-0
23. Vowinkel T, Mori M, Krieglstein CF, Russell J, Saijo F, Bharwani S, et al. Apolipoprotein A-IV inhibits experimental colitis. *J Clin Invest.* (2004) 114:260–9. doi: 10.1172/JCI200421233
24. Roula D, Theiler A, Luschnig P, Sturm GJ, Tomazic PV, Marsche G, et al. Apolipoprotein A-IV acts as an endogenous anti-inflammatory protein and is reduced in treatment-naive allergic patients and allergen-challenged mice. *Allergy.* (2020) 75:392–402. doi: 10.1111/all.14022
25. Schwaiger JP, Kollerits B, Steinbrenner I, Weissensteiner H, Schonherr S, Forer L, et al. Apolipoprotein A-IV concentrations and clinical outcomes in a large chronic kidney disease cohort: results from the GCKD study. *J Intern Med.* (2021) 291:622–36. doi: 10.1111/joim.13437
26. Osborne JC Jr. Delipidation of plasma lipoproteins. *Methods Enzymol.* (1986) 128:213–22. doi: 10.1016/0076-6879(86)28069-6
27. Rye KA. Interaction of apolipoprotein A-II with recombinant HDL containing egg phosphatidylcholine, unesterified cholesterol and apolipoprotein A-I. *Biochim Biophys Acta.* (1990) 1042:227–36. doi: 10.1016/0005-2760(90)90013-N
28. Weisweiler P. Isolation and quantitation of apolipoproteins A-I and A-II from human high-density lipoproteins by fast-protein liquid chromatography. *Clin Chim Acta.* (1987) 169:249–54. doi: 10.1016/0009-8981(87)90325-1
29. Matz CE, Jonas A. Micellar complexes of human apolipoprotein A-I with phosphatidylcholines and cholesterol prepared from cholate-lipid dispersions. *J Biol Chem.* (1982) 257:4535–40. doi: 10.1016/S0021-9258(18)34756-2
30. Rye KA. Interaction of the high density lipoprotein conversion factor with recombinant discoidal complexes of egg phosphatidylcholine, free cholesterol, and apolipoprotein A-I. *J Lipid Res.* (1989) 30:335–46. doi: 10.1016/S0022-2275(20)38362-0
31. Staros JV, Morgan DG, Appling DR. A membrane-impermeant, cleavable cross-linker. Dimers of human erythrocyte band 3 subunits cross-linked at the extracytoplasmic membrane face. *J Biol Chem.* (1981) 256:5890–3. doi: 10.1016/S0021-9258(19)69292-6
32. Kotite NJ, Staros JV, Cunningham LW. Interaction of specific platelet membrane proteins with collagen: evidence from chemical cross-linking. *Biochemistry.* (1984) 23:3099–104. doi: 10.1021/bi00308a038
33. Smith PK, Krohn RI, Hermanson GT, Mallia AK, Gartner FH, Provenzano MD, et al. Measurement of protein using bicinchoninic acid. *Anal Biochem.* (1985) 150:76–85. doi: 10.1016/0003-2697(85)90442-7
34. Takayama M, Itoh S, Nagasaki T, Tanimizu I. A new enzymatic method for determination of serum choline-containing phospholipids. *Clin Chim Acta.* (1977) 79:93–8. doi: 10.1016/0009-8981(77)90465-X
35. Stahler F, Gruber W, Stinshoff K, Roschlau P. A practical enzymatic cholesterol determination. *Med Lab.* (1977) 30:29–37.
36. Clay MA, Rye KA, Barter PJ. Evidence in vitro that hepatic lipase reduces the concentration of apolipoprotein A-I in rabbit high-density lipoproteins. *Biochim Biophys Acta.* (1990) 1044:50–6. doi: 10.1016/0005-2760(90)90217-L
37. Wu BJ, Chen K, Shrestha S, Ong KL, Barter PJ, Rye KA. High density lipoproteins inhibit vascular endothelial inflammation by increasing 3β-Hydroxysteroid-Δ24 reductase expression and inducing heme oxygenase-1. *Circ Res.* (2012) 112:278–88. doi: 10.1161/CIRCRESAHA.111.300104
38. Koike T, Kitajima S, Yu Y, Li Y, Nishijima K, Liu E, et al. Expression of human apoAII in transgenic rabbits leads to dyslipidemia: a new model for combined hyperlipidemia. *Arterioscler Thromb Vasc Biol.* (2009) 29:2047–53. doi: 10.1161/ATVBAHA.109.190264
39. Patel S, Di Bartolo BA, Nakhla S, Heather AK, Mitchell TW, Jessup W, et al. Anti-inflammatory effects of apolipoprotein A-I in the rabbit. *Atherosclerosis.* (2010) 212:392–7. doi: 10.1016/j.atherosclerosis.2010.05.035
40. Green PH, Glickman RM, Riley JW, Quinet E. Human apolipoprotein A-IV. Intestinal origin and distribution in plasma. *J Clin Invest.* (1980) 65:911–9. doi: 10.1172/JCI109745
41. Makino Y, Noguchi E, Takahashi N, Matsumoto Y, Kubo S, Yamada T, et al. Apolipoprotein A-IV is a candidate target molecule for the treatment of seasonal allergic rhinitis. *J Allergy Clin Immunol.* (2010) 116:e5. doi: 10.1016/j.jaci.2010.06.031
42. Ghiselli G, Krishnan S, Beigel Y, Gotto AM Jr. Plasma metabolism of apolipoprotein A-IV in humans. *J Lipid Res.* (1986) 27:813–27. doi: 10.1016/S0022-2275(20)38785-X
43. Segrest JP, Jones MK, De Loof H, Brouillette CG, Venkatachalapathi YV, Anantharamaiah GM. The amphipathic helix in the exchangeable apolipoproteins: a review of secondary structure and function. *J Lipid Res.* (1992) 33:141–66. doi: 10.1016/S0022-2275(20)41536-6
44. Saito H, Lund-Katz S, Phillips MC. Contributions of domain structure and lipid interaction to the functionality of exchangeable human apolipoproteins. *Prog Lipid Res.* (2004) 43:350–80. doi: 10.1016/j.plipres.2004.05.002
45. Navab M, Anantharamaiah GM, Reddy ST, Hama S, Hough G, Grijalva VR, et al. Apolipoprotein A-I mimetic peptides. *Arterioscler Thromb Vasc Biol.* (2005) 25:1325–31. doi: 10.1161/01.ATV.0000165694.39518.95
46. Anantharamaiah GM, Mishra VK, Garber DW, Datta G, Handattu SP, Palgunachari MN, et al. Structural requirements for antioxidative and anti-inflammatory properties of apolipoprotein A-I mimetic peptides. *J Lipid Res.* (2007) 48:1915–23. doi: 10.1194/jlr.R700010-JLR200
47. D'Souza W, Stonik JA, Murphy A, Demosky SJ, Sethi AA, Moore XL, et al. Structure/function relationships of apolipoprotein A-I mimetic peptides: implications for antiatherogenic activities of high-density lipoprotein. *Circ Res.* (2010) 107:217–27. doi: 10.1161/CIRCRESAHA.110.216507
48. Gareus R, Kotsaki E, Xanthoulea S, van der Made I, Gijbels MJ, Kardakaris R, et al. Endothelial cell-specific NF-kappaB inhibition protects mice from atherosclerosis. *Cell Metab.* (2008) 8:372–83. doi: 10.1016/j.cmet.2008.08.016
49. Schmidt A, Geigenmuller S, Volker W, Buddecke E. The antiatherogenic and antiinflammatory effect of HDL-associated lysosphingolipids operates via Akt –>NF-kappaB signalling pathways in human vascular endothelial cells. *Basic Res Cardiol.* (2006) 101:109–16. doi: 10.1007/s00395-005-0582-z

50. Zeiher AM, Fisslthaler B, Schray-Utz B, Busse R. Nitric oxide modulates the expression of monocyte chemoattractant protein 1 in cultured human endothelial cells. *Circ Res.* (1995) 76:980–6. doi: 10.1161/01.RES.76.6.980
51. De Caterina R, Libby P, Peng HB, Thannickal VJ, Rajavashisth TB, Gimbrone MA Jr., et al. Nitric oxide decreases cytokine-induced endothelial activation. Nitric oxide selectively reduces endothelial expression of adhesion molecules and proinflammatory cytokines. *J Clin Invest.* (1995) 96:60–8. doi: 10.1172/JCI118074
52. Andrews KL, Moore XL, Chin-Dusting JP. Anti-atherogenic effects of high-density lipoprotein on nitric oxide synthesis in the endothelium. *Clin Exp Pharmacol Physiol.* (2010) 37:736–42. doi: 10.1111/j.1440-1681.2010.05387.x
53. Uittenbogaard A, Shaul PW, Yuhanna IS, Blair A, Smart EJ. High density lipoprotein prevents oxidized low density lipoprotein-induced inhibition of endothelial nitric-oxide synthase localization and activation in caveolae. *J Biol Chem.* (2000) 275:11278–83. doi: 10.1074/jbc.275.15.11278
54. Witting PK, Song C, Hsu K, Hua S, Parry SN, Aran R, et al. The acute-phase protein serum amyloid A induces endothelial dysfunction that is inhibited by high-density lipoprotein. *Free Radic Biol Med.* (2011) 51:1390–8. doi: 10.1016/j.freeradbiomed.2011.06.031
55. Wong WM, Gerry AB, Putt W, Roberts JL, Weinberg RB, Humphries SE, et al. Common variants of apolipoprotein A-IV differ in their ability to inhibit low density lipoprotein oxidation. *Atherosclerosis.* (2007) 192:266–74. doi: 10.1016/j.atherosclerosis.2006.07.017
56. Qin X, Swertfeger DK, Zheng S, Hui DY, Tso P. Apolipoprotein AIV: a potent endogenous inhibitor of lipid oxidation. *Am J Physiol.* (1998) 274:H1836–40. doi: 10.1152/ajpheart.1998.274.5.H1836
57. Yoshida LS, Tsunawaki S. Expression of NADPH oxidases and enhanced H(2)O(2)-generating activity in human coronary artery endothelial cells upon induction with tumor necrosis factor-alpha. *Int Immunopharmacol.* (2008) 8:1377–85. doi: 10.1016/j.intimp.2008.05.004
58. Kim HJ, Park KG, Yoo EK, Kim YH, Kim YN, Kim HS, et al. Effects of PGC-1alpha on TNF-alpha-induced MCP-1 and VCAM-1 expression and NF-kappaB activation in human aortic smooth muscle and endothelial cells. *Antioxid Redox Signal.* (2007) 9:301–7. doi: 10.1089/ars.2006.1456
59. Liang CJ, Wang SH, Chen YH, Chang SS, Hwang TL, Leu YL, et al. Viscolin reduces VCAM-1 expression in TNF-alpha-treated endothelial cells via the JNK/NF-kappaB and ROS pathway. *Free Radic Biol Med.* (2011) 51:1337–46. doi: 10.1016/j.freeradbiomed.2011.06.023
60. Tabet F, Lambert G, Cuesta Torres LF, Hou L, Sotirchos I, Touyz RM, et al. Lipid-free apolipoprotein A-I and discoidal reconstituted high-density lipoproteins differentially inhibit glucose-induced oxidative stress in human macrophages. *Arterioscler Thromb Vasc Biol.* (2011) 31:1192–200. doi: 10.1161/ATVBAHA.110.222000

Conflict of Interest: The authors declare that the research was conducted in the absence of any commercial or financial relationships that could be construed as a potential conflict of interest.

Publisher's Note: All claims expressed in this article are solely those of the authors and do not necessarily represent those of their affiliated organizations, or those of the publisher, the editors and the reviewers. Any product that may be evaluated in this article, or claim that may be made by its manufacturer, is not guaranteed or endorsed by the publisher.

frontiers | Frontiers in Cardiovascular Medicine

METHODS
published: 14 July 2022
doi: 10.3389/fcvm.2022.926631

Using Synthetic ApoC-II Peptides and nAngptl4 Fragments to Measure Lipoprotein Lipase Activity in Radiometric and Fluorescent Assays

*Dean Oldham[1], Hong Wang[1], Juliet Mullen[2], Emma Lietzke[3], Kayla Sprenger[3], Philip Reigan[2], Robert H. Eckel[1] and Kimberley D. Bruce[1]**

[1] Division of Endocrinology, Metabolism and Diabetes, Department of Medicine, University of Colorado Anschutz Medical Campus, Aurora, CO, United States, [2] Department of Pharmaceutical Sciences, Skaggs School of Pharmacy and Pharmaceutical Sciences, University of Colorado Anschutz Medical Campus, Aurora, CO, United States, [3] Department of Chemical Engineering, University of Colorado Boulder, Boulder, CO, United States

OPEN ACCESS

Edited by:
Mary G. Sorci-Thomas, Medical College of Wisconsin, United States

Reviewed by:
Scott M. Gordon, University of Kentucky, United States
Robert Hegele, Western University, Canada
Werner J. Geldenhuys, West Virginia University, United States

***Correspondence:**
Kimberley D. Bruce
kimberley.bruce@cuanschutz.edu

Specialty section:
This article was submitted to Lipids in Cardiovascular Disease, a section of the journal Frontiers in Cardiovascular Medicine

Received: *22 April 2022*
Accepted: *16 June 2022*
Published: *14 July 2022*

Citation:
Oldham D, Wang H, Mullen J, Lietzke E, Sprenger K, Reigan P, Eckel RH and Bruce KD (2022) Using Synthetic ApoC-II Peptides and nAngptl4 Fragments to Measure Lipoprotein Lipase Activity in Radiometric and Fluorescent Assays. Front. Cardiovasc. Med. 9:926631. doi: 10.3389/fcvm.2022.926631

Lipoprotein lipase (LPL) plays a crucial role in preventing dyslipidemia by hydrolyzing triglycerides (TGs) in packaged lipoproteins. Since hypertriglyceridemia (HTG) is a major risk factor for cardiovascular disease (CVD), the leading cause of death worldwide, methods that accurately quantify the hydrolytic activity of LPL in clinical and pre-clinical samples are much needed. To date, the methods used to determine LPL activity vary considerably in their approach, in the LPL substrates used, and in the source of LPL activators and inhibitors used to quantify LPL-specific activity, rather than other lipases, e.g., hepatic lipase (HL) or endothelial lipase (EL) activity. Here, we describe methods recently optimized in our laboratory, using a synthetic ApoC-II peptide to activate LPL, and an n-terminal Angiopoietin-Like 4 fragment (nAngptl4) to inhibit LPL, presenting a cost-effective and reproducible method to measure LPL activity in human post-heparin plasma (PHP) and in LPL-enriched heparin released (HR) fractions from LPL secreting cells. We also describe a modified version of the triolein-based assay using human serum as a source of endogenous activators and inhibitors and to determine the relative abundance of circulating factors that regulate LPL activity. Finally, we describe how an ApoC-II peptide and nAngptl4 can be applied to high-throughput measurements of LPL activity using the EnzChek™ fluorescent TG analog substrate with PHP, bovine LPL, and HR LPL enriched fractions. In summary, this manuscript assesses the current methods of measuring LPL activity and makes new recommendations for measuring LPL-mediated hydrolysis in pre-clinical and clinical samples.

Keywords: lipoprotein lipase, hydrolysis, enzyme activity assay, lipase, microglia, post-heparin plasma

Abbreviations: Angptl4, Angiopoietin-Like 4; bLPL, bovine LPL; BSA, Bovine Serum Albumin; CVD, cardiovascular disease; CXN, calnexin; EL, endothelial lipase; ER, endoplasmic reticulum; fAngptl4, full-length Angptl4; FFA, free fatty acids; GPIHBP1, glycosylphosphatidylinositol-anchored high-density lipoprotein–binding protein 1; HDX-MS, Hydrogen Deuterium Exchange Mass Spectrometry; HL, hepatic lipase; HR, heparin release; HTG, hypertriglyceridemia; KRP, Krebs Ringer Phosphate; LMF1, lipase maturation factor; LPL, lipoprotein lipase; nAngptl4, N-terminal domain Angptl4; PC, proprotein convertase; PHP, post-heparin plasma; SorLA, sortilin-related receptor with type-A repeats; TG, triglyceride; TRL, TG-rich lipoproteins; VLDL, very-low density lipoproteins.

INTRODUCTION

Lipoprotein Lipase Function and Processing

Lipoprotein lipase (LPL) is a rate limiting enzyme in lipid and lipoprotein processing. LPL was initially described as "clearing factor" nearly 70 years ago, due to its ability to decrease the turbidity of lipid rich emulsions and hydrolyze neutral lipids in the presence of activating proteins (1–3). Since then, we have learned that LPL plays a critical role in lipoprotein processing throughout the body, which impacts the development of several cardiometabolic and neurodegenerative diseases. In its canonical role LPL serves as a secreted lipase that hydrolyzes triglycerides (TGs) from circulating TG-rich lipoproteins (TRLs) such as chylomicrons and very-low density lipoproteins (VLDL), making free fatty acids (FFAs) available to tissues for utilization or storage (4). Variations in the gene encoding LPL, and genes encoding factors that regulate LPL activity and processing, profoundly alter the efficiency of LPL-mediated TRL processing. The presence of such variants influences both plasma TG levels, the risk for coronary heart disease (5, 6), and the risk of Alzheimer's disease (7). Hence, methods that can accurately quantify both circulating LPL, and the activity and abundance of LPL in a range of tissues and cells are much needed to further understand LPL biology, and to develop LPL-targeted strategies that can ameliorate cardiometabolic and neurodegenerative disease.

The human LPL gene (synonyms include *LIPD* and *HDLCQ11*) is found on chromosome 8p21.3, and contains 10 exons and 11 introns, and encodes a 475 amino acid protein. LPL is secreted in an active and glycosylated from, but secretion is dependent on several critical steps that are facilitated by key molecular chaperones and binding partners. LPL is first synthesized as a proenzyme in the rough endoplasmic reticulum (ER), where it is later glycosylated and folded in the presence of calnexin (CXN) and lipase maturation factor 1 (LMF1) (8). A specific chaperone Sel1L stabilizes the LPL-LMF1 complex and facilitates trafficking to the Golgi apparatus (9). Active LPL then enters the Golgi, where sortilin-related receptor with type-A repeats (SorLA) chaperones LPL through further post-translational modifications, sorting, and secretion, where LPL is tethered to heparan sulfate-proteoglycans (HSPG) on the cell surface (10). In the capillary lumen LPL is also bound to the glycosylphosphatidylinositol-anchored high-density lipoprotein–binding protein 1 (GPIHBP1), which anchors and stabilizes the enzyme (11). The clinical significance of LPL-processing factors is highlighted by the fact that LMF1 and GPIHBP1 genetic variants are associated with compromised LPL function and severe hypertriglyceridemia (HTG) (12).

Lipoprotein Lipase Inhibition by Angiopoietin-Like 4

Once tethered to the cell surface or capillary lumen the activity of LPL is also dependent on the expression and availability of endogenous activators and inhibitors. For example, the Angiopoietin-Like proteins are a family of endogenous inhibitors of LPL, of which the Angiopoietin-Like 4 (Angptl4) is perhaps the best characterized. Native full-length Angptl4 (fAngptl4) is a fusion protein consisting of an N-terminal coiled-coil domain and a C-terminal fibrinogen-like domain (13) and is proteolytically cleaved by proprotein convertases (PCs) into its two isoforms with distinct functions. The N-terminal domain of Angptl4 (nAngptl4) inhibits LPL (14), whereas the C-terminus mediates antiangiogenic functions (15). Although fAngptl4 can inhibit LPL activity, proteolytic processing of fAngptl4 leads to nAngptl4 production and a greater effect on LPL activity and the ability to raise plasma TG levels (13), supporting the notion that nAngptl4 specifically inhibits LPL activity. Indeed, Angptl4-mediated inhibition of LPL activity is well established (16–20). Importantly, recent studies have shown that nAngptl4 specifically inhibits LPL activity by binding the lid domain and preventing substrate catalysis at the active site (21). For many years, the active form of LPL was thought to be a head-to-tail homodimer (22–24), and the prevailing model of Angptl4-mediated inactivation of LPL was the ability of Angptl4 to convert active LPL homodimers into readily unfolded and inactivated monomers (25). However, recent studies have shown that freshly secreted active LPL is found in a monomeric state, and that LPL-homodimer formation may be due to the presence of heparin, which is commonly used to purify or release LPL (26). In line with this paradigm shift, Angptl4 has since been shown to catalyze the unfolding of, and therefore inactivate, LPL monomers (20). Although more functional studies are needed to map the Angptl4 encounter site to LPL (20), recent Hydrogen Deuterium Exchange (HDX) Mass Spectrometry (HDX-MS) studies suggest that Angptl4 interacts with the lid (aa 89–102) and α-helix domain (aa 226–238) of LPL (21).

Lipoprotein Lipase Activation by ApoC-II

The LPL activator ApoC-II was initially discovered in 1970 as a protein bound to VLDL and was called glutamic acid (Glu) lipoprotein or ApoLP-Glu based on its C-terminus amino acid (27). A few years later, ApoC-II deficiency was identified as the first genetic cause of HTG (28). Since then, ApoC-II variants that lead to compromised LPL function have been associated with HTG, pancreatitis, familial chylomicronemia, and gestational HTG and pancreatitis (29–32). Investigations into the regulation of the human ApoC-II gene have shown that it resides within the *APOE-APOC1-APOC4-APOC-II* gene loci on Chromosome 19 and is subject to complex tissue specific transcriptional control (33). For example, macrophage specific expression of the *APOE-APOC1-APOC4-APOC-II* locus depends on the two 620-bp macrophage-specific multi-enhancer elements termed ME.1 and ME.2 upstream of the APOC-II promoter (33, 34). Both RXR and STAT1 transcriptionally activate ApoC-II and stimulate LPL expression resulting in increased local LPL activity (34, 35). After translation, cleavage of a 22 aa signal peptide results in a 79 aa full-length protein, which does not undergo N-linked or O-linked glycosylation (33). Based on the function of known ApoC-II variants, mutagenesis studies, and investigations using synthetic ApoC-II peptides, LPL activation is mediated by the C-terminal helix of ApoC-II (36, 37). Although the precise ApoC-II-LPL interaction is unknown, it is thought that residues 63, 66, 69, and 70 bind to the lid region of LPL to facilitate TG entry into its active

site (38, 39). However, considering the new crystal structures for LPL and new insights regarding the active monomeric forms of LPL, the interaction between ApoC-II and LPL, in addition to other the regulatory factors should be re-assessed.

Existing Methods to Measure Lipoprotein Lipase Activity

The standard of care for HTG involves lifestyle, dietary (e.g., polyunsaturated fatty acid supplementation) and pharmacological (e.g., statins) interventions (40). However, these approaches are not tailored to the underlying cause of HTG. Accurately quantifying the function and activity of LPL may guide the diagnosis of LPL deficiency to highlight individuals at risk of severe and life-threatening complications such as pancreatitis, and therefore need to be followed more closely (41). While western blot analyses or ELISAs can accurately determine the abundance of the LPL protein, this does not consider the presence or absence of activating (e.g., ApoC-II and ApoA-V), inhibiting (e.g., Angptl4, ApoC-I, and ApoC-III) factors, whether LPL has been unfolded, or is in an inactive state. Therefore, the presence of the protein itself does not necessarily indicate activity. Historically, radiometric assays using ^{3}H or ^{14}C labeled triolein have been used to determine lipase activity in post-heparin plasma (PHP) (42, 43). These assays have been instrumental in furthering our understanding of LPL biology, however, the separation of hydrolyzed fatty acids from non-hydrolyzed trioleyl glycerol can be time consuming, low-throughput and the use of radiation is associated with health and environmental risks (44). Perhaps a greater concern, is that PHP also contains other enzymes capable of TG-hydrolysis, which could interfere with the data analysis and interpretation of radiometric lipase assays (45). Several strategies have been employed that aim to measure LPL-specific activity rather than the activity of other lipases. For example, LPL activity is very responsive to salt concentrations and high-salt conditions can inhibit LPL activity. However, high salt can also increase hepatic lipase (HL) activity; manipulating salt concentrations alone does not accurately determine LPL-specific activity (46). Therefore, assays which use LPL-specific inhibitors and activators is a more suitable approach. Here, we describe a radiometric assay to measure LPL-specific enzyme activity in PHP using a C-terminal peptide of ApoC-II, which we propose binds directly to LPL. This is a relevant admission to the protocol since this peptide is not subject to the variability associated with isolating human VLDL or serum to use as an LPL activator. In addition, in our assay we use an N-terminal peptide of the recombinant nAngptl4 protein to measure LPL activity in the presence and absence of nAngptl4, allowing us to calculate Angptl4-sensitive lipase activity, and therefore LPL-mediated hydrolysis.

Measuring LPL activity in PHP is needed to determine whether a patient or sample has compromised LPL function leading to HTG and its co-morbidities. However, we are increasingly aware that lesser degrees of HTG may result from genetic variants in one of many molecular factors that regulate LPL-mediated lipoprotein metabolism, rather than variations in the LPL gene/protein itself (29, 47–50). Hence, we have developed a modified form of the triolein-based assay that uses a patient's preheparin serum (henceforth referred to as just serum) as an activator/inhibitor for a standardized source of LPL. For example, determining whether a patient's serum can decrease the activity of LPL, compared to a control sample, indicates whether endogenous LPL-regulating factors are altered rather LPL being directly compromised. Although this assay does not discriminate which activator or inhibitor is affecting LPL function, it is a relatively time-efficient first-step experiment to determine that LPL regulating factors, rather than LPL, are contributing to HTG. While not the standard-of-care to date, this may guide a patient's clinical support toward emerging strategies that specifically target LPL regulating factors, such as Angptl4 (51), ApoC-II, and ApoC-III (52, 53). Indeed, this methodology may be particularly useful for assessing lipase activity in subjects that have received treatments that specifically target ApoC-II and ApoC-III, rather than LPL (52, 53). Moreover, this experiment does not require the somewhat invasive administration of a heparin bolus to the patient and retrieval of PHP.

The PHP and serum activation/inhibition protocols described here are validated radiometric assays that allow accurate measurement of LPL activity using physiologically relevant lipid substrates, which can be tailored to answer the specific research question at hand. However, as described previously these assays are laborious, fairly low-throughput, and require the use of radiation and dedicated equipment. Therefore, for drug development studies or studies with large numbers of biological pre-clinical samples, a higher-throughput and time efficient process is needed. Therefore, here we also describe a modified fluorescent assay using a commercially available fluorogenic TG-analog, the EnzChek^{TM} lipase substrate (54), where we also include both ApoC-II and nAngptl4 to determine LPL-specific activity. Although this has previously been demonstrated (54), here for the first time to our knowledge we also show how the EnzChek^{TM} lipase substrate can be used to quantify LPL activity in PHP and heparin released (HR) fractions from cell types known to express and secrete LPL (BV-2 microglia). In summary, here we will provide detailed descriptions of optimized assays to determine; 1. radiometric detection of LPL activity using ApoC-II, nAngptl4 and a triolein substrate; 2. serum activation/inhibition of LPL; and 3. fluorescence detection of LPL activity using the EnzChek^{TM} substrate. We will also make recommendations for assay selection and study design throughout, as well as highlighting caveats for each assay that may guide protocol selection for a given research question.

MATERIALS AND EQUIPMENT

Radiometric Detection of Lipoprotein Lipase Activity Using Triolein, ApoC-II and Angiopoietin-Like 4

Reagents

- 1,α-phosphatidylcholine (lecithin), Sigma P3556
- ^{3}H-triolein, Perkin Elmer NET431001MC (1 mCi/mL, Specific activity: 41.6 Ci/mmol)

- ^{3}H-oleic acid, Perkin Elmer NET289001MC (1 mCi/mL, Specific activity 54.6 Ci/mmol)
- Glycerol Trioleate, Sigma T7140 (500 mg)
- SCINTISAFE 30% (Fisher Scientific SX235)
- Untagged ApoC-II peptide (Genscript; Sequence: STAAMSTYTGIFTDQVLSVLKGE; untagged)
- Molecular biology grade H_2O (Corning, 46-000-CV)
- Recombinant Human Angiopoietin-Like 4 N-Terminal Frag (R&D systems, 8249-AN-050), reconstituted in molecular biology grade H_2O to a final concentration of 200 μg/mL
- Source of LPL [bLPL (Sigma, L2254), PHP, HR source of LPL from cells or tissues].

Buffers/Solutions

- Working solution of Glycerol Trioleate. Add 10 mL chloroform to yield a solution of 50 mg/mL.
- 5 M NaCl
- Tris Buffer, 2 M pH = 8.2
- 10% (FFA free) Bovine Serum Albumin (BSA) in dH_2O, (Sigma, A-6003)
- For 50 mL no salt Krebs Ringer Phosphate (KRP) Buffer (Adjust to pH 7.4, sterile filter) (store at 4°C), 3.2 mL (1.15% KCl) (10 mM), 0.5 mL (1.52% $CaCl_2{\cdot}2H_2O$) (1 mM), 0.16 mL (3.82% $MgSO_4{\cdot}7H_2O$) (1 mM), 1 mL (Phosphate Buffer, 14.2 g Na_2HPO_4 + 20 mL 1 N HCl, dilute up to 1 L with dH_2O, Adjust to pH 7.4) (2 mM Na_2HPO_4). This KRP buffer can be used to add salt to the desired concentration. We recommend (0.175 M) for optimal LPL activity.
- 100 and 1 μg/mL in 0.9% saline (Fisher Scientific, #H-19)
- Belfrage Extraction Mix (store at RT), Chloroform (683.0 mL) 34%, Methanol (770.5 mL) 39%, Heptane (546.5 mL) 27%, Bicarbonate Buffer (store at RT), Na_2CO_3 (2.92 g) + $NaHCO_3$ (1.89 g), dilute up to 1 L, adjust pH to 10.5.

Equipment and Software

- Eppendorf pipettes
- Parafilm
- Dispensette dispensers
- Beckman Polyallomer Centrifuge Tubes 1 × 3 1/2″
- Fisher 13 × 100 mm glass test tubes
- Savit tube caps
- Beckman TJ6 centrifuge
- Beckman LS 600 TA scintillation counter
- Fisher HDPE 7 mL Scintillation Vial (catalog number 03-337-1)
- 1.7 mL Fisher polypropylene microcentrifuge tubes
- Fisher Scientific 550 Sonic Dismembrator
- Excel and Prism (GraphPad).

Serum Activation/Inhibition of Lipoprotein Lipase

Reagents

- See section "Reagents" in Radiometric Detection of Lipoprotein Lipase Activity Using Triolein, ApoC-II, and Angiopoietin-Like 4, with the addition of preheparin human serum.

Buffers/Solutions

- See section "Buffers/Solutions" in Radiometric Detection of Lipoprotein Lipase Activity Using Triolein, ApoC-II, and Angiopoietin-Like 4.

Equipment and Software

- See section "Equipment and Software" in Radiometric Detection of Lipoprotein Lipase Activity Using Triolein, ApoC-II, and Angiopoietin-Like 4.

Fluorescence Detection Lipoprotein Lipase Activity Using the EnzChek™ Substrate

Reagents

- EnzChek™ Lipase Substrate, green fluorescent, 505/51 CAT: E33955
- Heparin Sodium (Fisher #BP2425)
- DMSO
- Zwittergent® 3-12 Detergent CAT: 693015
- Molecular Grade Methanol
- 1 M NaCl
- 1 M Tris–HCl pH 8.0.

Buffers/Solutions

- 10 mg/ml Heparin Sodium stock (aliquot in 50 μL, store at −20°C)
- Heparin containing KRP (25 μL 10 mg/ml Heparin Sodium, and 4.975 μL KRP)
- Dissolve EnzChek in 20% DMSO to a final molarity of 100 μM
- Dissolve Zwittergent with a final concentration of 8% Zwittergent in molecular grade H_2O and molecular grade 1% Methanol
- 4× assay Buffer (600 mM NaCl, 80 mM Tris, molecular grade H_2O).

Equipment and Analysis Software

- 96-well black-walled plate for fluorescence
- Plate reader capable of temperature control and fluorescent detection
- Graph pad (or other software capable of fitting a Michaelis–Menten curve).

METHODS

Radiometric Detection of Lipoprotein Lipase Activity Using Triolein, ApoC-II, and Angiopoietin-Like 4

Radiometric detection of LPL activity is an appropriate method for determining the activity of heparin-released LPL activity in PHP from humans or from pre-clinical animal models. Importantly, the protocol, can be modified to answer a specific

research question e.g., changes to the substrate and PHP dilution or treatment can easily be implemented. A schematic describing the workflow of the method detailed in this section is shown in **Figure 1**.

Method

Make the Organic Portion of the Triolein Substrate

In a Beckman Polyallomer Centrifuge Tube mix together 20 μL ^{3}H-triolein (1 mCi/mL), 200 μL Glycerol Triolate (50 mg/mL), and 20 μL lecithin (12.5 mg/mL). Dry mixture under N_2 for 10 min, or until no liquid visibly moves when the tube is rotated.

Make the Aqueous Portion of the Triolein Substate

Add 1.9 ml dH_2O, 1 mL Tris (2 M, pH = 8.2), 0.8 ml 10% BSA, ApoC-II synthetic peptide (5–10 μM).

Sonicate the Mixture to Make an Emulsion

Ensure the part of the tube containing the substrate is submerged within an ice-slush bath. Insert sonicator probe 1–2 mm into the substrate mixture. Pulse-sonicate [output frequency: 20 kHz, 10 s on, 10 s off, (duty cycle = 0.05%) for 32 cycles]. The clear mixture should now be an opaque emulsion. Cover with parafilm and place on ice until ready to add to LPL source. Although the substrate should be made fresh the day of the assay, the substrate can stay on ice for several hours while preparing samples. However, ensure to gently mix the substrate prior to adding to the source of LPL.

Prepare Lipoprotein Lipase Samples

For human PHP samples we recommend 1:100 dilution with KRP (0.175 M NaCl). For different samples that have not been tested previously a concentration range optimization experiment may be appropriate. Keep the samples on ice while preparing the assay, and work quickly once the samples are diluted. Once all samples are diluted, add 100 μL of each sample (in triplicate) to a glass test tube. Prepare two sets of samples,

Angiopoietin-Like 4 Inhibition

Add Angptl4 to each "+Angptl4" sample, at 10 μg/ml, and incubate at RT for 15 min. Add an equal volume of vehicle (molecular grade H_2O), to the remaining samples. Due to the effect on LPL activity, ensure all + and − Angptl4 samples are incubated at RT for the same amount of time.

Prepare Internal Standards

For each assay a number of internal standards are required in order to control for variability in the substrate generation (substrate dose), oleic acid dilution [oleic acid dose fatty acid recovery (oleic acid recovery)], KRP buffer composition (KRP Blank), as well as measurement of a known source of LPL that can be used in each assay and is consistent across a given research project [quality control (QC)]. To prepare a final volume of 100 μL for each standard:

- **Substrate dose** = 100 μL substrate into 5 ml Scintillation fluid. Does not require processing through the hydrolysis reaction but should be processed at the same time to account for degradation.
- **Oleic Acid dose** = 20 μL ^{14}C-Oleic acid into 5 ml Scintillation fluid. Does not require processing through the hydrolysis reaction but should be processed at the same time to account for degradation.
- **Blank** = 100 μL KRP.
- **Oleic acid recovery dose** = ^{14}C-Oleic acid (20 μL 1 mCi/mL) + KRP (80 μ L).
- **Bovine LPL QC** = 100 μL 1:1,000 dilution (in KRP) of bovine LPL (Sigma L2254, 1 unit per μ L).
- **PHP control QC** = 100 μL 1:100 dilution of PHP from typical patient or pooled sample from typical and healthy population (in KRP).

Hydrolysis Reaction

Add 100 μL of substrate to each sample and standard. Incubate all tubes in a shaking water bath at 37°C for 45 min exactly. To terminate the reaction, add 3.4 mL of Belfrage to all samples, followed by 0.96 mL of bicarbonate buffer to each tube. Ensure all tubes are carefully capped and shake vigorously for 5 min.

Phase Separation

To separate the hydrolyzed FAs from non-hydrolyzed triolein centrifuge at 4°C for 20 min × 3,000 rpm (Beckman, TJ6). When removing and handling samples after centrifugation be careful not to disturb the interface. Transfer 500 μL of the top aqueous phase to a scintillation vial containing 5 ml SCINTISAFE. Vortex each sample for 10 s, and then read all samples in a scintillation counter capable of measuring ^{3}H for 2 min, providing ^{3}H counts per minute (CPMs) for each sample.

Data Analysis

1. Subtract the blank CPMs from each sample CPM.
2. Determine total lipase activity for each sample using the following formula:

$$Activity\ (nmol\ \mathrm{FFA}/mL/min) = \frac{\mathrm{Sample\ CPM} \times K \times 10}{DOSE\ counts \times Recovery}$$

Where K equals

$$K = \frac{mL\ upper\ phase}{mL\ counted} \times nEq\ TG\ oleic\ acid/tube \times \frac{dilution}{inc.time} \times 100$$

$$nEq\ TG\ oleic = \frac{50\frac{mg}{ml} \times \frac{0.2}{4.0}}{885.5\ g} \times 0.100\ mL \times 3\ oleic\ acid\ per\ mole \times 10^6 = 423$$

$$\frac{2.45\ mL\ upper\ phase}{0.5\ mL\ counted} \times 100 = 490$$

$$Recovery = \frac{OARS\ counts}{OAD\ counts} \times 490$$

1. To calculate LPL-specific activity subtract +Angptl4 lipase activity (Angptl4 resistant lipase) away from total lipase activity. Express data as nmol FFA/mL/min. Transform to other units (e.g., per hour) if required.

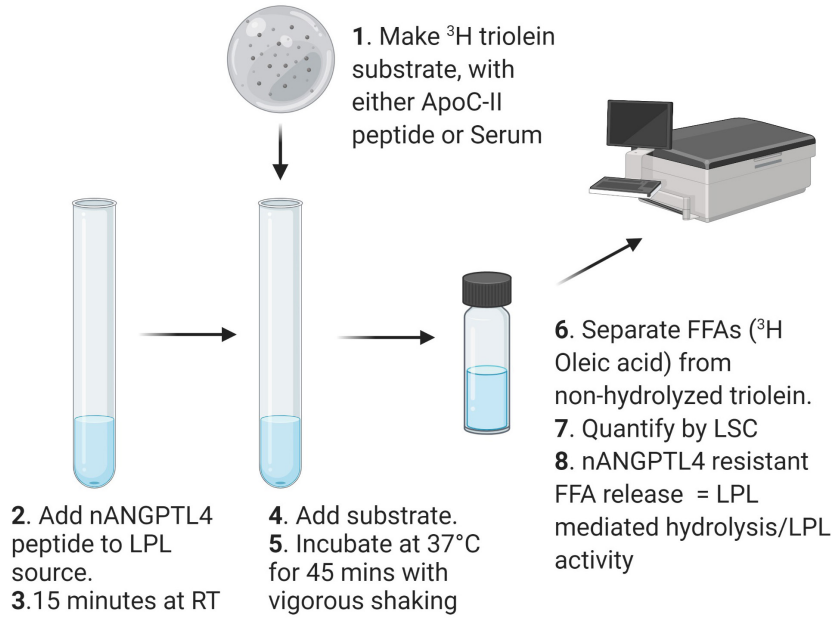

FIGURE 1 | Schematic workflow for measuring LPL activity with a triolein substrate.

Assessing Ability of Preheparin Serum to Inhibit or Activate Lipoprotein Lipase

In many instances, HTG is not caused by LPL variants leading to compromised LPL protein structure and function, but by a change in the endogenous circulating factors that are necessary to maintain LPL activity in each state. As a first-step approach to determine whether reduced lipase activity is a product of endogenous inhibition we have developed the following assay. The method outlined above is almost identical to the method described in section "Radiometric Detection of Lipoprotein Lipase Activity Using Triolein, ApoC-II, and Angiopoietin-Like 4," therefore, here we only detail the steps that differ from the above protocol.

Method

Make the Aqueous Portion of the Triolein Substate

Add 1.9 ml dH_2O, 1 mL Tris (2 M, pH = 8.2), 0.8 mL 10% BSA, 0.3 mL preheparin serum (substitute for ApoC-II).

Prepare Lipoprotein Lipase Samples

To ensure that the serum substrate is the only variable for these assays we suggest using a constant and known source of LPL (not patients PH), such as bovine LPL (bLPL) (Sigma). A working concentration of 1:1,000, bLPL is sufficient to determine differences in serum mediated activation/inhibition of LPL-mediate hydrolysis.

Data Analysis

Determine LPL activity using the same standards and formulas shown above. Importantly, for each substrate a complete set of standards should also be generated for accurate determination of LPL activity, e.g., substrate dose, blank, oleic acid recovery dose. For clinical research studies, comparison against a typical healthy patient sample, or patient sample pool should be considered. For drug intervention studies over time, ability for a patient's serum to increase.

Fluorescence Detection of Lipoprotein Lipase Activity Using the EnzChek™ Substrate

Fluorescent detection of LPL activity presents a 96-well plate assay format and relatively high-throughput alternative to the measuring LPL activity using a range of LPL sources where biological and technical replicates are too high to perform the triolein-substrate assay, or in laboratories where studies using radioactive materials are prohibited. A schematic workflow for this protocol is shown in **Figure 2**.

Method

Heparin Released LPL From Surface of Heparin Secreting Cells

Grow LPL secreting cells to confluency. Aspirate media and wash cells 3× with room temperature sterile PBS. Aspirate PBS. Leave plate tilted for 1 min to ensure that remaining buffer pools, can be aspirated, and will not dilute the LPL-enriched HR fraction. Add heparin–containing KRP buffer (300 μL per confluent 10 cm^2 plate) for 5 min, then immediately place on ice before quantification of lipase activity. A minimum volume of 100 μL HR per well is needed for EnzChek™ assay.

Prepare bLPL stock. Dilute bLPL in phenol free DMEM media without FBS 1:500.

Prepare PHP stock. A final dilution of 40× was needed to read LPL activity in PHP. Higher concentrations appeared to be affected by the natural yellow color of PHP resulting

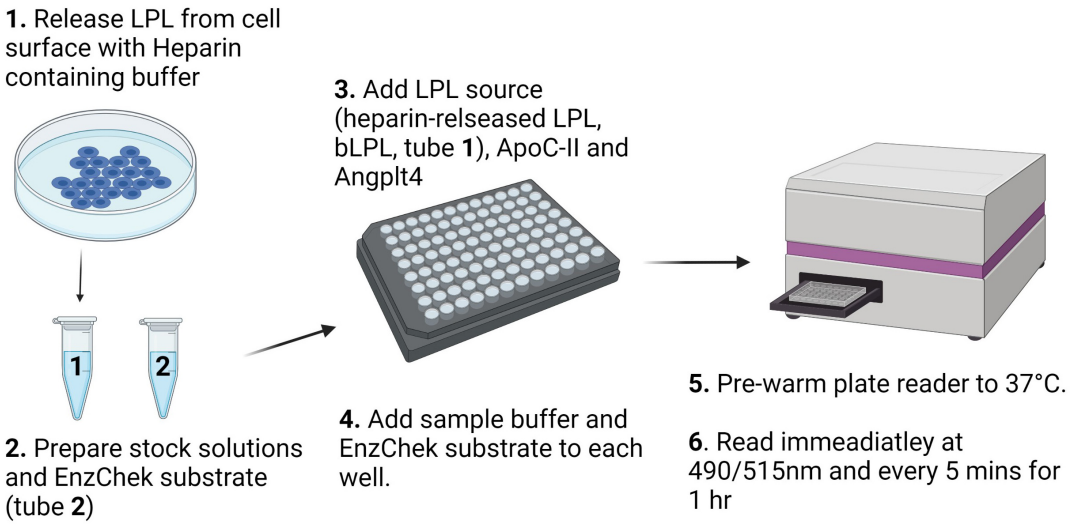

FIGURE 2 | Schematic description of the workflow for the fluorescence detection of LPL activity using the EnzChek^{TM} substrate.

in inconclusive, or "noisy," readings. Therefore, for each well combine 5 μL of the PHP sample with 95 μL molecular grade H_2O for each well per condition.

Prepare Plate. Four conditions/controls were tested per LPL source at equal volumes: Blank, LPL, LPL + ApoC-II, and LPL + Angptl4 in quadruplicate. ApoC-II was added at a concentration of 1 μM to increase LPL activity. Angptl4 was added at 2.7 μg/mL (for a final dose of 200 ng/well) to decrease LPL activity in each LPL source (i.e., HR, bLPL, or PHP) and incubated for 15 min at RT along with a control. During the 15-min incubation aliquot 100 μL of each sample into each well. Add molecular grade H_2O to each well to a final volume of 150 μL. bLPL could be read at a smaller volume with just 75 μL bLPL with no added H_2O in each well.

Pre-warm fluorescent plate reader to 37°C.

Prepare EnzChek^{TM} Stock solutions. A Final EnzChek^{TM} concentration of 0.625 μM is necessary. While the plate reader is warming, prepare 80× EnzChek^{TM}/Zwittergent by mixing EnzChek and Zwittergent in equal parts (50 μM EnzChek and 4% Zwittergent). Dilute the 50 μM EnzChek^{TM}/Zwittergent stock in 4× Sample buffer 1:20 for a 200 μL well volume or 1:40 for a 100 μL well volume. Immediately before read, add the EnzChek^{TM} stock to each well to dilute 4× buffer to 1×.

Read Plate. Read the plate immediately at 490/515 excitation/emission at 37°C every 5 min for 1 h.

Data Analysis

A blank is comprised of the 4× buffer, diluted to 1× in each well, DMEM, H_2O, and EnzChek/Zwittergent spike without any LPL. The average blank value is subtracted from each well per timepoint, producing a blank subtracted data set. Each technical replicate was then divided by the average fluorescent value of the first time point of the control group to produce a fold change from baseline. All wells in each condition are then averaged and the standard error calculated in GraphPad Prism V8. These values are then plotted, and a Michaelis–Menten line is fitted to each curve. The proper use of the Michaelis–Menten fit is tested as the best model by GraphPad. Differences are calculated by two-way ANOVA at each individual time point of Angptl4 and ApoC-II treated compared to Control.

RESULTS

Salt Concentration of Working Buffer Is Important for Accurately Measuring Lipoprotein Lipase Activity in Postheparin Plasma

Historically, LPL activity has been shown to be sensitive to the concentration of NaCl in the working buffer solution. Previous assays have reported the use of "low salt" potassium phosphate buffers either as a component of the lipid substrates or as a diluent for the LPL source (e.g., PHP) to measure LPL activity where the NaCl concentration ranges from 0.1 to 0.3 M NaCl (46, 55–57). To determine the optimal NaCl concentration to use as a diluent buffer for the triolein-substrate assay, we diluted PHP taken from four "typical" healthy subjects in KRP buffer containing 0.01–0.4 M NaCl and measured LPL activity using the triolein substrate assay described in "Radiometric Detection of Lipoprotein Lipase Activity Using Triolein, ApoC-II, and Angiopoietin-Like 4." We found that LPL activity was highest when PHP was diluted in 0.175 M NaCl (**Figure 3A**), and therefore we recommend using 0.175 M NaCl when measuring LPL activity.

N-Terminal Angiopoietin-Like 4 Peptide Robustly Inhibits Lipoprotein Lipase Activity in Triolein-Based Assays

Previous reports have taken advantage of the salt-sensitivity of LPL by using "high salt" concentrations to specifically inhibit LPL

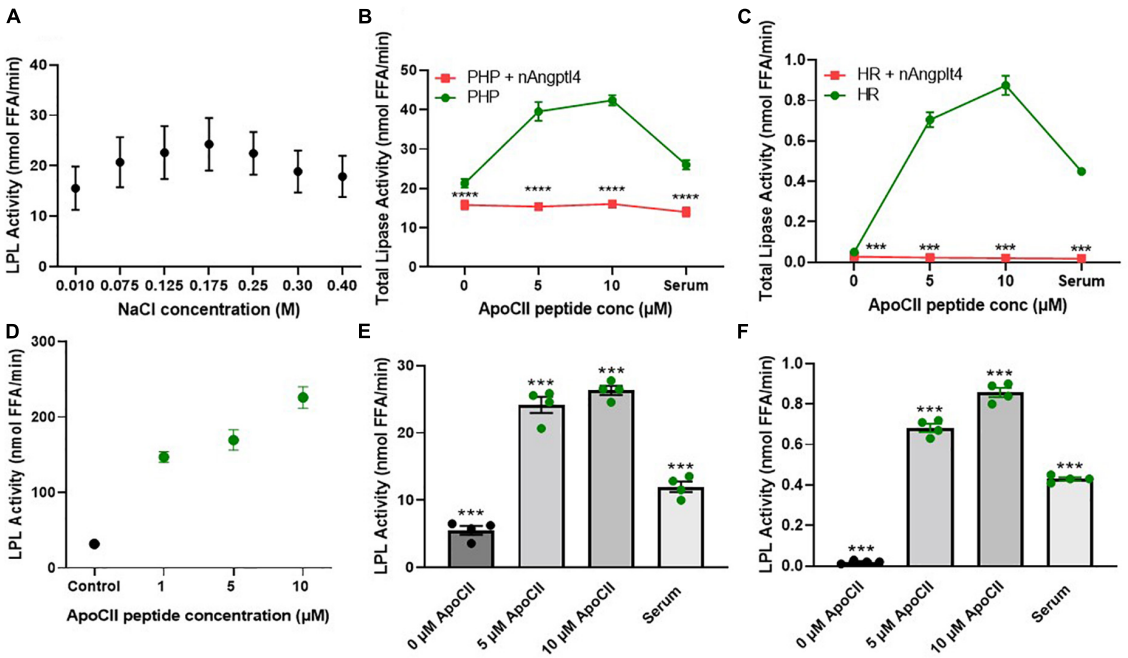

FIGURE 3 | NaCl, inhibitor (nAngptl4) and activator (ApoC-II peptide) standardization of the triolein substate method of measuring LPL activity. **(A)** Optimization of NaCl concentrations within KRP buffer used to dilute PHP (1:100) isolated from pool of healthy subjects. **(B)** Total lipase activity in PHP (1:100 dilution in 0.175 M NaCl KRP) + and – 5 μg/mL nAngptl4 in presence of 0, 5, or 10 μM ApoC-II peptide. **(C)** Total lipase activity in HR + and – 5 μg/ml nAngptl4 in presence of 0, 5, or 10 μM ApoC-II peptide. **(D)** Activation of bLPL with increasing ApoC-II peptide concentration. **(E)** LPL activity in PHP with increasing concentrations of ApoC-II peptide compared to serum as a source of ApoC-II. **(F)** LPL activity in KH with increasing concentrations of ApoC-II peptide compared to serum as a source of ApoC-II. ***$P < 0.001$; ****$P < 0.0001$.

activity in PHP. Although both HL and LPL are the major lipases in human PHP, in contrast to LPL, HL activity is increased in the presence of high salt and does not require further activation by circulating serum-derived factors (58). Therefore, HL activity has previously been calculated by inhibiting LPL activity with 1 M NaCl and measuring the salt-resistant lipase activity (59). However, 1 M NaCl only partially inhibits LPL activity in PHP from HL-deficient mice, suggesting that "high salt" is not an optimal method of LPL inhibition (46). Immunochemical inhibition of HL using HL-specific antibodies partially resolves this issue (55, 56, 60, 61). However, all forms of immunoassays are dependent on variations in antibody titer and specificity, whether the antibody was raised against a polypeptide or protein, or even between batches of the same antibody. Since the N-terminal domain of Angptl4 (nAngptl4) is a reversible, noncompetitive inhibitor of LPL (62), we established whether nAngptl4 would be a suitable alternative mode of LPL inhibition in triolein-substrate assays. Using a method initially adapted from Basu et al. (54), we established that 10 μg/mL nAngptl4 peptide could specifically inhibit LPL activity PHP (**Figure 3B**), and in LPL-enriched HR fractions isolated from cell lines that abundantly express and secrete LPL (BV-2 murine microglia) (**Figure 3C**), even in the presence of synthetic ApoC-II peptide or human serum as a source of ApoC-II. Since the circulating levels of Angptl4 have been reported to range from 455 to 961 ng/mL in patients with varying degrees of atherosclerosis (63). Hence, 10 μg/mL is sufficient to saturate LPL activity when LPL is within the typical range. However, in severe HTG or other non-representative samples a range of 5–20 μg/mL may be considered. As expected, in our study nAngptl4-mediated inhibition of LPL activity only depleted half of the total lipase activity in typical human PHP, with the nAngptl4-resistant lipase activity most likely being HL, and to a much lesser extent endothelial lipase (EL) (**Figure 3B**). Interestingly, all lipase activity in the HR LPL-enriched fractions taken from LPL-producing BV-2 murine microglia cells was lost following nAngptl4 supplementation, suggesting that LPL accounts for all lipases present on the cell surface of microglia (**Figure 3C**). Overall, we recommend the use of nAngptl4 in all assays measuring LPL activity.

ApoC-II Peptide Robustly Activates Lipoprotein Lipase Activity in Triolein-Based Assays

Like the methods used to specifically inhibit LPL activity, the methods used to activate LPL vary considerably across protocols. While almost all assays rely on ApoC-II mediated activation of LPL, the source of ApoC-II can range from serum samples taken from individuals or a pool of healthy individuals (46, 55, 56, 64), VLDL (65), ApoC-II protein (66), or ApoC-II peptide (27), leading to variable substrate composition and inconsistent results. In response, we have synthesized an ApoC-II peptide fragment corresponding to amino acids 55–78, and tested its ability to activate LPL in PHP, HR LPL from microglia, and bLPL

(**Figures 3B–D**). Previous studies have shown that this ApoC-II peptide is just as potent as the full length ApoC-II protein at activating LPL (27). Here, we show that a final concentration of 5 μM ApoC-II can robustly increase LPL activity in PHP, HR fractions, and bLPL (**Figures 3B–F**). Unexpectedly, substrates made with 0 ApoC-II were able to minimally activate LPL within PHP from a pool of typical subjects (**Figure 3B**). This suggests that the ApoC-II concentrations within a concentrated PHP sample is sufficient to activate LPL. In support of this, samples with no endogenous ApoC-II (HR LPL fractions from microglia), showed no LPL activity when serum or ApoC-II was absent from the substrate, yet showed a significant increase in LPL activity with addition of ApoC-II or serum to the substrate (**Figure 3C**). Overall, these findings corroborate the fact that circulating concentrations of ApoC-II are approximately 4.5 μM (67). However, considering ApoC-II is a component of VLDL and can be increased in patients with HTG, we recommend using 5 μM ApoC-II peptide 55–78 as an LPL activator in triolein-substrate LPL activity assays, but would also recommend testing with 10 μM in samples from patients or pre-clinical samples with increased TGs.

Using Preheparin Serum to Activate Lipoprotein Lipase Can Determine the Presence of Endogenous Activators and Inhibitors

Previous reports have suggested that the utility of measuring lipase activity in PHP is limited, since low LPL activity (68) is not always related to LPL polymorphisms (60). In addition, studies using triolein substrates and preheparin serum as a source of ApoC-II have also shown poor relationships between the activity of PHP lipases and the absolute turnover of serum TGs (61). Although these studies have reported important outcomes, it is also plausible that these inconsistencies stem from caveats in the experimental approach. For example, HTG can be caused by genetic variation in an array of molecular factors that enhance or inhibit LPL activity (29, 47–50). Therefore, in an individual with HTG the structure and function of the LPL enzyme may be uncompromised but, for example, an LPL activator such as ApoC-II may be compromised. In such a case, examining LPL activity in PHP using serum from a healthy/typical donor would not be able to resolve altered endogenous inhibition of LPL. To counter this problem, we designed an assay where serum from an individual is used as a source of circulating endogenous activators and inhibitors. Specifically, the serum is included as a component of the triolein-containing substrate emulsion. This substrate is added to a known and well characterized source of LPL. Here, we used bLPL, since no other LPL-regulating factors are present, but this assay could also be performed with HR LPL, or recombinant commercially available human LPL. The presence of LPL-regulating factors was evaluated by comparing LPL activation when the substrates contained serum from a typical healthy sample pool, versus LPL activation when the substrates contained serum from individuals with known HTG (**Figure 4**). We found serum from four individuals with HTG was less able to activate bLPL compared to serum from a typical patient pool (**Figure 4**). We would recommend employing this study design when LPL-independent mechanisms of HTG are suspected, or if PHP lipase activity appear normal despite HTG. In addition, this approach would be an appropriate study design when testing anti-hyperlipidemic drugs when a serum from the same individual can be compared over time.

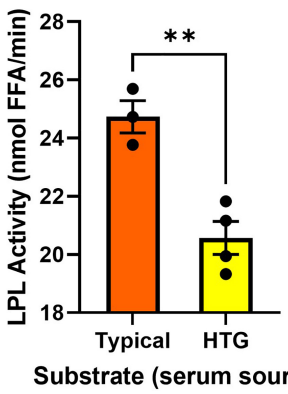

FIGURE 4 | Serum activation/inhibition of a known LPL source. $^{**}P < 0.01$.

ApoC-II Activation and Angiopoietin-Like 4 Inhibition Can Accurately Determine Lipoprotein Lipase Activity Using the EnzChek™ Substrate in Post-heparin Plasma, Heparin Released Lipoprotein Lipase, and Bovine Lipoprotein Lipase

Although determining LPL activity using physiologically relevant triolein substrates with ApoC-II and nAngptl4 provides an accurate and gold-standard approach for measuring lipase activity, particularly in PHP, the methodology remains cumbersome, lengthy, and reliant on radiolabeled lipids that are a health and environmental hazard. Therefore, several research groups have aimed to develop novel TG-like substrates that can be used in a high-throughput 96-well assay format, does not require the use of radioisotopes, nor complex procedures to separate hydrolyzed from non-hydrolyzed substrate (54, 69, 70). While these assays are cost-effective and efficient, particularly when measuring LPL activity in pre-clinical samples, in samples derived from cultured cells, or in drug-development screens, they have not been evaluated with PHP samples. Here we have shown that the EnzChek™ substrate can be used to quantify LPL activity in bLPL, (**Figure 5A**), LPL enriched HR fractions from BV-2 microglia, but not in HF fractions from BV-2 microglia where LPL expression has been knocked out using CRISPR-Cas9 (**Figure 5B**), and PHP (**Figure 5C**). Several optimization experiments were needed to accurately and reproducibly measure LPL activity in PHP, with optimal activity being observed at a dilution of 2:0.4 (EnzChek™ reagent and buffer:PHP). Moreover, we have shown that LPL-mediated hydrolysis of the EnzChek™ substrate can be robustly inhibited by 5 μg/ml nAngptl4 and increased by 10 μM ApoC-II peptide

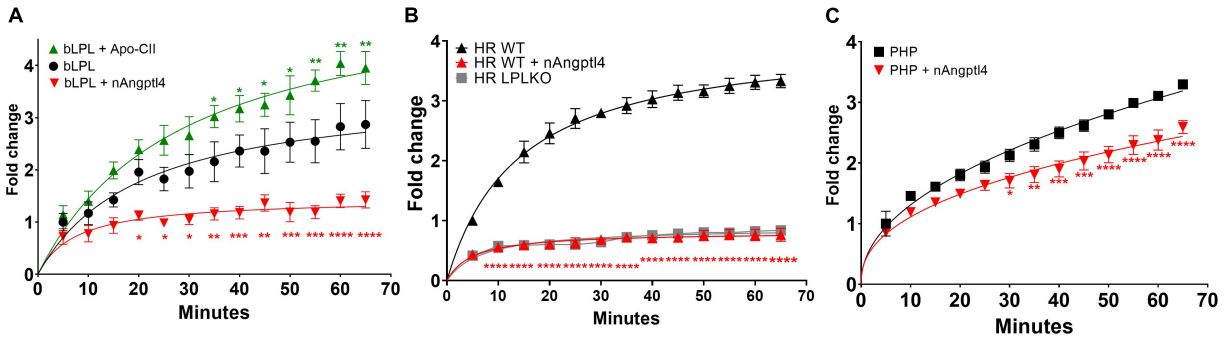

FIGURE 5 | Fluorescence detection of LPL activity using the EnzChek^{TM} substrate, ApoC-II activation and nAngptl4 inhibition to determine LPL activity using **(A)** bLPL **(B)** heparin-released (HR) LPL from LPL secreting BV-2 microglia, and LPL knock out (LPL KO) cells as a control, and **(C)** PHP as a source of LPL. *$P < 0.05$; **$P < 0.01$; ***$P < 0.001$; ****$P < 0.0001$.

using bLPL as a source of LPL (**Figure 5A**). Interestingly ApoC-II-mediated activation did not increase LPL activity in HR or PHP, which may reflect the structure of the TG analog substrate, the relative composition of the biological sample, and the presence of endogenous ApoC-II (data not shown). However, hydrolysis of the EnzChek^{TM} substrate was inhibited by the n-terminal Angptl4 fragment in HR and PHP. Therefore, we recommend inclusion of the ApoC-II and nAngptl4 peptide in the experimental design of studies aiming to the measure LPL activation using the EnzChek^{TM} assay.

DISCUSSION

While there are several methods to determine LPL activity, each has several caveats precluding its applicability to a given research, or diagnostic objective. Here, we describe, evaluate, and optimize methods to; (1) measure LPL activity in PHP; (2) determine presence of circulating factors that may inhibit or activate LPL; and (3) to determine LPL activity in PHP and heparin-released LPL-enriched fractions using the EnzChek fluorescent substrate. We have made a number of changes to existing protocols, most notably, the use of defined salt concentrations (0.175 M NaCl) in the working buffer, the use of an ApoC-II peptide as a potent, readily available and cost-effective LPL activator, and the use of the nAngptl4 peptide as an LPL-specific inhibitor. Here, we describe these methods in detail and recommend the use of ApoC-II peptides and nAngptl4 to reduce variation and increase reproducibility when quantifying LPL activity in a range of samples.

In our analysis we observe a robust reduction in total lipase activity following supplementation with the nAngptl4 fragment. There is considerable data to support the notion that Angptl4 regulates LPL activity at a post-translational level (16–20). Indeed, recent studies have shown that nAngptl4 specifically inhibits LPL activity by binding the lid domain and preventing substrate catalysis at the active site (21). Since the reciprocal studies have not been performed to assess whether nAngptl4 can inhibit the activity of other lipases such as HL, and to a lesser extent EL, that may be present in PHP, we cannot rule out the possibility that nAngptl4 may reduce total lipase activity. However, in recent studies using Angptl4 knockout mice, no effects on HL or total lipase were observed, whereas LPL activity was modified following Angptl4 depletion (71). In addition, in the present study, we show that nAngptl4 treatment completely abolishes lipase activity in extracellular fractions from microglia that only express LPL, whereas nAngptl4 only partially inhibits lipase activity in PHP, suggesting that HL, the second most abundant in PHP, is at least partially resistant to nAngptl4-mediated inhibition. Additionally, EL is mostly a phospholipase and has very little TG lipolytic activity (44). Further studies that directly assess the ability of nAngptl4 to inhibit HL and EL, while beyond the scope of this manuscript, should be considered going forward. Nonetheless, the addition of both ApoC-II and Angptl4 in our study design provides an additional layer of control when measuring LPL-specific catalysis of triolein.

While the triolein-substrate method for quantifying LPL activity is fairly well established, there are variations in its execution from laboratory to laboratory, that require consideration when interpreting the results. For example, while almost all assays rely on ApoC-II mediated activation of LPL, the source of ApoC-II can range from serum samples taken from individuals or a pool of healthy individuals (46, 55, 56, 64), VLDL (65), ApoC-II protein (66), or ApoC-II peptide (27). However, using human serum as a source of ApoC-II is subject to considerable variability, between individuals, and even within the same individual over time, nutritional status, and other exposures that may affect TG and ApoC-II levels. Although using a pooled sample of human preheparin serum may prevent variation within a single testing laboratory, different laboratories across the world generate their own reference pool of healthy human serum, which is subject to regional variability and may not be replicated by other research teams. Using VLDL prepared by ultracentrifugation as a source of TG and ApoC-II is advantageous, but harsh ultracentrifugation procedures can non-discriminately de-proteinate lipoproteins leading to variation in substrate composition. Using recombinant and purified sources of ApoC-II may limit variability, but recombinant apoproteins are very expensive and the quality may vary depending on the expression system and purification procedure. To counter

these issues, here we present the use of a synthetic ApoC-II peptide, which is a potent LPL activator, is not subject to biological variation, is readily available, and is relatively cost-effective. Notably, in recent studies other ApoC-II peptides have been used to mimic the ApoC-II activation of LPL while also blocking the LPL-inhibiting effect of ApoC-III and lower plasma TG (53). Therefore, the peptides described in the study by Wolska et al. (53), could easily be incorporated into the experimental approaches described in this manuscript as an additional measure of LPL-specific activity. Overall, we recommend the simultaneous use of an ApoC-II peptide, in addition to the nAngptl4 peptide for a reproducible method of determining LPL-specific lipase activity in a range of biological samples.

However, it is important to note that even following our recommendations, the ^{3}H-triolein-based assay still requires specialized equipment and accommodations for using radioactive isotopes and remains low-throughput compared to the 96-well plate format colorimetric and fluorometric methods of detecting LPL activity. Hence, we would recommend making these changes to an existing protocol or reserving this method for clinical or pre-clinical evaluation of LPL activity.

Drug development studies have utilized Angptl4 to determine whether small molecule LPL activators can enhance LPL activity and reverse Angptl4-mediated inhibition (72). Hence, how nAngptl4 and ApoC-II peptides interact with LPL is of major interest to researchers pursuing LPL-focused drug development studies, to elucidate the mechanism-of-action of potential drugs, and to determine the utility of this specific assay design for their studies. Here, we used HDOCK to perform rigid-body docking calculations to predict the preferred binding interactions between the ApoC-II peptide (aa 56–78) and the N-terminal Angptl4 fragment with LPL (73). The visualization software Visual Molecular Dynamics (VMD) was used to analyze the results from the docking calculations (74). As input to HDOCK, we used the AlphaFold structure of human LPL, which closely resembles recently elucidated crystal structures of LPL, but also includes predicted coordinates for missing amino acid residues that were not resolved by crystallography (75). The AlphaFold structures for LPL (76), ApoC-II (77), and Angptl4 (78) were modified prior to docking so that they more closely represented the structures used in the experiments (i.e., LPL without the signal peptide, the region of ApoC-II covered by the synthetic peptide only, and the N-terminal fragment of Angptl4, respectively). Separate HDOCK calculations were performed with the ApoC-II peptide and LPL, and with Angptl4 and LPL. **Figure 6** shows VMD snapshots of the overlay of the top HDOCK-scored complexes for the two separate calculations. The results show that both the ApoC-II peptide and the N-terminal Angptl4 fragment preferentially bind to the ligand binding site and lid domain of LPL. Furthermore, the preferred interactions predicted by HDOCK are consistent with previous studies using full-length ApoC-II and Angptl4 (27, 38, 39). This suggests that both the ApoC-II peptide and nAngptl4 fragment interact with LPL like the full-length proteins, supporting their functionality in the LPL assays described above. Moreover, this highlights the utility of this assay as a physiologically relevant method in drug development studies.

While triolein assays are often used to determine whether a patient may have LPL deficiently leading to HTG, many patients do not carry an LPL variant leading to compromised LPL activity, and LPL activity can appear normal in the cell-free triolein substrate assay described above. For these patients, an alternative methodology can be adopted to assess the presence and relative abundance of circulating endogenous factors that may inhibit LPL activity, leading to HTG. Here, we also present a modified version of the triolein-based substrate assay to answer specific research questions pertaining to the relative abundance of circulating factors that may inhibit LPL. Although this assay will determine whether activating/inhibiting factors are present in each sample the assay will not indicate which molecular factors are dysregulated to alter LPL activity. In addition, outcomes from this assay may be challenging to interpret, since in patients with HTG, LPL-regulating factors may fall or rise to compensate for the dysregulated or variant factor. Nonetheless, this assay will indicate whether LPL-regulating factors, rather than LPL enzymatic activity, is compromised and will generate pre-requisite data to necessitate further characterization of LPL-regulating factors.

Importantly, methods to assess LPL activity have been instrumental in the discovery of LPL structure and function, and its preferred substrate(s). For example, it is often forgotten that although the canonical role of LPL is the hydrolysis of TGs within TRLs, LPL also has phospholipase A_1 activity (79, 80), and can hydrolyze lipoprotein phospholipids, and sonicated phosphatidylcholine vesicles when activated by ApoC-II (81). Using isolated lipoproteins to interrogate LPL biology can be challenging due to the complexity and heterogeneity of the lipoprotein particle, in addition to the relative abundance of activating and inhibiting factors that may confound interpretation. In response, non-lipoprotein substrates have been developed to further interrogate LPL function. *P*-nitrophenyl butyrate (PNBP) was initially developed as a short-chain fatty acid (SCFA) substrate for LPL (82), based on the fact that LPL can also catalyze the hydrolysis of SCFA esters such as tributyrin, and, *p*-nitrophenyl acatate in the absence of ApoC-II (83, 84). Although the colorimetric change that occurs following LPL-mediated hydrolysis of PNBP provides a convenient way of assessing LPL-mediated hydrolysis, using PNBP as a substrate to measure LPL activity in biological samples is not physiologically relevant since PNBP prevents LPL-mediated TG hydrolysis, and the hydrolysis of PNBP itself is inhibited, rather than activated by, ApoC-II (83, 85).

In the search to identify more physiologically relevant non-lipoprotein substrates, several TG analogs were developed where the lipolytic products could be visualized, and hence LPL activity, quantified by fluorescence (54, 86). Arguably the most sensitive, and well characterized TG-analog, with the most stable lipolytic end products is the EnzChek^{TM} substrate (54). However, the utility of this method to measure LPL activity in human PHP has not been previously demonstrated. Here we show that a 1:40 dilution (in assay buffer) of PHP is sufficient to quantify lipase activity. However, it is important to note that since the EnzChek^{TM} substrate contains a C12 fatty acid side chain in the *sn-1* position, this is subject to hydrolysis by LPL

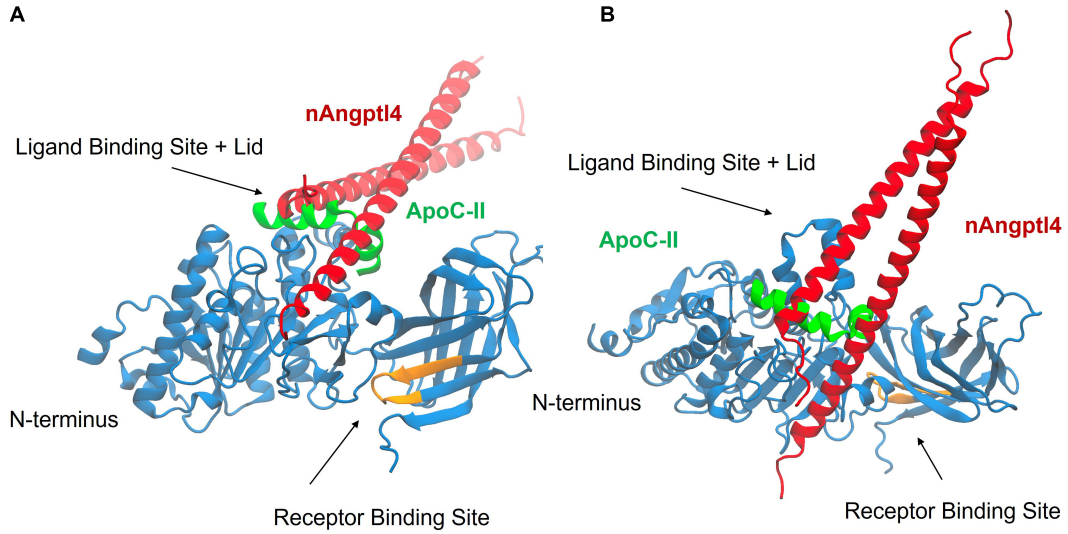

FIGURE 6 | Results from molecular docking of LPL (blue) with the synthetic ApoC-II peptide (green), and nAngptl4 fragment (red) used in the experimental protocol, showing the top HDOCK-scored complex from both a front view **(A)** and top view **(B)**. The receptor binding site of LPL is highlighted in orange. The results show that the ApoC-II peptide and nAngptl4 fragments are expected to bind to the ligand binding site and lid domain of LPL, consistent with our experimental data.

and HL, and therefore nAngptl4-mediated inhibition of LPL is a requisite control. In addition, the inability of ApoC-II to increase LPL activity in HR LPL enriched fractions, when ApoC-II has such a profound ability to increase LPL activity in the triolein-based assay suggests that the interaction between the EnzChek^{TM} substrate, LPL, ApoC-II and Angptl4 needs to be further evaluated. Overall, although questions remain regarding the physiological relevance of the EnzChek^{TM} substrate we recommend this assay in studies using a large volume of biological replicates. Moreover, due to its high-throughput nature this assay can be readily applied to drug discovery screens, but we would also recommend testing promising drug candidates using the triolein-based method to recapitulate key findings.

CONCLUSION

In summary, we have shown that including synthetic ApoC-II peptides and nAngptl4 fragments in triolein and EnzChek^{TM}-based lipase assays can accurately determine LPL-specific activity using a range of biological samples, such as PHP, HR LPL fractions from LPL secreting cells, and bLPL. We recommend the addition of ApoC-II and nAngptl4 as a cost-effective and reproducible way to measure LPL activity avoiding the variability of human serum or isolated human-VLDL. Moreover, in samples with increased TGs where the LPL activity appears uncompromised, we also advise trialing triolein-based assays using a patient's serum to determine the relative abundance of factors that may compromise LPL-activity, although further studies will be needed to identify these factors. Finally, in instances requiring high-throughput measurements of LPL activity, we recommend using the EnzChek^{TM} fluorescence substrate, in combination with ApoC-II and nAngptl4 controls to ensure LPL-specific lipase activity is being measured.

DATA AVAILABILITY STATEMENT

The raw data supporting the conclusions of this article will be made available by the authors, upon request.

ETHICS STATEMENT

The studies involving human participants were reviewed and approved by the Colorado Institutional Review Board. The patients/participants provided their written informed consent to participate in this study.

AUTHOR CONTRIBUTIONS

KB and RE contributed to the conceptual design of the study. KB, DO, HW, JM, and EL carried out the experimental studies and data analysis. KB, DO, RE, PR, and KS wrote the manuscript. All authors edited the manuscript.

FUNDING

This work was in part supported by a SPARK-REACH grant from the NIH and State of Colorado awarded to KB, and an ABNEXUS grant awarded by the University of Colorado to KB and KS.

SUPPLEMENTARY MATERIAL

The Supplementary Material for this article can be found online at: https://www.frontiersin.org/articles/10.3389/fcvm.2022.926631/full#supplementary-material

REFERENCES

1. Korn ED. Properties of clearing factor obtained from rat heart acetone powder. *Science.* (1954) 120:399–400. doi: 10.1126/science.120.3114.399-a
2. Korn ED. Clearing factor, a heparin-activated lipoprotein lipase. II. Substrate specificity and activation of coconut oil. *J Biol Chem.* (1955) 215:15–26.
3. Korn ED. Clearing factor, a heparin-activated lipoprotein lipase. I. Isolation and characterization of the enzyme from normal rat heart. *J Biol Chem.* (1955) 215:1–14.
4. Kersten S. Physiological regulation of lipoprotein lipase. *Biochim Biophys Acta.* (2014) 1841:919–33. doi: 10.1016/j.bbalip.2014.03.013
5. Khera AV, Won HH, Peloso GM, O'Dushlaine C, Liu D, Stitziel NO, et al. Myocardial infarction genetics consortium DSGCEC, global lipids genetics c. association of rare and common variation in the lipoprotein lipase gene with coronary artery disease. *JAMA.* (2017) 317:937–46. doi: 10.1001/jama.2017.0972
6. Myocardial Infarction G, Investigators CAEC, Stitziel NO, Stirrups KE, Masca NG, Erdmann J, et al. Coding variation in ANGPTL4, LPL, and SVEP1 and the risk of coronary disease. *N Engl J Med.* (2016) 374:1134–44. doi: 10.1056/NEJMoa1507652
7. Db K, Tang M, Reigan P, He R. Genetic variants of lipoprotein lipase and regulatory factors associated with Alzheimer's disease risk. *Int J Mol Sci.* (2020) 21:8338. doi: 10.3390/ijms21218338
8. Doolittle MH, Ehrhardt N, Peterfy M. Lipase maturation factor 1: structure and role in lipase folding and assembly. *Curr Opin Lipidol.* (2010) 21:198–203. doi: 10.1097/MOL.0b013e32833854c0
9. Sha H, Sun S, Francisco AB, Ehrhardt N, Xue Z, Liu L, et al. The ER-associated degradation adaptor protein Sel1L regulates LPL secretion and lipid metabolism. *Cell Metab.* (2014) 20:458–70. doi: 10.1016/j.cmet.2014.06.015
10. Obunike JC, Lutz EP, Li Z, Paka L, Katopodis T, Strickland DK, et al. Transcytosis of lipoprotein lipase across cultured endothelial cells requires both heparan sulfate proteoglycans and the very low density lipoprotein receptor. *J Biol Chem.* (2001) 276:8934–41. doi: 10.1074/jbc.M008813200
11. Goulbourne CN, Gin P, Tatar A, Nobumori C, Hoenger A, Jiang H, et al. The GPIHBP1-LPL complex is responsible for the margination of triglyceride-rich lipoproteins in capillaries. *Cell Metab.* (2014) 19:849–60. doi: 10.1016/j.cmet.2014.01.017
12. Surendran RP, Visser ME, Heemelaar S, Wang J, Peter J, Defesche JC, et al. Mutations in LPL, APOC2, APOA5, GPIHBP1 and LMF1 in patients with severe hypertriglyceridaemia. *J Intern Med.* (2012) 272:185–96. doi: 10.1111/j.1365-2796.2012.02516.x
13. Lei X, Shi F, Basu D, Huq A, Routhier S, Day R, et al. Proteolytic processing of angiopoietin-like protein 4 by proprotein convertases modulates its inhibitory effects on lipoprotein lipase activity. *J Biol Chem.* (2011) 286:15747–56. doi: 10.1074/jbc.M110.217638
14. Backhed F, Ding H, Wang T, Hooper LV, Koh GY, Nagy A, et al. The gut microbiota as an environmental factor that regulates fat storage. *Proc Natl Acad Sci USA.* (2004) 101:15718–23. doi: 10.1073/pnas.0407076101
15. Cazes A, Galaup A, Chomel C, Bignon M, Brechot N, Le Jan S, et al. Extracellular matrix-bound angiopoietin-like 4 inhibits endothelial cell adhesion, migration, and sprouting and alters actin cytoskeleton. *Circ Res.* (2006) 99:1207–15. doi: 10.1161/01.RES.0000250758.63358.91
16. Desai U, Lee EC, Chung K, Gao C, Gay J, Key B, et al. Lipid-lowering effects of anti-angiopoietin-like 4 antibody recapitulate the lipid phenotype found in angiopoietin-like 4 knockout mice. *Proc Natl Acad Sci USA.* (2007) 104:11766–71. doi: 10.1073/pnas.0705041104
17. Dijk W, Kersten S. Regulation of lipoprotein lipase by Angptl4. *Trends Endocrinol Metab.* (2014) 25:146–55. doi: 10.1016/j.tem.2013.12.005
18. Kersten S. New insights into angiopoietin-like proteins in lipid metabolism and cardiovascular disease risk. *Curr Opin Lipidol.* (2019) 30:205–11. doi: 10.1097/MOL.0000000000000600
19. Aryal B, Price NL, Suarez Y, Fernandez-Hernando C. ANGPTL4 in metabolic and cardiovascular disease. *Trends Mol Med.* (2019) 25:723–34. doi: 10.1016/j.molmed.2019.05.010
20. Kristensen KK, Leth-Espensen KZ, Mertens HDT, Birrane G, Meiyappan M, Olivecrona G, et al. Unfolding of monomeric lipoprotein lipase by ANGPTL4: Insight into the regulation of plasma triglyceride metabolism. *Proc Natl Acad Sci USA.* (2020) 117:4337–46. doi: 10.1073/pnas.1920202117
21. Gutgsell AR, Ghodge SV, Bowers AA, Neher SB. Mapping the sites of the lipoprotein lipase (LPL)-angiopoietin-like protein 4 (ANGPTL4) interaction provides mechanistic insight into LPL inhibition. *J Biol Chem.* (2019) 294:2678–89. doi: 10.1074/jbc.RA118.005932
22. Kobayashi Y, Nakajima T, Inoue I. Molecular modeling of the dimeric structure of human lipoprotein lipase and functional studies of the carboxyl-terminal domain. *Eur J Biochem.* (2002) 269:4701–10. doi: 10.1046/j.1432-1033.2002.03179.x
23. van Tilbeurgh H, Roussel A, Lalouel JM, Cambillau C. Lipoprotein lipase. Molecular model based on the pancreatic lipase x-ray structure: consequences for heparin binding and catalysis. *J Biol Chem.* (1994) 269:4626–33.
24. Wong H, Yang D, Hill JS, Davis RC, Nikazy J, Schotz MC. A molecular biology-based approach to resolve the subunit orientation of lipoprotein lipase. *Proc Natl Acad Sci USA.* (1997) 94:5594–8. doi: 10.1073/pnas.94.11.5594
25. Sukonina V, Lookene A, Olivecrona T, Olivecrona G. Angiopoietin-like protein 4 converts lipoprotein lipase to inactive monomers and modulates lipase activity in adipose tissue. *Proc Natl Acad Sci U \SA.* (2006) 103:17450–5. doi: 10.1073/pnas.0604026103
26. Beigneux AP, Allan CM, Sandoval NP, Cho GW, Heizer PJ, Jung RS, et al. Lipoprotein lipase is active as a monomer. *Proc Natl Acad Sci USA.* (2019) 116:6319–28. doi: 10.1073/pnas.1900983116
27. Kinnunen PK, Jackson RL, Smith LC, Gotto AM Jr., Sparrow JT. Activation of lipoprotein lipase by native and synthetic fragments of human plasma apolipoprotein C-II. *Proc Natl Acad Sci USA.* (1977) 74:4848–51. doi: 10.1073/pnas.74.11.4848
28. Breckenridge WC, Little JA, Steiner G, Chow A, Poapst M. Hypertriglyceridemia associated with deficiency of apolipoprotein C-II. *N Engl J Med.* (1978) 298:1265–73. doi: 10.1056/NEJM197806082982301
29. Ueda M, Dunbar RL, Wolska A, Sikora TU, Escobar MDR, Seliktar N, et al. A novel APOC2 missense mutation causing apolipoprotein C-II deficiency with severe triglyceridemia and pancreatitis. *J Clin Endocrinol Metab.* (2017) 102:1454–7. doi: 10.1210/jc.2016-3903
30. Chait A, Brunzell JD. Chylomicronemia syndrome. *Adv Intern Med.* (1992) 37:249–73.
31. Xie SL, Chen TZ, Huang XL, Chen C, Jin R, Huang ZM, et al. Genetic variants associated with gestational hypertriglyceridemia and pancreatitis. *PLoS One.* (2015) 10:e0129488. doi: 10.1371/journal.pone.0129488
32. Okubo M, Hasegawa Y, Aoyama Y, Murase T. A G+1 to C mutation in a donor splice site of intron 2 in the apolipoprotein (apo) C-II gene in a patient with apo C-II deficiency. A possible interaction between apo C-II deficiency and apo E4 in a severely hypertriglyceridemic patient. *Atherosclerosis.* (1997) 130:153–60. doi: 10.1016/s0021-9150(96)06061-3
33. Wolska A, Dunbar RL, Freeman LA, Ueda M, Amar MJ, Sviridov DO, et al. Apolipoprotein C-II: new findings related to genetics, biochemistry, and role in triglyceride metabolism. *Atherosclerosis.* (2017) 267:49–60. doi: 10.1016/j.atherosclerosis.2017.10.025
34. Trusca VG, Fuior EV, Florea IC, Kardassis D, Simionescu M, Gafencu AV. Macrophage-specific up-regulation of apolipoprotein E gene expression by STAT1 is achieved via long range genomic interactions. *J Biol Chem.* (2011) 286:13891–904. doi: 10.1074/jbc.M110.179572
35. Mak PA, Laffitte BA, Desrumaux C, Joseph SB, Curtiss LK, Mangelsdorf DJ, et al. Regulated expression of the apolipoprotein E/C-I/C-IV/C-II gene cluster in murine and human macrophages. A critical role for nuclear liver X receptors alpha and beta. *J Biol Chem.* (2002) 277:31900–8. doi: 10.1074/jbc.M202993200
36. Amar MJ, Sakurai T, Sakurai-Ikuta A, Sviridov D, Freeman L, Ahsan L, et al. A novel apolipoprotein C-II mimetic peptide that activates lipoprotein lipase and decreases serum triglycerides in apolipoprotein E-knockout mice. *J Pharmacol Exp Ther.* (2015) 352:227–35. doi: 10.1124/jpet.114.220418
37. Shen Y, Lookene A, Zhang L, Olivecrona G. Site-directed mutagenesis of apolipoprotein CII to probe the role of its secondary structure for activation of lipoprotein lipase. *J Biol Chem.* (2010) 285:7484–92. doi: 10.1074/jbc.M109.022046
38. Hill JS, Yang D, Nikazy J, Curtiss LK, Sparrow JT, Wong H. Subdomain chimeras of hepatic lipase and lipoprotein lipase. Localization of heparin and

cofactor binding. *J Biol Chem.* (1998) 273:30979–84. doi: 10.1074/jbc.273.47.30979

39. Shen Y, Lookene A, Nilsson S, Olivecrona G. Functional analyses of human apolipoprotein CII by site-directed mutagenesis: identification of residues important for activation of lipoprotein lipase. *J Biol Chem.* (2002) 277:4334–42. doi: 10.1074/jbc.M105421200
40. Mason RP, Eckel RH. Mechanistic insights from REDUCE-IT STRENGTHen the case against triglyceride lowering as a strategy for cardiovascular disease risk reduction. *Am J Med.* (2021) 134:1085–90. doi: 10.1016/j.amjmed.2021.03.014
41. Neelamekam S, Kwok S, Malone R, Wierzbicki AS, Soran H. The impact of lipoprotein lipase deficiency on health-related quality of life: a detailed, structured, qualitative study. *Orphanet J Rare Dis.* (2017) 12:156. doi: 10.1186/s13023-017-0706-1
42. Donahoo WT, Jensen DR, Shepard TY, Eckel RH. Seasonal variation in lipoprotein lipase and plasma lipids in physically active, normal weight humans. *J Clin Endocrinol Metab.* (2000) 85:3065–8. doi: 10.1210/jcem.85.9.6816
43. Duncan GE, Perri MG, Theriaque DW, Hutson AD, Eckel RH, Stacpoole PW. Exercise training, without weight loss, increases insulin sensitivity and postheparin plasma lipase activity in previously sedentary adults. *Diabetes Care.* (2003) 26:557–62. doi: 10.2337/diacare.26.3.557
44. McCoy MG, Sun GS, Marchadier D, Maugeais C, Glick JM, Rader DJ. Characterization of the lipolytic activity of endothelial lipase. *J Lipid Res.* (2002) 43:921–9. doi: 10.1016/S0022-2275(20)30466-1
45. Jin W, Marchadier D, Rader DJ. Lipases and HDL metabolism. *Trends Endocrinol Metab.* (2002) 13:174–8. doi: 10.1016/s1043-2760(02)00589-1
46. Dallinga-Thie GM, Zonneveld-de Boer AJ, van Vark-van der Zee LC, van Haperen R, van Gent T, Jansen H, et al. Appraisal of hepatic lipase and lipoprotein lipase activities in mice. *J Lipid Res.* (2007) 48:2788–91. doi: 10.1194/jlr.D700021-JLR200
47. Goldberg RB, Chait A. A comprehensive update on the chylomicronemia syndrome. *Front Endocrinol (Lausanne).* (2020) 11:593931. doi: 10.3389/fendo.2020.593931
48. Lima JG, Helena CNL, Moura Bandeira FT, Pires Sousa AG, Medeiros de Araujo Macedo TB, Cavalcante Nogueira AC, et al. A novel GPIHBP1 mutation related to familial chylomicronemia syndrome: a series of cases. *Atherosclerosis.* (2021) 322:31–8. doi: 10.1016/j.atherosclerosis.2021.02.020
49. Sundaram M, Curtis KR, Amir Alipour M, LeBlond ND, Margison KD, Yaworski RA, et al. The apolipoprotein C-III (Gln38Lys) variant associated with human hypertriglyceridemia is a gain-of-function mutation. *J Lipid Res.* (2017) 58:2188–96. doi: 10.1194/jlr.M077313
50. Glodowski M, Christen S, Saxon DR, Hegele RA, Eckel RH. Novel PPARG mutation in multiple family members with chylomicronemia. *J Clin Lipidol.* (2021) 15:431–4. doi: 10.1016/j.jacl.2021.03.006
51. Singh AK, Chaube B, Zhang X, Sun J, Citrin KM, Canfran-Duque A, et al. Hepatocyte-specific suppression of ANGPTL4 improves obesity-associated diabetes and mitigates atherosclerosis in mice. *J Clin Invest.* (2021) 131:e140989. doi: 10.1172/JCI140989
52. Huynh K. Dual apoC-II mimetic and apoC-III antagonist for hypertriglyceridaemia. *Nat Rev Cardiol.* (2020) 17:201. doi: 10.1038/s41569-020-0351-6
53. Wolska A, Lo L, Sviridov DO, Pourmousa M, Pryor M, Ghosh SS, et al. A dual apolipoprotein C-II mimetic-apolipoprotein C-III antagonist peptide lowers plasma triglycerides. *Sci Transl Med.* (2020) 12:eaaw7905. doi: 10.1126/scitranslmed.aaw7905
54. Basu D, Manjur J, Jin W. Determination of lipoprotein lipase activity using a novel fluorescent lipase assay. *J Lipid Res.* (2011) 52:826–32. doi: 10.1194/jlr.D010744
55. Nikkila EA, Huttunen JK, Ehnholm C. Postheparin plasma lipoprotein lipase and hepatic lipase in diabetes mellitus. Relationship to plasma triglyceride metabolism. *Diabetes.* (1977) 26:11–21. doi: 10.2337/diab.26.1.11
56. Huttunen JK, Ehnholm C, Kinnunen PK, Nikkila EA. An immunochemical method for the selective measurement of two triglyceride lipases in human postheparin plasma. *Clin Chim Acta.* (1975) 63:335–47. doi: 10.1016/0009-8981(75)90055-8
57. Imamura S, Kobayashi J, Nakajima K, Sakasegawa S, Nohara A, Noguchi T, et al. A novel method for measuring human lipoprotein lipase and hepatic lipase activities in postheparin plasma. *J Lipid Res.* (2008) 49:1431–7. doi: 10.1194/jlr.M700528-JLR200
58. Cheng CF, Bensadoun A, Bersot T, Hsu JS, Melford KH. Purification and characterization of human lipoprotein lipase and hepatic triglyceride lipase. Reactivity with monoclonal antibodies to hepatic triglyceride lipase. *J Biol Chem.* (1985) 260:10720–7.
59. Greten H, DeGrella R, Klose G, Rascher W, de Gennes JL, Gjone E. Measurement of two plasma triglyceride lipases by an immunochemical method: studies in patients with hypertriglyceridemia. *J Lipid Res.* (1976) 17:203–10.
60. van Hoek M, Dallinga-Thie GM, Steyerberg EW, Sijbrands EJ. Diagnostic value of post-heparin lipase testing in detecting common genetic variants in the LPL and LIPC genes. *Eur J Hum Genet.* (2009) 17:1386–93. doi: 10.1038/ejhg.2009.61
61. Huttunen JK, Ehnholm C, Kekki M, Nikkila EA. Post-heparin plasma lipoprotein lipase and hepatic lipase in normal subjects and in patients with hypertriglyceridaemia: correlations to sex, age and various parameters of triglyceride metabolism. *Clin Sci Mol Med.* (1976) 50:249–60. doi: 10.1042/cs0500249
62. Lafferty MJ, Bradford KC, Erie DA, Neher SB. Angiopoietin-like protein 4 inhibition of lipoprotein lipase: evidence for reversible complex formation. *J Biol Chem.* (2013) 288:28524–34. doi: 10.1074/jbc.M113.497602
63. Sun T, Zhan W, Wei L, Xu Z, Fan L, Zhuo Y, et al. Circulating ANGPTL3 and ANGPTL4 levels predict coronary artery atherosclerosis severity. *Lipids Health Dis.* (2021) 20:154. doi: 10.1186/s12944-021-01580-z
64. Pfeifer MA, Brunzell JD, Best JD, Judzewitsch RG, Halter JB, Porte D Jr. The response of plasma triglyceride, cholesterol, and lipoprotein lipase to treatment in non-insulin-dependent diabetic subjects without familial hypertriglyceridemia. *Diabetes.* (1983) 32:525–31. doi: 10.2337/diab.32.6.525
65. Di Filippo M, Marcais C, Charriere S, Marmontel O, Broyer M, Delay M, et al. Post-heparin LPL activity measurement using VLDL as a substrate: a new robust method for routine assessment of plasma triglyceride lipolysis defects. *PLoS One.* (2014) 9:e99721. doi: 10.1371/journal.pone.0099721
66. Goldberg IJ, Scheraldi CA, Yacoub LK, Saxena U, Bisgaier CL. Lipoprotein ApoC-II activation of lipoprotein lipase. Modulation by apolipoprotein A-IV. *J Biol Chem.* (1990) 265:4266–72.
67. Hortin GL, Sviridov D, Anderson NL. High-abundance polypeptides of the human plasma proteome comprising the top 4 logs of polypeptide abundance. *Clin Chem.* (2008) 54:1608–16. doi: 10.1373/clinchem.2008.108175
68. Glaser DS, Yost TJ, Eckel RH. Preheparin lipoprotein lipolytic activities: relationship to plasma lipoproteins and postheparin lipolytic activities. *J Lipid Res.* (1992) 33:209–14.
69. Tsujita T, Ninomiya H, Okuda H. p-nitrophenyl butyrate hydrolyzing activity of hormone-sensitive lipase from bovine adipose tissue. *J Lipid Res.* (1989) 30:997–1004.
70. Rajan S, de Guzman HC, Palaia T, Goldberg IJ, Hussain MM. A simple, rapid, and sensitive fluorescence-based method to assess triacylglycerol hydrolase activity. *J Lipid Res.* (2021) 62:100115. doi: 10.1016/j.jlr.2021.100115
71. Spitler KM, Shetty SK, Cushing EM, Sylvers-Davie KL, Davies BSJ. Regulation of plasma triglyceride partitioning by adipose-derived ANGPTL4 in mice. *Sci Rep.* (2021) 11:7873. doi: 10.1038/s41598-021-87020-5
72. Geldenhuys WJ, Aring D, Sadana P. A novel Lipoprotein lipase (LPL) agonist rescues the enzyme from inhibition by angiopoietin-like 4 (ANGPTL4). *Bioorg Med Chem Lett.* (2014) 24:2163–7. doi: 10.1016/j.bmcl.2014.03.021
73. Yan Y, Zhang D, Zhou P, Li B, Huang SY. HDOCK: a web server for protein-protein and protein-DNA/RNA docking based on a hybrid strategy. *Nucleic Acids Res.* (2017) 45:W365–73. doi: 10.1093/nar/gkx407
74. Humphrey W, Dalke A, Schulten K. VMD: visual molecular dynamics. *J Mol Graph.* (1996) 14:33–8. doi: 10.1016/0263-7855(96)00018-5
75. Tunyasuvunakool K, Adler J, Wu Z, Green T, Zielinski M, Zidek A, et al. Highly accurate protein structure prediction for the human proteome. *Nature.* (2021) 596:590–6. doi: 10.1038/s41586-021-03828-1
76. EMBL-EBI. *Lipoprotein Lipase (Human). AlphaFold Structure Prediction P06858.* (n.d.). Available online at: https://alphafold.ebi.ac.uk/entry/P06858
77. EMBL-EBI. *Apolipoprotein C-II (Human). AlphaFold Structure Prediction.P02655.* (n.d.). Available online at: https://alphafold.ebi.ac.uk/entry/P02655

78. EMBL-EBI. *Angiopoietin-Related Protein 4 (mus musculus). AlphaFold Structure Prediction.Q9Z1P8*. (n.d.). Available online at: https://alphafold.ebi.ac.uk/entry/Q9Z1P8
79. Groot PH, Van Tol A. Metabolic fate of the phosphatidylcholine component of very low density lipoproteins during catabolism by the perfused rat heart. *Biochim Biophys Acta.* (1978) 530:188–96. doi: 10.1016/0005-2760(78)90004-8
80. Scow RO, Egelrud T. Hydrolysis of chylomicron phosphatidylcholine in vitro by lipoprotein lipase, phospholipase A2 and phospholipase C. *Biochim Biophys Acta.* (1976) 431:538–49. doi: 10.1016/0005-2760(76)90219-8
81. Stocks J, Galton DJ. Activation of the phospholipase A1 activity of lipoprotein lipase by apoprotein C-II. *Lipids.* (1980) 15:186–90. doi: 10.1007/BF02540967
82. Shirai K, Jackson RL. Lipoprotein lipase-catalyzed hydrolysis of p-nitrophenyl butyrate. Interfacial activation by phospholipid vesicles. *J Biol Chem.* (1982) 257:1253–8.
83. Shirai K, Jackson RL, Quinn DM. Reciprocal effect of apolipoprotein C-II on the lipoprotein lipase-catalyzed hydrolysis of p-nitrophenyl butyrate and trioleoylglycerol. *J Biol Chem.* (1982) 257:10200–3.
84. Egelrud T, Olivecrona T. Purified bovine milk (lipoprotein) lipase: activity against lipid substrates in the absence of exogenous serum factors. *Biochim Biophys Acta.* (1973) 306:115–27. doi: 10.1016/0005-2760(73)90215-4
85. Quinn DM, Shirai K, Jackson RL, Harmony JA. Lipoprotein lipase catalyzed hydrolysis of water-soluble p-nitrophenyl esters. Inhibition by apolipoprotein C-II. *Biochemistry.* (1982) 21:6872–9. doi: 10.1021/bi00269a038
86. Duque M, Graupner M, Stutz H, Wicher I, Zechner R, Paltauf F, et al. New fluorogenic triacylglycerol analogs as substrates for the determination and chiral discrimination of lipase activities. *J Lipid Res.* (1996) 37:868–76.

Conflict of Interest: The authors declare that the research was conducted in the absence of any commercial or financial relationships that could be construed as a potential conflict of interest.

Publisher's Note: All claims expressed in this article are solely those of the authors and do not necessarily represent those of their affiliated organizations, or those of the publisher, the editors and the reviewers. Any product that may be evaluated in this article, or claim that may be made by its manufacturer, is not guaranteed or endorsed by the publisher.

frontiers | Frontiers in Cardiovascular Medicine

TYPE Original Research
PUBLISHED 26 July 2022
DOI 10.3389/fcvm.2022.916031

OPEN ACCESS

EDITED BY
Nathalie Pamir,
Oregon Health and Science University, United States

REVIEWED BY
Federico Vancheri,
S. Elia Hospital, Italy
Krzysztof Dyrbuś,
Silesian Center for Heart Diseases, Poland
Oliver Weingärter,
University Hospital Jena, Germany

*CORRESPONDENCE
Sonia Ruiz-Bustillo
sruiz@psmar.cat

SPECIALTY SECTION
This article was submitted to Lipids in Cardiovascular Disease, a section of the journal Frontiers in Cardiovascular Medicine

RECEIVED 08 April 2022
ACCEPTED 08 July 2022
PUBLISHED 26 July 2022

CITATION
Ruiz-Bustillo S, Badosa N, Cabrera-Aguilera I, Ivern C, Llagostera M, Mojón D, Vicente M, Ribas N, Recasens L, Martí-Almor J, Cladellas M and Farré N (2022) An intensive, structured, mobile devices-based healthcare intervention to optimize the lipid-lowering therapy improves lipid control after an acute coronary syndrome.
Front. Cardiovasc. Med. 9:916031.
doi: 10.3389/fcvm.2022.916031

An intensive, structured, mobile devices-based healthcare intervention to optimize the lipid-lowering therapy improves lipid control after an acute coronary syndrome

Sonia Ruiz-Bustillo[1,2,3,4]*, Neus Badosa[1,2], Ignacio Cabrera-Aguilera[1,5,6], Consol Ivern[1,2], Marc Llagostera[2], Diana Mojón[2], Miren Vicente[2], Núria Ribas[1,2], Lluis Recasens[1,2], Julio Martí-Almor[1,2,3], Mercè Cladellas[1,2,3] and Núria Farré[1,2,3,4]

[1]Heart Diseases Biomedical Research Group, IMIM (Hospital del Mar Medical Research Institute), Barcelona, Spain, [2]Cardiac Rehabilitation Unit, Department of Cardiology, Hospital del Mar, Barcelona, Spain, [3]Departament of Medicine, Autonomous University of Barcelona, Barcelona, Spain, [4]Department of Medicine, Pompeu Fabra University, Barcelona, Spain, [5]Unitat de Biofísica i Bioenginyeria, Facultat de Medicina i Ciéncies de la Salut, Universitat de Barcelona, Barcelona, Spain, [6]Department of Human Movement Sciences, Faculty of Health Sciences, School of Kinesiology, Universidad de Talca, Talca, Chile

Aims: Despite the evidence, lipid-lowering treatment (LLT) in secondary prevention remains insufficient, and a low percentage of patients achieve the recommended LDL cholesterol (LDLc) levels by the guidelines. We aimed to evaluate the efficacy of an intensive, mobile devices-based healthcare lipid-lowering intervention after hospital discharge in patients hospitalized for acute coronary syndrome (ACS).

Methods and results: Ambiespective register in which a mobile devices-based healthcare intervention including periodic follow-up, serial lipid level controls, and optimization of lipid-lowering therapy, if appropriate, was assessed in terms of serum lipid-level control at 12 weeks after discharge. A total of 497 patients, of which 462 (93%) correctly adhered to the optimization protocol, were included in the analysis. At the end of the optimization period, 327 (70.7%) patients had LDLc levels $\leq$ 70 mg/dL. 40% of patients in the LDLc $\leq$ 70 mg/dL group were upgraded to very-high intensity lipid-lowering ability therapy vs. 60.7% in the LDLc $>$ 70 mg/dL group, $p < 0.001$. Overall, 38.5% of patients had at least a change in their LLT. Side effects were relatively infrequent (10.7%). At 1-year follow-up, LDLc levels were measured by the primary care physician in 342 (68.8%) of the whole cohort of 497 patients. In this group, 71.1% of patients had LDLc levels $\leq$ 70 mg/dL.

Conclusion: An intensive, structured, mobile devices-based healthcare intervention after an ACS is associated with more than 70% of patients reaching the LDLc levels recommended by the clinical guidelines. In patients with LDLc measured at 1-year follow-up, 71.1% had LDLc levels ≤ 70 mg/dL.

KEYWORDS

ischemic heart disease, secondary prevention, cardiovascular risk factors, lipid-lowering therapy, mobile devices-based healthcare

Introduction

There is extensive evidence confirming the benefit of cardiac rehabilitation programs (CRP) in patients with ischemic heart disease (IHD) (1). An intensive CRP reduces cardiovascular risk through lifestyle changes (2). However, correct pharmacological treatment is also crucial for optimal cardiovascular risk factors control, including dyslipidemia. The drop in low-density lipoprotein cholesterol (LDLc) levels in secondary prevention significantly reduces mortality, coronary events, coronary revascularization procedures, and ischemic strokes (3).

Despite the evidence, lipid-lowering treatment (LLT) in secondary prevention remains insufficient, and a low percentage of patients achieve the LDLc levels recommended by the guidelines (4–6). One factor explaining this contradiction is the so-called therapeutic inertia, defined as the failure of physicians to initiate or intensify an indicated therapy (7). Other significant barriers are lack of infrastructure and availability of CRP, lack of perceived importance of secondary prevention among professionals, and low patient motivation and financial difficulties to pay the LLT (8).

Mobile devices-based healthcare (mHealth) aimed at improving patients' living standards (9) can be an effective tool to improve the suboptimal results in dyslipidemia control (10). Considering the disappointing results in secondary prevention, we conducted a randomized pilot study to evaluate whether an intensive mHealth lipid-lowering intervention implemented after a hospitalization due to IHD was associated with a lower LDLc level. We demonstrated that this strategy was associated with improved management of LDLc levels compared with standard care alone (11). Our current study aimed to assess whether this same structured mHealth-based protocol helped improve LDLc levels after a hospitalization due to IHD in a real-life population.

Materials and methods

Study design and participants

The Risk Optimization Acute Coronary Syndrome (RiskOp-ACS) study was a single-center ambispective register assessing the efficacy and safety of a lipid-lowering intervention to improve the management of LDLc levels in patients hospitalized for IHD (ClinicalTrials.gov Identifier: NCT03619395). Between July 2018 and September 2019, all patients hospitalized for IHD in our hospital not meeting any exclusion criteria (inability or refusal to sign the informed consent or presenting comorbidities with a life expectancy of less than 1 year) and willing to participate in the CRP were screened for inclusion in this study. All patients providing written informed consent were included in the RiskOp-ACS register. The Ethics Committee of the Hospital del Mar approved the study and was conducted per the Declaration of Helsinki. The Ethics Committee approved the retrospective inclusion of patients who followed the same protocol since November 2016 to increase the sample size and waived the need for written informed consent. Therefore, all patients included in the study (both prospectively and retrospectively) followed the same optimization protocol.

Cardiac rehabilitation program

The multidisciplinary CRP performed in our center is coordinated by specialized nurses. It includes interventions performed by cardiologists, nurses, rehabilitation physicians, and professionals specialized in managing anxiety and other mental health disorders. All patients discharged after a hospitalization for an acute IHD event and with no severe cognitive impairment are invited to the CRP. As part of the program activities, nurses educate patients in healthy habits during the in-hospital stage and at follow-up visits at 3 and 12 months after discharge; provide and monitor the quality of life, anxiety, and depression symptoms using validated tests, and coordinate the follow-up plan and visits. Rehabilitation physicians and physiotherapists assess the patient's functional status and indicate and supervise physical activity during follow-up. All professionals involved in the CRP participate in monthly group sessions aimed at reinforcing the health education of the patients, with a particular focus on increasing the patients' understanding of the pathophysiology of IHD, on the role of cardiovascular risk factors, and the importance of optimal risk factor management, mainly through physical activity,

control of anxiety, and adherence to guideline-recommended pharmacotherapies.

Intervention

All patients were discharged under LLT. Serum lipid levels were measured at week 6 after discharge, and a virtual visit with the cardiologist was made within 1 week of the blood test. The laboratory test results were evaluated using a pre-specified algorithm based on clinical practice guidelines (**Supplementary Figure 1**). If there was a need to modify the LLT, the electronic prescription was changed accordingly, and the patient was informed by phone. Thus, the protocol avoided the need to come to the hospital or primary care center since the medication could be retrieved directly from the local pharmacy or printed/seen in the personal health record through a dedicated app/website created by the Health Department (*Lamevasalut*). This intervention was repeated every 6 weeks after every pharmacological change until the target LDLc levels (calculated by the Friedewald formula) advised in the clinical guidelines were achieved, or maximum lipid-lowering therapy according to local regulation was reached. Thus, the duration of the intervention was a maximum of 3 months ("optimization period"). From that moment, the follow-up was performed by the patient's primary care general physician and primary care cardiologist. Creatinine kinase and liver tests were measured in all blood tests following LLT modification.

The LLT intensity was defined according to its ability to reduce LDLc (12, 13). The moderate lipid-lowering ability group comprises moderate-intensity statins and low-intensity statin plus ezetimibe. High-intensity statins, and medium-intensity statins plus ezetimibe are the high-reduction group. High-potency statins plus ezetimibe are the very-high reduction group. Finally, PCSK9 inhibitor added at maximally tolerated doses to LLT is considered extreme reduction ability treatment (**Supplementary Table 1**). In our country, the prescription of PCSK9 inhibitors is allowed in the public health system for patients with established cardiovascular disease and no optimal control defined as LDLc > 100 mg/dL despite the maximum tolerated dose of statins, patients intolerant to statins, or in whom statins are contraindicated (14).

Study endpoints

The primary study endpoint was the proportion of patients with serum LDLc levels ≤ 70 mg/dL at the end of the optimization period, which was the treatment goal supported by current ESC guidelines (15) when the study was conducted. Other variables related to lipid management assessed during the intervention included lipid-lowering medication use, changes in lipid-lowering medication, and the presence of side effects, among others. As an exploratory analysis, the number of patients who reached LDLc levels < 55 mg/dL at the end of the optimization period was also analyzed. Finally, we assessed also as an exploratory analysis, clinical outcomes with the achievement of LDL ≤ 70 mg/dL at the end of the optimization period.

Statistical analyses

Data for continuous variables are expressed as mean ± standard deviation (SD) or median and interquartile range (IQR) based on normality distribution assessed by Kolmogorov-Smirnov test. Categorical variables were expressed as percentages. Differences in baseline characteristics between groups were tested using the χ^2-test (categorical variables) and Student's *t*-test or Mann–Whitney *U*-test, one-way analysis of variance, or Kruskal-Wallis test for continuous variables. All analysis was performed using IBM SPSS Statistics v25 (Armonk, NY, United States). For all tests, $p < 0.05$ was considered as statically significant.

Results

The whole cohort included 497 patients, of which 462 (93%) correctly adhered to the optimization protocol and were included in the analysis. At the end of the optimization period, 327 (70.7%) patients had LDLc levels ≤ 70 mg/dL, and 159 (34.7%) had LDLc levels < 55 mg/dL.

According to LDLc levels achieved, baseline characteristics of patients are described in **Table 1**. Interestingly, the only differences between both groups were a higher prevalence of chronic obstructive pulmonary disease in the LDLc ≤ 70 mg/dL group and different history of smoking.

Table 2 shows LDLc levels at baseline and during follow-up, the type of LLT given, and the presence of side effects. Interestingly, LLT did not differ at discharge from the hospital, with 65% of patients on high lipid-lowering ability treatment. However, by the end of the optimization therapy, 40% of patients in the LDL ≤ 70 mg/dL levels were upgraded to very-high intensity lipid-lowering ability vs. 60.7% in the LDL levels > 70 mg/dL, $p < 0.001$. Overall, 38.5% of patients had at least a change in their LLT. The LDLc levels > 70 mg/dL group had a higher number of changes in medications (61.4 vs. 27.5%, $p < 0.001$). However, this treatment modification was not enough to achieve good LDLc control in this group. During the optimization period, only 14 (2.8%) received extreme lipid-lowering ability treatment with PCSK-9 inhibitors, 5 (1.5%) patients in the LDLc ≤ 70 mg/dL, and 9 (6.9%) patients in the LDL levels > 70 mg/dL, $p = 0.003$.

Side effects were relatively infrequent, with 53 reports (10.7%) of the cohort (patients could have more than one side

TABLE 1 Baseline characteristics of patients according to LDLc levels after the optimization protocol.

	LDLc ≤ 70 mg/dL (*n* = 327)	LDLc > 70 mg/dL (*n* = 135)	*P*-value
Age (years)	62.9 ± 11.6	62.9 ± 11.9	0.98
Women (*n*, %)	56 (17.1)	30 (22.9)	0.15
BMI (Kg/m2)	27.7 ± 4.0	27.7 ± 4.6	0.95
Risk factors and comorbidities			
Hypertension (*n*, %)	185 (56.6)	72 (55)	0.75
Hyperlipidemia (*n*, %)	207 (63.3)	94 (71.8)	0.09
Diabetes mellitus (*n*, %)	100 (30.6)	33 (25.2)	0.25
Current smoker (*n*, %)	119 (36.4)	65 (49.6)	0.008
Previous smoker > 1 year (*n*, %)	114 (34.9)	29 (22.1)	
Previous smoker < 1 year (*n*, %)	16 (4.9)	2 (1.5)	
Previous ACS-MI (*n*, %)	60 (18.3)	25 (19.1)	0.86
COPD (*n*, %)	32 (9.8)	5 (3.8)	0.02
Cerebrovascular disease (*n*, %)	18 (5.5)	5 (3.8)	0.46
Peripheral vascular disease (*n*, %)	25 (7.6)	9 (6.9)	0.78
Anemia (*n*, %)	53 (16.2)	28 (21.4)	0.19
Chronic kidney disease (*n*, %)	21 (6.4)	7 (5.3)	0.66
Index hospitalization			
STEMI (*n*, %)	140 (42.8)	60 (45.8)	0.79
NSTEMI (*n*, %)	118 (36.1)	43 (32.8)	
Unstable Angina (*n*, %)	69 (21.1)	28 (21.4)	
One vessel disease (*n*, %)	170 (52)	76 (58)	0.29
Two vessel disease (*n*, %)	85 (26)	28 (21.4)	
Three vessel disease (*n*, %)	63 (19.3)	20 (15.3)	
Left main disease (*n*, %)	14 (4.3)	9 (6.9)	0.25
Coronary percutaneous angioplasty (*n*, %)	280 (85.6)	107 (81.7)	0.29
Ejection fraction (%)	56.4 ± 10.0	55.6 ± 10.2	0.42

Data are mean ± SD, median (IQR), or n (%). BMI, Body mass index; COPD, chronic obstructive pulmonary disease; CV, Cardiovascular; STEMI, ST-elevation myocardial infarction; NSTEMI, non-ST-elevation myocardial infarction; ACS-MI, Acute coronary syndrome-myocardial infarction.

effect reported). The more common side effects were abnormal asymptomatic liver tests, increased creatine-kinase levels, and myalgia. However, these side effects were rarely associated with LLT discontinuation. In most cases, side effects led to a change or temporary suspension in LLT in 4.3% of patients, without differences in both groups.

At 1-year follow-up, LDLc levels were measured by the local cardiologist or primary care physician in 342 (68.8%) of the whole cohort of 497 patients. In this group, 71.1% of patients had LDLc levels ≤ 70 mg/dL. Interestingly, 77.4% of patients with LDL ≤ 70 mg/dL at the end of optimization still had LDL levels ≤ 70 mg/dL at 1-year follow-up, whereas 59.6% of patients who did not reach LDLc ≤ 70 mg/dL did so at 1 year.

At a median follow-up of 30 (p25–75: 21–38) months, patients who achieved an LDLc ≤ 70 mg/dL after the optimization protocol had a numerically lower incidence of myocardial infarction [12 (3.6%) patients vs. 10 (7.5%), $p = 0.08$], need of new revascularization [22 (6.7%) patients vs. 10 (7.5%), $p = 0.77$), death (12 (3.6%) patients vs. 8 (6%), $p = 0.27$], and the composite end-point that comprised the 3 outcomes [33 (10%) vs. 22 (16.4%), $p = 0.054$] compared to those who did not achieve an LDLc ≤ 70 mg/dL.

Discussion

Our study showed that an intensive, structured, mHealth post-discharge follow-up plan to optimize the lipid-lowering pharmacotherapy was associated with achieving a target LDLc ≤ 70 mg/dL in 70.7% of patients after an acute coronary syndrome (ACS). Reduction and achievement of LDLc target value were obtained early (between 6 and 12 weeks after the ACS) as recommended in the literature (16). It is also important to emphasize that the intervention was carried out using low-cost phone-based telemedicine techniques (mHealth) that facilitate its implementation and patient follow-up. The use of mHealth might explain why less than 8% of the patients did not adhere to follow-up.

Considering the few significant baseline characteristics differences between the LDLc ≤ 70 mg/dL and

10.3389/fcvm.2022.916031

TABLE 2 Baseline LDL levels and medication changes according to LDL levels reached.

	LDLc ≤ 70 mg/dL (*n* = 327)	LDLc > 70 mg/dL (*n* = 135)	*P*-value
Baseline LDLc	103.9 ± 36.6	115.2 ± 45.2	0.012
End of optimization LDLc	53.4 ± 10.1	85.0 ± 16.7	< 0.001
Δ LDLc at the end of optimization (absolute reduction)	−50.0 (−21, −77)	−31.0 (+ 2, −53)	< 0.001
Δ LDLc at the end of optimization (relative reduction)	−47.5 (−25, −60.1)	−26.2 (+ 2.6, −41.0)	< 0.001
1-year LDLc levels	61.5 ± 18.3	69.9 ± 25.4	0.003
Baseline LLT			
Moderate lowering ability (*n*, %)	17 (5.3)	7 (5.4)	0.21
High lowering ability (*n*, %)	206 (63.8)	88 (68.2)	
Very high lowering ability (*n*, %)	96 (29.7)	30 (23.3)	
LLT end of optimization			
Moderate lowering ability (*n*, %)	15 (4.5)	3 (2.2)	< 0.001
High lowering ability (*n*, %)	171 (52.2)	40 (29.6)	
Very high lowering ability (*n*, %)	131 (40)	82 (60,7)	
Extreme lowering ability (*n*, %)	5 (1.5)	10 (7.4)	
Number of side effects reported (*n*, %)	38 (11.8)	15 (11.6)	0.97
Side effects			
Liver test abnormalities (*n*, %)	24 (7.3)	6 (4.4)	0.30
Creatine Kinase increase (*n*, %)	6 (1.8)	4 (2.9)	
Myalgia (*n*, %)	3 (0.9)	4 (2.9)	
Change in LLT (*n*, %)	90 (27.5)	83 (61.4)	< 0.001
LLT at 1 year			
Moderate lowering ability (*n*, %)	11 (4.5)	2 (2)	0.46
High lowering ability (*n*, %)	113 (46.1)	45 (45)	
Very high lowering ability (*n*, %)	117 (47.8)	51 (51)	

Data are mean ± SD, median (IQR), or n (%). LDLc, low-density lipoprotein cholesterol LLT; lipid lowering therapy.

LDLc > 70 mg/dL groups, these differences did not allow us to identify those patients who would achieve proper LDLc control. It is worth mentioning that the percentage of patients achieving LDLc ≤ 70 mg/dL in this real-life study is even better than the results we obtained in a previous randomized study in which we used the same strategy, where an LDLc ≤ 70 mg/dL was achieved in 62% of the patients (10). Moreover, these results contrast positively with the poor results described in our hospital before implementing the study intervention (4). This insufficient control of dyslipidemia in very high-risk patients coincides with that described more recently in the literature. The ESC-EORP Euroaspire V survey performed in 27 European countries showed that the prevalence of LDLc ≤ 70 mg/dL in the entire cohort was 30% (5). Similar findings were found in a retrospective analysis of patients with ACS in Finland, where two-thirds of patients on statin therapy did not achieve the LDLc level target recommended by the guidelines (6). According to these data, our strategy could more than double the number of patients with adequate LDLc level control after a hospitalization due to IHD.

The most recent ESC/EAS guidelines for the management of dyslipidemias published in 2019 advise an LDLc < 55 mg/dL for high and very high-risk patients. The recommendations regarding the treatment goals for LDLc are based in the studies that have shown that the lower the LDLc level the better (17). These guidelines were not published during the performance of our study. In our cohort, 34.7% of the patients achieved an LDLc < 55 mg/dL. It is worth noting that it was not the target level of our study and, thus, there was some room for LLT optimization. This result improves that reported in the DA VINCI study; being one of the first comparative analyses evaluating 2019 risk-based goal attainment, showed that three-quarters of patients did not meet their 2019 LDLc goals (18).

The inability to achieve an LDLc level ≤ 70 mg/dl was not due to therapeutic inertia. Intensifications or treatment changes were done in 64% of the patients. When changes were not made, patients were already on the maximum dose of oral treatment, did not tolerate a higher dose or did not meet the local criteria for using PCSK9 inhibitors. This intensification effort is superior to the ones described in the literature. The GOULD prospective observational registry study was carried out simultaneously in the United States. A total of 5,006 patients with established atherosclerotic cardiovascular disease were enrolled. Surprisingly, only 17%

had LLT intensification after 2 years, while two-thirds remained at an LDLc level > 70 mg/dL (19). Another important finding in our study is that 95% of the patients at the end of the optimization period were treated with drugs included in the high, very high, or extreme lipid-lowering ability groups. In the register published by Navar et al., of almost 3,297 patients analyzed, only 47% of the patients who required secondary prevention were treated with the appropriate intensity of treatment (20). One of the hypotheses that may justify not achieving an optimal decrease in LDLc, despite treatment is the described lack of response to statin treatment. A meta-analysis of genome-wide association studies showed that two loci of the genome are responsible for about 5% of the variation in an individual's response to statin treatment (21). The JUPITER study highlights that 43% of high-risk patients had an LDLc reduction < 50 and 11% showed no reduction or even an increase in LDLc with statin treatment (22).

Large cardiovascular outcomes trials showed a prognostic benefit with PCSK9 inhibitors monoclonal antibodies (23, 24), and it has been estimated that 30% of patients could be candidates of PCSK9 inhibitors (25). However, the use of PCSK9 inhibitors in our study was low due to prescription restrictions in our country. PCSK9 inhibition obtains further lowering of LDLc beyond that achieved with statin therapy and cholesterol absorption inhibitors; an incremental reduction in LDLc of 50% from baseline has been shown (26). Knowing that the LDLc levels in the group with LDLc > 70 mg/dL were 85.0 ± 16.7 mg/dL and the hypothetical additional reduction of 50%, we theorized that we could have even achieved 100% of patients with LDLc target levels if we had been allowed to expand the use of PCSK9 inhibitors.

Numerous studies with lipid-lowering drugs have shown that the reduction of LDLc levels translates into a reduction in cardiovascular events, giving rise to the current recommendations in secondary prevention (17). We saw that patients who achieved an LDLc ≤ 70 mg/dL after the optimization protocol had numerically fewer clinical endpoints. However, it is important to remark that the study was underpowered to detect hard endpoint due to the relatively small sample size and the number of events.

One of the reasons that might limit LLT is side effects. Some physicians and patients might be reluctant to begin or maintain statins, most commonly because of perceived side effects that are not confirmed (i.e., the nocebo effect) (27). However, statins are generally well-tolerated drugs (25). 11% of the patients had any side effects in our cohort, with no significant differences between the LDLc group ≤ 70 mg/dL and the LDLc group > 70 mg/dL. The most frequent side effect was the liver tests abnormalities (79%), followed by an increase in creatinine kinase (26%) and finally myalgias (18%). These data are comparable to those previously described (15, 28).

After the treatment optimization period, the patient's primary care general physician and primary care cardiologist performed the follow-up. We decided to analyze whether the good results achieved in the first 3 months were maintained after 12 months. Surprisingly, 31% of the patients did not have a follow-up blood test at month 12. In those patients who did have an LDLc assessment at 1 year, 71.1% of the patients maintained an LDLc ≤ 70 mg/dl. This group comprises 77.4% of the patients who already had an LDLc ≤ 70 mg/dl initially and patients who had not reached this target level originally (59.6%). This percentage of patients with a target LDLc level after 12 months remains significantly higher than the results reported in the literature (4–6).

Our study used the simplest and most readily usable form of mHealth, such as telephone calls. We believe that it was a determining factor in the success of this follow-up protocol. A randomized study in Sweden (29) and a meta-analysis of randomized controlled trials (10) showed improved LDLc levels with mHealth.

Limitations

As a single-center study, the results might not apply to other settings. Some of the patients were included retrospectively, potentially leading to bias. Still, given that all patients followed the same protocol and that the information was documented in the medical record, we believe that the risk of bias in this study is negligible.

Conclusion

An intensive, structured, mobile devices-based healthcare intervention after an ACS is associated with more than 70% of patients reaching the LDLc levels recommended by the clinical guidelines. This strategy uses low-cost and easy-to-apply telemedicine techniques that can be replicated in various clinical settings.

Data availability statement

The original contributions presented in this study are included in the article/**Supplementary material**, further inquiries can be directed to the corresponding author.

Ethics statement

The patients/participants prospectively included in the study provided their written informed consent. The patients/participants included retrospectively did not require informed consent after evaluation by the Research Ethics Committee of the Hospital del Mar.

Author contributions

SR-B: conceptualization and writing original draft preparation. SR-B and NF: methodology, project administration, and validation. NF: formal analysis and writing – review and editing. SR-B, NB, CI, NF, and NR: investigation. IC-A, MV, DM, ML, LR, SR-B, and NF: data curation. NB, CI, IC-A, DM, MV, ML, NR, LR, JM-A, and MC: visualization. NF, JM-A, and MC: supervision. All authors contributed to the article and approved the submitted version.

Conflict of interest

The authors declare that the research was conducted in the absence of any commercial or financial relationships that could be construed as a potential conflict of interest.

Publisher's note

Supplementary material

The Supplementary Material for this article can be found online at: https://www.frontiersin.org/articles/10.3389/fcvm.2022.916031/full#supplementary-material

SUPPLEMENTARY FIGURE 1
Lipid-lowering treatment optimization algorithm.

References

1. Visseren FLJ, Mach F, Smulders YM, Carballo D, Koskinas KC, Bäck M, et al. 2021 ESC guidelines on cardiovascular disease prevention in clinical practice. *Eur Heart J.* (2021) 42:3227–337. doi: 10.1093/eurheartj/ehab484

2. Wood DA, Kotseva K, Connolly S, Jennings C, Mead A, Euroaction Study Group, et al. Nurse-coordinated multidisciplinary, family-based cardiovascular disease prevention programme (EUROACTION) for patients with coronary heart disease and asymptomatic individuals at high risk of cardiovascular disease: a paired, cluster-randomised controlled trial. *Lancet.* (2008) 371:1999–2012. doi: 10.1016/S0140-6736(08)60868-5

3. Cannon CP, Braunwald E, McCabe CH, Rader DJ, Rouleau JL, Belder R, et al. Intensive versus moderate lipid lowering with statins after acute coronary syndromes. *N Engl J Med.* (2004) 350:1495–504. doi: 10.1056/NEJMoa040583

4. Ribas N, García-García C, Meroño O, Recasens L, Pérez-Fernández S, Bazán V, et al. Secondary prevention strategies after an acute ST-segment elevation myocardial infarction in the AMI code era: beyond myocardial mechanical reperfusion. *BMC Cardiovasc Disord.* (2017) 17:54. doi: 10.1186/s12872-017-0493-6

5. De Backer G, Jankowski P, Kotseva K, Mirrakhimov E, Reiner Ž, Rydén L, et al. Management of dyslipidaemia in patients with coronary heart disease: results from the ESC-EORP EUROASPIRE V survey in 27 countries. *Atherosclerosis.* (2019) 285:135–46. doi: 10.1016/j.atherosclerosis.2019.03.014

6. Leskelä RL, Torvinen A, Rissanen TT, Virtanen V, Herse F, Nuutinen M, et al. Outcomes of lipid control in secondary prevention of coronary artery disease in Finland: a 24-month follow-up after acute coronary syndrome. *Atherosclerosis.* (2020) 296:4–10. doi: 10.1016/j.atherosclerosis.2020.01.018

7. Lázaro P, Murga N, Aguilar D, Hernández-Presa MA. Therapeutic inertia in the outpatient management of dyslipidemia in patients with ischemic heart disease. The inertia study. *Rev Esp Cardiol.* (2010) 63:1428–37. doi: 10.1016/s1885-5857(10)70277-2

8. Fitzsimons D, Stępińska J, Kerins M, Piepoli MF, Hill L, Nuutinen M, et al. Secondary prevention and cardiovascular care across Europe: a survey of European society of cardiology members' views. *Eur J Cardiovasc Nurs.* (2020) 19:201–11. doi: 10.1177/1474515119877999

9. Akter S, Roy P. mHealth – an ultimate platformto serve the unserved. *Yearbook Med Inform.* (2010) 1:94–100.

10. Akbari M, Lankarani KB, Naghibzadeh-Tahami A, Tabrizi R, Honarvar B, Kolahdooz F, et al. The effects of mobile health interventions on lipid profiles among patients with metabolic syndrome and related disorders: a systematic review and meta-analysis of randomized controlled trials. *Diabetes Metab Syndr.* (2019) 13:1949–55. doi: 10.1016/j.dsx.2019.04.011

11. Ruiz-Bustillo S, Ivern C, Badosa N, Farre N, Marco E, Bruguera J, et al. Efficacy of a nurse-led lipid-lowering secondary prevention intervention in patients hospitalized for ischemic heart disease: a pilot randomized controlled trial. *Eur J Cardiovasc Nurs.* (2019) 18:366–74. doi: 10.1177/1474515119831511

12. Masana L, Pedro-Botet J, Civeira F. IMPROVE-IT clinical implications. Should the "high-intensity cholesterol-lowering therapy" strategy replace the "high-intensity statin therapy"? *Atherosclerosis.* (2015) 240:161–2. doi: 10.1016/j.atherosclerosis.2015.03.002

13. Escobar C, Anguita M, Arrarte V, Barrios V, Cequier A, Cosín-Sales J, et al. Recommendations to improve lipid control. Consensus document of the Spanish society of cardiology. *Rev Esp Cardiol.* (2020) 73:161–7. doi: 10.1016/j.rec.2019.08.012

14. Agencia Española de Medicamentos y Productos Sanitarios. *Informe de Posicionamiento Terapéutico de Evolocumab en Hipercolesterolemia. Fecha de Adopción de la Actualización de la Fase I del Informe Por el GCPT.* Madrid: Agencia Española de Medicamentos y Productos Sanitarios (2020).

15. Piepoli MF, Hoes AW, Agewall S, Albus C, Brotons C, Catapano AL, et al. ESC scientific document group. 2016 European guidelines on cardiovascular disease prevention in clinical practice: the sixth joint task force of the European society of cardiology and other societies on cardiovascular disease prevention in clinical practice (constituted by representatives of 10 societies and by invited experts). Developed with the special contribution of the European association for cardiovascular prevention & rehabilitation (EACPR). *Eur Heart J.* (2016) 37:2315–81. doi: 10.1093/eurheartj/ehw106

16. Schiele F, Farnier M, Krempf M, Bruckert E, Ferrières J. A consensus statement on lipid management after acute coronary syndrome. *Eur Heart J Acute Cardiovasc Care.* (2018) 7:532–43. doi: 10.1177/2048872616679791

17. Mach F, Baigent C, Catapano AL, Koskinas KC, Casula M, Badimon L, et al. 2019 ESC/EAS guidelines for the management of dyslipidaemias: lipid modification to reduce cardiovascular risk. *Eur Heart J.* (2020) 41:111–88. doi: 10.1093/eurheartj/ehz455

18. Vrablik M, Seifert B, Parkhomenko A, Banach M, Jóźwiak JJ, Kiss RG, et al. Lipid-lowering therapy use in primary and secondary care in central and Eastern Europe: DA VINCI observational study. *Atherosclerosis.* (2021) 334:66–75. doi: 10.1016/j.atherosclerosis.2021.08.035

19. Cannon CP, de Lemos JA, Rosenson RS, Ballantyne CM, Liu Y, Gao Q, et al. Use of lipid-lowering therapies over 2 years in GOULD, a registry of patients with atherosclerotic cardiovascular disease in the US. *JAMA Cardiol.* (2021) 6:1–9. doi: 10.1001/jamacardio.2021.1810

20. Navar AM, Wang TY, Li S, Robinson JG, Goldberg AC, Virani S, et al. Lipid management in contemporary community practice: results from the provider

assessment of lipid management (PALM) registry. *Am Heart J.* (2017) 193:84–92. doi: 10.1016/j.ahj.2017.08.005

21. Postmus I, Trompet S, Deshmukh HA, Barnes MR, Jóźwiak JJ, Kiss RG, et al. Pharmacogenetic meta-analysis of genome-wide association studies of LDL cholesterol response to statins. *Nat Commun.* (2014) 5:5068. doi: 10.1038/ncomms6068

22. Ridker PM, Mora S, Rose L, Jupiter Trial Study Group. Percent reduction in LDL cholesterol following high-intensity statin therapy: potential implications for guidelines and for the prescription of emerging lipid-lowering agents. *Eur Heart J.* (2016) 37:1373–9. doi: 10.1093/eurheartj/ehw046

23. Sabatine MS, Giugliano RP, Keech AC, Honarpour N, Wiviott SD, Murphy SA, et al. FOURIER Steering Committee and Investigators. Evolocumab and clinical outcomes in patients with cardiovascular disease. *N Engl J Med.* (2017) 376:1713–22. doi: 10.1056/NEJMoa1615664

24. Schwartz GG, Steg PG, Szarek M, Bhatt DL, Bittner VA, Diaz R, et al. ODYSSEY OUTCOMES committees and Investigators. Alirocumab and cardiovascular outcomes after acute coronary syndrome. *N Engl J Med.* (2018) 379:2097–107. doi: 10.1056/NEJMoa1801174

25. Elamin AFM, Grafton-Clarke C, Chen KW, Obafemi T, Luvai A, Katira R, et al. Potential use of PCSK9 inhibitors as a secondary preventative measure for cardiovascular disease following acute coronary syndrome: a UK real-world study. *Postgrad Med J.* (2019) 95:61–6. doi: 10.1136/postgradmedj-2018-136171

26. Furtado RHM, Giugliano RP. What lessons have we learned and what remains to be clarified for PCSK9 inhibitors?. A review of FOURIER and ODYSSEY Outcomes Trials. *Cardiol Ther.* (2020) 9:59–73. doi: 10.1007/s40119-020-00163-w

27. Howard JP, Wood FA, Finegold JA, Nowbar AN, Thompson DM, Arnold AD, et al. Side effect patterns in a crossover trial of statin, placebo, and no treatment. *J Am Coll Cardiol.* (2021) 78:1210–22. doi: 10.1016/j.jacc.2021.07.022

28. Collins R, Reith C, Emberson J, Armitage J, Baigent C, Blackwell L, et al. Interpretation of the evidence for the efficacy and safety of statin therapy. *Lancet.* (2016) 388:2532–61. doi: 10.1016/S0140-6736(16)31357-5

29. Jakobsson S, Irewall AL, Bjorklund F, Mooe T. Cardiovascular secondary prevention in high-risk patients: a randomized controlled trial sub-study. *BMC Cardiovasc Disord.* (2015) 15:125. doi: 10.1186/s12872-015-0115-0

frontiers | Frontiers in Cardiovascular Medicine

TYPE Original Research
PUBLISHED 17 August 2022
DOI 10.3389/fcvm.2022.948332

OPEN ACCESS

EDITED BY
Mary G. Sorci-Thomas,
Medical College of Wisconsin,
United States

REVIEWED BY
Liwu Li,
Virginia Tech, United States
Darukeshwara Joladarashi,
Temple University, United States

*CORRESPONDENCE
Vincenza Cifarelli
vcifarelli@slu.edu
Yongjian Liu
yongjianliu@wustl.edu
Nada A. Abumrad
nabumrad@wustl.edu

SPECIALTY SECTION
This article was submitted to
Lipids in Cardiovascular Disease,
a section of the journal
Frontiers in Cardiovascular Medicine

RECEIVED 19 May 2022
ACCEPTED 22 July 2022
PUBLISHED 17 August 2022

CITATION
Cifarelli V, Kuda O, Yang K, Liu X, Gross RW, Pietka TA, Heo GS, Sultan D, Luehmann H, Lesser J, Ross M, Goldberg IJ, Gropler RJ, Liu Y and Abumrad NA (2022) Cardiac immune cell infiltration associates with abnormal lipid metabolism.
Front. Cardiovasc. Med. 9:948332.
doi: 10.3389/fcvm.2022.948332

Cardiac immune cell infiltration associates with abnormal lipid metabolism

Vincenza Cifarelli[1,2]*, Ondrej Kuda[3], Kui Yang[1,4], Xinping Liu[1], Richard W. Gross[1], Terri A. Pietka[1], Gyu Seong Heo[5], Deborah Sultan[5], Hannah Luehmann[5], Josie Lesser[5], Morgan Ross[2], Ira J. Goldberg[6], Robert J. Gropler[5], Yongjian Liu[5]* and Nada A. Abumrad[1,7]*

[1]Department of Medicine, Washington University School of Medicine, St. Louis, MO, United States, [2]Department of Pharmacology and Physiology, Saint Louis University School of Medicine, St. Louis, MO, United States, [3]Institute of Physiology, Czech Academy of Sciences, Prague, Czechia, [4]Division of Complex Drug Analysis, Office of Testing and Research, U.S. Food and Drug Administration, St. Louis, MO, United States, [5]Department of Radiology, Washington University School of Medicine, St. Louis, MO, United States, [6]Division of Endocrinology, Department of Medicine, New York University Grossman School of Medicine, New York, NY, United States, [7]Department of Cell Biology and Physiology, Washington University School of Medicine, St. Louis, MO, United States

CD36 mediates the uptake of long-chain fatty acids (FAs), a major energy substrate for the myocardium. Under excessive FA supply, CD36 can cause cardiac lipid accumulation and inflammation while its deletion reduces heart FA uptake and lipid content and increases glucose utilization. As a result, CD36 was proposed as a therapeutic target for obesity-associated heart disease. However, more recent reports have shown that CD36 deficiency suppresses myocardial flexibility in fuel preference between glucose and FAs, impairing tissue energy balance, while CD36 absence in tissue macrophages reduces efferocytosis and myocardial repair after injury. In line with the latter homeostatic functions, we had previously reported that CD36$^{-/-}$ mice have chronic subclinical inflammation. Lipids are important for the maintenance of tissue homeostasis and there is limited information on heart lipid metabolism in CD36 deficiency. Here, we document in the hearts of unchallenged CD36$^{-/-}$ mice abnormalities in the metabolism of triglycerides, plasmalogens, cardiolipins, acylcarnitines, and arachidonic acid, and the altered remodeling of these lipids in response to an overnight fast. The hearts were examined for evidence of inflammation by monitoring the presence of neutrophils and pro-inflammatory monocytes/macrophages using the respective positron emission tomography (PET) tracers, ^{64}Cu-AMD3100 and ^{68}Ga-DOTA-ECL1i. We detected significant immune cell infiltration in unchallenged CD36$^{-/-}$ hearts as compared with controls and immune infiltration was also observed in hearts of mice with cardiomyocyte-specific CD36 deficiency. Together, the data show that the CD36$^{-/-}$ heart is in a

non-homeostatic state that could compromise its stress response. Non-invasive immune cell monitoring in humans with partial or total CD36 deficiency could help evaluate the risk of impaired heart remodeling and disease.

KEYWORDS

CD36, PET tracers, cardiac inflammation, lipidomics, eicosanoids, macrophage

Introduction

Myocardial energy metabolism is a highly dynamic process important for tissue health and optimal cardiac function. Long-chain fatty acids (FAs) are a major metabolic substrate of myocardial tissue. Rates of tissue FA uptake are dependent on the FA transporter CD36 (1, 2) and its vesicular recycling between endosomes and the sarcolemma (3). CD36 deficiency reduces heart FA uptake and prevents the fasting-induced metabolic remodeling by the myocardium from glucose utilization to more reliance on FAs; following an overnight fast, mice with global Cd36 deletion ($CD36^{-/-}$) displayed atrioventricular block and bradycardia, and increased incidence of sudden death (4). Suppressed or absent myocardial FA uptake has been reported in people with *CD36* gene variants that reduce protein levels (5–7). In addition, relatively common single nucleotide polymorphisms (SNPs) in the *CD36* gene have been associated with cardiac function and with increased susceptibility to cardiovascular disease, as reviewed elsewhere (8). Despite the above findings, how CD36 deficiency impacts heart lipid metabolism and its ability for adaptive remodeling remains unexplored.

The heart is a continuously working organ that adapts to various stresses and its ability to cope and recover is integral to maintaining its health and function. In addition to metabolic remodeling, myocardial recovery relies on the sequential mobilization of immune cells (i.e., neutrophils, monocytes, and macrophages) that serve diverse roles in the reparative process (9, 10), including removal of dead cells and renewal of extracellular matrix (11). Immune cell recruitment in the heart is orchestrated by chemokines interacting with corresponding receptors on leukocytes, mediating their activation and extravasation into the injured area (12–14). Of these chemokine receptors, C-C chemokine receptor type 2 (CCR2), expressed on monocytes and macrophages (15), plays an important role in regulating the phenotype and function of cell types involved in myocardial remodeling, while C-X-C motif chemokine receptor 4 (CXCR4), highly expressed on neutrophils (16), regulates phenotype and function of all cell types involved in tissue healing, making it an important target for both imaging and therapy (17–19). Mice with myeloid CD36 deficiency present defective heart remodeling and repair following injury (20, 21); however, there is no information on whether CD36 deficiency causes immune cell infiltration in unchallenged hearts, as we previously reported in the intestine of $CD36^{-/-}$ mice (22). Such information would be important for evaluating cardiac ability for optimal recovery from injury and potential risk of disease. CD36 deficiency is relatively common in certain populations (3–10%) and *CD36* SNPs that reduce CD36 levels result in dyslipidemia and increase the risk of type 2 diabetes (23, 24).

In this study, we profiled lipid metabolism in the hearts of fed and overnight-fasted mice. Our data identified significant changes in the content of plasmalogens, cardiolipins, and eicosanoids suggesting that CD36-mediated FA delivery is important for maintaining the normal heart lipid profile during the adaptation to fasting. Unbiased global assessment of gene expression by microarray analysis in hearts from $CD36^{-/-}$ mice, as compared to WT, identified upregulation of pathways regulating both innate and adaptive immunity. To gain insight into the dynamic expression and spatial localization of immune cells in unchallenged $CD36^{-/-}$ mice heart, we employed a novel positron emission tomography (PET) imaging approach to non-invasively image neutrophils and pro-inflammatory monocytes/macrophages, using validated tracers ^{64}Cu-AMD3100 for CXCR4 and ^{68}Ga-DOTA-ECL1i for CCR2 (25, 26). We show that the hearts of unchallenged $CD36^{-/-}$ mice have increased pro-inflammatory immune infiltration as compared to controls. The presence of inflammation in hearts with CD36 deletion specific to cardiomyocytes supported the interpretation that a healthy heart lipid profile is needed to prevent inflammation.

Abbreviations: PET, Positron emission tomography; CT, Computed Tomography; CXCR4, CXCR4; CCR2, C-C chemokine receptor type 2; DHA, Docosahexaneoic Acid; LA, Linoleic acid; LPC, Lysophosphatidylcholine; LPE, Lysophosphatidylethanolamine; LC, Lysocardiolipins; AC, Acylcarnitine; 5-HEPE, Hydroxyeicosapentaenoic acid; 17-HDHA, 17-Hydroxy-docosahexaenoic acid; 13-HODE, 13-Hydroxyoctadecadienoic acid; PGD2, Prostaglandin D2; PGF1, Prostaglandin F1; PGE, Prostaglandin E; DGLA, Dihomo-γ-linolenic acid; TXB2, Thromboxane B2; LTB4, Leukotriene B4; HETEs, Hydroxyeicosatetraenoic acids; EETs, Epoxyeicosatrienoic acids.

Materials and methods

Mice

Mice were bred and maintained at the Washington University School of Medicine and all experimental procedures followed the guidelines of the animal use oversight committee. The studies used cohorts of male and female C57Bl6 wild-type (WT) and CD36-null ($CD36^{-/-}$) mice that were age-matched (12–14 weeks), unless indicated otherwise. Myocardial CD36 deficiency (MHC-$CD36^{-/-}$) was obtained by crossing CD36 floxed (Fl/Fl) mice with mice expressing the myosin heavy chain alpha (MHC) Cre as previously described (27). Mice housed in a 12-h light-dark facility were fed chow *ad libitum* (Purina) or 12 h fasted. Genotypes were confirmed by PCR and immunohistochemistry.

Lipid analysis

Lipids were extracted and analyzed by mass spectrometry. In brief, hearts from mice killed by carbon dioxide inhalation were rapidly removed, rinsed with ice-cold PBS, freeze-clamped, and pulverized at liquid nitrogen temperature. The tissue was homogenized in LiCl solution (50 mM) using a Potter-Elvehjem tissue grinder. Methanol and chloroform, as well as internal standards for major lipids, were added and the lipids extracted. Multidimensional shotgun lipidomic analysis of extracted lipids used a Thermo Electron TSQ Quantum Ultra spectrometer (San Jose, CA) equipped with an electrospray ion source, and individual molecular species were identified and quantified by 2D mass spectrometry (28–30).

Metabolite assays

ATP was extracted from hearts (31) and quantified using mass spectrometry (32). Analysis of carnitine and acylcarnitines was performed as described (33). Around 20 mg of heart tissue was lyophilized for 12 h after the addition of a set of deuterium-labeled carnitine and acylcarnitine standards (Cambridge Isotope Laboratories, Andover, MA). The lyophilized tissue was grounded to powder using an Eppendorf micropestle and dissolved in 1 mL of 8:2 (v/v) acetonitrile/water. After sonification and centrifugation, the supernatants were dried and derivatized (33). Carnitine and acylcarnitines were analyzed as their butyl esters by precursor ion scanning of m/z 85 utilizing a TSQ Quantum Ultra Plus triple-quadrupole mass spectrometer (Thermo Fisher Scientific, San Jose, CA). Protein content was measured (Bradford assay, Bio-Rad) with BSA as standard.

Mitochondria isolation and functional studies

The heart was minced, added to the buffer (10 mM HEPES, 250 mM sucrose, 1mM EGTA, pH 7.0), and homogenized using a Dounce grinder. Heart mitochondria were isolated by differential centrifugation. After centrifugation (500 × g, 2 min) to remove tissue debris, the supernatant was centrifuged at 10,000 xg (10 min) to pellet mitochondria, which were washed once and resuspended at 20 ∼ 30 mg/mL protein at 4°C (0.1 M KCl, 0.05 M Tris-HCl, 2 mM EGTA, pH 7.4). Mitochondrial FA oxidation was measured by monitoring either CO_2 or water release using [^{14}C]-palmitate as substrate. In brief, mitochondria (0.5 mg protein/mL) were incubated with 100 μM FA complexed to BSA (FA:BSA = 1.7) in respiration buffer (120 mM KCl, 5 mM KH2PO4, 3 mM HEPES, 3 mM MgCl2, 1 mM EGTA, 5 mM ATP 1mM NAD, 0.5 mM Carnitine, 0.1 mM Coenzyme A, 5 mM Malate, pH 7.2) aerated with 95% O_2 and 5% CO_2. The reaction was terminated by adding hydrochloric acid and radiolabeled products were quantified. Oxygen consumption was measured polarographically using a dual channel Instech Dissolved O_2 Measuring system. Mitochondria were placed in the electrode chamber in 150 mM KCl, 1 mM EGTA, 5 mM DTT, pH 7.0 at 20°C and the O_2 consumed was measured for 5 min with no additives and with 5 mM malate added. ADP was added to determine the substrate-supported O_2 consumption and the ability to generate ATP.

Gene expression analysis

Gene expression was analyzed by microarray as previously described (4) or by RNA-Seq (27) as indicated. In brief, total RNA was isolated from tissues using Trizol (Invitrogen, Carlsbad, CA). In brief, flash frozen hearts were homogenized in Trizol and chloroform was added (0.2 mL/mL Trizol) followed by centrifugation. The supernatant was removed, an equal volume of isopropanol was added, and the samples were centrifuged again to pellet the RNA, which was washed in 75% ethanol, dried, and resuspended in UltraPure Distilled Water (GIBCO, Carlsbad, CA). Microarray analyses were performed using the Whole Mouse Genome Oligo Microarray Kit (Agilent Technologies, Santa Clara, CA). The array was scanned by Axon 4000B scanner, and the data were extracted by GenePix Pro 6.1 software (Molecular Devices, Sunnyvale, CA). For the RNAseq, raw sequencing data were obtained as previously described in FASTQ format. Read mapping used Tophat 2.0.9 against the mm10 mouse reference genome. The resulting BAM alignment files were processed using HTSeq 0.6.1 python framework and respective mm10 GTF gene annotation (UCSC database). The Bioconductor package DESeq2 (3.2) was used to identify differentially expressed genes (DEGs) and for statistical

analysis based on the negative binomial distribution model. The resulting values were adjusted (Benjamini–Hochberg method for FDR determination). Genes with adjusted *P*-value < 0.05 were determined to be differentially expressed. KEGG analysis was used to identify the top canonical pathways being altered. RNA-seq data were deposited in the NCBI's Gene Expression Omnibus (GEO) database (GEO GSE116350).

Macrophage polarization and treatments

Bone marrow-derived macrophages were isolated and cultured in RPMI with 10% FBS, 10% L929 conditioned media, and 1% PenStrep for 5 days. For M1 polarization, macrophage media was supplemented with 20 ng/mL IFNγ (Peprotech) and 20 ng/mL lipopolysaccharides (all from Sigma). For M2 polarization, macrophage media was supplemented with 20 ng/mL interleukin-4 (Peprotech). For linoleic acid (LA) and docosahexaenoic acid (DHA) solution: 25 μM LA or DHA (Cayman) complexed with 8 μM FA-Free BSA in PBS supplemented with glucose and 2 μM calcium chloride. Solutions were prepared fresh 24 h before treatment and rotated at 4°C overnight to allow for complete complexing to BSA. Eicosanoids were measured by liquid chromatography–mass spectrometry (LC–MS) as previously described (34).

Positron emission tomographic/computed tomography imaging

Mice were fasted for 4 h, anesthetized with isoflurane, and injected with 3.7 MBq of ^{64}Cu-AMD3100 (^{64}Cu: $t_{1/2}$ = 12.7 h) or 9.25 MBq ^{68}Ga-DOTA-ECL1i (^{68}Ga: $t_{1/2}$ = 68 min) in 100 μL of saline *via* the tail vein. Small animal PET/CT scans (40–60 min dynamic scan) were performed on the Inveon PET/CT system (Siemens, Malvern, PA). The PET images were corrected for attenuation, scatter, normalization, and camera dead time and co-registered with CT images. The PET images were reconstructed with the maximum *a posteriori* (MAP) algorithm and analyzed by Inveon Research Workplace. The uptake was calculated as the percent injected dose per gram (%ID/g) of tissue in three-dimensional regions of interest (ROIs) without the correction for partial volume effect (26).

Flow cytometry

Single-cell suspensions were generated from saline perfused hearts by finely mincing and digesting them in DMEM with Collagenase 1 (450 U/mL), Hyaluronidase (60 U/mL), and DNase I (60 U/mL) for 1 h at 37°C. All enzymes were purchased from Sigma. To deactivate the enzymes, samples were washed with HBSS that was supplemented with 2% FBS and 0.2% BSA and filtered through 40 μM cell strainers. Red blood cell lysis was performed with ACK lysis buffer (Thermo Fisher Scientific). Samples were washed with HBSS and resuspended in 100 μL of FACS buffer (DPBS with 2% FBS and 2 mM EDTA). Cells were stained with monoclonal antibodies at 4°C for 30 min in the dark. All the antibodies were obtained from Biolegend: CD45-PerCP/Cy5.5, clone 30-F11; CD64-APC and PE, clone X54-5/7.1; CCR2-BV421, clone: SA203G11; MHCII-APC/Cy7, clone M5/114.15.2; Ly6G-PE/Cy7, clone 1A8; and Ly6C-FITC, clone HK1.4. Samples were washed two times, and final resuspension was made in 300 μL FACS buffer. DAPI or LIVE/DEAD^{TM} Aqua dyes were used for the exclusion of dead cells. Flow cytometric analysis were performed on the BD Fortessa platform. Neutrophils were gated as CD45 + Ly6G^{high}. Macrophages were gated as Ly6G^{neg}CD64^{high}Ly6C^{low} cells.

Statistics

Statistical analyses were made using GraphPad Prism 8 or MATLAB Student's *t*-test, one-way or two-way ANOVA with *post hoc* comparison. Principal component analysis (PCA) using Umetrics SIMCA-P + 12 software (Umetrics AB) was conducted for non-biased evaluation of lipidomic data (22). All data presented are means ± standard error (SE). Significance was for $p < 0.05$.

Results

Cardiac lipidomic profile

FAs are structural components of membranes, signaling molecules, and energy sources. In addition, they regulate gene expression by providing substrate for histone acetylation (35, 36). The inability of the myocardium to adapt FA utilization and FA oxidation to FA availability disrupts homeostasis and can associate with stress and inflammation. We examined the lipid profile of the CD36$^{-/-}$ heart by conducting an unbiased global assessment using hearts from fed or overnight fasted CD36$^{-/-}$ and WT mice. Turnover of intramyocardial triglycerides (TAG) contributes an estimated 10% of cardiac energy (37); TAG content was similar in hearts of fed WT and CD36$^{-/-}$ mice (**Figure 1A**). TAG increased after fasting in WT hearts as previously reported (30, 34), in contrast, CD36$^{-/-}$ hearts showed a marked (∼60%) reduction of TAG stores (**Figure 1A**). We examined FA composition of the TAG to gain insight into TAG remodeling. Saturated FA (**Figure 1B**) and PUFA (**Figure 1D**) were significantly increased

in the hearts of CD36$^{-/-}$ mice as compared to controls during the fed state. Fasting is associated in WT hearts with increases in TAG content of monounsaturated (>200%) and polyunsaturated (160%) FAs more than saturated FAs (~130%). In CD36$^{-/-}$ hearts, fasting reduced all FAs in TAG with a larger drop in monounsaturated (-65%) and polyunsaturated (-62%) FAs as compared to saturated FAs (-45%). These results suggested abnormalities of FA desaturation (**Figures 1B–D**). In line with the results in the fasting state, expression of the myocardial isoform of stearoyl-CoA desaturase increased three-fold in the hearts of fasted WT mice and was 60% reduced in the hearts of fed or fasted CD36$^{-/-}$ mice (data not shown). Myocardial plasmalogens and cardiolipins (CL), two classes of lipids important for the function of peroxisomes and mitochondria in FA oxidation (38) were altered in CD36$^{-/-}$ mice. Plasmalogen levels were reduced (~25%) in fed and fasted states, as compared with hearts of WT mice (**Figure 1E**). Fasting increased lysocardiolipin levels in hearts from both genotypes, although the increase was larger in hearts from CD36$^{-/-}$ as compared to those of WT mice, 1.6-, and 2.8-fold, respectively (**Figure 1F**). Fasting changed FA composition of cardiolipin acyl chains, which is regulated in concert with the remodeling of other phospholipids. Lysocardiolipin is formed by phospholipase removal of FA-acyl chains and acyltransferase mediates reacylation back to cardiolipin. The larger increase in lysocardiolipin in fasted CD36$^{-/-}$ hearts involved all species with the most affected acyl chains being linoleic acid (C18:2) and DHA (C22:6) (**Figure 1G**).

Tissue renewal relies on lipid metabolism, notably FA oxidation which maintains competent stem cells (39) and regulates cardiac function and homeostasis (8, 40). In the fed state, there was little change in levels of total acylcarnitines (ACs) in CD36$^{-/-}$ hearts (**Figure 2A**), but while total acylcarnitine levels increased with fasting in WT hearts, they trended lower in CD36$^{-/-}$ hearts, although total AC content is not as meaningful with respect to the status of FA oxidation as that of long-chain ACs. The WT hearts sustained FA oxidation in fasting (**Figure 2B**) and mitochondrial CD36 protein content increased (**Figure 2C**) while relative FAO decreased with fasting in CD36$^{-/-}$ hearts (**Figure 2B**). The heart during fasting normally reduces its glucose utilization and increases its reliance on FA uptake and FA oxidation. However, this metabolic flexibility is lost in the hearts of CD36$^{-/-}$ mice which continue to rely on glucose utilization during fasting (8). In line with this, ACs increased during fasting in the hearts of WT mice, but the increase was uniformly muted in CD36$^{-/-}$ mice as ACs showed little change or decreased (**Figure 2D**). Levels of acylcarnitines were similar in the fed state in WT and CD36$^{-/-}$ hearts, but during fasting, long-chain AC species (12:0, 16:0, 18:0, 18:1, and 18:2) trended lower but only AC 12:0 and 18:0 reached significance. As compared to the WT heart, long-chain acylcarnitines (12:0, 14:0, 16:0, 18:0, 18:1, and 18:2) were significantly reduced in the hearts of CD36$^{-/-}$ mice indicating reduced mitochondrial FA oxidation. These results are consistent with findings showing that during feeding, the CD36$^{-/-}$ heart can utilize FAs from chylomicrons as uptake of chylomicron FA is not limited by CD36 (8).

The FAs liberated by phospholipases serve as the primary precursor pool for the formation of the pleiotropically bioactive arachidonic acid-derived eicosanoid generated by cyclooxygenases (COX), lipoxygenases (LOX), and cytochromes P450. The generated eicosanoids are involved in multiple signaling pathways in the heart (41). The role of CD36 in phospholipase A2 activation, release of arachidonic acid, and generation of prostaglandin E2 (PGE2) was previously reported in isolated macrophages (42). We found that levels of many eicosanoids were elevated in the hearts of fed CD36$^{-/-}$ mice as compared to those of WT mice (**Figure 3A**, black to white bars). This included several LOX-generated hydroxyeicosatetraenoic acids; 8, 12, and 15 HETE and P450 generated epoxyeicosatrienoic acids; 5–6, 8–9, 11–12, and 14–15 EET and 20-HETE. The COX-derived PGE2, PGF2a, and PGD2 were not affected but they increased with fasting only in WT hearts (**Figures 3A,B**). CD36 deficiency is associated with higher gene expression of the CYP4A arachidonic acid ω-hydroxylases *Cyp4a12* and epoxygenase *Cyp2c70* (**Figure 3C**). The increase in arachidonic acid-derived eicosanoids during feeding could reflect the presence of inflammation in the myocardium.

Unbiased global assessment of gene expression by microarray analysis in hearts of CD36$^{-/-}$ mice, as compared to WT, identified upregulation of pathways regulating both innate and adaptive immunity (**Figure 4A** and **Supplementary Table 1**). Excessive or abnormal FA metabolism can promote cardiac inflammation and heart disease which could involve effects on macrophage (MAC) polarization (43). We examined the response of M1-like vs. M2-like MACs to pro-inflammatory (e.g., ω-6 linoleic acid, LA) or anti-inflammatory (e.g., ω-3 docosahexaenoic acid, DHA) polyunsaturated long chain FAs (PUFAs) and the effect of CD36 deficiency. The ω-3 and ω-6 PUFAs are metabolized to various eicosanoids that can, respectively, promote (*via* prostaglandins) or resolve (*via* resolvins) inflammation (44, 45). As reported (46), alternatively polarized M2-like bone marrow-derived MACs have higher CD36 expression when compared to classical M1 MACs (**Figure 4B**). Untreated WT M1 MACs produced much more PGD2, a metabolite of the ω-6 FA arachidonic acid, than WT untreated M2 MACs (~843 ± 15 vs. 35 ± 2 AU, respectively, $p < 0.0001$), and M1 PGD2 production was unaffected by FA treatment (**Figure 4C**). The WT M2 MACs generated low amounts of PGD2 that modestly increased upon addition of DHA (65 ± 4 AU; $p < 0.05$) or LA (80 ± 4 AU; $p < 0.05$) (**Figure 4C**). We then examined the production of 5-HEPE, a common anti-inflammatory metabolite of ω-3 FAs. Wildtype M1 MACs produced low amounts of 5-HEPE, which modestly increased in response to DHA while a much larger (~six-fold) increase in 5-HEPE was observed in DHA-treated WT M2 MACs (**Figure 4D**).

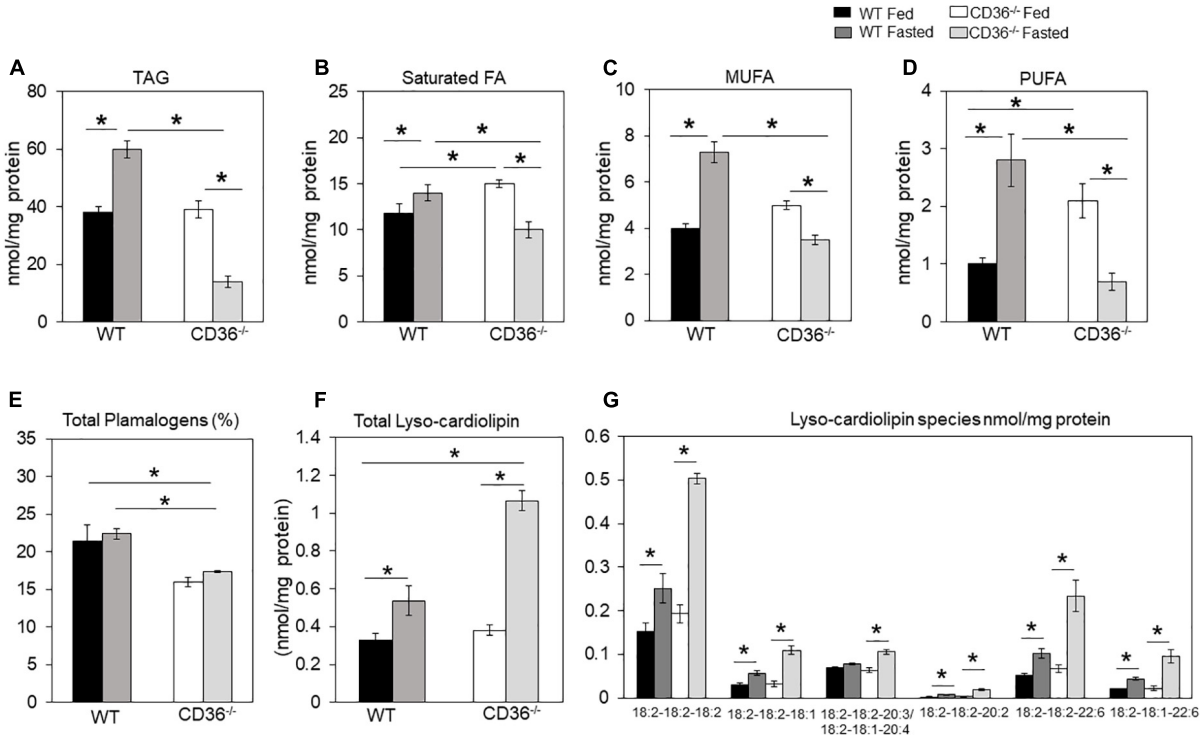

FIGURE 1
CD36-mediated alterations in myocardial triglycerides and lysocardiolipin. Myocardial lipids in fed and fasted WT and CD36$^{-/-}$ mice were analyzed using shotgun lipidomics mass spectrometry. Levels of **(A)** total triglycerides, **(B)** saturated, **(C)** monounsaturated (MUFA), and **(D)** polyunsaturated (PUFA) FAs in TGs. **(E)** Levels of total plasmalogens (%). **(F)** Levels of lysocardiolipins. **(G)** Lysocardiolipin species. Labels denote the number of carbons: number of double bonds. Results are reported as nmol/mg of protein. Data (n = 5/group) are means ± SE with n representing the number of mice per group, *$p < 0.05$.

Similar data were observed with the anti-inflammatory metabolite 18-HEPE (data not shown). The effect of CD36 deletion on MAC production of eicosanoids was examined next (**Figures 4E–G**). CD36 deletion increased by ∼nine-fold basal PGD2 levels in M1 MACs (49,862 ± 3,708 AU; $p < 0.0001$) with no further increase observed with LA treatment. DHA suppressed PGD2 levels (12,364 ± 1,377 AU; $p < 0.001$) less efficiently in CD36$^{-/-}$ cells (**Figure 4E** left panel). DHA treatment increased PGD2 in CD36$^{-/-}$ M2 MACs by ∼ two-fold (to 2,741 ± 811; $p < 0.05$) while LA was ineffective (**Figure 4E** right panel). These data show that a major effect of CD36 deficiency was to dramatically increase basal PGD2 secretion by M1 MACs. Levels of the anti-inflammatory DHA metabolite 17-HDHA were modestly higher in untreated CD36$^{-/-}$ M1 MACs (1,980 ± 295 AU) as compared to untreated WT M1 MACs (362 ± 242 AU; $P < 0.01$) (**Figure 4F**). Addition of DHA increased 17-HDHA (11,353 ± 2,530 AU) in WT M1 MACs with a significantly larger effect in CD36$^{-/-}$ cells (99,242 ± 11,230 AU; $p < 0.001$) indicating that CD36 deficiency also increases ω-3 conversion into eicosanoids. A similar pattern was observed in M2 MACs, while LA treatment was generally ineffective (**Figure 4F**). CD36 deficiency increased (∼10-fold) production of the linoleic acid metabolite 13-HODE in M1 MACs (291,575 ± 57,607 AU) as compared to untreated WT M1 MACs (29,562 ± 5,744 AU; $p < 0.01$), and in response to DHA or LA in both M1 and M2 (**Figure 4G**). Together, these data suggest that MAC CD36 influences eicosanoid formation, and CD36 loss results in process dysregulation with blunting of differences in eicosanoid production between M1 and M2 MACs.

Cardiac C-X-C motif chemokine receptor 4 and C-C chemokine receptor type 2 imaging

The above data together suggested the presence of inflammation in the myocardium of the CD36$^{-/-}$ mouse, so we next examined the presence of inflammation non-invasively *in vivo*. Neutrophils are the first cell type to respond when the heart is subjected to stress, infection, or injury. Short-term neutrophil infiltration initiates inflammation and helps with its resolution, while the long-term presence of neutrophils can damage the myocardium (47, 48). High CXCR4 expression is typical of activated neutrophils that can cause tissue damage (49). MAC subsets in the heart

10.3389/fcvm.2022.948332

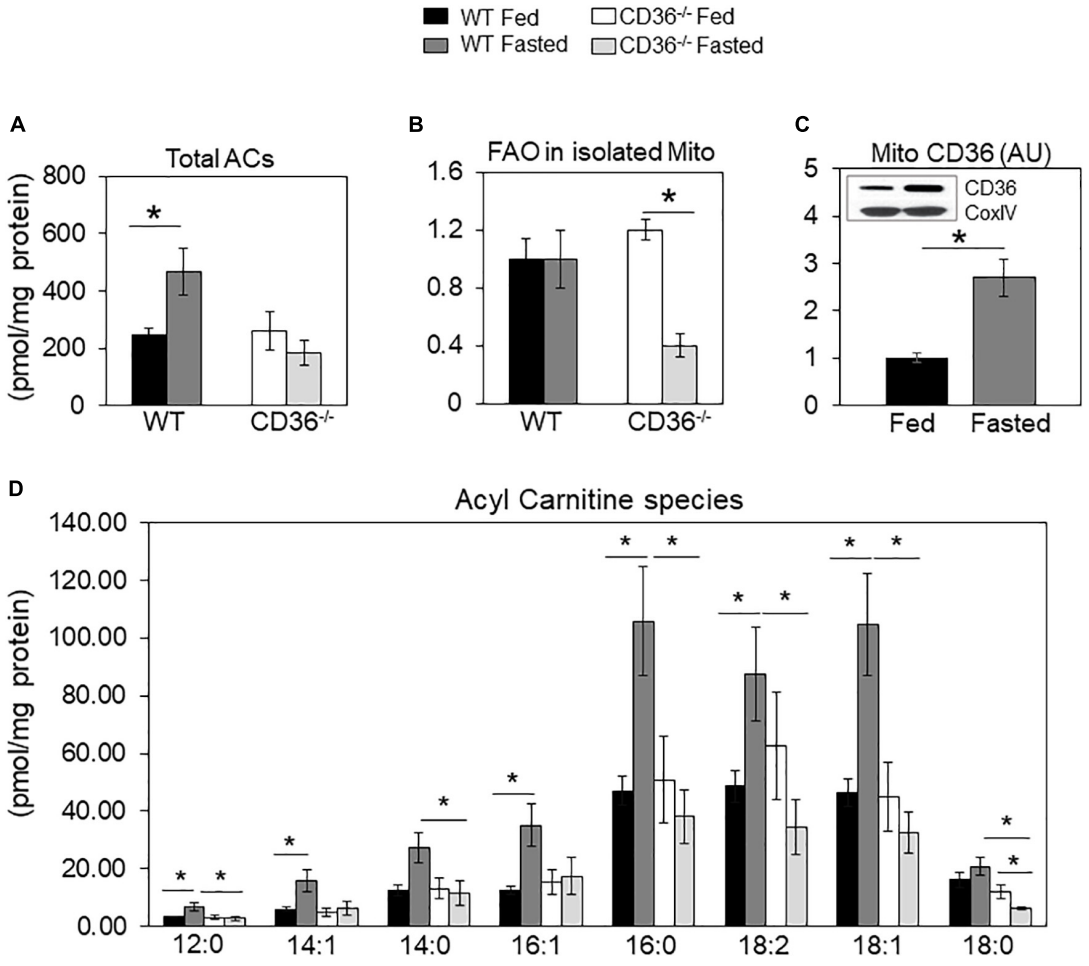

FIGURE 2
Acylcarnitines and fatty acid oxidation (FAO) of mitochondria isolated from fed and fasted WT and CD36$^{-/-}$ hearts. **(A)** Levels of total acylcarnitines (ACs). **(B)** Mitochondria were isolated to measure CD36 content and fatty acid oxidation (FAO) rate determined from CO_2 or ^3H water release from radiolabeled substrates as described in Methods. Data are expressed as ratios of FAO rates from fasted and fed hearts. **(C)** CD36 expression and densitometry in mitochondrial lysates relative to COX IV expression by western blotting. **(A,B)** n = 5/group; **(C)** n = 7/group; **(D)** n = 3/group. Results are reported as pmol/mg of protein. Data are means ± SE with n representing the number of mice per group, *$p < 0.05$.

play different roles in the tissue's response to stress. While tissue-resident CCR2^{neg} MACs inhibit monocyte recruitment, CCR2^{+} tissue MACs recruit monocytes and promote cardiac inflammation (50) and contribute to adverse heart remodeling and the pathogenesis of heart failure in humans (51, 52). To non-invasively assess real-time cardiac inflammation in unchallenged CD36$^{-/-}$ mice, we took advantage of a PET-based molecular imaging strategy using ^{64}Cu-AMD3100 tracer detecting CXCR4^{+} neutrophils (CXCR4 PET) and ^{68}Ga-DOTA-ECL1i tracer detecting CCR2+ macrophages (CCR2 PET) as previously described (25, 26, 53). In CD36$^{-/-}$ mice, robust CXCR4 PET signals were observed in the hearts compared to the low tracer retention measured in wild type controls (**Figure 5A**). Quantitative analysis showed that tracer uptake in the hearts of CD36$^{-/-}$ mice was significantly higher (3.36 ± 0.36%ID/g, $p < 0.001$, $n = 7$) than that in WT mice (2.17 ± 0.25%ID/g, $n = 10$) (**Figure 5B**). Moreover, *ex vivo* autoradiography performed immediately after PET/CT imaging showed stronger tracer uptake in heart slices from CD36$^{-/-}$ mice relative to slices from WT mice (**Figure 5C**). To further validate the CXCR4 PET findings, we determined level of CXCR4^{+} neutrophils in mouse hearts using flow cytometry. CD36$^{-/-}$ hearts as compared to WT hearts, had more CXCR4^{+} neutrophils but not more total neutrophils (CD45^{+}Ly6G^{+}) (**Figure 5D**). For CCR2 imaging, higher tracer uptake was measured in CD36$^{-/-}$ mice that contrasted with the low retention of ^{68}Ga-DOTA-ECL1i seen in WT mice (**Figures 6A,B**). Heart uptake quantification revealed nearly doubled signals in CD36$^{-/-}$ mice (1.33 ± 0.16%ID/g, $n = 5$, $p < 0.001$)

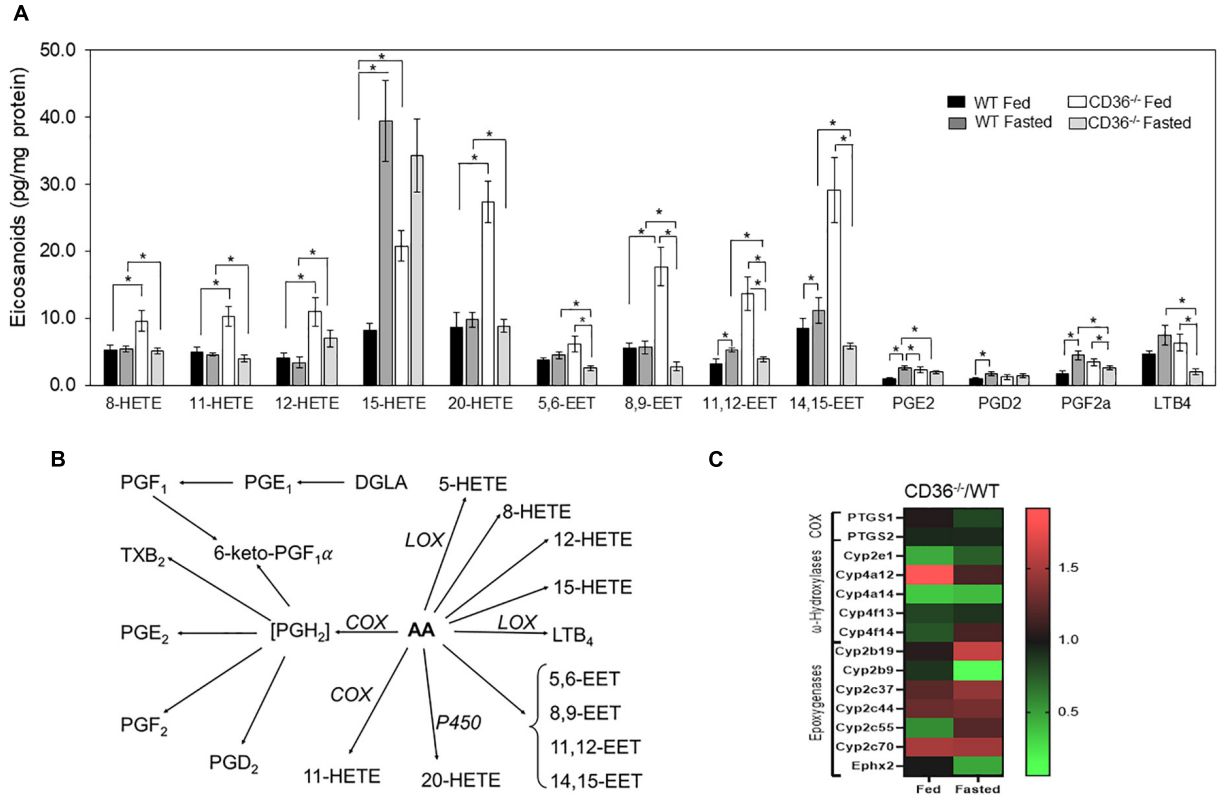

FIGURE 3
CD36 deficiency affects cardiac eicosanoid content. **(A)** Eicosanoid content in fed or fasted WT and CD36$^{-/-}$ heart (n = 5/group). Results are reported as pg/mg of protein. **(B)** Gene expression fold change of key enzymes regulating eicosanoid production. Data are means ± SE with n representing the number of mice per group, *$p < 0.05$. **(C)** The scheme represents downstream metabolites of arachidonic acid (AA) *via* cyclooxygenase (COX), lipoxygenase (LOX), or cytochrome (P450) pathways.

relative to those in WT mice (0.72 ± 0.06%ID/g, n = 5). Moreover, in CCR2$^{-/-}$ mice, minimal ^{68}Ga-DOTA-ECL1i accumulation was observed (0.59 ± 0.04%ID/g, n = 4, $p < 0.001$), validating CCR2-targeting specificity of ^{68}Ga-DOTA-ECL1i (Figures 6A,B). Flow cytometry analysis confirmed increased CCR2 expression on heart MACs isolated from CD36$^{-/-}$ mice (Figure 6C).

CD36 deletion in cardiomyocyte associates with cardiac inflammation

The alterations in lipid metabolism measured in the hearts of CD36$^{-/-}$ mice would be predicted to cause significant stress to the myocardium, which could promote inflammation. To assess the role of cardiomyocyte CD36 deficiency on cardiac inflammation independent of the context of CD36 deficiency in immune cells, we examined whether inflammation can be observed in hearts from mice with CD36 deletion restricted to cardiomyocytes, MHC-CD36$^{-/-}$ (27). Hearts of MHC-CD36$^{-/-}$ mice had significant increases in the macrophage CCR2 PET tracer as compared to hearts of WT mice (Figures 7A,B). In addition, an unbiased global assessment of gene expression in hearts from MHC-CD36$^{-/-}$ mice showed upregulation of pathways involved in immune cell activation and infiltration. In contrast, pathways relevant to cellular respiration, mitochondrial function, and FA metabolism were downregulated as compared to littermate controls (Figure 7C). These data suggested that CD36 deficiency in cardiomyocytes likely contributes to tissue inflammation and immune infiltration.

Discussion

Our study examined metabolic and immune adaptation of the heart in the context of CD36-mediated impaired lipid metabolism. Lipidomic analysis in hearts from CD36$^{-/-}$ mice showed abnormal remodeling of TAG and mitochondrial cardiolipin in fasting, and reduced levels of peroxisomal plasmalogens, a major glycerophospholipid class in the myocardium (54). In line with this, fasting associated with suppressed mitochondrial FA oxidation and with reduced FA

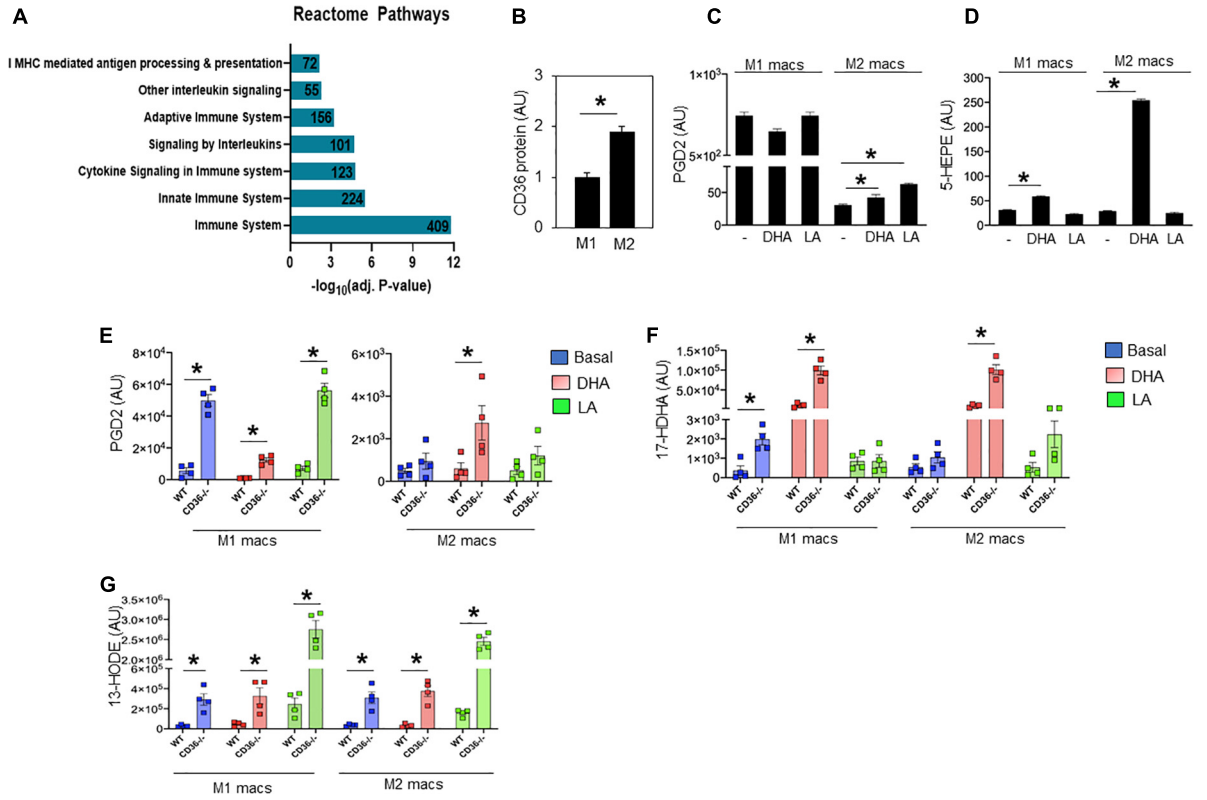

FIGURE 4
CD36 deletion associates with markers of inflammation in heart tissue and isolated macrophages. **(A)** Microarray analysis in CD36$^{-/-}$ heart shows upregulated biological pathways involved in immune cell activation and inflammation (n = 3/group). Pathway analysis obtained from Reactome analysis database using differentially regulated genes (>1.6 or <0.7). Number of differentially regulated genes is indicated on the significance bar for each pathway. **(B)** WT bone marrow-derived macrophages (BMDM) were subjected to a polarization protocol to yield M1- and M2-like macrophages and were assayed for CD36 expression levels by western blotting. WT M1- and M2-like macrophages were assayed for the content of **(C)** PGD2 and **(D)** 5-HEPE at baseline and following DHA or LA treatment. **(E–G)** BMDM were obtained from WT or CD36$^{-/-}$ mice and subjected to the polarization protocol. M1- and M2-like macrophages were then treated with DHA or LA to measure the content of **(E)** PGD2, **(F)** the DHA metabolite 17-Hydroxy-ocosahexaenoic acid (17-HDHA) and **(G)** the linoleic acid metabolite 13-Hydroxyoctadecadienoic acid (13-HODE). Eicosanoids were measured by LC–MS. All data (n = 4/group) are means ± SE with n representing the number of mice per group. Statistical significance is determined by Student's t test. *$p < 0.05$.

acylcarnitine levels. Eicosanoid production was dysregulated in fed CD36$^{-/-}$ mice with high levels of multiple pro-inflammatory arachidonic acid derivatives. Analysis of heart gene expression showed that CD36 deficiency promotes the downregulation of genes involved in cellular respiration and mitochondrial function while upregulating the expression of genes involved in immune cell activation and inflammation. Using a novel non-invasive PET imaging approach, we further showed that CD36 deficiency promotes cardiac immune cell infiltration in unchallenged mice. Increases were observed in PET signals for CXCR4, a marker of old activated neutrophils that cause tissue damage (49), and for CCR2 which marks a pro-inflammatory subset of monocytes-macrophages, that associates with adverse left ventricle remodeling and heart failure progression (26, 55). CD36 regulates macrophage polarization to the anti-inflammatory phenotype and improves macrophage efferocytosis after ischemic injury (56). Deficiency in myeloid-CD36 delays the clearing of apoptotic cells, including neutrophils and cardiac repair after injury (21). Uncleared apoptotic neutrophils are implicated in tissue injury through the generation of pro-inflammatory cytokines, extracellular traps, and reactive oxygen species (57). Although neutrophils were recently shown to have a protective role in polarizing macrophages toward a healing function, the absence of CD36 on macrophages would at least in part impede this effect (58, 59). The observation that CD36 deficiency restricted to cardiomyocytes promotes macrophage infiltration and upregulation of pathways related to immune activation and migration in the heart suggests that dysregulation of lipid metabolism might drive the immune infiltration in CD36$^{-/-}$ hearts.

CD36 deficiency in rodents was reported to associate with intolerance to prolonged fasting with increases in arrhythmias and sudden death (4). One contributor to fasting intolerance

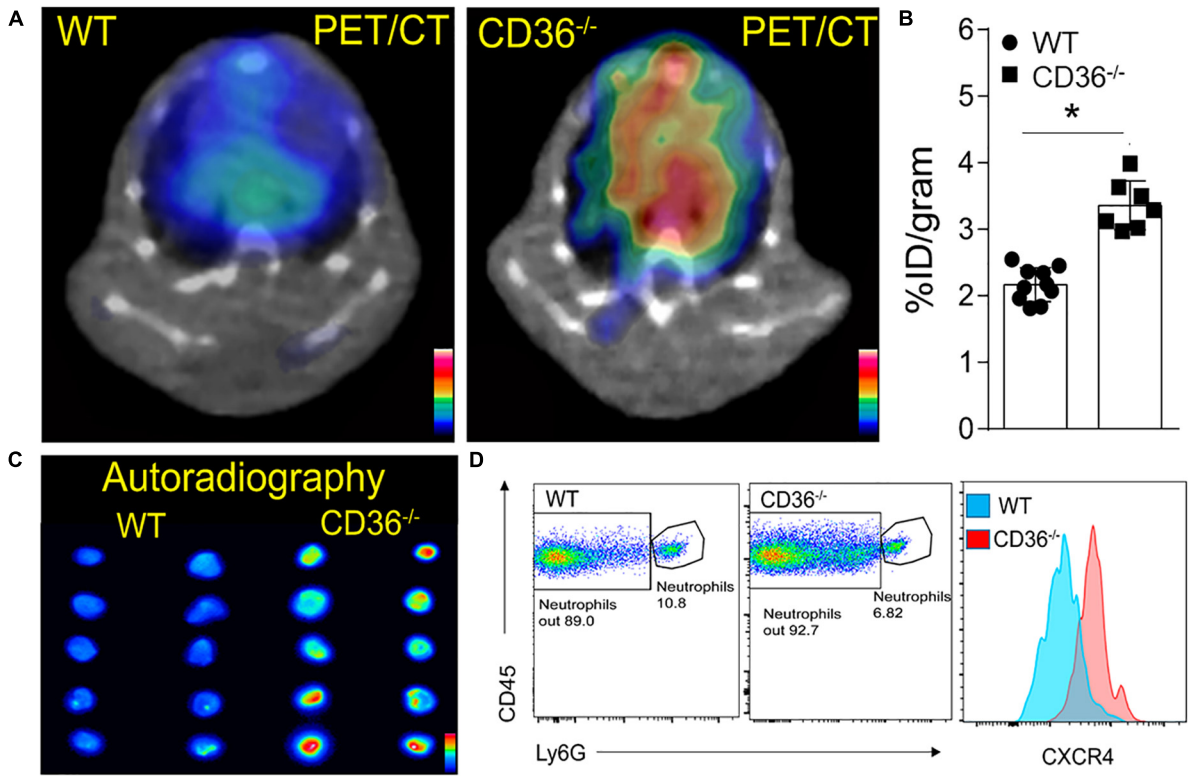

FIGURE 5
Visualization of activated neutrophils in the heart of wild type (WT) and CD36 *null* ($CD36^{-/-}$) mice. **(A)** Neutrophils are visualized non-invasively using ^{64}Cu-AMD3100 tracer and PET/CT scanning. **(B)** Quantification of ^{64}Cu-AMD3100 tracer in the heart (n = 10 in WT mice, n = 7 in $CD36^{-/-}$ mice). **(C)** *Ex vivo* autoradiography of heart slices collected from WT and $CD36^{-/-}$ mice immediately after the PET scan to further document uptake of ^{64}Cu-AMD3100 (n = 2/group). **(D)** Flow cytometric analysis of CXCR4 expression on cardiac neutrophils isolated from WT and $CD36^{-/-}$ mice (n = 3/group). All data are means ± SE with n representing the number of mice per group. Statistical significance is determined by the unpaired non-parametric Mann–Whitney t-test. *$p < 0.05$.

of $CD36^{-/-}$ mice is likely the fasting-induced TAG depletion. The fasted $CD36^{-/-}$ heart relies more heavily than the WT heart on glucose and endogenous lipid stores and is unable to replenish them by FA supply during fasting. However, in the fed state, the $CD36^{-/-}$ heart can derive FAs from chylomicrons. The heart utilizes FFAs bound to albumin, as well as FFAs, released from very low-density lipoproteins (VLDL) or from intestinally derived chylomicrons *via* vascular lipoprotein lipase (LpL)-mediated enzymatic cleavage of triacylglycerol (TG) ester bonds. A comparison of myocardial FA uptake from VLDL and chylomicrons in mice showed that CD36 was important for FA uptake from VLDL but not from chylomicrons, as the effect of CD36 deletion on FA uptake from chylomicrons was negligible (60). Therefore, in the fed state, the $CD36^{-/-}$ heart can replenish endogenous lipids from chylomicrons. In the fasting state, $CD36^{-/-}$ hearts fail to replenish TAG stores as uptake of FA and VLDL is CD36 dependent (8, 60). Targeting cardiac FA uptake can provide a primary approach for preventing excess lipid accumulation and lipotoxicity as proposed (61) but our findings indicate that very low FA uptake rates can negatively impact myocardial adaptation and the remodeling required for the maintenance of tissue health. In line with the current results with $CD36^{-/-}$ hearts, mice with LpL deficiency restricted to cardiomyocytes showed altered cardiac expression of genes involved in lipid and glucose metabolism (62) and developed heart dysfunction with aging and increased afterload (63).

Altered remodeling of cardiolipins and plasmalogens

We previously reported that $CD36^{-/-}$ hearts had higher contents of lysophospholipids, LPC, and LPE (4). These earlier findings together with the current observations of abnormal increases in lysocardiolipins are consistent with the interpretation that FA acyl supply might be rate-limiting for phospholipid remodeling in fasted $CD36^{-/-}$ hearts in line with the reduction in FA acyl sources, namely myocardial TAG and FA uptake. However, alternative or additional mechanisms cannot be ruled out. Phospholipid remodeling is regulated by signal transduction events, including changes in

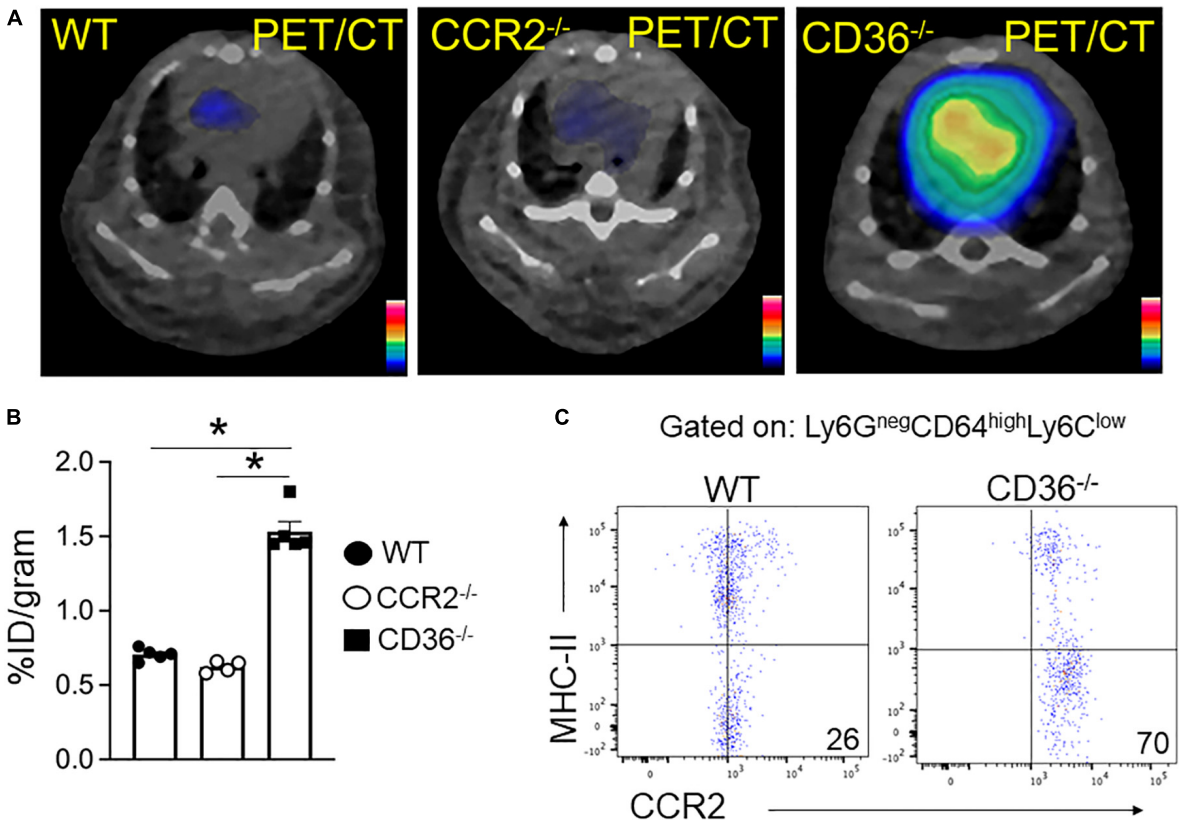

FIGURE 6
^{68}Ga-DOTA-ECL1i PET/CT imaging the infiltration of CCR2 + monocyte/macrophages in hearts. **(A,B)** Representative ^{68}Ga-DOTA-ECL1i PET/CT images and quantitative analysis showed higher tracer accumulation in the heart of CD36$^{-/-}$ (n = 5) compared with WT mice (n = 5) and CCR2$^{-/-}$ mice (n = 4/group). **(C)** Flow cytometric analysis of CCR2 expression in macrophages isolated from WT and CD36$^{-/-}$ hearts (n = 3/group). All data are means ± SE with n representing the number of mice per group. Statistical significance is determined by One-way ANOVA. *$p < 0.05$.

calcium dynamics, which are altered in CD36$^{-/-}$ hearts (4). Dysfunction of calcium flux, or activation of phospholipases A2, or lysophospholipid acyltransferases could result in abnormal tissue remodeling. We observed 50% suppression of gene expression for heart cytoplasmic cPLA2 and iPLA2γ, enzymes that mobilize arachidonic from PC and PE to yield lysoPC and lysoPE, and a two to fourfold increase in expression of the acyltransferases LPCAT2 and LPCAT3 that reacylate lysoPC to PC (data not shown). It remains to be determined whether these changes are compensatory in the context of dysregulated enzymatic activity.

Remodeling of cardiolipin side-chains is important for mitochondrial function (64, 65). Linoleic, oleic, arachidonic, and docosahexaenoic acids are major side-chains of mouse heart cardiolipin (66) and are maintained preferentially through acyl chain transfer from the *sn*-2 position of PC (67). Maintaining appropriate levels of the key C18:2 and C22:6 cardiolipin might be suboptimal in CD36$^{-/-}$ hearts. Remodeling of phospholipids is important for myocardial adaptation to stress and is thought to boost sarcoplasmic reticulum Ca^{2+} uptake. For example, altered DHA content of heart phospholipids in mice with deficiency of the very-long-chain acyl-CoA dehydrogenase that initiates oxidation of FA with 14–20 carbons is associated with abnormal Ca^{2+} handling, tachycardia, and prolonged QT interval (68, 69), similar to dysfunctions noted in fasted CD36$^{-/-}$ mice (4). The dysregulated phospholipid (PC, PE, and CL) remodeling induced by CD36 ablation appears maladaptive and might contribute to impairing calcium handling.

Level of plasmalogens was reduced in fed and fasted CD36$^{-/-}$ hearts as compared to controls. Plasmalogens are enriched in plasma membrane lipid-raft microdomains (70) and function as potent endogenous antioxidants regulating susceptibility to oxidative damage in many diseases (71–73). In addition, they are important for mitochondrial FA oxidation (38). Plasmalogens can also generate toxic lysolipids and hydroxy fatty aldehydes and are the target of activated neutrophils (74), but whether the reduction in plasmalogen levels is in part linked to neutrophil infiltration is unclear.

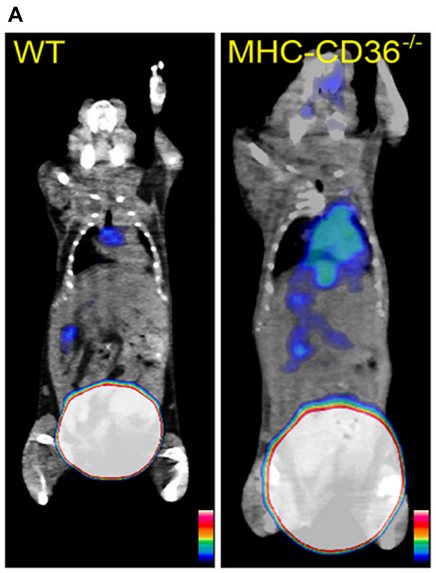

C

Direction	GAGE analysis - MHC-CD36$^{-/-}$/Control	Statistics	Genes	Adj. p-value
Down	Cellular respiration	-5.48	137	2.6e-04
	Mitochondrial respiratory chain complex assembly	-5.42	75	6.0e-04
	Generation of precursor metabolites and energy	-4.9	356	8.5e-04
	Energy derivation by oxidation of organic compounds	-4.89	210	8.5e-04
	Acetyl-CoA metabolic process	-4.80	78	1.3e-03
	Thioester metabolic process	-4.80	79	1.3e-03
Up	Extracellular matrix organization	6.49	250	2.8e-07
	Leukocyte migration	5.77	310	1.0e-05
	Myeloid activation	5.04	198	4.4e-04

FIGURE 7
Myocardial CD36 deletion associates with cardiac inflammation and impaired FA metabolisms. **(A,B)** Representative ^{68}Ga-DOTA-ECL1i PET/CT images and quantitative analysis showed higher tracer accumulation in the heart of MHC-CD36$^{-/-}$ (n = 4/group) compared with those isolated from control mice (n = 5/group). Data are means ± SE with n representing the number of mice per group, *$p < 0.05$. **(C)** Gene expression of MHC-CD36$^{-/-}$ and control hearts obtained by RNA-seq. Up- and downregulated biological pathways from Reactome analysis using differentially regulated genes (MHC-CD36$^{-/-}$ vs. WT, > 1.6 or < 0.7-fold change). All data are (n = 3/group) with n representing the number of mice per group. Number of genes on the differentially regulated list is indicated on significance bar for each pathway.

Changes in eicosanoids

The altered phospholipid remodeling in CD36$^{-/-}$ hearts is associated with increased production of various eicosanoids especially in the fed state when the supply of FAs is abundant. The data suggest that eicosanoid production is dysregulated and that it is normally suppressed by CD36 presence. This is in line with the findings in macrophages where CD36 deficiency upregulated basal or FA-induced eicosanoid production (**Figures 4E–G**). In macrophages, CD36 deficiency markedly increased levels of the pro-inflammatory PGD2 in M1 macrophages and those of the linoleic acid metabolite 13-HODE by both M1 and M2 macrophages. These lipid mediators influence diverse signaling pathways in the heart including activation of ion channels, modulation of calcium flux, and their resultant effects on cardiac hypertrophy, myocardial preconditioning, infarction, and arrhythmogenesis (41).

CD36$^{-/-}$ hearts have higher levels of most arachidonic-derived eicosanoids as compared to WT hearts. Arachidonic acid metabolism generates mostly pro-inflammatory mediators but can also yield metabolites that help resolve inflammation (75). Arachidonic acid metabolism to prostaglandins *via* the COX pathway or to leukotrienes *via* the LOX pathway is associated with acute inflammation (75). In addition to the increased production of pro-inflammatory eicosanoids, we observed a fourfold increase in cytochrome P450-derived epoxy cardioprotective compounds (76). The CYP pathway produces the pro-resolution mediator epoxyeicosatrienoic acid, thought to increase the recruitment of dendritic cells and monocytes important for repair (75). The EETs, present in the heart, endothelium, and plasma have vasodilatory, anti-inflammatory, antioxidative, anti-migratory, and pro-fibrinolytic effects in the heart, with 11,12-EET being the most efficacious. Some of these anti-inflammatory effects might be mediated by the inhibitory role of EETs on pro-inflammatory mediators in the vascular wall, ICAM-1, VCAM-1, and E-selectin. The 11,12-EET also inhibits phosphorylation of IκB-α, which is necessary for nuclear translocation of NF-κB, preventing activation of NF-κB target genes (77). However, it is worth noting that the changes in EET levels in CD36$^{-/-}$ hearts occurred in opposite direction to those in WT hearts. Levels were much higher in the fed state and declined after fasting to levels below those of WT hearts (e.g., 11,12-EET, and 14,15-EET). Overall, eicosanoid metabolism appears dysregulated in CD36$^{-/-}$ hearts, and further studies are needed to understand the molecular mechanisms driving the changes.

Is CD36 good or bad for heart homeostasis?

The current findings and our previous observations support the importance of CD36 for maintaining heart metabolic

flexibility and optimal adaptation to energy fluctuations. They also suggest an important role of the protein in the regulation of phospholipid remodeling important for membrane function. Emerging research show that CD36 has dual actions in the inflammatory process, as the receptor is reported to regulate both induction and resolution of inflammation possibly due to its capability to bind different ligands. For example, CD36-mediated uptake of oxLDL (78) contributes to cholesterol accumulation in arterial wall macrophages (79). CD36 induces inflammation by forming a complex with TLR4 (80) was shown to regulate nucleation and accumulation of cholesterol crystals within macrophages resulting in activation of the NLRP3 inflammasome (75). On the other hand, as a pattern recognition receptor, CD36 is involved in the clearance of cell debris and phagocytosis, which is important for resolving inflammation by contributing to the clearance of apoptotic neutrophils (81). In the heart, CD36 may be important for the resolution of cardiac inflammation after injury by contributing to monocyte clearance of apoptotic cells (21, 82). Impaired resolution of inflammation is also observed with CD36 deletion in lymphatic endothelial cells and the resulting impairment of the lymphatic barrier (83). These dual actions of CD36 in helping mount and resolve inflammation would be consistent with the concept that normally inflammation is tightly controlled, self-limited, and programs its own resolution (84). In summary, the heart of unchallenged $CD36^{-/-}$ mice is in a non-homeostatic state and displays strikingly abnormal remodeling of tissue lipids. This includes lipids important for energy production, TAG, and cardiolipin, which are associated with diminished mitochondrial oxidation and the reduced production of acylcarnitines during fasting. Abnormal remodeling of membrane phospholipids, important for tissue adaptation to stress, associated with dysregulated production of the bioactive eicosanoids, which play important roles in multiple physiological pathways, including the initiation and resolution of inflammation.

Potential relevance to humans

CD36 genetic variants that reduce protein level by ∼50% are relatively common, with a minor allele incidence of ∼20% in African Americans. Partial or total CD36 deficiency is associated with abnormal blood lipid profile (24, 85) and with vascular stiffening (23), which are predictors of obesity/diabetes-associated cardiovascular events. Humans deficient in CD36 have impaired FA uptake as visualized by spectral imaging using the FA analog BMIPP. Myocardial BMIPP uptake is almost undetectable in CD36 deficient humans and is significantly reduced in subjects with partial CD36 deficiency (6, 86) suggesting a quantitative gene-dosage dependency. The dysregulated eicosanoid secretion in the hearts of $CD36^{-/-}$ mice might signal the presence of subclinical tissue damage in line with the observed immune infiltration. High levels of eicosanoids have been associated with myocardial vulnerability. Increases in LOX-generated AA-derived HETEs, notably 12-HETE and 15-HETE, and of P450-generated AA-derived 11,12-EET and 14,15-EET were shown to correlate with the N-terminal pro-B-type natriuretic peptide, a cardiac biomarker predictive of the acute coronary syndrome and heart failure. They are also associated with the subsequent onset of acute myocardial infarct in patients with coronary artery disease (87). Our findings warrant further investigation of interventions that would mitigate the negative effects of the dysregulated lipid metabolism in CD36 deficient hearts. It would be important to determine whether polymorphisms that significantly reduce CD36 levels might be predictive of myocardial vulnerability to stress and could be a useful biomarker of individual susceptibility to (i) immune cell-induced cardiac pathological remodeling and (ii) electrical instability during fasting or other catabolic states.

Data availability statement

RNA-seq data were deposited in the NCBI's Gene Expression Omnibus (GEO) database (GEO GSE116350).

Ethics statement

This animal study was reviewed and approved by the Washington University Animal Studies Committee.

Author contributions

VC, OK, RWG, YL, RG, and NAA designed the research studies and analyzed the data. VC, OK, GSH, DS, HL, JL, KY, MR, TP, IJG, and YL contributed to data collection and analysis. VC, OK, and NAA wrote the manuscript. All authors reviewed the manuscript.

Funding

This work was supported by the Saint Louis University Research Institute (VC), the Ministry of Education, Youth and Sports of the Czech Republic (grant no. LTAUSA18104 to OK), the National Institutes of Health (grant nos. R01HL118639 and R01HL133178 to RWG, R35HL145212, R01HL151685, P41EB025815 to YL, R01HL045095 to NAA and IJG, R01DK111175 to NAA, and P30 DK056341), and the Cellular and Molecular Biology Core of the Nutrition and Obesity Research Center at Washington University.

Conflict of interest

The authors declare that the research was conducted in the absence of any commercial or financial relationships that could be construed as a potential conflict of interest.

Publisher's note

All claims expressed in this article are solely those of the authors and do not necessarily represent those of their affiliated organizations, or those of the publisher, the editors and the reviewers. Any product that may be evaluated in this article, or claim that may be made by its manufacturer, is not guaranteed or endorsed by the publisher.

Supplementary material

The Supplementary Material for this article can be found online at: https://www.frontiersin.org/articles/10.3389/fcvm.2022.948332/full#supplementary-material

References

1. Hames KC, Vella A, Kemp BJ, Jensen MD. Free fatty acid uptake in humans with CD36 deficiency. *Diabetes.* (2014) 63:3606–14.

2. Carley AN, Bi J, Wang X, Banke NH, Dyck JR, O'Donnell JM, et al. Multiphasic triacylglycerol dynamics in the intact heart during acute in vivo overexpression of CD36. *J Lipid Res.* (2013) 54:97–106. doi: 10.1194/jlr.M029991

3. Glatz JFC, Luiken J, Nabben M. CD36 (SR-B2) as a target to treat lipid overload-induced cardiac dysfunction. *J Lipid Atheroscler.* (2020) 9:66–78. doi: 10.12997/jla.2020.9.1.66

4. Pietka TA, Sulkin MS, Kuda O, Wang W, Zhou D, Yamada KA, et al. CD36 protein influences myocardial Ca2+ homeostasis and phospholipid metabolism: conduction anomalies in CD36-deficient mice during fasting. *J Biol Chem.* (2012) 287:38901–12. doi: 10.1074/jbc.M112.413609

5. Okamoto F, Tanaka T, Sohmiya K, Kawamura K. CD36 abnormality and impaired myocardial long-chain fatty acid uptake in patients with hypertrophic cardiomyopathy. *Jpn Circ J.* (1998) 62:499–504. doi: 10.1253/jcj.62.499

6. Tanaka T, Nakata T, Oka T, Ogawa T, Okamoto F, Kusaka Y, et al. Defect in human myocardial long-chain fatty acid uptake is caused by FAT/CD36 mutations. *J Lipid Res.* (2001) 42:751–9.

7. Tanaka T, Sohmiya K, Kawamura K. Is CD36 deficiency an etiology of hereditary hypertrophic cardiomyopathy? *J Mol Cell Cardiol.* (1997) 29:121–7.

8. Abumrad NA, Goldberg IJ. CD36 actions in the heart: lipids, calcium, inflammation, repair and more? *Biochim Biophys Acta.* (2016) 1861:1442–9. doi: 10.1016/j.bbalip.2016.03.015

9. Forte E, Furtado MB, Rosenthal N. The interstitium in cardiac repair: role of the immune-stromal cell interplay. *Nat Rev Cardiol.* (2018) 15:601–16. doi: 10.1038/s41569-018-0077-x

10. Gentek R, Hoeffel G. The innate immune response in myocardial infarction repair, and regeneration. *Adv Exp Med Biol.* (2017) 1003:251–72.

11. Weinberger T, Schulz C. Myocardial infarction: a critical role of macrophages in cardiac remodeling. *Front Physiol.* (2015) 6:107. doi: 10.3389/fphys.2015.00107

12. Shinagawa H, Frantz S. Cellular immunity and cardiac remodeling after myocardial infarction: role of neutrophils, monocytes, and macrophages. *Curr Heart Fail Rep.* (2015) 12:247–54.

13. Swirski FK. Inflammation and repair in the ischaemic myocardium. *Hamostaseologie.* (2015) 35:34–6.

14. Cavalera M, Frangogiannis NG. Targeting the chemokines in cardiac repair. *Curr Pharm Des.* (2014) 20:1971–9.

15. Geissmann F, Jung S, Littman DR. Blood monocytes consist of two principal subsets with distinct migratory properties. *Immunity.* (2003) 19:71–82. doi: 10.1016/s1074-7613(03)00174-2

16. Nahrendorf M, Swirski FK. PET Imaging of Leukocytes in Patients With Acute Myocardial Infarction. *JACC Cardiovasc Imaging.* (2015) 8:1427–9.

17. Frangogiannis NG. The stromal cell-derived factor-1/CXCR4 axis in cardiac injury and repair. *J Am Coll Cardiol.* (2011) 58:2424–6.

18. Nishimura Y, Ii M, Qin G, Hamada H, Asai J, Takenaka H, et al. CXCR4 antagonist AMD3100 accelerates impaired wound healing in diabetic mice. *J Invest Dermatol.* (2012) 132(3 Pt 1):711–20.

19. Jujo K, Hamada H, Iwakura A, Thorne T, Sekiguchi H, Clarke T, et al. CXCR4 blockade augments bone marrow progenitor cell recruitment to the neovasculature and reduces mortality after myocardial infarction. *Proc Natl Acad Sci USA.* (2010) 107:11008–13. doi: 10.1073/pnas.0914248107

20. Irie H, Krukenkamp IB, Brinkmann JF, Gaudette GR, Saltman AE, Jou W, et al. Myocardial recovery from ischemia is impaired in CD36-null mice and restored by myocyte CD36 expression or medium-chain fatty acids. *Proc Natl Acad Sci USA.* (2003) 100:6819–24.

21. Dehn S, Thorp EB. Myeloid receptor CD36 is required for early phagocytosis of myocardial infarcts and induction of Nr4a1-dependent mechanisms of cardiac repair. *FASEB J.* (2018) 32:254–64. doi: 10.1096/fj.201700450R

22. Cifarelli V, Ivanov S, Xie Y, Son NH, Saunders BT, Pietka TA, et al. CD36 deficiency impairs the small intestinal barrier and induces subclinical inflammation in mice. *Cell Mol Gastroenterol Hepatol.* (2017) 3:82–98. doi: 10.1016/j.jcmgh.2016.09.001

23. Shibao CA, Celedonio JE, Ramirez CE, Love-Gregory L, Arnold AC, Choi L, et al. A common CD36 variant influences endothelial function and response to treatment with phosphodiesterase 5 inhibition. *J Clin Endocrinol Metab.* (2016) 101:2751–8. doi: 10.1210/jc.2016-1294

24. Love-Gregory L, Kraja AT, Allum F, Aslibekyan S, Hedman AK, Duan Y, et al. Higher chylomicron remnants and LDL particle numbers associate with CD36 SNPs and DNA methylation sites that reduce CD36. *J Lipid Res.* (2016) 57:2176–84. doi: 10.1194/jlr.P065250

25. Zhao Y, Detering L, Sultan D, Cooper ML, You M, Cho S, et al. Gold nanoclusters doped with (64)Cu for CXCR4 positron emission tomography imaging of breast cancer and metastasis. *ACS Nano.* (2016) 10:5959–70. doi: 10.1021/acsnano.6b01326

26. Heo GS, Kopecky B, Sultan D, Ou M, Feng G, Bajpai G, et al. Molecular imaging visualizes recruitment of inflammatory monocytes and macrophages to the injured heart. *Circ Res.* (2019) 124:881–90. doi: 10.1161/CIRCRESAHA.118.314030

27. Son NH, Basu D, Samovski D, Pietka TA, Peche VS, Willecke F, et al. Endothelial cell CD36 optimizes tissue fatty acid uptake. *J Clin Invest.* (2018) 128:4329–42. doi: 10.1172/JCI99315

28. Han X, Yang K, Gross RW. Multi-dimensional mass spectrometry-based shotgun lipidomics and novel strategies for lipidomic analyses. *Mass Spectrom Rev.* (2012) 31:134–78. doi: 10.1002/mas.20342

29. Liu X, Moon SH, Mancuso DJ, Jenkins CM, Guan S, Sims HF, et al. Oxidized fatty acid analysis by charge-switch derivatization, selected reaction monitoring, and accurate mass quantitation. *Anal Biochem.* (2013) 442:40–50. doi: 10.1016/j.ab.2013.06.014

30. Han X, Yang J, Cheng H, Ye H, Gross RW. Toward fingerprinting cellular lipidomes directly from biological samples by two-dimensional electrospray ionization mass spectrometry. *Anal Biochem.* (2004) 330:317–31. doi: 10.1016/j.ab.2004.04.004

31. Ford DA, Han X, Horner CC, Gross RW. Accumulation of unsaturated acylcarnitine molecular species during acute myocardial ischemia: metabolic compartmentalization of products of fatty acyl chain elongation in the acylcarnitine pool. *Biochemistry.* (1996) 35:7903–9. doi: 10.1021/bi960552n

32. Su X, Han X, Mancuso DJ, Abendschein DR, Gross RW. Accumulation of long-chain acylcarnitine and 3-hydroxy acylcarnitine molecular species in diabetic myocardium: identification of alterations in mitochondrial fatty acid processing in diabetic myocardium by shotgun lipidomics. *Biochemistry.* (2005) 44:5234–45. doi: 10.1021/bi047773a

33. Spiekerkoetter U, Tokunaga C, Wendel U, Mayatepek E, Ijlst L, Vaz FM, et al. Tissue carnitine homeostasis in very-long-chain acyl-CoA dehydrogenase-deficient mice. *Pediatr Res.* (2005) 57:760–4.

34. Kuda O, Rombaldova M, Janovska P, Flachs P, Kopecky J. Cell type-specific modulation of lipid mediator's formation in murine adipose tissue by omega-3 fatty acids. *Biochem Biophys Res Commun.* (2016) 469:731–6. doi: 10.1016/j.bbrc.2015.12.055

35. McDonnell E, Crown SB, Fox DB, Kitir B, Ilkayeva OR, Olsen CA, et al. Lipids reprogram metabolism to become a major carbon source for histone acetylation. *Cell Rep.* (2016) 17:1463–72. doi: 10.1016/j.celrep.2016.10.012

36. Clemot M, Senos Demarco R, Jones DL. Lipid mediated regulation of adult stem cell behavior. *Front Cell Dev Biol.* (2020) 8:115. doi: 10.3389/fcell.2020.00115

37. Saddik M, Lopaschuk GD. Triacylglycerol turnover in isolated working hearts of acutely diabetic rats. *Can J Physiol Pharmacol.* (1994) 72:1110–9. doi: 10.1139/y94-157

38. Park H, He A, Tan M, Johnson JM, Dean JM, Pietka TA, et al. Peroxisome-derived lipids regulate adipose thermogenesis by mediating cold-induced mitochondrial fission. *J Clin Invest.* (2019) 129:694–711. doi: 10.1172/JCI120606

39. Ito K, Carracedo A, Weiss D, Arai F, Ala U, Avigan DE, et al. A PML-PPAR-delta pathway for fatty acid oxidation regulates hematopoietic stem cell maintenance. *Nat Med.* (2012) 18:1350–8. doi: 10.1038/nm.2882

40. Shu H, Peng Y, Hang W, Nie J, Zhou N, Wang DW. The role of CD36 in cardiovascular disease. *Cardiovasc Res.* (2022) 118:115–29.

41. Jenkins CM, Cedars A, Gross RW. Eicosanoid signalling pathways in the heart. *Cardiovasc Res.* (2009) 82:240–9.

42. Kuda O, Jenkins CM, Skinner JR, Moon SH, Su X, Gross RW, et al. CD36 protein is involved in store-operated calcium flux, phospholipase A2 activation, and production of prostaglandin E2. *J Biol Chem.* (2011) 286:17785–95. doi: 10.1074/jbc.M111.232975

43. Mouton AJ, Li X, Hall ME, Hall JE. Obesity, hypertension, and cardiac dysfunction: novel roles of immunometabolism in macrophage activation and inflammation. *Circ Res.* (2020) 126:789–806. doi: 10.1161/CIRCRESAHA.119.312321

44. Werz O, Gerstmeier J, Libreros S, De la Rosa X, Werner M, Norris PC, et al. Human macrophages differentially produce specific resolvin or leukotriene signals that depend on bacterial pathogenicity. *Nat Commun.* (2018) 9:59. doi: 10.1038/s41467-017-02538-5

45. Panigrahy D, Gilligan MM, Serhan CN, Kashfi K. Resolution of inflammation: an organizing principle in biology and medicine. *Pharmacol Ther.* (2021) 227:107879. doi: 10.1016/j.pharmthera.2021.107879

46. Orecchioni M, Ghosheh Y, Pramod AB, Ley K. Macrophage polarization: different gene signatures in M1(LPS+) vs. classically and M2(LPS-) vs. alternatively activated macrophages. *Front Immunol.* (2019) 10:1084. doi: 10.3389/fimmu.2019.01084

47. Eash KJ, Means JM, White DW, Link DC. CXCR4 is a key regulator of neutrophil release from the bone marrow under basal and stress granulopoiesis conditions. *Blood.* (2009) 113:4711–9. doi: 10.1182/blood-2008-09-177287

48. De Filippo K, Rankin SM. CXCR4, the master regulator of neutrophil trafficking in homeostasis and disease. *Eur J Clin Invest.* (2018) 48(Suppl. 2):e12949. doi: 10.1111/eci.12949

49. Vafadarnejad E, Rizzo G, Krampert L, Arampatzi P, Arias-Loza AP, Nazzal Y, et al. Dynamics of cardiac neutrophil diversity in murine myocardial infarction. *Circ Res.* (2020) 127:e232–49.

50. Bajpai G, Bredemeyer A, Li W, Zaitsev K, Koenig AL, Lokshina I, et al. Tissue resident CCR2- and CCR2+ cardiac macrophages differentially orchestrate monocyte recruitment and fate specification following myocardial injury. *Circ Res.* (2019) 124:263–78. doi: 10.1161/CIRCRESAHA.118.314028

51. Bajpai G, Schneider C, Wong N, Bredemeyer A, Hulsmans M, Nahrendorf M, et al. The human heart contains distinct macrophage subsets with divergent origins and functions. *Nat Med* (2018) 24:1234–45. doi: 10.1038/s41591-018-0059-x

52. Xia Y, Frangogiannis NG. MCP-1/CCL2 as a therapeutic target in myocardial infarction and ischemic cardiomyopathy. *Inflamm Allergy Drug Targets.* (2007) 6:101–7.

53. Luehmann HP, Pressly ED, Detering L, Wang C, Pierce R, Woodard PK, et al. PET/CT imaging of chemokine receptor CCR5 in vascular injury model using targeted nanoparticle. *J Nucl Med.* (2014) 55:629–34. doi: 10.2967/jnumed.113.132001

54. Hazen SL, Hall CR, Ford DA, Gross RW. Isolation of a human myocardial cytosolic phospholipase A2 isoform. Fast atom bombardment mass spectroscopic and reverse-phase high pressure liquid chromatography identification of choline and ethanolamine glycerophospholipid substrates. *J Clin Invest.* (1993) 91:2513–22. doi: 10.1172/JCI116487

55. Li W, Hsiao HM, Higashikubo R, Saunders BT, Bharat A, Goldstein DR, et al. Heart-resident CCR2(+) macrophages promote neutrophil extravasation through TLR9/MyD88/CXCL5 signaling. *JCI Insight.* (2016) 1:e87315. doi: 10.1172/jci.insight.87315

56. Ren Y, Silverstein RL, Allen J, Savill J. CD36 gene transfer confers capacity for phagocytosis of cells undergoing apoptosis. *J Exp Med.* (1995) 181:1857–62. doi: 10.1084/jem.181.5.1857

57. Zlatanova I, Pinto C, Silvestre JS. Immune modulation of cardiac repair and regeneration: the art of mending broken hearts. *Front Cardiovasc Med.* (2016) 3:40. doi: 10.3389/fcvm.2016.00040

58. Phillipson M, Kubes P. The healing power of neutrophils. *Trends Immunol.* (2019) 40:635–47.

59. Horckmans M, Ring L, Duchene J, Santovito D, Schloss MJ, Drechsler M, et al. Neutrophils orchestrate post-myocardial infarction healing by polarizing macrophages towards a reparative phenotype. *Eur Heart J.* (2017) 38:187–97. doi: 10.1093/eurheartj/ehw002

60. Bharadwaj KG, Hiyama Y, Hu Y, Huggins LA, Ramakrishnan R, Abumrad NA, et al. Chylomicron- and VLDL-derived lipids enter the heart through different pathways: in vivo evidence for receptor- and non-receptor-mediated fatty acid uptake. *J Biol Chem.* (2010) 285:37976–86. doi: 10.1074/jbc.M110.174458

61. Glatz JFC, Zuurbier CJ, Larsen TS. Targeting metabolic pathways to treat cardiovascular diseases. *Biochim Biophys Acta Mol Basis Dis.* (2020) 1866:165879.

62. Augustus A, Yagyu H, Haemmerle G, Bensadoun A, Vikramadithyan RK, Park SY, et al. Cardiac-specific knock-out of lipoprotein lipase alters plasma lipoprotein triglyceride metabolism and cardiac gene expression. *J Biol Chem.* (2004) 279:25050–7. doi: 10.1074/jbc.M401028200

63. Augustus AS, Buchanan J, Park TS, Hirata K, Noh HL, Sun J, et al. Loss of lipoprotein lipase-derived fatty acids leads to increased cardiac glucose metabolism and heart dysfunction. *J Biol Chem.* (2006) 281:8716–23.

64. Li J, Romestaing C, Han X, Li Y, Hao X, Wu Y, et al. Cardiolipin remodeling by ALCAT1 links oxidative stress and mitochondrial dysfunction to obesity. *Cell Metab.* (2010) 12:154–65.

65. Mancuso DJ, Sims HF, Han X, Jenkins CM, Guan SP, Yang K, et al. Genetic ablation of calcium-independent phospholipase A2gamma leads to alterations in mitochondrial lipid metabolism and function resulting in a deficient mitochondrial bioenergetic phenotype. *J Biol Chem.* (2007) 282:34611–22. doi: 10.1074/jbc.M707795200

66. Minkler PE, Hoppel CL. Separation and characterization of cardiolipin molecular species by reverse-phase ion pair high-performance liquid chromatography-mass spectrometry. *J Lipid Res.* (2010) 51:856–65. doi: 10.1194/jlr.D002857

67. Xu Y, Malhotra A, Ren M, Schlame M. The enzymatic function of tafazzin. *J Biol Chem.* (2006) 281:39217–24.

68. Werdich AA, Baudenbacher F, Dzhura I, Jeyakumar LH, Kannankeril PJ, Fleischer S, et al. Polymorphic ventricular tachycardia and abnormal Ca2+ handling in very-long-chain acyl-CoA dehydrogenase null mice. *Am J Physiol Heart Circ Physiol.* (2007) 292:H2202–11. doi: 10.1152/ajpheart.00382.2006

69. Gelinas R, Thompson-Legault J, Bouchard B, Daneault C, Mansour A, Gillis MA, et al. Prolonged QT interval and lipid alterations beyond beta-oxidation in very long-chain acyl-CoA dehydrogenase null mouse hearts. *Am J Physiol Heart Circ Physiol.* (2011) 301:H813–23. doi: 10.1152/ajpheart.01275.2010

70. Pike LJ, Han X, Chung KN, Gross RW. Lipid rafts are enriched in arachidonic acid and plasmenylethanolamine and their composition is independent of caveolin-1 expression: a quantitative electrospray ionization/mass spectrometric analysis. *Biochemistry.* (2002) 41:2075–88. doi: 10.1021/bi0156557

71. Khaselev N, Murphy RC. Susceptibility of plasmenyl glycerophosphoethanolamine lipids containing arachidonate to oxidative degradation. *Free Radic Biol Med.* (1999) 26:275–84. doi: 10.1016/s0891-5849(98)00211-1

72. Skaff O, Pattison DI, Davies MJ. The vinyl ether linkages of plasmalogens are favored targets for myeloperoxidase-derived oxidants: a kinetic study. *Biochemistry.* (2008) 47:8237–45. doi: 10.1021/bi800786q

73. Dean JM, Lodhi IJ. Structural and functional roles of ether lipids. *Protein Cell.* (2018) 9:196–206.

74. Thukkani AK, Hsu FF, Crowley JR, Wysolmerski RB, Albert CJ, Ford DA. Reactive chlorinating species produced during neutrophil activation target tissue plasmalogens: production of the chemoattractant, 2-chlorohexadecanal. *J Biol Chem.* (2002) 277:3842–9. doi: 10.1074/jbc.M109489200

75. Sheedy FJ, Grebe A, Rayner KJ, Kalantari P, Ramkhelawon B, Carpenter SB, et al. CD36 coordinates NLRP3 inflammasome activation by facilitating intracellular nucleation of soluble ligands into particulate ligands in sterile inflammation. *Nat Immunol.* (2013) 14:812–20. doi: 10.1038/ni.2639

76. Batchu SN, Lee SB, Qadhi RS, Chaudhary KR, El-Sikhry H, Kodela R, et al. Cardioprotective effect of a dual acting epoxyeicosatrienoic acid analogue towards ischaemia reperfusion injury. *Br J Pharmacol.* (2011) 162:897–907. doi: 10.1111/j.1476-5381.2010.01093.x

77. Spiecker M, Liao JK. Vascular protective effects of cytochrome p450 epoxygenase-derived eicosanoids. *Arch Biochem Biophys.* (2005) 433:413–20.

78. Huh HY, Pearce SF, Yesner LM, Schindler JL, Silverstein RL. Regulated expression of CD36 during monocyte-to-macrophage differentiation: potential role of CD36 in foam cell formation. *Blood.* (1996) 87:2020–8.

79. Goyal T, Mitra S, Khaidakov M, Wang X, Singla S, Ding Z, et al. Current concepts of the role of oxidized LDL receptors in atherosclerosis. *Curr Atheroscler Rep.* (2012) 14: 150–9.

80. Stewart CR, Stuart LM, Wilkinson K, van Gils JM, Deng J, Halle A, et al. CD36 ligands promote sterile inflammation through assembly of a Toll-like receptor 4 and 6 heterodimer. *Nat Immunol.* (2010) 11:155–61. doi: 10.1038/ni.1836

81. Ballesteros I, Cuartero MI, Pradillo JM, de la Parra J, Perez-Ruiz A, Corbi A, et al. Rosiglitazone-induced CD36 up-regulation resolves inflammation by PPARgamma and 5-LO-dependent pathways. *J Leukoc Biol.* (2014) 95:587–98. doi: 10.1189/jlb.0613326

82. Glinton KE, Ma W, Lantz CW, Grigoryeva LS, DeBerge M, Liu X, et al. Macrophage-produced VEGFC is induced by efferocytosis to ameliorate cardiac injury and inflammation. *J Clin Invest.* (2022) 132:e140685. doi: 10.1172/JCI140685

83. Cifarelli V, Appak-Baskoy S, Peche VS, Kluzak A, Shew T, Narendran R, et al. Visceral obesity and insulin resistance associate with CD36 deletion in lymphatic endothelial cells. *Nat Commun.* (2021) 12:3350. doi: 10.1038/s41467-021-23808-3

84. Serhan CN, Chiang N, Dalli J. The resolution code of acute inflammation: novel pro-resolving lipid mediators in resolution. *Semin Immunol.* (2015) 27:200–15. doi: 10.1016/j.smim.2015.03.004

85. Love-Gregory L, Abumrad NA. CD36 genetics and the metabolic complications of obesity. *Curr Opin Clin Nutr Metab Care.* (2011) 14:527–34.

86. Kintaka T, Tanaka T, Imai M, Adachi I, Narabayashi I, Kitaura Y. CD36 genotype and long-chain fatty acid uptake in the heart. *Circ J.* (2002) 66:819–25.

87. Huang CC, Chang MT, Leu HB, Yin WH, Tseng WK, Wu YW, et al. Association of arachidonic acid-derived lipid mediators with subsequent onset of acute myocardial infarction in patients with coronary artery disease. *Sci Rep.* (2020) 10:8105. doi: 10.1038/s41598-020-65014-z

Advantages of publishing in Frontiers

OPEN ACCESS
Articles are free to read for greatest visibility and readership

FAST PUBLICATION
Around 90 days from submission to decision

HIGH QUALITY PEER-REVIEW
Rigorous, collaborative, and constructive peer-review

TRANSPARENT PEER-REVIEW
Editors and reviewers acknowledged by name on published articles

Frontiers
Avenue du Tribunal-Fédéral 34
1005 Lausanne | Switzerland

Visit us: www.frontiersin.org
Contact us: frontiersin.org/about/contact

REPRODUCIBILITY OF RESEARCH
Support open data and methods to enhance research reproducibility

DIGITAL PUBLISHING
Articles designed for optimal readership across devices

FOLLOW US
@frontiersin

IMPACT METRICS
Advanced article metrics track visibility across digital media

EXTENSIVE PROMOTION
Marketing and promotion of impactful research

LOOP RESEARCH NETWORK
Our network increases your article's readership